A global to regional scale assessment of dam-induced agricultural change by means of remote sensing

DISSERTATION

Zur Erlangung des akademischen Grades
doctor rerum naturalium
(Dr. rer. nat.)
im Fach Geographie

Eingereicht an der
Mathematisch-Naturwissenschaftlichen Fakultät
der Humboldt-Universität zu Berlin

von
M.Sc. Philippe Rufin

Präsidentin der Humboldt-Universität zu Berlin
Prof. Dr.-Ing. habil. Dr. Sabine Kunst

Dekan der Mathematisch-Naturwissenschaftlichen Fakultät
Prof. Dr. Elmar Kulke

Gutachter:
Prof. Dr. Patrick Hostert
Prof. Dr. habil. Claudia Künzer
Prof. Dr. Volker Radeloff

Eingereicht am 29.01.2019
Datum der Verteidigung: 15.04.2019

Acknowledgments

I want to thank Patrick Hostert for introducing me to Earth observation, providing a great work environment, and spreading so much enthusiasm for our field. I would like to thank all co-authors for their invaluable contributions to this thesis. Too many to name them here, but I want to thank *all* members of the Earth Observation Lab, Conservation Biogeography Lab, and the Applied Geoinformation Science Lab for making the daily work routines so enjoyable. I want to thank the many people whom I met through the field of Geography, but are now among my very close friends. In particular, Dennis Funke, Cornelius Senf, Florian Gollnow, and Marcel Schwieder. Thanks to my life-long friends in Berlin, Europe, and the rest of the world. Furthermore, I want to thank my family for their ever-lasting motivation and support, which helped me to follow my ideas and find my way into research. Lastly and most importantly - thank you Emma & Ava for bringing so much curiosity, joy, and *mys* into my life. Let's keep on going!

Abstract

Humans used land over the course of millennia. A growing world population, and its increasing demands for food, feed, fuel and fiber, substantially add pressure on the global land system. The construction of dams is a common strategy for increasing water storage capacities and boosting production outputs through irrigation. Reservoirs represent the most important source of irrigation water globally, but their effects on land systems, and agriculture in particular, are only poorly understood. Remote sensing emerges as a key tool for enabling spatially explicit assessments of dam-induced land system change due to its ability to provide spatially detailed, frequent, and synoptic observations of the land surface. The overall goal of this thesis was to assess the effects of irrigation dams on agricultural land systems on a global and regional scale, by making use of state-of-the art remote sensing data products and methods. A synthesis of the current scientific literature offered novel insights into dam-induced changes in agricultural systems, and raised the hypothesis that irrigation dams caused overall increases in agricultural land use intensity. On a global scale, satellite-based measurements of cropping frequency derived from MODIS-based map products attested to this finding. However, a high regional variability of cropping frequency was apparent, which could partly be explained through the biophysical, socio-economic and technological characteristics of irrigation dams and their command areas. Due to the recent acceleration in dam construction activities, Turkey was identified as a relevant case for regional-scale investigations. Landsat-based time series methods were assessed in order to produce spatially and thematically detailed representations of the national cropping system. The resulting insights on time series analyses facilitated a long-term characterization of irrigated summer cropping in the largest dam-and-canal irrigation scheme of Turkey. This regional study further emphasized the enormous spatio-temporal dynamics of irrigated agriculture and revealed current trends of land use intensification. This thesis demonstrates that remote sensing technologies can contribute to accurate and consistent characterization of agricultural land systems and the spatial and temporal dynamics therein. Current requirements for consistent, spatially detailed, and frequent data on land use in irrigated agriculture can thereby be supported by remote sensing technologies. The findings, methods, and datasets generated in this thesis add to the knowledge on the effects of dams on agricultural land systems and can thereby aid in exploring future pathways of agricultural intensification.

Zusammenfassung

Die terrestrischen Ökosysteme der Erde unterliegen seit Jahrtausenden menschlicher Nutzung. Im Laufe des letzten Jahrhunderts stieg der Druck auf die globale Landoberfläche, zeitgleich mit einer wachsenden Nachfrage nach landwirtschaftlichen Erzeugnissen, drastisch an. In vielen Weltregionen ist Landwirtschaft von künstlicher Bewässerung abhängig. Staudämme stellen einen Großteil der Wasserressourcen und ermöglichen hierdurch Produktionssteigerungen. Die Zusammenhänge zwischen Staudämmen und Veränderungen des Landsystems wurden bis heute jedoch kaum erforscht. Im Hinblick auf die steigende Nachfrage nach landwirtschaftlichen Erzeugnissen bedarf es eines besseren Verständnisses des Einflusses von Staudämmen und Bewässerung auf landwirtschaftliche Produktionssysteme. Daten und Methoden der Fernerkundung liefern regelmäßige, synoptische und räumlich detaillierte Aufnahmen der Erdoberfläche mit großem Potential für die Untersuchung von landwirtschaftlichen Produktionssystemen. Das Hauptziel dieser Arbeit war es, das gegenwärtige Verständnis des Zusammenhangs von Bewässerungsstaudämmen und Landsystemen mit Mitteln der Fernerkundung zu verbessern. Eine Synthese der wissenschaftlichen Literatur verdeutlichte die Komplexität des Zusammenspiels zwischen Staudämmen und Landsystemen. Insbesondere wurde ein Zusammenhang zwischen Bewässerungsstaudämmen und gesteigerter Landnutzungsintensität deutlich. Um diesen Prozess zu untersuchen, wurde eine globalskalige Analyse der Anbaufrequenz im Einflussbereich von Bewässerungsstaudämmen mittels MODIS-basierten Kartenprodukten durchgeführt. Die Ergebnisse dieser Studie bestätigten den Zusammenhang zwischen Dämmen und erhöhter Landnutzungsintensität, wobei diese Muster einer hohen inter-regionalen Variabilität unterlagen. Die biophysikalischen, sozio-ökonomischen und technologischen Gegebenheiten der Untersuchungsgebiete konnten die Variabilität in Teilen erklären. Die Türkei erlebte in den vergangenen Jahrzehnten einen rasanten Anstieg des Baus von Bewässerungsstaudämmen und stellte daher ein interessantes Studiengebiet dar, um die globalen Hypothesen aus regionaler Perspektive zu untersuchen. Landsat-basierte Zeitreihenanalysen ermöglichten eine räumlich und thematisch detaillierte Kartierung der dominanten landwirtschaftlichen Anbaupraktiken im Jahr 2015. Die methodischen Erkenntnisse aus dieser Arbeit wurden im Rahmen einer Kartierung von Bewässerungsfeldwirtschaft im größten Bewässerungsdistrikt der Türkei angewendet, welche die globalskaligen Ergebnisse in Bezug auf erhöhte Landnutzungsintensität, sowie die enorme raumzeitliche Variabilität der regionalen Bewässerungslandwirtschaft untermauerten. In dieser Arbeit wurden großflächige Beschreibungen heterogener Agrarsysteme generiert, welche nachdrücklich das Potential von Daten und Methoden aus der Fernerkundung hervorheben. Das hohe thematische, räumliche und zeitliche Detail erlaubte einzigartige Einblicke in die raum-zeitlichen Dynamiken von Bewässerungsfeldwirtschaft. Die im Zuge dieser Arbeit entstandenen Ergebnisse, Methoden, und Datensätze tragen maßgeblich zum heutigen Wissensstand in Bezug auf den Zusammenhang zwischen Bewässerungsstaudämmen und Landnutzungsintensität bei und liefern wichtige Einblicke zur Verbesserung zukünftiger Produktionsstrukturen.

Contents

List of Figures

List of Tables

Chapter 1

Introduction

1.1 Scientific background

1.1.1 Agriculture in the Land System

Earth's land surface is of unique value for humanity, as it regulates water cycles and the global climate, supports the production of food, feed, fuel, and fiber, provides habitat and shelter to plants and animals, and offers recreational values (Verburg et al., 2015). Humans have used land throughout millennia in order to profit from these ecosystem goods and services (Ellis et al., 2013). Ecosystems respond to human modifications with altered environmental conditions and ecosystem properties, including changes in climate or freshwater cycles (DeFries et al., 2004; Robinson et al., 2018). During the last century, these interactions between humans and ecosystems have accelerated at an unprecedented rate, thereby threatening the stability of the Earth system as a whole, and posing risks for global-scale disruptions of ecosystems or societies, and economies (Steffen et al., 2018).

In recognition of the feedback between humans and their environment, novel scientific frameworks with a focus on the interactions between biogeophysical and anthropogenic components of the Earth system gained importance in recent years (e.g., coupled human and natural systems or social-ecological systems; Liu and et al., 2007; Ostrom, 2009). The pivotal role of land for current societal challenges including food and water security (Godfray et al., 2010; Vörösmarty et al., 2010), as well as climate change (IPCC, 2018; Steffen et al., 2015), further demanded for a framework with a specific focus on land and its interactions with humans. In this light, the scientific community coined the term land system, which represents *"the terrestrial component of the Earth system and encompasses all processes and activities related to the human use of land, including socioeconomic, technological and organizational investments and arrangements, as well as the benefits gained from land and the unintended social and ecological outcomes of societal activities"* (Verburg et al., 2013, p.433). Among all anthropogenic activities in the land system, agriculture is of particular relevance, because it covers around one-third of the global land surface and is strongly interlinked with global biogeochemical cycles and human well-being (Foley et al., 2005; Pongratz et al., 2008).

Agriculture allows societies to appropriate ecosystem goods and services in order to generate food, feed, fuel, and fiber. Historically, population growth increased the requirements for land resources, which substantially altered the land system (Ellis, 2011; Ellis et al., 2013). Until the middle of the 20^{th} century, production increases were widely sustained through agricultural expansion, which resulted in the extensive conversion of natural ecosystems into cultivated or grazed land, with severe effects on the global carbon cycle and biodiversity (Ramankutty and Foley, 1998; Gibbs et al., 2010). The Green Revolution marked a turning point in this regard,

as it provided the key technological developments for boosting the productivity of global agricultural production (Evenson and Gollin, 2003). During the second half of the 20^{th} century, production gains were increasingly supported through the adoption of high-yielding varieties, synthetic fertilizers, pesticides, and modernized land management, which compensated for cropland expansion through more intensive use of land (Stevenson et al., 2013). By the middle of the 21^{st} century, nine billion people will inhabit Earth, and their requirements for agricultural produce will further increase the pressure on the land system (Gerland et al., 2014; Godfray et al., 2010). Future restrictions in land and water resources, as well as uncertainties in climatic conditions, require an improved understanding of the production potential, as well as the social and ecological externalities of land use intensification (Foley et al., 2011; Pretty, 2018; Rasmussen et al., 2018).

Land use intensity is multi-dimensional. It encompasses the inputs and outputs of the production systems, as well as the properties of production systems (Erb et al., 2013). Inputs include labor, agro-chemicals, water, or land (for instance regarding cropping frequency; Boserup, 1965; Turner and Doolittle, 2010). Outputs mostly refer to quantities of production output per unit area and time, such as yields in tons per hectare. The properties of the production system include biogeochemical and ecological patterns and processes such as carbon storage, water, and nutrient cycles, or soil quality. System properties are thus directly coupled to the input, as well as the output components of the system, and vice versa. Agricultural intensification often involves trade-offs between the benefits of agricultural production and the costs for social-ecological systems (Rasmussen et al., 2018). However, the impacts of various intensification strategies, e.g., regarding input-output relationships, or environmental externalities, remain only poorly understood, partly due to a lack of information on the spatial patterns of different land use intensity indicators (Kümmerle et al., 2013; Pongratz et al., 2017).

Drastic gains in agricultural production are required in the future, with estimates ranging from 60% increases in production value (Alexandratos and Bruinsma, 2012), to a doubling of food calorie production between 2005 and 2050 (Tilman et al., 2011). Given the global scarcity of suitable agricultural land (Lambin and Meyfroidt, 2011) and the severe environmental consequences of land conversion for agricultural expansion (Gibson et al., 2011; Fearnside, 2005), the intensification of land use will likely play a pivotal role for meeting future demands for agricultural produce (Ramankutty et al., 2018). A major controversy arises from the need for production increases because the extent and intensity of contemporary land-based agriculture readily approach the physical boundaries of multiple Earth system components (Campbell et al., 2017; Conijn et al., 2018). The current intensity of agricultural production disturbs the balance of global biogeochemical flows through increased nitrogen

and phosphorous inputs (Power, 2010). Irrigation of agricultural land accounts for around 70% of the planetary freshwater withdrawals (Siebert and Döll, 2010), and overexploitation of water resources poses a risk of severe ecosystem degradation in many parts of the globe (Jägermeyr et al., 2017). The identification of pathways for sustainable intensification is thus one of the grand societal challenges of the 21^{st} century (Rockström et al., 2016). However, the limited understanding of past effects of agricultural intensification, their mechanisms and outcomes, hamper advances in designing sustainable intensification pathways.

At the beginning of the 21^{st} century, approximately one-third of the terrestrial land area was used for agriculture, including 12% of croplands and 26% of pasturelands (Foley et al., 2011). Between 1985 and 2005, the global cropland extent increased by 3%, while in the same period, intensification processes boosted the production of major crops by 28%. Disentangling the underlying processes of intensification revealed that the causes for rising production were two-fold. Roughly two-thirds of these production gains resulted from increased yields, while the remainder was supported through improved land management, which enabled a reduction of fallow periods, or multiple cropping cycles within a year (Alexandratos and Bruinsma, 2012; Foley et al., 2011).

Increasing land input regarding cultivation and harvest frequency offers solutions for closing productivity gaps on the global scale (Ray and Foley, 2013; Wu et al., 2018). For instance, increasing cropping frequency is expected to allow for a 10% gain in agricultural production until 2050 (Alexandratos and Bruinsma, 2012), and regional investigations suggested double cropping as means for adapting production systems to changes in climate (Seifert and Lobell, 2015; Kawasaki, 2018). An improved understanding of how reductions of fallow years and increases in multicropping can be achieved while minimizing social and environmental externalities is urgently required (Ray and Foley, 2013; Wu et al., 2018). To this end, irrigation emerges as a potential mechanism to enable and sustain agricultural production in water-constrained production regions, seasons, and conditions (Rosegrant et al., 2009).

1.1.2 Irrigation for agricultural intensification

Irrigation is a key mechanism to increase agricultural production outputs (Rosa et al., 2018; Rosegrant et al., 2009). Increased water availability and the development of irrigation infrastructure enable increased land input through three distinct processes (Figure 1.1). First, irrigation enables cropland expansion, resulting in the conversion of marginal lands or vegetated ecosystems into irrigated agriculture. Secondly, the conversion of rainfed into irrigated production enables a reduction of fallow years. Third, land inputs can increase intra-annually through the introduc-

tion of multiple cropping cycles. Irrigation improves yields, and further supports productivity gains through co-occurring changes in additional inputs, e.g., diversification of crop types, increased fertilizer application and mechanization (Rosegrant et al., 2009; You et al., 2011).

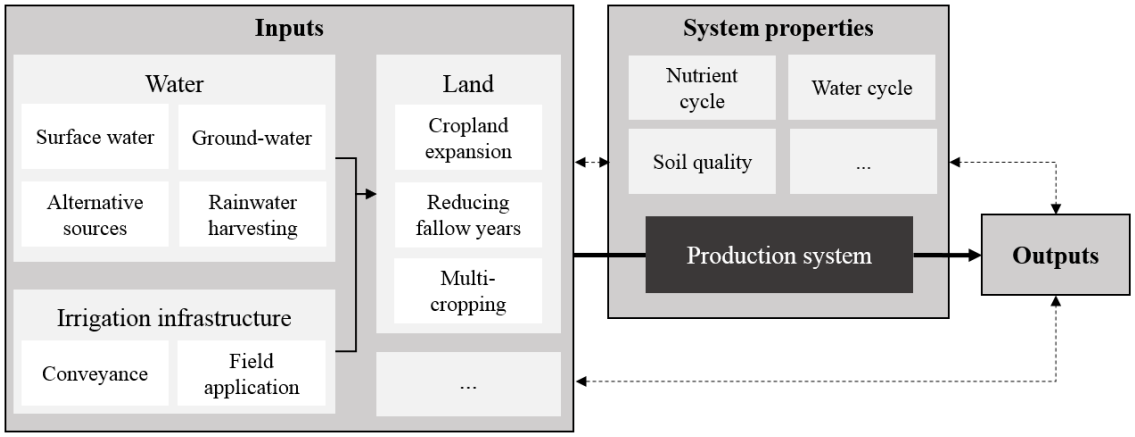

Figure 1.1: Schematic representation of irrigation-induced input intensification within the land use intensity framework. Combined water and irrigation infrastructure relate to increased land input through expansion and increased cropping frequency. Figure adapted from (Erb et al., 2013).

Globally, irrigation brought vast new areas of land into production and further increased the use intensity of existing croplands. Since 1950, the area equipped for irrigation across the globe tripled, exceeding 300 million ha in 2005 (Siebert et al., 2015). The contribution of irrigation to global crop production is substantial, as it, e.g., sustains 20% of the global cereal production (Siebert and Döll, 2010). At the same time, irrigation can alter the properties of the production system. Excessive irrigation can lead to the depletion of the regional water resource base, as observed in the Aral Sea basin (Micklin, 2007), and regions with high reliance on groundwater irrigation, such as the US High Plains (Scanlon et al., 2012). Furthermore, irrigation-induced soil salinization degrades the fertility of 1.5 million ha of croplands per year (Wood et al., 2000). In part, these degraded areas are permanently unusable, causing reductions in land inputs (Qadir et al., 2014).

Irrigation can - under appropriate management - offer sustainable pathways for closing yield gaps in specific world regions, and major crop types (Mueller et al., 2012; Rosa et al., 2018). Irrigated agriculture is envisioned to expand by 20 million ha until 2050 (Alexandratos and Bruinsma, 2012), mostly in regions where irrigation potential is widely untapped, such as in Sub-Sahara Africa (You et al., 2011). Future scenarios of irrigation expansion must consider the pivotal role of irrigation for water scarcity (Mekonnen and Hoekstra, 2016). Limitations in freshwater availability will be exacerbated under climate change, and efficient use of water resources through better water management is a precondition for expanding irrigation activities and

sustaining ecosystem services in the long run (Grafton et al., 2018; Jägermeyr et al., 2017).

Water use efficiency (i.e., the ratio between effective water use and actual water withdrawal; Stanhill, 1986) is determined by the configuration of the water transfer system and the application methods, which vary across the globe (Jägermeyr et al., 2015). Irrigation water transfer from the source to the field occurs through pipes or canals, where water is applied to the field through surface-, sprinkler-, or drip-irrigation (FAO, 1985). Water losses due to evaporation and seepage during water allocation and application translate into water use efficiencies below 50% in many irrigated systems (Rohwer et al., 2007). Specifically, gravity-based water transfer in open, unlined canals and surface irrigation operate under low efficiency (Brouwer, 1989), but are, nevertheless, the dominant configuration of irrigation systems globally (Jägermeyr et al., 2015).

The sources of irrigation water comprise surface water, groundwater, and non-conventional sources such as treated wastewater, which vary across the globe. The dominant share of the global irrigated areas (62%), however, taps open water surfaces (Siebert et al., 2013). In this context, dams play a pivotal role, as they provide a total of 40% of the global irrigation water withdrawals (Biemans et al., 2011). Despite this substantial contribution, enormous social and environmental costs were frequently associated with dam construction and operation (McCully, 2001; Scudder, 2019).

1.1.3 Dams: past, present, and future perspectives

More than 59,000 large dams are registered globally (ICOLD, 2015) and the global number of small dams likely ranges beyond the order of millions (Lehner et al., 2011; Wisser et al., 2010). Irrigation is the dominant purpose of existing dams. As much as half of all single-purpose dams and a quarter of all multi-purpose dams globally were built for irrigation (ICOLD, 2015). Dams provide a significant share of global irrigation water (Biemans et al., 2011), generate an estimated 3,200 terrawatt hours of electricity at an annual basis (Zeng et al., 2017), aid in meeting water requirements of industry, rural and urban populations, and protect the livelihoods of those living in flood-prone regions (Muller et al., 2015).

The pace of dam construction accelerated in the second half of the 20^{th} century, driven by increasing demands for irrigation water and hydropower (Figure 1.2). Dam construction peaked in the mid-1970s when two to three large dams were commissioned every day (WCD, 2000). In an era of increasing environmental concerns following the Stockholm conference in 1972, the perception on dams as a means for water storage and electricity production changed markedly, resulting in emerging disputes between dam advocates and opponents (Biswas, 2012). As a result, the World Bank and the International Union for Conservation of Nature (IUCN)

founded an internal working group in 1997, in order to compile knowledge about the costs and benefits of large dams across the globe.

The World Commission on Dams (WCD) released its final report in 2000, which outlined the economic, technical, environmental, and social performance of large dams. The report strengthened the evidence on severe negative effects of dams on humans and the environment (WCD, 2000), and thereby sparked further scientific inquiry to investigate the effects of dams on humans and the environment at scales ranging from local to the global. To date, research documented the diverse and interlinked effects of dam construction, encompassing the anticipated societal and economic benefits, as well as undesired consequences for humans and the environment (Kirchherr and Charles, 2016; McCully, 2001).

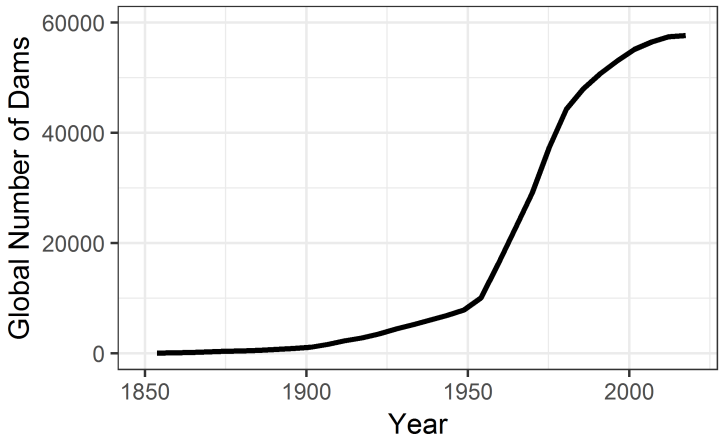

Figure 1.2: Cumulative number of large dams constructed since 1850. Data obtained from ICOLD (2015).

The societal impacts of dams directly concern the adjacent and downstream population. Reservoir construction displaced 40 - 80 million people by the year 2000 (WCD, 2000; Scudder, 2012). This estimate is increasing rapidly in light of recent projects (Scudder, 2019), including the Chinese Three Gorges Dam, which displaced 1.3 million people with adverse effects on well-being and livelihoods (Wilmsen, 2018). Irrigation dams can aid to alleviate the poverty of rural populations (Awlachew et al., 2008; Lipton et al., 2003) and bring economic development to society at large (Muller et al., 2015). On the contrary, flow regulation has implications for food security, e.g., in the case of flood-cycle dependent fisheries (Sabo et al., 2017), or floodplain agriculture (Thomas and Adams, 1999). Negative impacts on human health can follow reservoir construction and the development of irrigation schemes. For instance, irrigation development globally increased malaria incidence rates (Keiser et al., 2005), which counterbalanced the positive economic effects of irrigation investments (Ersado, 2005). The notion of dam construction as a tool for economic development (Biswas and Tortajada, 2001; Hall et al., 2014;

Tortajada, 2014) was therefore increasingly challenged in recent years (Ansar et al., 2014; Zeitoun et al., 2016).

The environmental consequences of dam construction concern, among others, the hydrosphere, biosphere, and atmosphere on local to global scales. Currently, large dams affect 48% of the global river volume through flow regulation or river fragmentation, which is projected to double given the realization of currently planned dams (Grill et al., 2015). River regulation changes riparian ecosystems (Nilsson and Berggren, 2000), and wetlands (Feng et al., 2016; Han et al., 2018). Alterations in the hydrological regime and landscape configuration further induce changes in habitat availability and species composition, which threaten the integrity of riparian ecosystems (Diamond, 2001). Dam-related flow regulation for hydropower and irrigation affected hydroclimate on a global scale (Destouni et al., 2013) and reservoirs emit substantial amounts of greenhouse gases (St. Louis et al., 2000). Anoxic decomposition of flooded vegetation and soil organic matter in reservoirs increases the carbon and methane footprint of hydro-energy, specifically for newly flooded reservoirs in tropical regions (Barros et al., 2011). In these regions, the greenhouse gas emissions per unit electricity approach the levels of fossil-based energy production (de Faria et al., 2015).

While dam construction rates in the developed nations of Europe and North America stagnated in recent decades, they recently started to gain traction in other nations (Figure 1.3). Turkey is one such example. Dam-based irrigation was heavily promoted to enable the expansion and intensification of Turkey's agricultural production in recent decades (Kibaroğlu et al., 2011). To date, agriculture plays a pivotal role to the Turkish economy, as the country is among the top exporters of cereal grain, and staple crop production alone accounts for nearly 10% of the national GDP (FAO, 2009b). Currently, 972 dams are operational in Turkey, 86% of which serve irrigation purposes (ICOLD, 2017). The relevance of dam-and-canal irrigation is, for instance, demonstrated by the Güneydoğu Anadolu Projesi (GAP) - a major infrastructure investment which now entails Turkey's largest irrigation scheme. The GAP comprised the installation of 22 large dams, and the envisioned expansion of irrigation on 1.8 million ha in semi-arid conditions (GAP, 2017). To date, the GAP region provides more than half of the national production of cotton, Turkey's most important non-food crop (USDA, 2018; TSI, 2015). Irrigation consumes 74% of the nationally extracted water resources, and further development of water storage capacities is a key priority for the national development policy (Kibaroğlu et al., 2012). Irrigation expansion is foreseen on more than three million hectares until 2030 and offers opportunities for achieving sustainable production increases in the future, which are, however, heavily dependent on appropriate regulation and management of land and water resources (Malek et al., 2018).

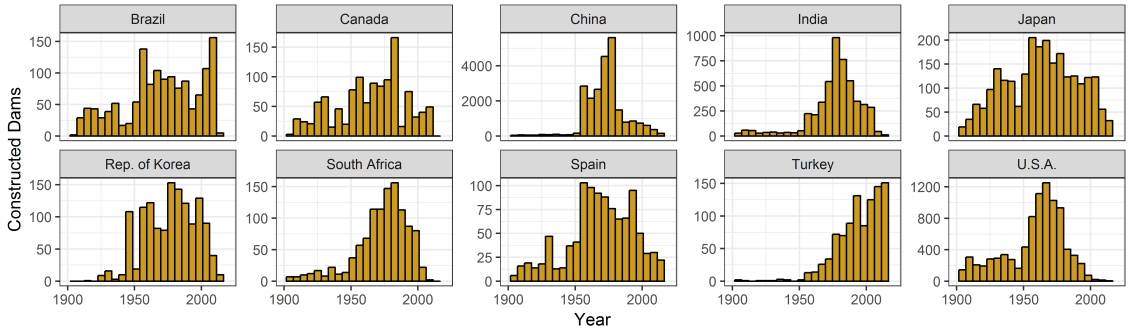

Figure 1.3: The number of dams constructed in five-year intervals. Data are shown for the top ten countries regarding the number of dams. Data obtained from ICOLD (2015).

An additional 3,700 dams will be operational until 2030, the majority of which is located in biodiversity hotspots, such as the Amazon basin, or the Caucasus (Winemiller et al., 2016; Zarfl et al., 2015). Dam-and-canal schemes are part of the option space for future irrigation expansion and provide opportunities for increasing global agricultural production (Shumilova et al., 2018; You et al., 2011). While the societal and economic benefits of dams are continuously motivating dam construction across the globe (Muller et al., 2015), our understanding of their costs and benefits remains limited in many respects. Most strikingly, there are only limited insights on the benefits of irrigation dams for agricultural production, including where and under which conditions these unfold (Perry, 2001).

An improved understanding of dam-induced agricultural change is vital to disentangle the relationships between land and water resource inputs and production outputs, specifically in light of the societal challenge of feeding a growing world population. A land system perspective offers opportunities for investigating the effects of dams, including the types and magnitudes of dam-induced land changes, or their spatial distribution. Specifically, the relationship between irrigation and land inputs can contribute to understanding the role of dams for agricultural production. In the past, knowledge gains were hampered by a lack of information on the command areas (i.e., the target areas of irrigation development), and land use intensity indicators with sufficient spatial, temporal, and thematic detail. The recent emergence of novel methods, datasets, and analysis capabilities, leverage promising opportunities to overcome past constraints for investigating dam-induced land change.

1.2 Methodological framework

1.2.1 Assessing dam-induced agricultural change

Only a few selected effects of dams are investigated on a global scale, including alterations in hydrology (Grill et al., 2015) and climate (Destouni et al., 2013), health effects (Keiser et al., 2005), or economic indicators (Ansar et al., 2014). Knowledge of the benefits of irrigation dams for agricultural production is very limited (Perry, 2001). Particularly little is known concerning dam-induced land system change at small geographic scales, and analyses of general patterns or theories lack to date. For instance, there are currently no estimates on the cumulative area of inundated land, and more specifically, which types of land cover or land use were lost in the light of dam construction. Changes in agricultural land extent and use intensity, e.g., regarding land input, can be expected in the light of irrigation expansion, but these changes were, to date, not assessed. Therefore, the question remains if changes across large areas can be observed, what their magnitudes are, and how these processes interact with other land system components. Novel approaches for assessing dam-induced land system change in the context of agriculture can profit from the insights gained in previous studies with a focus on the economic performance of irrigation dams.

The WCD (2000) provided the first global assessment of general patterns and trends of dam performance by compiling a multitude of social, environmental, technical, and economic indicators from multiple case studies. Concerning irrigation performance, the assessment was limited to a quantitative assessment of the fraction of developed irrigated area of the anticipated irrigated area across 52 dams (Figure 1.4). The analysis revealed a general trend for delayed irrigation infrastructure development, specifically in the initial years after commissioning. The resulting economic underperformance had drastic consequences for the livelihoods of people reliant on the anticipated irrigation infrastructure but did not facilitate insights on the costs, or benefits that arise from the achieved irrigation infrastructure expansion (Perry, 2001).

The assessment of the WCD was the first of its kind to offer insights into general patterns of performance of dam projects. However, its replicability is limited by the high costs for expert consultation and the aggregation of various data types and sources with varying levels of uncertainty. Approaches based on standardized methods to quantify dam-induced changes in land system indicators offer means for consistent estimates of general patterns of change. One key challenge for measuring dam-induced changes in agricultural landscapes is that the exact locations of command areas are commonly unknown. A few selected studies approached a spatially explicit identification of command areas in order to quantify the impacts of

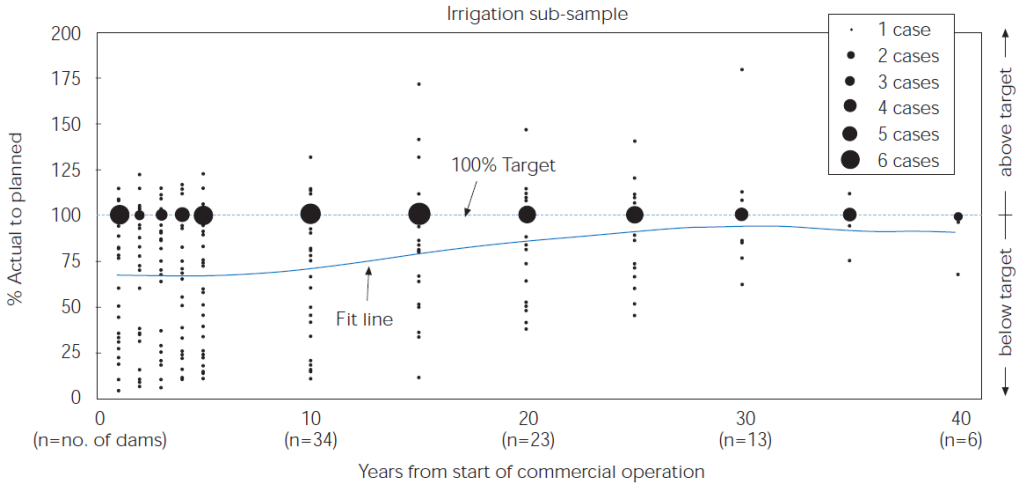

Figure 1.4: The performance of 52 irrigation dams projects concerning the timeliness of anticipated irrigation infrastructure development (WCD, 2000).

irrigation dams on rural poverty (Duflo and Pande, 2007), or cropland productivity (Strobl and Strobl, 2011; Blanc and Strobl, 2014), and for identifying potential areas for further irrigation expansion (You et al., 2011).

Duflo and Pande (2007) assessed the relationship between dams and changes in agricultural production across India. This study was among the first to investigate the effects of irrigation dams across a larger number of dams with a spatially explicit component. The spatial distribution of dam-induced changes was hypothetically defined based on the topographic relationship of dams and administrative districts. Either no, or partly even negative effects on agricultural production were found in proximity to the dam location, whereas positive effects were found downstream, where the majority of irrigation dam command areas were located. Strobl and Strobl (2011) expanded the spatial dimension of this framework to link dams and changes in cropland productivity across hydrological basins in Africa. Basin-level cropland productivity was derived by combining remotely sensed data products on land cover (Bartholomé and Belward, 2005) and net primary production (Cao et al., 2004). You et al. (2011) identified potential areas for future irrigation expansion in several African countries, assuming gravity-based irrigation and a 150 km maximum distance between dams and cropland areas. All three studies targeted the quantification of the significance of dams for the economic value of agricultural production and found overall positive effects of dams. The economic perspective, however, does not yield insights on land use intensification patterns, which are essential for investigating future intensification pathways in an era of limited land and water resources.

Assessments on small geographic scales are vital for improving our understanding of general patterns and trends of land change and can motivate further inquiry to

deepen the resulting insights at the regional level (Verburg et al., 2011). However, common trade-offs between spatial extent and spatial detail cannot easily be overcome. Two of the studies mentioned above related the number of dams to changing output indicators in aggregate spatial units (Duflo and Pande, 2007; Strobl and Strobl, 2011). Thereby, average patterns could be revealed, but the sub-unit variability and determinants thereof could not be explored in detail. For instance, the storage capacity of an individual reservoir was suggested to co-determine the magnitude of dam-induced productivity increases (Blanc and Strobl, 2014), strengthening the notion that dam-induced agricultural changes vary on a case-by-case basis. Additionally, the geographies of dam locations vary strongly across space, e.g., regarding biophysical, socio-economic, or institutional settings (Poff and Hart, 2002; Tortajada et al., 2012).

A synthesis of dam-induced land system change ideally covers a large spatial extent to account for the variability of dam geographies, while at the same time it should be conducted at sufficient spatial detail. However, existing trade-offs between spatial extent and detail hamper such analyses to date. Regional-scale studies commonly profit from data at finer spatial, temporal, or thematic detail, which allows for insights into the variability within the unit of analysis. Analyses at varying scales can complement each other in this regard, and transferring investigations of similar indicators across scales offers opportunities to improve our understanding of the magnitude, spatial distribution, and variability of dam-induced agricultural change. Spatially explicit information on the land change processes of interest is a detrimental prerequisite in this context. Optical remote sensing offers great potential for facilitating analyses on a regional and a global scale, specifically in the context of land use, and land use intensity changes (Kümmerle et al., 2013; Pongratz et al., 2017).

1.2.2 Remote sensing in agricultural systems

In recent years, major technological and political developments supported the advent of innovative remote-sensing based analysis techniques that enabled spatially explicit characterizations of land cover and land use with high spatial, temporal, and thematic detail, using optical remote sensing data (Wulder et al., 2018). Recent governmental initiatives, spearheaded by the United States Geological Survey, opened satellite image archives and provided cost-free access to a vast amount of image datasets. These resulted in a broad user base for remote sensing data, stimulating a "democratization" of remote sensing analyses (Wulder and Coops, 2014). Technological developments increased data storage capacities and processing power, which currently facilitate the storage of image data in petabyte order of magnitude. Innovative algorithms allow for efficient pre-processing of such data including geometric,

radiometric, atmospheric correction (Frantz et al., 2016; Masek et al., 2006) as well as cloud detection (Frantz et al., 2018; Zhu et al., 2015). Advances in the field of machine learning provided algorithms for robust and computationally efficient image classification or regression analyses to map patterns and processes in land systems from remotely sensed imagery (Maxwell et al., 2018). As a consequence, spatially detailed mapping across large areas was made possible (Hansen and Loveland, 2012) and fuelled analyses that revealed global-scale changes in forests (Hansen et al., 2013), shrublands, bare soil (Song et al., 2018), or surface water (Pekel et al., 2016).

Openly accessible remote sensing data archives offer opportunities for a broad range of applications. The suitability of a specific dataset for a given purpose is determined by the technical properties of the specific sensor, and thus the choice of suitable image datasets is dependent on the application. For the case of capturing dam-induced agricultural change, i.e., changes in cropland extent and use intensity, the process characteristics superimpose specific requirements to the data. Namely, these are a spectral, spatial, temporal resolution as well as a temporal coverage of the input data, which is appropriate to identify the target attributes of agricultural production systems at sufficient thematic detail and with low uncertainties.

Remote sensing systems can be categorized into passive or active systems. Active systems emit electromagnetic radiation and measure the amount of energy returned and comprise light detection and ranging (Lidar), or radio detection and ranging (Radar) sensors. Active systems provide opportunities for structural characterizations of the land surface. For instance, Lidar data is considered a gold-standard for assessing the vertical structure of forests (Pflugmacher et al., 2012). Similarly, Synthetic Aperture Radar (SAR) systems have great potential for characterizing terrain topography, biomass, soil moisture, or inundation patterns, since they operate independently of atmospheric conditions or sun illumination. Despite these advantages, frequent global data coverage of Lidar systems is not available, and for SAR systems, this has only recently been made possible (Torres et al., 2012).

Passive systems measure the sun's radiation reflected by the Earth surface or thermal energy emitted by the Earth surface. Optical remote sensing systems are of prime importance to derive spatially explicit characterizations of land cover, land use, and land use intensity, due to their ability to measure the reflectance of surfaces in various parts of the electromagnetic spectrum. Such reflectance measurements allow for deriving indicators of surface properties, such as land cover, or the state of vegetation. The spectral properties of a sensor system are defined through the number and position of spectral bands as well as their resolution. For the characterization of land surface properties in the optical domain, many sensors are designed to capture the visible (∼400 nm - ∼700 nm), near infrared (∼700 nm - ∼1,300 nm),

and shortwave infrared (∼1,300 nm - ∼3,000 nm) parts of the electromagnetic spectrum (Lillesand et al., 2011). While sensors with a visible red and near infrared band could theoretically allow for describing the status of vegetation, operational optical systems are commonly equipped with multi-, or hyperspectral sensors, which allow for capturing reflectance in a few, or up to hundreds of different regions of the electromagnetic spectrum. These measurements allow for nuanced characterizations of land and water surfaces and their attributes, such as vigor and water content of vegetation, which is of great use for applications in agriculture (Atzberger, 2013).

The spatial resolution of remotely sensed data is critical for accurate descriptions of agricultural systems, as the size and shape of cropland parcels vary strongly across the globe (Fritz et al., 2015). Currently, operational optical sensors have spatial resolutions ranging from kilometers to centimeters. Their suitability depends on the landscape characteristics of the studied system, e.g., regarding agricultural field sizes (Figure 1.5). The Advanced Very High Resolution Radiometer (AVHRR; 1,150 m) and the Satellite Pour l'Observation de la Terre Vegetation (SPOT VEGETATION; 1,100 m), acquire kilometer-scale spatial resolution imagery. The Moderate Resolution Imaging Spectroradiometer (MODIS) spectral bands allow for analyses at 250 m to 1,000 m, and the OLCI sensors onboard the Sentinel 3A and 3B satellites at 300 m spatial resolution. While these sensors provide global coverage at near-daily intervals, their relatively coarse spatial resolution can lead to biased estimates of agricultural land extent, both in consolidated systems, and even more so when fields are small (Jain et al., 2013; Özdoğan and Woodcock, 2006a; Senf et al., 2015).

Satellites such as Landsat 4 - 8 and Sentinel 2A and B provide great opportunities to capture fragmented landscapes, as their sensors provide a spatial resolution of less than 30 m in the spectral bands of the visible to shortwave infrared regions of the electromagnetic spectrum. The increased spatial detail improves characterizations of diverse agricultural systems, ranging from consolidated systems with large parcels to fragmented mosaic landscapes. Recent studies demonstrated the great potential of the Landsat and Sentinel 2 sensors to cover large areas while characterizing the spectral variability within parcels and thus offers novel opportunities for agriculture (Griffiths et al., 2019; Immitzer et al., 2016). A spatial resolution below ten meters is, e.g., provided by the Rapid Eye (5 m), IKONOS (3.28 m), or WorldView-2 (1.8 m) sensors. While such a fine resolution offers unique opportunities for the characterization of agricultural lands, the data commonly underlie commercial licenses and are thus costly to acquire. Additionally, wall-to-wall coverage over large areas is commonly not available, specifically at appropriate temporal intervals for characterizing agricultural systems.

Agricultural landscapes are highly dynamic in terms of their spectral behavior over time, due to diverse crop growth cycles and management interventions such

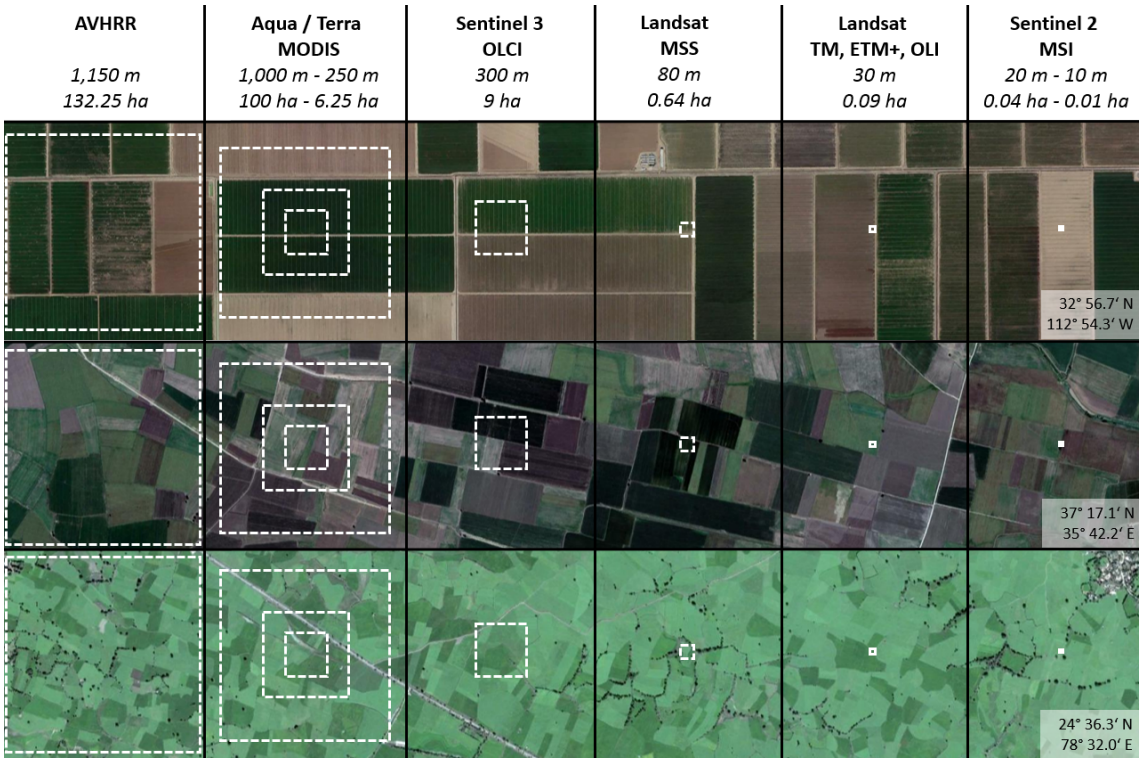

Figure 1.5: Pixel size of selected optical Earth observation sensors in agricultural landscapes in the United States (top), Turkey (middle), and India (bottom). Image data obtained from Digital Globe, Google Earth.

as irrigation, plowing, mowing, and harvesting. The spectral similarities between different agricultural land uses, such as croplands and grasslands, can further complicate mapping (Müller et al., 2015). Exploring information of the temporal change of land surfaces - often referred to as land surface phenology - was recognized as a means for improving mapping efforts in agricultural systems. Sensors with a daily or near-daily revisit-frequency such as MODIS allow for capturing land surface phenology at high detail, and thereby identify multi-cropping, distinguish crop types, or map management interventions such as irrigation (Estel et al., 2016; Özdoğan and Gutman, 2008; Xiao et al., 2006). However, due to the lack of spatial detail of these data, sensors such as Landsat TM, ETM+, OLI or Sentinel 2 MLCI are increasingly considered for time-series based mapping in agricultural systems (Atzberger, 2013). The nominal repeat frequency of these sensors is commonly lower, as, for instance, the Landsat satellites have a 16-day repeat cycle. By combining data from two Landsat sensors, 8-day repeat cycles can be achieved, which can be even higher in across-track overlap areas. Using integrated data from the Sentinel 2A and 2B satellites, nominal repeat frequencies of 5 days can be achieved, again with higher revisit frequencies in the across-track overlap areas. However, cloud cover and sensor errors decrease the nominal repeat frequency at the pixel-level, which can result in extended periods without clear observations (Whitcraft et al., 2015).

Recent mapping efforts in agricultural systems investigated the use of time series analysis techniques to overcome the limitations of low and spatially varying data availability. For instance, temporal binning of dense time series can be used for integrating clear observations within specified time windows. Using, for instance, all available annual or seasonal observations allows for producing gap-free image datasets over large areas. Data gaps can be filled with data from other acquisitions within the specified time window, e.g., through pixel-based compositing (Griffiths et al., 2013a) or time series gap filling (Vuolo et al., 2017). Alternatively, all available observations can be compressed into a statistical description of the reflectance signal and its variability in a specified period - commonly referred to as spectral-temporal metrics (Müller et al., 2015; Schug et al., 2018). Dense intra-annual time series further enable detailed characterizations of land surface phenology, from which phenological metrics can be derived (Schwieder et al., 2016). Seasonal to weekly temporal intervals, for instance, are suitable for discriminating crop types based on their growing-season phenology (Griffiths et al., 2019), or management practices, which are visible only for short periods (Jakimow et al., 2018). These time series analysis techniques increasingly allow for large-area characterization of agricultural systems at 30 m spatial resolution, e.g., in terms of cropland extent on a national, and continental scale (Phalke and Özdoğan, 2018; Waldner et al., 2017) or with higher thematic detail including crop types, or irrigated agriculture (Deines et al., 2017; Griffiths et al., 2019; Roy and Yan, 2018).

The temporal coverage of a dataset is specifically relevant for assessing long-term processes and land change over decadal timeframes. An expansive temporal coverage allows to move from static descriptions of land cover or land use towards the characterization of processes such as long-term changes in surface water (Pekel et al., 2016), changes in tidal zones (Murray et al., 2018), or deforestation (Hansen et al., 2013). In terms of land use intensity, long-term characterization of simple indicators of land cover or land use reveals indicators of cropping intensity (Estel et al., 2016), cropland abandonment (Dara et al., 2018) or post-deforestation land use intensity (Griffiths et al., 2018; Müller et al., 2016; Rufin et al., 2015). Landsat provides unique opportunities in this regard, as the Landsat image archive provides more than three decades of global coverage at 30 m spatial resolution (Figure 1.6). However, Landsat data availability varies across space and time due to past limitations in onboard data storage, data downlink capacities, and ground receiving stations.

In the past, long-term data acquisition plans were formulated which steered precisely when and where data was collected and downloaded (Arvidson et al., 2001). To date, increased downlink capacities, and an extended network of ground receiving stations widely overcome such restrictions, as, for instance, Landsat 8 provides a continuous stream of Earth surface measurements. Since 2010, more than five

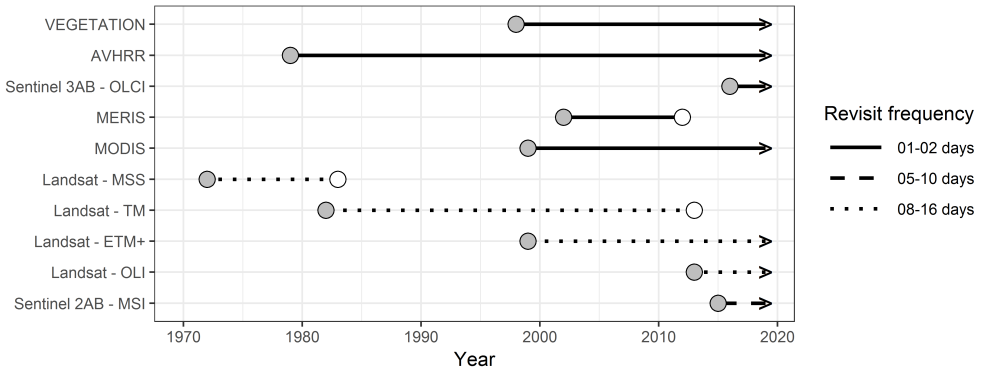

Figure 1.6: Lifetime and nominal revisit frequency of selected optical sensor systems.

million images have been migrated from international data holdings into a centralized archive, in order to fill historic data gaps in many world regions (Wulder et al., 2016). These efforts comprised, for instance, nearly one million images from European data holdings (Labahn, 2018). Currently, the Landsat archive provides more than three decades (or four, albeit with reduced spatial resolution) worth of global coverage. The spectral, spatial and temporal resolution of these data is highly suitable for long-term and large-area characterizations of agricultural systems, including indicators of land use or land use intensity. However, global-scale processing at 30 m spatial resolution is still a challenging endeavor, and global indicators of land use intensity do therefore only exist at lower spatial detail.

A variety of coarser spatial resolution products might fulfill criteria for global-scale investigations of dam-induced agricultural changes (Table 1.1). Besides their limited spatial detail, however, these products often have restricted temporal coverage of one or two points in time, and high levels of uncertainty related to the confusion of thematically or spectrally proximate classes, which is reflected in lacking agreement between products (Fritz et al., 2011). Additionally, map errors are not evenly distributed across space (Foody, 2005), and the regional suitability of available products might vary (Waldner et al., 2016b). Detailed assessments the quality of selected map products might be available for certain regions (Pflugmacher et al., 2011), or target classes (Pérez-Hoyos et al., 2017). Selected products feature a spatially explicit representation of classification uncertainty (Friedl et al., 2010). The application-specific suitability of existing map products needs to be assessed, whereas the spatial and temporal resolution, thematic detail, and accuracy of the product limit the applicability of some products over others (Verburg et al., 2011).

Table 1.1: Name, spatial and temporal resolution, years covered, thematic detail in the cropland domain and overall accuracy for selected global-scale land cover products, derived from remotely sensed data.

Name	Spatial resolution	Temporal resolution	Period	Cropland classes	Overall accuracy
IIASA IFPRI (Fritz et al., 2015)	1 km	static	2005	Cropland (%) per grid cell	82.4%
GlobCover (Bontemps et al., 2011; Defourny et al., 2006)	300 m	static	2005, 2009	Post-flooding or irrigated croplands; Rainfed-croplands; Two cropland mosaic classes	67.5% / 70.7%
GLC2000 (Bartholomé and Belward, 2005)	1 km	static	2000	Cultivated and managed areas (sub-classes at regional level); Two cropland mosaic classes	68.6%
MODIS Collection 5 LC (Friedl et al., 2010)	500 m	annual	2001 - 2012	Croplands; Cropland/natural vegetation mosaics	75.0%
ESA CCI v. 1 (Defourny et al., 2012)	300 m	5-yearly	1995 - 2015	Cropland rainfed; Cropland irrigated; Two cropland mosaic classes	71.7% (2015)
GFSAD 30 (Thenkabail, 2013; Congalton et al., 2017)	30 m	static	2015	Cropland	91.7%

1.3 Conceptual framework

1.3.1 Research questions

Dams were built to enhance water storage capacities across the globe. Surprisingly, dam-induced land change processes in agricultural systems are only poorly understood. Designing future intensification pathways requires a better understanding of past patterns of land change, which can allow for determining whether dam-based irrigation could contribute to achieving a more sustainable agricultural production in the future. The work presented in this thesis targets two overarching research questions:

Research Question I: *How did irrigation dams affect agricultural land systems on a global and regional scale?*

Irrigation dams expectedly affect the extent and land use intensity of agricultural land over different spatial extents and periods. The first research question of this thesis aims at capturing the patterns and trends of dam-induced land system change. Compiling evidence from multiple study regions across the globe can thereby allow for outlining relevant processes of dam-induced land change, and the magnitudes thereof. Accounting for the heterogeneous geographies of different case studies can improve our understanding of determinants of land use intensity, or changes therein. Investigations on a global scale can further be used to formulate hypotheses, which can subsequently be investigated on a regional scale. Assessing the potential of remote sensing datasets and methods to overcome these limitations is central to the second research question of this thesis:

Research Question II: *How can remote sensing contribute to our understanding of dam-induced agricultural change?*

Two major methodological challenges currently hamper the identification of dam-induced land system change. Namely, these are lack of spatially explicit knowledge about the locations of irrigation dam command areas, as well as limited availability of data on the land system response processes, such as changes in cropland extent or land use intensity. On a global scale, combining remote sensing data products, such as multi-temporal land cover and land use maps can improve existing approaches for identifying command areas and indicators of cropland use intensity. On a regional scale, state-of-the-art methods of Landsat time-series analysis offer great potential to derive indicators of land input over large areas and long time frames, and thereby to enable spatially detailed analysis of dam-induced agricultural land change.

1.3.2 Objectives and workflow

This thesis explores dam-induced agricultural change on two scales: the global and the regional. Analyses on varying scales superimpose specific requirements towards the analytical frameworks, methods, and data used. Five objectives arise from the two overarching research questions, three of which pursue global-scale insights:

Objective 1) *Synthesize observed processes of dam-induced land system change, and assess their relevance for agricultural systems.*

Objective 2) *Employ global remote sensing data products to map cropping frequency and to identify the command areas of recently constructed irrigation dams.*

Objective 3) *Assess cropping frequency and its determinants in the command areas of recently constructed irrigation dams on a global scale.*

Objective 1 targeted the synthesis of case study knowledge through a meta-study framework in order to improve the understanding of dam-induced land system change, as well as the underlying processes. Patterns and processes of agricultural change were focused upon, which motivated further scientific inquiry concerning dam-induced land use intensity changes. Objective 2 entailed the development of a global-scale approximation of irrigation dam command areas. Moreover, options for using land cover products to characterize cropping frequency across the globe were explored. Based on these outcomes, objective 3 targeted a global-scale characterization of cropping frequency in irrigation dam command areas, and an investigation of its biophysical, socio-economic and technological determinants. The two objectives focusing on a regional scale formulate as follows:

Objective 4) *Investigate the potential of Landsat time series for thematically detailed mapping of cropping systems on a regional scale.*

Objective 5) *Characterize patterns and long-term trends of cropping frequency in a dam-and-canal irrigation scheme on a regional scale.*

Objective 4 targeted the development of Landsat-based methods for mapping agricultural land use intensity indicators at 30 m spatial resolution. Due to the recent acceleration of dam construction, Turkey served as a case study to test and develop state-of-the-art methods of Landsat time series analysis for mapping cropping practices. The insights gained in the context of objective 4 indicated time series analysis techniques applicable for regional characterizations of dam-induced agricultural change. For objective 5, the suggested methods for mapping irrigated summer cropping were employed over decadal time frames in a regional setting. Due to its relevance for the national agricultural production, the Güneydoğu Anadolu Projesi (GAP) - Turkey's largest irrigation scheme - was selected as a study region. Each of the five objectives thus concerns one of the two research questions and targets insights on a global, or regional scale (Figure 1.7).

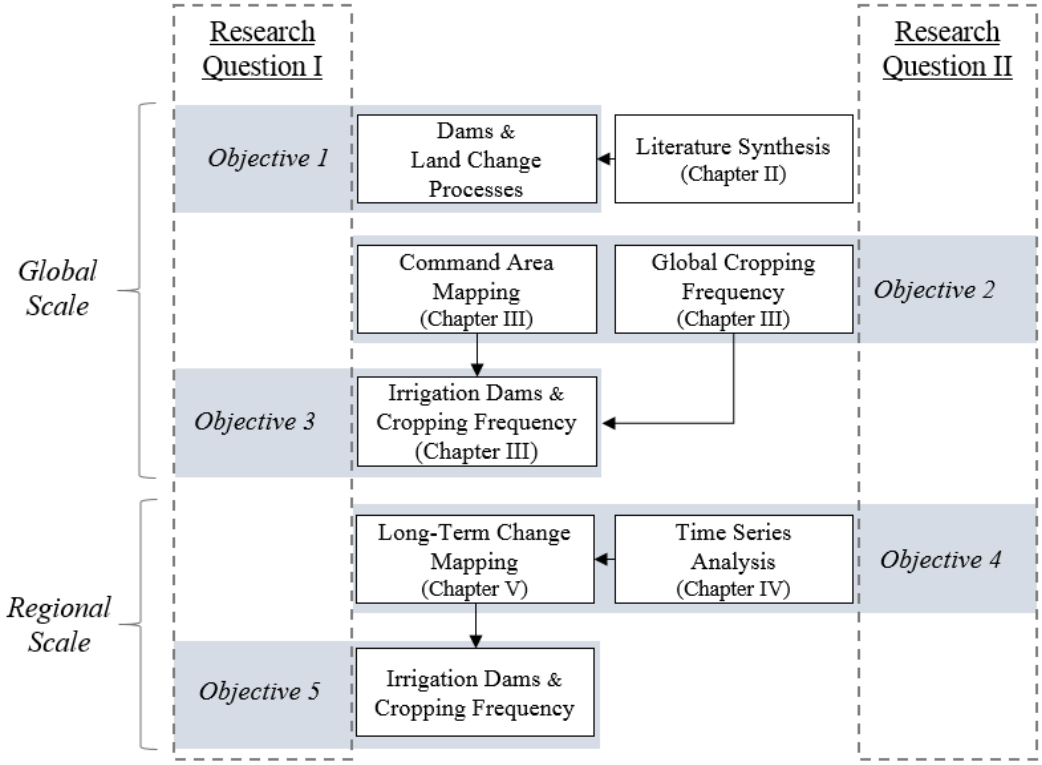

Figure 1.7: Thesis workflow, illustrating the relations between research questions, geographic scales, and individual objectives.

1.3.3 Thesis structure

This thesis consists of six chapters. Chapter I served the wider framing in the scientific literature and motivated the research questions and objectives which receive further attention in the following chapters. Chapters II - V represent the core scientific chapters of this thesis. Each of these four chapters is either published in

international peer-reviewed journals, or in preparation for submission. The thesis concludes with a synthesis section in chapter VI, in which a general summary and the main conclusions, implications, as well as an outlook, are presented.

Chapter II:) Philippe Rufin, Florian Gollnow, Daniel Müller and Patrick Hostert (2019). Synthesizing dam-induced land system change. *AMBIO*.

Chapter III:) Philippe Rufin, Christian Levers, Matthias Baumann, Jonas Jägermeyr, Tobias Krüger, Tobias Kümmerle and Patrick Hostert (2018). Global-scale patterns and determinants of cropping frequency in irrigation dam command areas. *Global Environmental Change*.

Chapter IV:) Philippe Rufin, David Frantz, Stefan Ernst, Andreas Rabe, Patrick Griffiths, Mutlu Özdoğan and Patrick Hostert (2019). Mapping cropping practices on a national scale using intra-annual Landsat time series binning. *Remote Sensing*.

Chapter V:) Philippe Rufin, Daniel Müller, Marcel Schwieder, Dirk Pflugmacher and Patrick Hostert: Mapping the extent and intensity of irrigated summer cropping in Southeastern Anatolia using Landsat data. *In preparation for submission*.

Chapter 2

Synthesizing dam-induced land system change

Philippe Rufin, Florian Gollnow, Daniel Müller, and Patrick Hostert
Ambio, 2019

DOI: 10.1007/s13280-018-01144-z
Submitted 11 June 2018; Revised 20 September 2018; Accepted 29 December 2018

Abstract

Dam construction and operation modify land systems. We synthesized 178 observations of dam-induced land system changes from 54 peer-reviewed case studies. Changing extents of forests (23%), agricultural land (21%), and built-up areas (11%) were reported frequently, alongside alterations in land use intensity (23%). Land cover changes were mostly related to hydropower and multi-purpose dams, while irrigation dams dominantly caused land use intensity changes. While a significant share of the changes were caused by reservoir flooding (29%), indirect effects which interact with societal and environmental systems (42%) were of utmost importance. We suggested the distance to the dam and the time since commissioning as potential controls for the direction of land system changes. Our insights provide opportunities for future inductive investigations across large populations of dams at regional to global scales and highlight that multi-disciplinary research perspectives are imperative for the production of generalizable knowledge.

2.1 Introduction

Globally, tens of thousands of dams and reservoirs provide societal and economic benefits, such as irrigation water for nearly one million square kilometers of agricultural land (ICOLD, 2017) and 3,000 terawatt hours of electricity per year (Zeng et al., 2017). The growing number of dams also causes a plethora of severe environmental and socio-economic side-effects with global-scale implications, including modifications of hydrological cycles (Rosenberg et al., 2000), hydroclimatic shifts (Destouni et al., 2013; Jaramillo and Destouni, 2015), increasing greenhouse gas emissions (Barros et al., 2011), as well as negative implications for human health (Keiser et al., 2005), livelihoods (Kirchherr and Charles, 2016), and food security (Fung et al., 2018). Furthermore, dams modify land systems, which encompass all processes and activities related to the human use of land, including its social and ecological benefits and unintended consequences (Verburg et al., 2013). Land submergence during reservoir flooding or repercussions from social or environmental side-effects can, for instance, alter the spatial patterns or intensity of land use (WCD, 2000; Tortajada et al., 2012). However, a globally consistent assessment of the effects of dams on land systems has been missing to date.

The effects of dams on land systems can be divided into direct and indirect effects. Direct effects of dams refer to land cover or land use changes caused by reservoir flooding, which encompass changes in area extent and modification within the land use and land cover categories, such as changes in the intensity of land use. Due to their spatially and temporally restricted nature, the direct effects can be captured with current methodological toolkits. For instance, remote sensing allows to detect the extent of reservoir inundation and the associated losses of natural ecosystems, built-up area (e.g., settlements, infrastructure), and agricultural land.

Indirect effects relate dams and land systems through more complex sequences of causes and effects. Indirect effects of dams are diverse, non-static, can occur in proximate or distal locations, and often unexpectedly. These effects are difficult to monitor and isolate with current methods, and are therefore only weakly understood. For instance, dams improved irrigation water availability globally (Biemans et al., 2011), thereby increasing the reliability and profitability of agricultural production, which can foster agricultural expansion and intensification (Thomas and Adams, 1999; de Fraiture et al., 2014). Novel livelihood strategies and economic opportunities emerge from such changes in agricultural production systems (Gordon and Meentemeyer, 2006; Casado et al., 2016), which in turn alter land ownership structures (Loker, 2003) or increase the competition for land and water resources (Thomas and Adams, 1999; Delang et al., 2013). Synthesizing these manifold repercussions of dam construction on land systems is a key for better understanding of dam-induced land system changes.

Empirical evidence concerning the impact of dams on land systems is currently limited to case study findings. Synthesizing case study evidence on the causes and effects of dam-induced land system change allows to attain a better understanding of the frequencies and characteristics of such interactions (van Vliet et al., 2015b; Magliocca et al., 2018). In this context, meta-studies integrating quantitative and qualitative observations of land system change can help to advance theory building, identify knowledge gaps for future scientific inquiry, and inform policy (Magliocca et al., 2015; van Vliet et al., 2015b). As dam construction is part of the option space to meet the increasing demands for hydropower and irrigation water (You et al., 2011; Zarfl et al., 2015), integrating and combining evidence of dam-induced land system change will help to advance empirical insights and provide stimuli for future research.

Dam-induced land system changes are characterized by complex causal chains, which involve a variety of land system components, actors, and processes. This complexity requires disentangling the causal chains of dam-induced land system change. Decomposing causal chains into single unidirectional links, defined as causal effects (Meyfroidt, 2016), allows for synthesizing findings across heterogeneous study sites and methodologies and thus facilitates a systemic understanding of the observed phenomena.

Isolating the causal effects of dams on land systems from other drivers or determinants of land system change, such as changing market forces or climate change, is challenging. Counterfactual study designs allow for setting up quasi-natural experiments, which render them valuable for common research questions in land system science (Meyfroidt, 2016; Butsic et al., 2017). Given the abundance of suitable datasets to support such applications, counterfactuals are cost-efficient and readily applicable tools for isolating the effects of dams on land systems (Braatne et al., 2008). Investigating the types of counterfactuals used in the existing literature can help to reveal suitable study designs and common analytical gaps to assess the effects of dams across diverse disciplinary perspectives, data types and coverages, study site contexts, and geographic scales.

This study aims at providing a descriptive overview of the current state of research concerning dam-induced land system change. We synthesized the literature of land system changes associated with the construction and operation of dams, the spatial distribution of such changes, as well as the datasets and counterfactual methodologies employed to isolate dam-induced effects. Our main research questions are:

- Which types of dam-induced land system change were commonly reported in the scientific literature?
- What are the most common processes and directionalities of dam-induced land

system changes?

- Which types of data and counterfactual methodologies were used for attributing land system change to dam construction or operation?

2.2 Materials and methods

2.2.1 Case selection

We gathered all available peer-reviewed studies, which focused on land system change associated with the construction or operation of dams. We searched research articles published in English since 1950 and listed in the ISI Web of Science (last accessed on Feb 1, 2018). We restricted our analysis to publications whose titles contain the keywords "dam*" or "reservoir*" and at least one of the following: "land*", "chang*", "ecosystem*", "settle*", "agricult*", "irrigat*", "crop*", "flood*", "pasture*", "grassland*", "urban*", "wetland*", whereas the asterisk acts as placeholder for additional characters.

The search resulted in 3,193 publications, which formed the literature corpus used for subsequent refinements. Based on the abstracts, we categorized the literature regarding its thematic scope, thereby excluding unrelated articles, which focused, e.g., on dam engineering (n = 485), modeling of dam failure (n = 238), effects of climate change and land use on water quality and quantity in man-made reservoirs (n = 194), oil and gas extraction (n = 150), geology and quaternary sciences (n = 124), and other unrelated fields. We focused on observed interactions of dam construction and operation and land systems and therefore also excluded studies that modeled the potential impacts of planned infrastructures, and studies that simulated test floods or the effects of dam removal or collapse. Our final literature corpus consisted of 54 case studies (all references are listed in Table S2.1).

2.2.2 Study site characteristics

We compared dam attributes, as well as socio-economic and biophysical context of the 54 case studies against a global sample (n = 8,444) of dams (FAO, 2015). We used Mann–Whitney U tests to assess differences in the statistical distribution of eleven attributes, namely latitude, longitude, elevation, mean annual temperature, total annual precipitation, commissioning year of the dam, reservoir storage capacity, travel time to major cities as a proxy for remoteness, population density, amount of irrigation water applied in 0.5° grid cell, and conveyance losses (Table S2.3). We further compared the shares of the four most frequent purposes of the dams (irrigation, hydropower, flood control, water supply) across the selected observations

and all dams registered in a non-spatial global database of large dams (ICOLD, 2017).

2.2.3 Synthesis of case study evidence

We extracted direct and indirect interactions between dam construction or operation and the land system (from here on called observations) from the 54 case studies. Each observation represents one link of a causal chain that relates dam construction or operation (cause) with a change in one or multiple land system components further down the causal chain (effect). Each observation thus consists of a cause, a directionality (increase, decrease, or general alteration), and a resulting effect in the land system or a related system component (e.g., agricultural land extent, population displacement, or changing water seasonality). To avoid replications, observations must be unique combinations of a study area, a cause, directionality, and an effect (van Vliet et al., 2015b). In the case of multiple dams or study areas being subject to one analysis, or one study site being studied multiple times, similar findings were counted once, whereas new findings were accounted for separately.

All extracted observations were thematically coded. We classified causes and effects into nine broad land system categories, including seven land use and land cover types (agriculture, bare land, grassland, forests and woody vegetation, wetlands, water, built-up) as well as land use intensity and land demand. While effects on the land use and land cover types exclusively relate to changing extents, effects on land use intensity include alterations of management strategies such as irrigation or fertilization, the cultivation of new crop types or varieties, increasing productivity in terms of multi-cropping, or yield improvements. Dam-induced effects on land demand include increasing land prices, increasing competition over land resources, and changes in land ownership. All aspects not directly affecting the land system categories per se were thematically aggregated into the categories of environmental change and societal change. Environmental changes include alterations in hydrological regimes, sediment load, river morphology, floral and faunal habitat, or local climate. Societal changes comprise population displacement, conflicts, changing livelihoods, alterations in water resource management, or changes in policy (see Table S2.2 for further examples).

We visualized all observations using chord diagrams, which allow for illustrating the overall system, while highlighting the most frequent interactions between individual system components. Note that feedbacks (i.e., when cause and effect were present within the same category) can be artifacts of the thematic aggregation, e.g., when population displacement (societal change category) caused shifts in livelihood strategies (also societal change category).

2.2.4 Spatial scales, data sources, and counterfactuals

For each article, we recorded the scale of analysis. Local scale analyses cover study sites of limited spatial extent, such as single villages. Regional scale analyses are characterized either by observations across multiple isolated study sites or wall-to-wall coverage of larger regions. National scale accounts for analyses of a whole country, larger cross-boundary areas, and continental scale covers several countries or entire continents. Further, we recorded the study location and stratified the observations by UN world regions.

We documented the start and end of the study period. In cases where multiple datasets were used, we recorded the earliest observation as the start and the latest as the end. We further recorded the types of data used. These include interviews and qualitative data, quantitative field data, including measurements or surveys, geospatial data, remote sensing data, and combinations thereof.

We classified the employed counterfactual study design of the case studies into temporal counterfactual (pre- vs. post-dam or sequences of revisits in the post-commissioning phase), spatial counterfactual (upstream vs. downstream; progressive downstream; dammed vs. freeflowing), spatio-temporal counterfactual (spatial and temporal combined), or no counterfactual (Braatne et al., 2008). Manipulative strategies (modifications of river flow, test floods, or dam removal) or biophysical modeling also qualify as potential counterfactuals. However, the first did not occur in the screened literature and the latter was excluded in our case selection.

2.3 Results

2.3.1 Study site characteristics

We compared dam attributes, as well as socio-economic and biophysical characteristics of the 54 case study locations to a global sample of dams. The examined case studies did not differ significantly from the global sample in case of most attributes ($p < 0.001$), except for latitude, mean annual temperature, commissioning year, and storage capacity (Table S2.3). Relative to the global sample, the dams listed in our selected cases were located in lower latitudes, and warmer regions, were commissioned later, and had larger storage capacities. Unsurprisingly, the full variability of the global sample was rarely covered by the dams contained in our case studies (Figure 2.1). For instance, our sample failed to include dams located in remote locations, in high elevations, or in areas of high population densities. Furthermore, our case study sample contained a larger share of dams with irrigation function and a lower share of hydropower and flood control dams as compared to the global sample (Table 2.1).

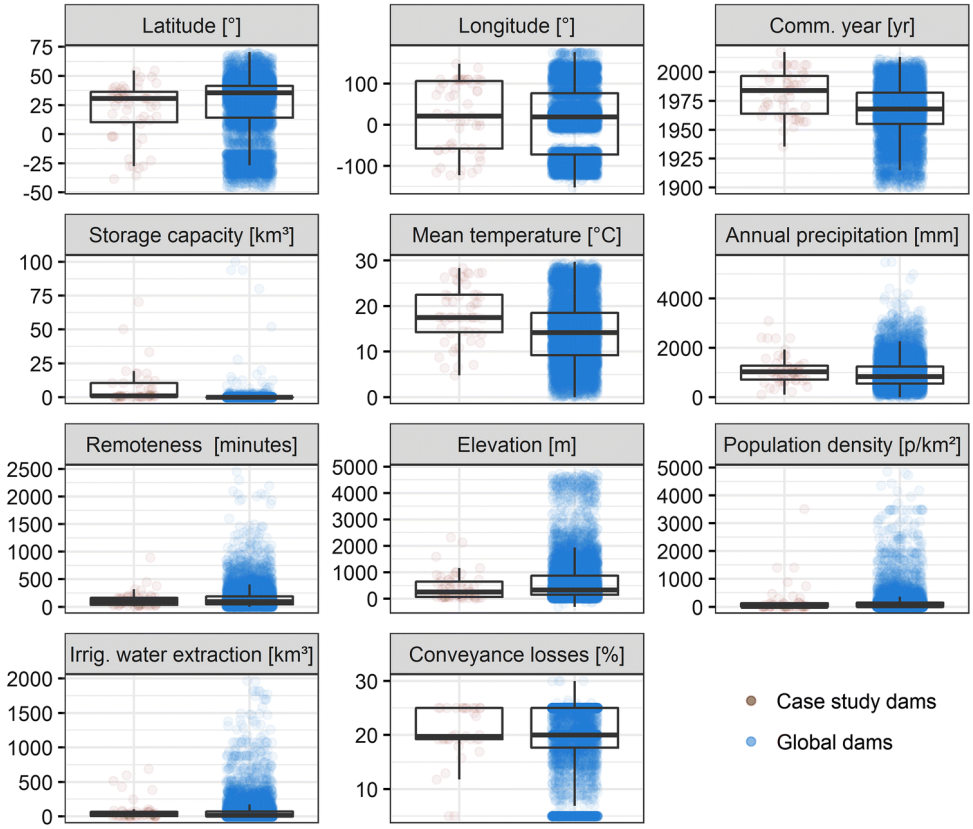

Figure 2.1: Comparison of selected dam attributes, socio-economic and biophysical characteristics of the case studies (red points) against a global sample of dams (blue points).

Table 2.1: Shares of dominant purposes for the dams selected from the case studies compared to the global sample of dams.

Purpose (single or multiple)	Selected cases (%)	Global sample (%)
Irrigation	55.2	34.7
Hydropower	27.1	16.5
Water supply	31.2	12.9
Flood control	2.2	12.4
Multi-purpose	15.9	16.7

2.3.2 Systematic view of dam-induced land system changes

We extracted a total of 332 observations from the 54 case studies. Of these, 178 observations affect the land system categories, whereas the remaining 154 relate to changes in non-land categories. Of the 178 observed land system changes, 29% were caused by reservoir flooding and affected five of the nine land system categories (Figure 2.2a), most frequently forests and natural vegetation, agricultural land, built-up area, and grasslands. Another 29% of the observations directly resulted from dam construction or operation (Figure 2.2b), such as changes in water surfaces, agri-

cultural land, forests, built-up land, or wetlands. The notion of "direct" describes the logic in which causal effects were formulated in the case studies, and does not necessarily reflect the actual causal pathway. For instance, dam-induced increases in built-up or agricultural land are in most cases a consequence of resettlement schemes, and hence not directly caused by dam operation.

Indirect effects on land systems accounted for 42% of the observations and can be further categorized according to their cause being a dam-induced environmental (12%) or societal change (12%; Figure 2.2c), or a change in one of the land system categories (18%; Figure 2.2d). Specifically, dam-induced changes in the environment most frequently led to alterations in forests, land use intensity, and agricultural land. Dam-induced societal change mainly affected land use intensity, built-up areas, and agricultural land extent. Dam-induced land system changes caused secondary effects in the land system, such as dam-induced changes in agricultural land extent which affected land use intensity. Land use intensity changes triggered additional repercussions, for instance if the introduction of irrigation allowed for the cultivation of more productive crop varieties. Altogether, we registered 24 unique types of indirect effects caused by previous dam-induced alterations in land systems.

Besides land system changes, the literature provided evidence of 154 causal effects in the non-land categories, 52% of which related to environmental and 44% to societal impacts, as well as 4%, in which dam operation itself was affected (Figure 2.2c). Dams caused most of these social and environmental effects, which in turn led to secondary effects in the other categories, including effects of environmental changes on societies (10%), and societal changes affecting the environment (3%). Additionally, initial changes triggered repercussions in the same category, for instance where resettlement schemes lead to changes in income structure. These repercussions occurred similarly frequent in the environmental (10%) and societal change (7%) category.

2.3.3 Directionality of land system changes

Land system changes operate in different directions, which unfold in increasing or decreasing extents of land use and land cover types, but also increases or decreases in land use intensity, or land demand. We accounted for the differences in directionality by stratifying the 178 effects on individual land system categories by their direction (Figure 2.3). Changes with unspecified or unclear directionalities (n = 17) were omitted from these analyses.

The most frequently reported land use and land cover changes were losses of forests and riparian vegetation (15%), almost exclusively due to flooding (10%), conversion to agriculture or built-up areas (3%), and hydrological changes (1%). In contrast, downstream alterations of the hydrological regimes led to woody vegetation

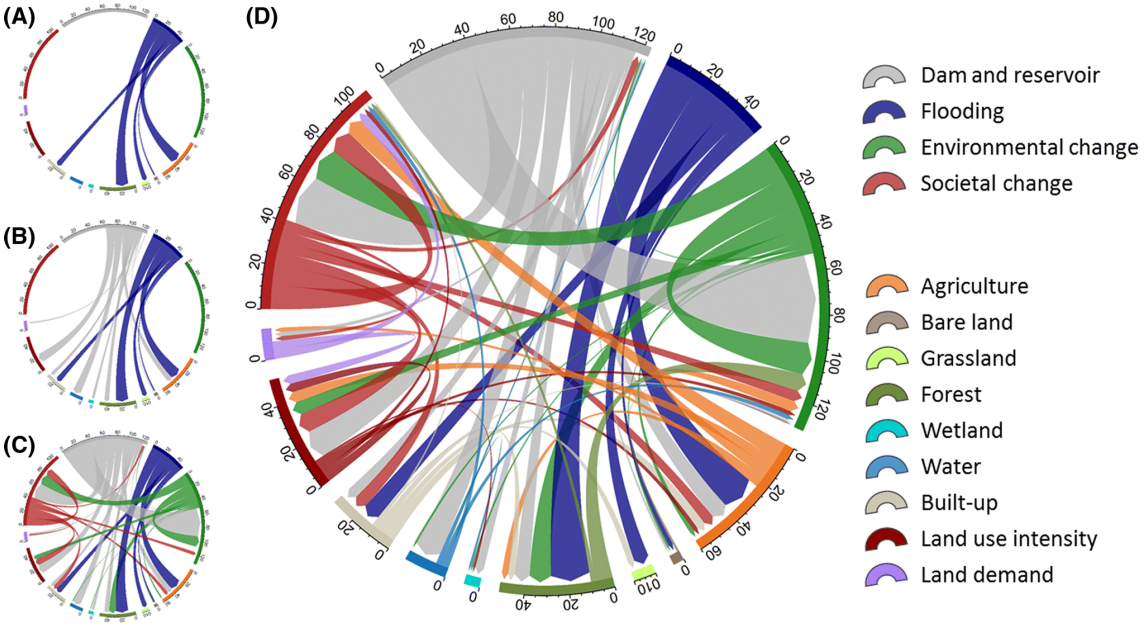

Figure 2.2: Chord diagrams visualizing *a)* the effects of reservoir flooding on land systems, *b)* dam-induced changes in the land system, *c)* dam-induced changes in society or environment which further affect the land system, and *d)* all effects between dams, society, environment, and land systems. Width of the connections represents frequency and arrow heads indicate the direction of the observed causal effects.

succession (7%). Losses of agricultural land (11%) occurred due to flooding (9%) and conversion to built-up land (2%). Increases of agricultural land (8%) occurred due to the displacement of submerged agricultural land and agricultural expansion in previously uncultivated areas.

Management-related increases in land use intensity were observed (11%), but also decreasing land use intensity (6%) was reported. Losses of built-up area, including settlements and transportation infrastructure, were found (5%), alongside expansion of housing areas due to resettlement schemes (7%). Moreover, dam construction has led to grassland loss (6%), specifically due to reservoir flooding (4%) and land conversions (2%), and to decreasing wetland areas (4%). Changes in land demand were rarely assessed in our case study sample but in the few reported cases overall increasing demand dominated (2%) over decreases (1%).

A stratification by reservoir purpose (Figure 2.4) revealed that hydropower and multi-purpose dams often negatively affected the extent of forests and agricultural land, while the majority of studies investigating irrigation dams reported increasing land use intensity. Differences across groups of commissioning year were less pronounced (Figure S2.3), while stratification of storage capacity revealed a tendency for agricultural land loss and increasing land demand for reservoirs with storage capacities above 1000 Mm^3 (Figure S2.4). Land use and land cover changes occurred similarly over time after dam commissioning (Supplementary Material, Figure S2.5).

Contrastingly, land use intensity and land demand increased frequently within initial years after dam commissioning, while decreases dominated from 30 years or more after dam commissioning.

2.3.4 Processes of dam-induced agricultural change

Our synthesis revealed frequent interactions between dams and agricultural land extent and land use intensity. Dam-induced agricultural changes were characterized by differing directionalities and are highly interlinked with societal and environmental changes caused by dam operation, e.g., resettlement schemes or changing flood regimes. Disentangling the nature of these changes allowed us to identify recurring processes in the context of dam-induced agricultural change, which we classified into six process categories.

- *Agricultural land loss* (n = 20) was primarily related to submergence during reservoir flooding, affecting both rainfed (Zhao et al., 2013; Keken et al., 2015) and irrigated croplands (Shao et al., 2005; Delang et al., 2013). Moreover, resettlement caused the loss of agricultural lands due to conversions from agricultural to built-up land (Cao et al., 2011; Jafari and Hasheminasab, 2017).

- In this context, *agricultural abandonment* (n = 2) occurred on cultivated floodplains following dam-induced alterations of hydrological regimes, which lead to reduced flooding and thus reduced suitability for cultivation (Thomas and Adams, 1999) or as a consequence of resettlement schemes and subsequent population displacement following dam construction (Main, 1990).

- *Agricultural expansion* (n = 14) was often reported in vicinity of newly constructed settlements, partly on less suitable lands, such as hillslopes (Shao et al., 2005; Wiejaczka et al., 2017). Additionally, agricultural land expanded in natural ecosystems or marginal lands (Thomas and Adams, 1999; Loker, 2003; Gordon and Meentemeyer, 2006).

- *Land use displacement* (n = 6) occurred in cases when agricultural land loss was compensated for through agricultural expansion elsewhere. For example, the loss of agricultural land due to submergence was offset by expanding agricultural land around newly constructed settlements (Loker, 2003; Yang et al., 2014). Partly, land use displacement occurred over long time frames, e.g., where the adoption of alternative management strategies resulted in the displacement of rainfed and irrigated croplands decades after the initial submergence of agricultural land (Thomas and Adams, 1999).

- *Land use intensification* (n = 20) related to alterations of agricultural management were typically induced by the construction or improvement of irrigation systems (Ashraf et al., 2007; Strobl and Strobl, 2011) and subsequent adoption of more productive crop varieties (Main, 1990; Thomas and Adams, 1999), increasing cropping frequency (Loker, 2003; Ashraf et al., 2007; de Fraiture et al., 2014), or higher livestock densities (Khlifi et al., 2010).
- *Land use dis-intensification* (n = 10) led to decreasing agricultural productivity, e.g., caused by reduced river flow (Blanc and Strobl, 2014; Jafari and Hasheminasab, 2017) or low agricultural suitability of the newly cultivated arable lands (Loker, 2003; Shao et al., 2005).

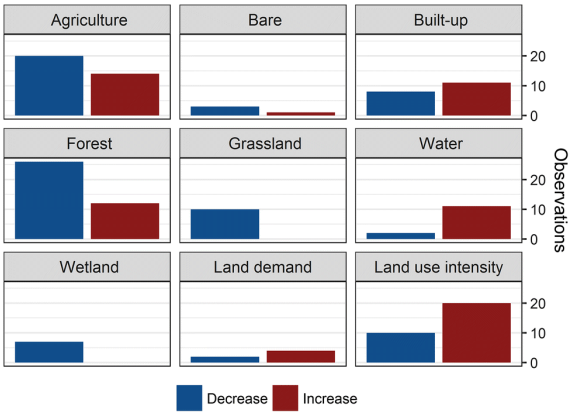

Figure 2.3: Counts of decreases (blue), and increases (red) of specific land system components.

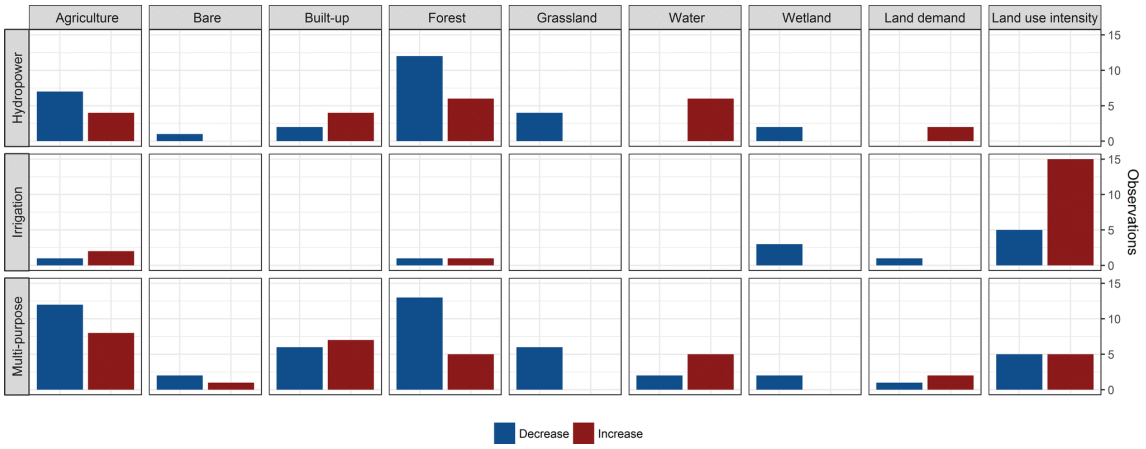

Figure 2.4: Counts of decreases (blue), and increases (red) of specific land system components, stratified by hydropower, irrigation, and multipurpose functions.

Stratification by world regions

We identified Asia as a hotspot of research on dams and land change (Table 2.2). Fourteen of the 54 studies examined dams in China, of which ten were dedicated to the Three Gorges Dam, the world's largest hydropower dam by installed capacity.

A stratification of all observations by world region revealed regional patterns of study foci (Figure 2.5). The role of environmental changes was pronounced in study sites in North America, whereas studies on the African continent widely focused on societal changes and their interactions with agricultural land extent and land use intensity. Changing land demands were studied solely in Latin America and Africa. Changes in built-up area were in the spotlight in Europe and Asia.

Regions with few studies of dam-induced land system change, such as Europe and North America, showed a smaller number of unique causal effects and thus affected fewer land system categories. This trend suggests that an increasing amount of research can help to unveil the complexity of dam-induced land system changes.

Table 2.2: Number of studies, causal effects, and effects on land systems per world region.

World Region	Studies	Causal effects	Effects on land systems
Africa	7	58	42
Asia	23	169	81
Australia	1	0	0
Europe	4	25	15
Latin America	11	59	32
North America	8	21	8

Data types, methods, and counterfactuals

Changes in the environment, society, and land systems were observed using diverse data types, study periods, and scales of analyses. Data were most frequently sourced using a combination of methods (n = 29), but some studies relied solely on remote sensing (n = 12), field measurements (n = 6), qualitative data (n = 4), or statistical and geospatial data (n = 3; Figure 2.6). Study periods ranged from single points in time up to 113 years with an average of 27 years. The scales of analyses ranged from local (n = 12), to regional (n = 39), national (n = 1) and continental (n = 2).

Concerning counterfactual types, 25 studies used temporal comparisons, of which 20 compared phases of pre and post dam-commissioning and two observed multiple periods in the post-commissioning phase (Figure 2.6). Only two studies pursued spatial comparisons, by comparing sites with different levels of hydrological alteration and with increasing distance to the impoundment. Combined spatial and temporal counterfactuals were used in 19 studies, dominated by comparisons of dammed and

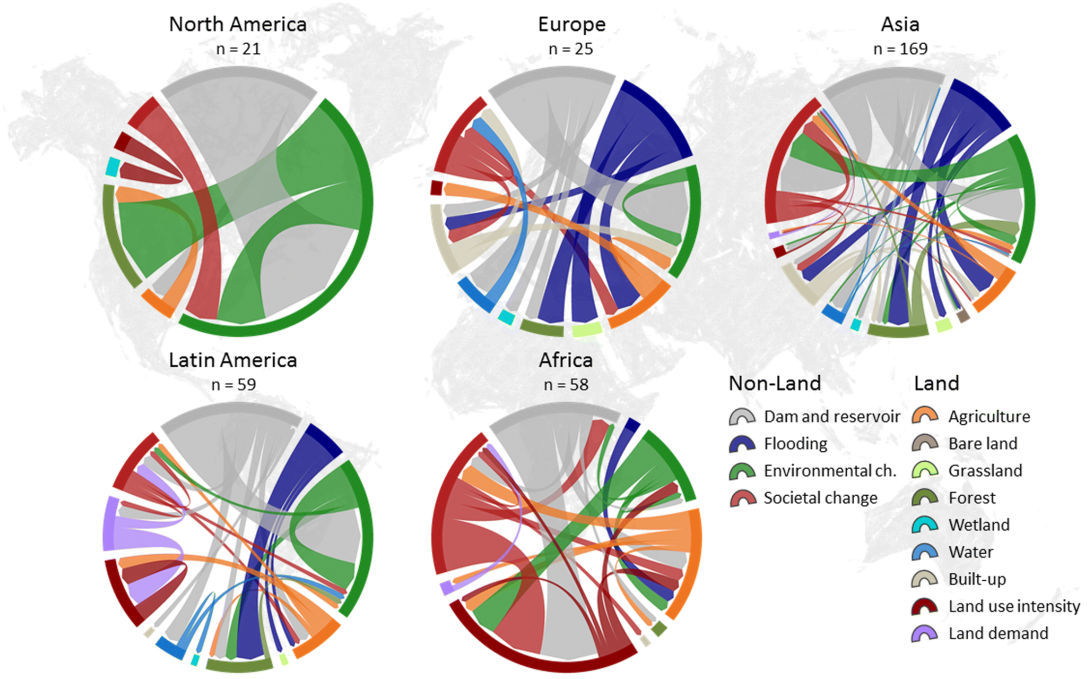

Figure 2.5: Chord diagrams of causal effects stratified by world region.

undammed sites before and after commissioning. A total of eight studies did not use any counterfactual. Accordingly, most of the observed land system changes were found through regional scale analyses using temporal counterfactuals or combined spatial and temporal counterfactuals (also see Figure S2.1 and S2.2).

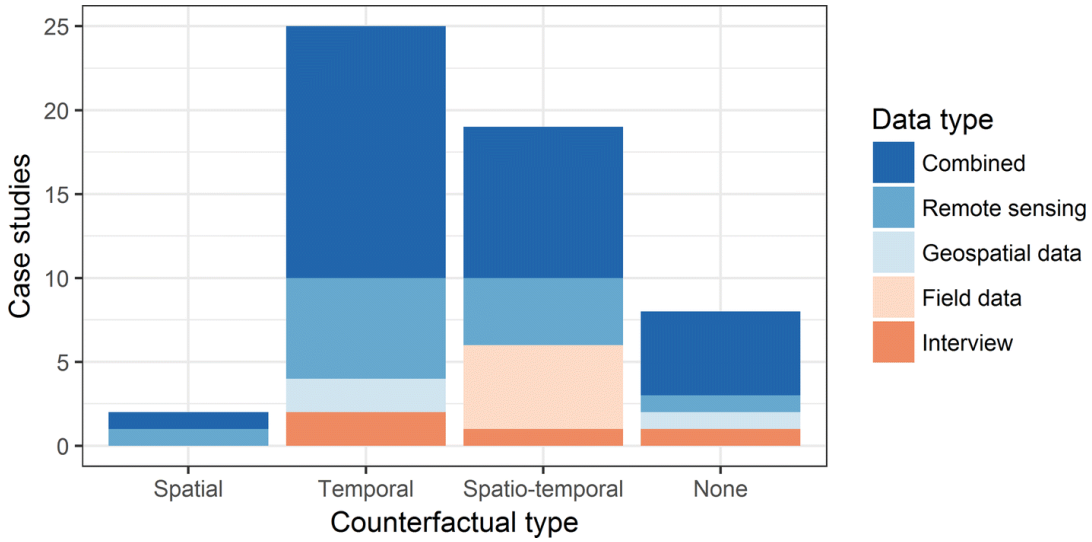

Figure 2.6: Number of case studies across data and counterfactual types.

2.4 Discussion

We synthesized the peer-reviewed literature focusing on dam-induced land system changes. Our study design allowed for incorporating quantitative and qualitative findings, which permitted systematic insights into the types, directions, and frequencies of specific change processes. The case studies included in our analysis suggest that dam construction and operation substantially affected the extent and intensity of agricultural land use as well as the extent of natural vegetation. Indirect effects shape a diverse array of land system change processes with societal and environmental consequences and thus play a significant role in the context of dam-induced land system change. The analysis allowed us to identify a set of commonalities and methodological limitations that help to guide future research activity concerning dam-induced land system changes.

2.4.1 Systemic complexity calls for additional research

Despite the global abundance of dams, scientific literature on dam-induced land system change is sparse. The majority of the cases we considered examined dams in Asia but the mere 24 studies that matched our criteria dwarf compared with the 33,000 large dams that are currently operational in Asia (ICOLD, 2017). The low number of studies may in part be due to the fact that we constrained our analyses to studies published in English, listed in the ISI Web of Science, and to those with an explicit focus on land. We thereby omitted other dam-induced changes with relevance for the land system, as for instance shifting evapotranspiration rates (Jaramillo and Destouni, 2015), changes in rural poverty (Duflo and Pande, 2007), or food production (Orr et al., 2012). The low number of studies contained in our meta-study also reflects that research about the interactions of dams and land systems has only recently gained traction, particularly with the advent of dam critics following the release of the Report of the World Commission on Dams in the late 1990s. This was reflected by the lack of studies published before 1990.

Globally, the frequency of direct effects was outweighed by indirect effects, which relate dams and land system components through multiple processes, partly with strong environmental and societal implications. World-region stratification demonstrated that the amount of research activity and the associated diversity of disciplinary perspectives, study sites, methodologies, and time frames studied, co-determined the complexity of the observed system by raising the number of unique causal effects. Future research on dam-induced land system change is thus essential for improving our understanding of social and environmental costs and benefits of dams and reservoirs.

2.4.2 Potential controls for effect directionality

Dam-induced land system changes partly operated in contradicting directions. We repeatedly encountered two factors that potentially affected the direction of dam-induced effects on land systems.

First, we observed the time since dam commission as a controlling factor for some land system changes. Temporal variations in the strength and direction of land system changes partly led to the inversion of land change processes with increasing operational lifetime of the dam. For instance, forest cover losses were observed immediately after dam construction, while forest succession at later stages of the operational phase led to increasing forest cover (Wiejaczka et al., 2017). Similarly, dam construction had negative effects on agricultural production systems immediately after commissioning, whereas multi-decadal adaptation processes of the population resulted in improved agricultural productivity, even compared to pre-commissioning levels (Thomas and Adams, 1999). These temporal non-linearities highlight the need for continuous monitoring of the land systems in post-commissioning phases to study the sequences of effects and feedbacks in a systematic manner.

Secondly, the spatial configuration of the study region appeared as a controlling factor for effect directions. For instance, the magnitude of riparian vegetation changes was found to be negatively related to the distance to the impoundment (Gordon and Meentemeyer, 2006) or elevation above the reservoir water level (Kellogg and Zhou, 2014). While some studies reported cropland productivity increases downstream of dams, with no changes in the vicinity of the reservoirs (Strobl and Strobl, 2011), others challenge this finding (de Fraiture et al., 2014). Other studies suggested dam-induced land use changes to occur mostly in upstream watersheds and predominantly within a distance of three kilometers to the dam (Zhao et al., 2013). Contrastingly, our findings reveal process-specific variations of distances, as for instance local changes in riparian vegetation communities (Azami et al., 2004) and tree mortality occurred hundreds of kilometers downstream of the impoundment (Assahira et al., 2017). Thus, variations of observed effects might occur in relation to the distance and the relative location to the dam (e.g., upstream or downstream). Unfortunately, a lack of detailed study site descriptions in relation to the investigated dam hampered an empirical analysis of these patterns. However, our insights into spatial and temporal controls are in line with earlier meta-synthesis efforts on the social impacts of dams (Kirchherr et al., 2016).

2.4.3 Methodical limitations and challenges

In line with other synthesis studies in land system science, the occurrence frequency of a studied process was seen as indicative of its existence and relevance in the

system (Geist and Lambin, 2001; van Vliet et al., 2015a). We can thereby learn which processes are well documented and identify knowledge gaps about processes that warrant further research. Due to the diversity of data types and sources, as well as strengths and caveats of the methods employed, the level of confidence associated with each observation varies. Specifically, the attribution of indirect effects over long time frames remains a challenge, as multiple external factors might co-determine the process of interest.

The observations included here represent causal effects in that a change in factor X causes a change in outcome Y, while evidence for causal mechanisms, which explain specifically how the cause produces an effect (see Meyfroidt, 2016, for terminology), was scarce. We thus suggested an array of agricultural change processes to provide a framework which allows for categorizing the processes underlying and following dam-induced agricultural changes.

Evaluating the robustness and suitability of the applied methodological toolkits is beyond the scope of this study. However, the majority of case studies included in this synthesis relied on counterfactual study designs. Typically, these included the use of time series to enable comparison of land systems before and after dam commissioning, mostly at the regional scale. While the dominance of regional analyses suggests that this spatial scale is appropriate for analyzing dam-induced land system change, it also points to a dearth of studies which examine dam-induced land system changes at smaller geographic scales.

The knowledge generated from synthesis efforts such as ours can fertilize theory development, yield policy recommendations, or serve for improving the calibration of process-based land change models (Magliocca et al., 2015). Compared to a global sample of dams, the dams included in our meta-study were relatively similar in terms of dam attributes and socio-economic and biophysical characteristics, but failed to capture the global variability of most attributes. Due to the relatively small number of studies, different methodologies, and scales of analysis included in the presented study, our findings are context-dependent and currently do not support the production of generalizable knowledge (Magliocca et al., 2018). We therefore call for reporting detailed descriptions of study site geographies (Margulies et al., 2016), as well as quantitative estimates of land system change in future studies, independent of the methods employed. This will foster the production of generalizable knowledge from case study synthesis. Further, current advances in statistical toolkits, such as counterfactuals, and increasing availability of geospatial data on dam locations (Lehner et al., 2011), forest loss (Hansen et al., 2013), or water surfaces (Pekel et al., 2016) bear potential for analyzing dam-induced land system change across larger populations of dams up to the global scale. This will grant novel opportunities for knowledge production using inductive approaches.

2.5 Conclusions

Dam-induced changes in agricultural systems, including changes in the extent of cultivated land and in land use intensity, are globally relevant phenomena that deserve further investigation on smaller geographic scales. We presented a descriptive representation of the current state of research about the effects of dam construction and operation on changes in land systems. To do so, we relied on observations from various scales, contextual settings, and disciplinary angles. Time-series analyses that trace land system changes in regular intervals on a regional scale have in the past shown potential to capture dam-induced land changes and the spatial and temporal variability therein. To enable and improve future synthesis efforts that quantitatively capture the processes in dam-induced land system change, we encourage researchers to report a detailed description of the study site location, period since dam commissioning, and, wherever possible, standardized quantities of change such as estimates of land cover change or changes in agricultural production.

Inferring the causal interactions between dams and land systems is methodically challenging and reliant on the abundance of suitable data and methodological toolkits. Considering the rapid growth of openly accessible data sets and the increasing connectedness between research disciplines, the emergence of innovative methods will hopefully guide novel research opportunities in the nexus of water, land, food, and energy, thus shedding new light on the effects of dams on land systems.

Acknowledgments

Philippe Rufin gratefully acknowledges funding from the Elsa Neumann Scholarship of the Federal State of Berlin, Germany. The presented research contributes to the Global Land Programme.

Supplementary materials

Table S2.1: Final literature corpus and dam characteristics.

Authors	Year	DOI or URL	Country	Scale	Dams	Purpose
Agnihotri, A.	2016	10.1007/978-3-319-19117-1_5	IND	Local	1	Irrigation
Aguiar, F. et al.	2016	10.1016/j.landurbplan.2016.04.009	PRT	Regional	3	Hydropower
Alcantara, F. et al.	2004	10.1016/j.soilbio.2004.04.018	BRA	Local	2	Hydropower
Ambers, R.	2001	10.1016/S0022-1694(01)00331-6	USA	Regional	1	Multi-purpose
Andersen, D. et al.	2007	10.1007/s00267-006-0294-7	USA	Regional	NA	Irrigation
Ashraf, M. et al.	2007	10.1016/j.agwat.2007.05.007	PAK	Regional	3	Irrigation
Assahira, C. et al.	2017	10.1016/j.foreco.2017.04.016	BRA	Local	1	Hydropower
Austin, N. et al.	2013	10.1080/01431161.2012.744528	CHN	Regional	1	Multi-purpose
Azami, K. et al.	2004	10.1002/rra.763	JPN	Regional	1	Hydropower
Bauni, V. et al.	2015	10.1016/j.rsase.2015.06.003	ARG	Regional	1	Hydropower
Begin, Y. et al.	2010	10.1007/978-90-481-8736-2_23	CAN	Local	1	Hydropower
Benchimol, M. and Peres, C.	2015	10.1016/j.biocon.2015.04.005	BRA	Local	1	Hydropower
Benchimol, M. and Peres, C.	2015	10.1371/journal.pone.0129818	BRA	Local	1	Hydropower
Blanc, E. and Strobl, E.	2014	10.1093/wber/lht026	ZAF	National	3371	Irrigation
Braatne, J. et al.	2008	10.1007/s00267-007-9048-4	USA	Regional	3	Hydropower
Burke, M. et al.	2009	10.1016/j.jenvman.2008.07.022	USA	Local	2	Multi-purpose
Canziani, G. et al.	2006	10.1007/s10113-006-0018-9	ARG	Regional	1	Hydropower
Cao, Y. et al.	2011	10.1007/s11629-011-2008-8	CHN	Regional	1	Multi-purpose
Cao, Y. et al.	2013	10.1007/s11629-013-2240-5	CHN	Regional	1	Multi-purpose
Casado, A. et al.	2016	10.1016/j.geomorph.2016.05.036	ARG	Local	1	Multi-purpose
Chen, G. et al.	2015	10.1016/j.apgeog.2015.06.001	BRA	Regional	1	Hydropower
Colonnello, G. and Medina, E.	1998	10.1023/A:1009785118019	VEN	Local	1	Multi-purpose
Cozar, A. et al.	2005	10.1016/j.scitotenv.2004.07.014	ARG	Local	1	Hydropower
de Fraiture, C.et al.	2014	10.1016/j.agwat.2013.07.001	BFA	Local	1	Irrigation
Delang, C. et al.	2013	10.1111/j.1475-4959.2012.00481.x	LAO	Regional	5	Hydropower
Feng, L. et al.	2016	10.1016/j.rse.2016.01.011	CHN	Regional	1	Multi-purpose
Gordon, E. and Meentemeyer, R.	2006	10.1016/j.geomorph.2006.06.001	USA	Regional	1	Hydropower
Guo, Z. et al.	2003	10.1023/A:1026042524839	CHN	Regional	1	Multi-purpose
Han, X. et al.	2018	10.1016/j.rse.2017.09.023	CHN	Regional	1	Multi-purpose
Huntley, B. et al.	1998	10.1046/j.1466-822X.1998.00302.x	GBR	Local	1	WS
Jafari, R. and Hasheminasab, S.	2017	10.1007/s10661-017-5792-y	IRN	Regional	1	Multi-purpose
Keken, Z. et al.	2015	10.1016/j.ecoleng.2014.11.002	Multiple	Regional	2	Hydropower
Kellogg, C. and Zhou, X.	2014	10.1016/j.jag.2014.03.021	CHN	Regional	1	Multi-purpose
Khlifi, S. et al.	2010	10.1016/j.agwat.2009.08.010	TUN	Regional	8	Irrigation
Kingsford, R. and Thomas, R.	2004	10.1007/s00267-004-0250-3	AUS	Regional	6	Hydropower
Le Stevens, A. et al.	2001	10.1890/1051-0761(2001)011[0701:PFACRR]2.0.CO;2	USA	Regional	1	Hydropower
Liang, C. et al.	2016	10.1016/j.ecoleng.2015.12.037	CHN	Regional	1	Hydropower
Loker, W.	2003	10.1086/379271	HND	Regional	1	Multi-purpose
Main, H.	1990	10.1111/j.1467-9493.1990.tb00020.x	NGA	Regional	2	Multi-purpose
Naik, D. et al.	2011	10.1007/s12524-011-0086-2	IND	Regional	1	Multi-purpose
Nasipuri, P. and Chatterjee, A.	2009	jstor.org/stable/24112078	IND	Regional	1	Multi-purpose
Rakhmatullaev, S. et al.	2013	10.1007/s12665-012-1802-0	UZB	Regional	16	Multi-purpose
Shao, J. et al.	2005	10.1007/s11769-005-0019-5	CHN	Regional	1	Hydropower
Strobl, E. and Strobl, O.	2011	10.1016/j.jdeveco.2010.08.005	Multiple	Continental	972	Irrigation
Sueltenfuss, J. et al.	2013	10.1007/s13157-013-0437-6	USA	Regional	16	Irrigation
Talukdar, S. and Pal, S.	2017	10.1016/j.iswcr.2017.05.003	BGD	Regional	1	Irrigation
Thomas, D. and Adams, W.	1999	10.1016/S0305-750X(99)00041-8	NGA	Regional	1	Multi-purpose
Uddin, F. et al.	2014	10.3161/104.062.0407	Multiple	Continental	16	Irrigation
Wang, L. et al.	2016	10.1007/s12665-016-5758-3	CHN	Regional	1	Multi-purpose
Wen, Z. et al.	2017	10.1016/j.scitotenv.2016.09.049	CHN	Regional	1	Multi-purpose
Wiejaczka, L. et al.	2017	10.1515/quageo-2017-0010	POL	Regional	1	Hydropower
Yang, J. et al.	2014	10.1007/s11355-013-0217-8	CHN	Regional	1	Hydropower
Zhang, J. et al.	2009	10.1016/j.jag.2009.07.004	CHN	Regional	1	Multi-purpose
Zhao, Q. et al.	2013	10.1016/j.ecoleng.2012.12.050	CHN	Regional	1	Hydropower

Table S2.2: Classification of categories and contained components used for coding causal effects in the scientific literature.

Category	Component
Land system	Agriculture (e.g., agricultural expansion, contraction of cropland)
	Bare land (e.g., changes in extent of unvegetated land)
	Grassland (e.g., flooding of floodplain grassland)
	Forest and woody vegetation (e.g., changes in riparian vegetation, shrubs, trees and forests)
	Wetlands (e.g., declining wetland extent)
	Water (e.g., reduced extent of downstream lakes)
	Built-up (e.g., flooding or construction of new settlements or infrastructure)
	Land use intensity (e.g., agricultural management, productivity, irrigation)
	Land demand (e.g., land expropriation, increasing land prices, competition for land ownership)
Environment	Atmosphere and climate (e.g., local to regional climate, greenhouse gas emissions
	Biosphere (e.g., ecosystem integrity, habitat loss, biodiversity decline)
	Hydrosphere (e.g., changing water seasonality, reduced water quality)
	Pedosphere (e.g., soil erosion, reduced sediment loads, changing channel morphology)
Society	People and livelihoods (e.g., conflict, livelihood strategies, cultural goods, population displacement)
	Economy (e.g., shifts in relevant economic sectors, reduced household income)
	Policy (e.g., improved water resource management, novel development strategies)

Study site characteristics

We aimed at investigating the considered case study geographies relative to a global sample of dam locations by comparing the distributions of the case study sample (CSS) with a global dam sample (GDS). Geolocations of CSS were extracted from the literature and global databases of dams (Lehner et al., 2011; FAO, 2015; ICOLD, 2017). The GDS contained all entries in the FAO AQUASTAT database with information on geolocation (n = 8,444), which reduced the sample size as compared to the overall number of dams in the database (n = 13,918), or other non-spatial databases (n = 58,519).

For each dam location, we compiled 11 attributes comprising geographic location (Lehner et al., 2011; FAO, 2015; ICOLD, 2017), biophysical (Hijmans et al., 2005; Jarvis et al., 2008) and socio-economic attributes (CIESIN et al., 2011; Nelson, 2008), as well as technological attributes relating to the dam characteristics (Lehner

et al., 2011; FAO, 2015; ICOLD, 2017) and regional irrigation systems (Jägermeyr et al., 2015) (Table S2.3).

For visualization purposes, we excluded commissioning years before 1900, storage capacities larger than 100,000 million m^3, irrigation water applied above 2000km^3 and population densities above 10,000 people / km^2 from the GDS.

For the twelve studies involving multiple dams, we calculated mean values for each attribute across the dams considered in the respective study. It is to note, that we could not reproduce the exact geolocations of all dams for six studies (Kingsford and Thomas, 2004; Andersen et al., 2007; Strobl and Strobl, 2011; Rakhmatullaev et al., 2013; Sueltenfuss et al., 2013; Blanc and Strobl, 2014). In these cases, we included all dams listed in the AQUASTAT database that fall within the geographic boundaries of the study region (e.g., irrigation district, watershed, country, and continent).

We performed Mann-Whitney-U tests to compare the statistical distributions of the selected attributes, finding that distributions are not significantly different (p<0.001) for seven variables, while in four cases, the CSS showed differing characteristics from the GDS (latitude, mean annual temperature, commissioning year, storage capacity; see Table S2.3).

Table S2.3: Attributes and datasets used for comparison of case study sample and global dam sample, as well as p-value of Mann-Whitney-U test when comparing the distributions of CSS and GDS.

Characteristics	Data sources	p-value
Geographic latitude in decimal degrees	Lehner et al. (2011); FAO (2015); ICOLD (2017), individual studies	0.006516
Geographic longitude in decimal degrees	Lehner et al. (2011); FAO (2015); ICOLD (2017), individual studies	0.4927
Elevation in m above sea level	Jarvis et al. (2008)	0.01657
Mean annual temperature in °C	Hijmans et al. (2005)	< 2.2e-16
Total annual precipitation in mm	Hijmans et al. (2005)	0.02386
Commissioning year of the dam	Lehner et al. (2011); FAO (2015); ICOLD (2017), individual studies	3.613e-06
Reservoir storage capacity in km^3	Lehner et al. (2011); FAO (2015); ICOLD (2017), individual studies	< 2.2e-16
Annual irrigation water applied for the period 2002-2008 per 0.5° grid cell in km^3	Jägermeyr et al. (2015)	0.303
Water conveyance losses for 2002-2008 in % of irrigation water extracted	Jägermeyr et al. (2015)	0.5243
Population density in capita per km^2	CIESIN et al. (2011)	0.6736
Remoteness, expressed in travel time to major cities in minutes	Nelson (2008)	0.7144

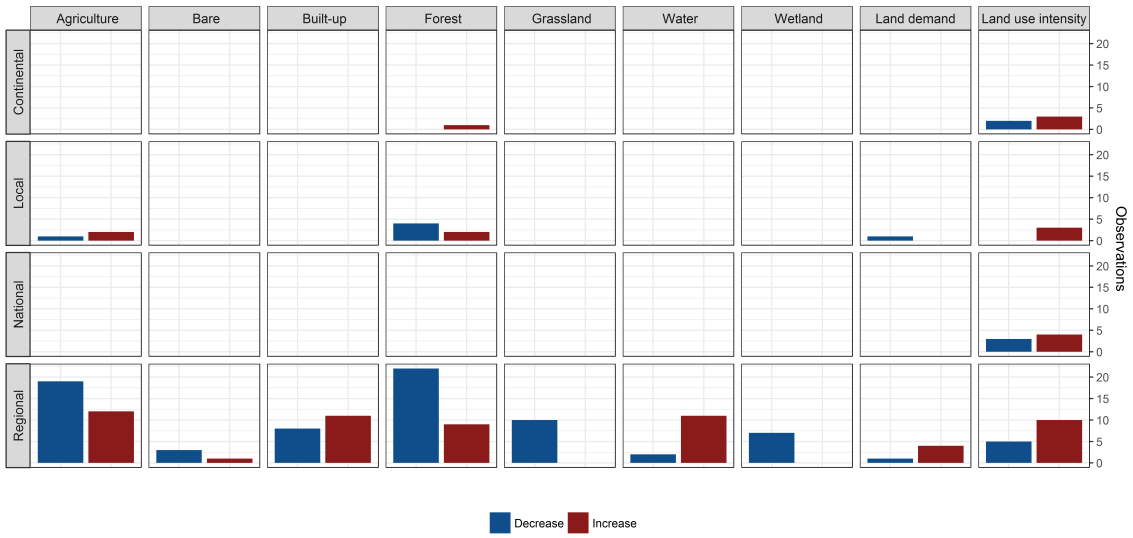

Figure S2.1: Count of observed land system changes, stratified by the scale of analysis in the respective study.

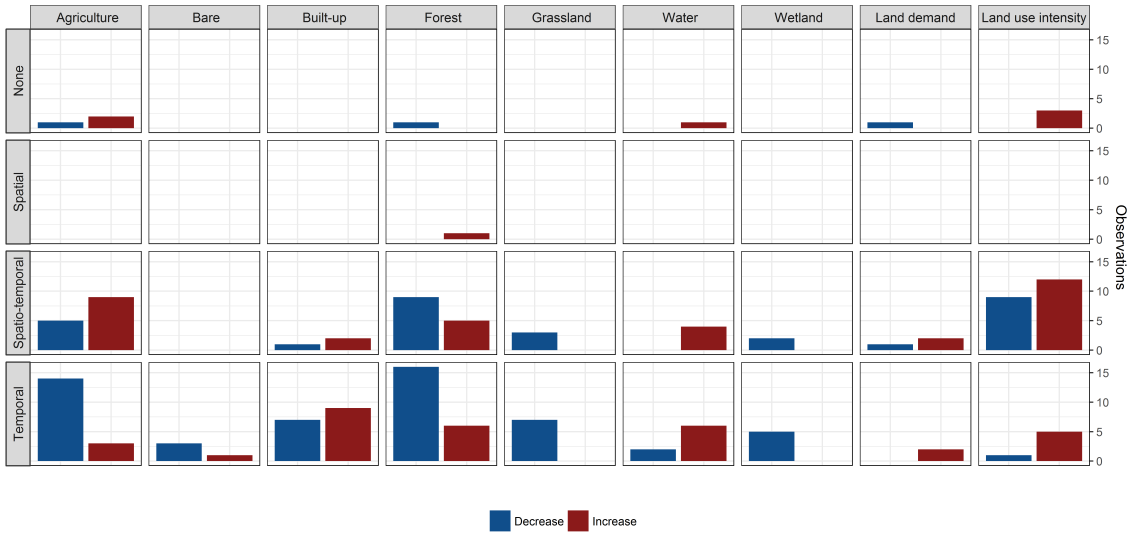

Figure S2.2: Count of observed land system changes, stratified by the counterfactual(s) used in the respective study.

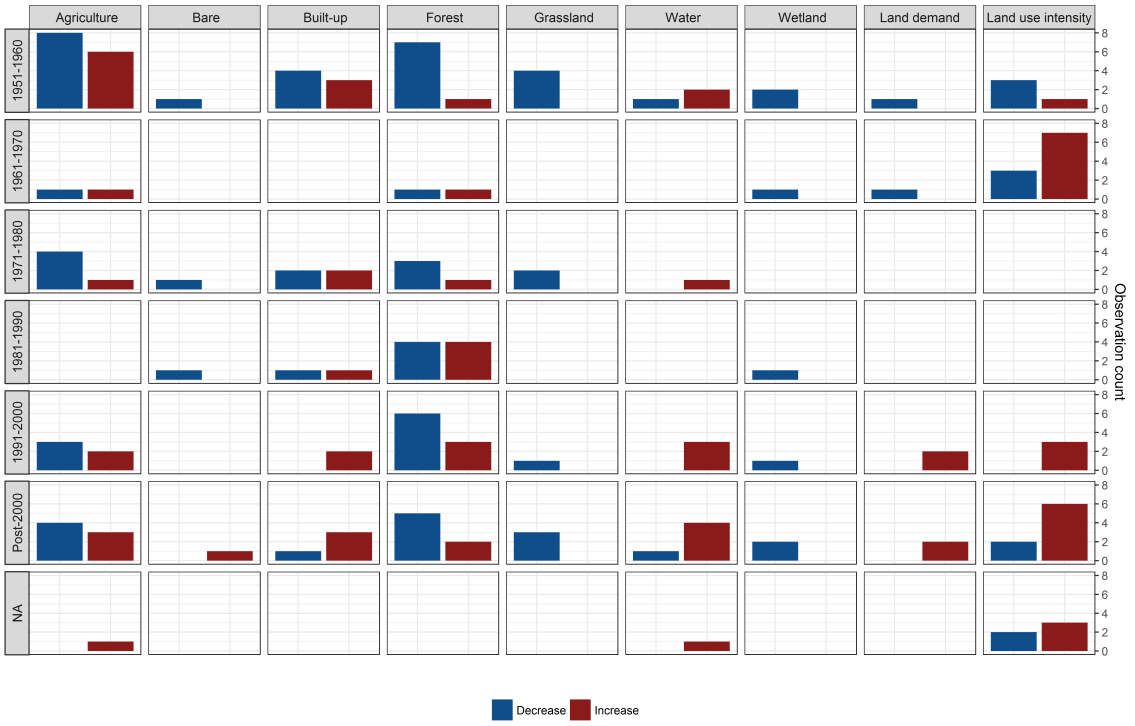

Figure S2.3: Count of observed land system changes, stratified by groups of (average) commissioning year of the investigated dam(s).

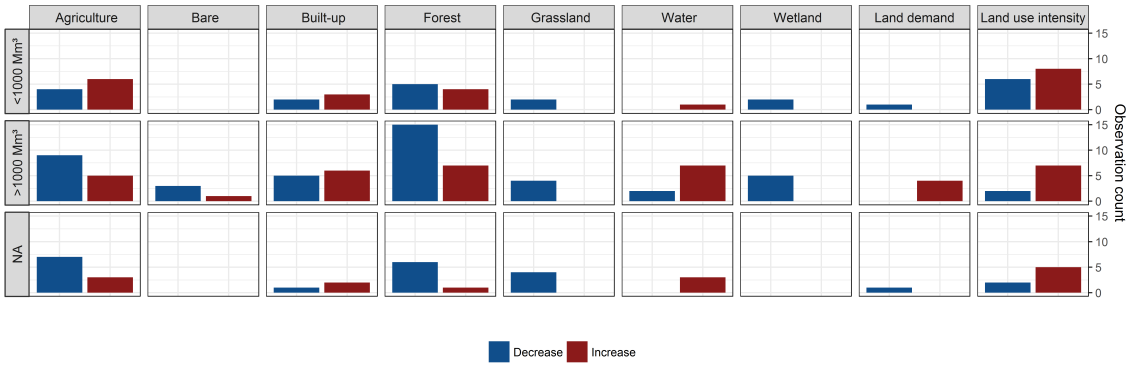

Figure S2.4: Count of observed land system changes, stratified by groups of (average) storage capacity of the investigated dam(s).

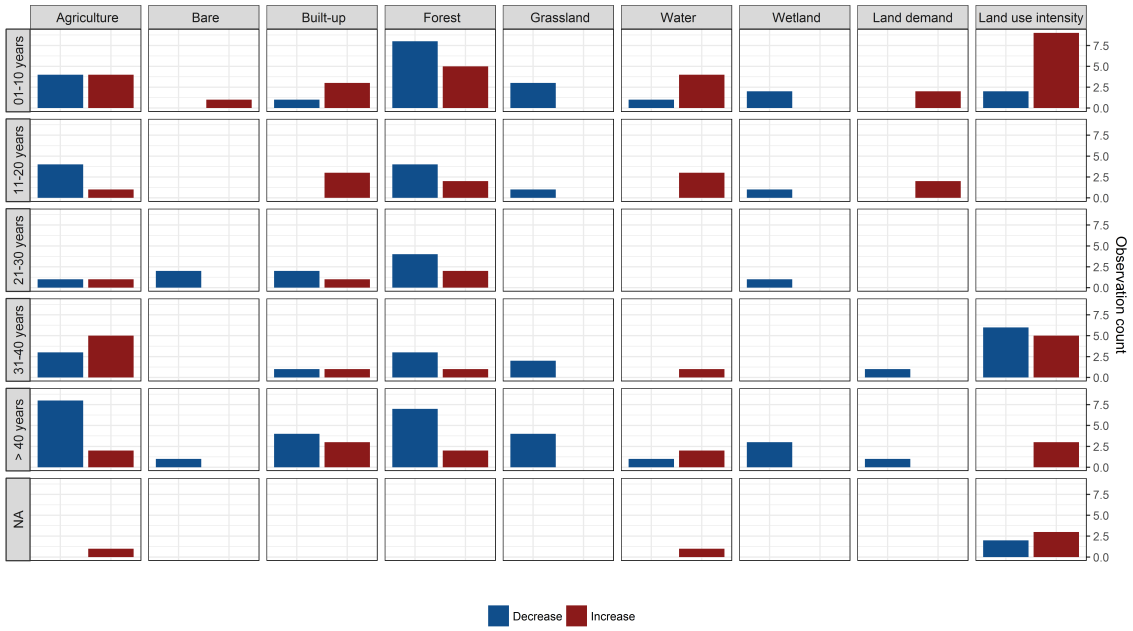

Figure S2.5: Count of observed land system changes, stratified by groups of time intervals inbetween (average) commissioning year (s) of the dam(s) and the latest observation year in the respective study.

Chapter 3

Global-scale patterns and determinants of cropping frequency in irrigation dam command areas

Philippe Rufin, Christian Levers, Matthias Baumann, Jonas Jägermeyr, Tobias Krüger, Tobias Kümmerle, and Patrick Hostert
Global Environmental Change, 2018

DOI: 10.1016/j.gloenvcha.2018.02.011
Submitted 2 June 2017; Revised 31 January 2018; Accepted 25 February 2018

Abstract

Growing human populations and shifting consumption patterns increase the pressure on agricultural production systems. Reservoir-based irrigation has generally boosted agricultural production through higher cropping frequencies, whereas the magnitude of this effect varies significantly across the globe. Technological, biophysical and socio-economic constraints often limit cropping frequency in the command areas of irrigation dams, yet the relationships with these factors remain poorly understood at the global scale. Here, we first determined the size and location of 1,288 command areas of irrigation dams commissioned since 1985. Within these areas, we studied cropping frequency during the period of 2001 to 2012 using a global time series of land cover information. We further investigated potential biophysical, socio-economic and technological constraints for intensive cropping using a Boosted Regression Trees modeling framework. Our results showed that the largest extent of reservoir-irrigated croplands are located in India (5.9 Mha), Indonesia (1.5 Mha), China (1.4 Mha), Vietnam (0.9 Mha), Turkey (0.7 Mha), Iran (0.7 Mha), and Thailand (0.6 Mha). Globally, cropping frequencies in irrigation dam command areas were on average 16% higher compared to rainfed control areas, yet pronounced differences in the strength and direction of this effect were apparent across world regions. Technological properties of dams and irrigation systems were amongst the most important variables for explaining global-scale variation in cropping frequency. Specifically, we observed low cropping frequencies in smaller command areas ($<$ 10,000 ha) and under long distance water allocation ($>$ 20 km). The command areas of small reservoirs (storage capacity $<$ 7.9 Mm^3) showed similar cropping frequencies compared to large reservoirs, yet with increased tolerance toward biophysical constraints. Our findings thus support arguments for de-centralized water storage facilities in order to reduce water losses and to improve access to irrigation water and infrastructure, thereby contributing to better meeting future agricultural production targets.

3.1 Introduction

Current population dynamics and shifts in diets increase the pressure on agricultural production systems (Foley et al., 2011). Globally limited availability of fertile land will further require intensification of existing agricultural land (Tilman et al., 2011; Lambin and Meyfroidt, 2011). Irrigation is a key component in this context, currently boosting productivity on 24% of the world's cultivated land (Portmann et al., 2010; Siebert and Döll, 2010). Man-made reservoirs are vital for agricultural production, as they provide 40% of the global surface water extracted for irrigation (Biemans et al., 2011). Thereby, irrigation reservoirs provide the water needed to overcome periodic scarcity and allow for the decoupling of agricultural production from intra- and inter-annual precipitation variability (Benhin, 2008; Hillel et al., 2008; Lipton et al., 2003). The improved access to water allows for stabilizing and intensifying agricultural production systems (Domènech, 2015; Mueller et al., 2012; Siebert and Döll, 2010) by minimizing undesired fallow periods and thus enabling more frequent cultivation (Gaur et al., 2008).

The benefits of irrigation reservoirs for agricultural production are frequently offset by technological, socio-economic and biophysical constraints of their location (hereafter collectively referred to as "operational reality"). On the technological side, extensive unlined canal schemes with high conveyance losses (Thakkar, 2000; World Bank, 2007; Rohwer et al., 2007), sediment accumulation in reservoirs (Alahiane et al., 2016; Hu et al., 2009), or increasing competition between multiple water uses in the water-energy-food nexus interfere with irrigation water supply (Bonsch et al., 2015; Lacombe et al., 2014; Scott et al., 2007). Further, benefits for agricultural production vary across differently sized water storage infrastructures (Blanc and Strobl, 2014; WCD, 2000). Regarding socio-economic factors, market accessibility and population density co-determine irrigation suitability and agricultural intensity (Neumann et al., 2011). Further, inefficient administration of water distribution, or weak governance structures hamper the use of irrigation infrastructure in readily equipped schemes (Yami, 2015; Singh, 2016; Klümper et al., 2017). Biophysical limitations include unsuitable topography (Koluvek et al., 1993) and climate (Neumann et al., 2011; Iizumi and Ramankutty, 2015), or declining soil productivity under excessive irrigation (Gómez-Limón and Picazo-Tadeo, 2012; Singh, 2016).

While these mostly local studies suggest that a reservoir's operational reality determines the intensity of agriculture in its command area, it remains unclear if case study insights are generalizable across larger geographic extents. A key reason for this knowledge gap is a scarcity of high-quality, spatial datasets on irrigation dam command areas. Several studies aimed at mapping irrigated lands globally (Salmon et al., 2015; Siebert et al., 2015), but the spatially explicit attribution of irrigated lands to dams has rarely been undertaken. First approaches associating

changes in agricultural production with dams were based on aggregated areal units, such as administrative districts (Duflo and Pande, 2007), or watershed boundaries (Strobl and Strobl, 2011). These approaches represent only indirect approximations of command areas, and may be improved by considering dam- and location-specific parameters (e.g., reservoir storage capacity or topography). Such a refined dataset is required for better understanding the spatial distribution and properties of irrigation dam command areas (Strobl and Strobl, 2011).

Agricultural intensification (i.e. increasing production output on agricultural land) is commonly achieved via increasing inputs, such as water, labor or fertilizer, or via an optimized land management that leads to a more efficient use of the same input resources (Erb et al., 2013). A common mechanism for increasing the output of cropland is to increase the frequency of cultivation, or cropping frequency, for instance via the introduction of multiple cropping cycles (Iizumi and Ramankutty, 2015) or by minimizing fallow years (Boserup, 1965; Estel et al., 2016). In the year 2000, 28% of the world's croplands were fallow (Siebert et al., 2010b), indicating a vast potential for agricultural intensification. Specifically in areas where access to water is critical for successful crop cultivation, insufficient irrigation water supply is causing undesired fallow periods (Gaur et al., 2008), which translate into lower cropping frequencies through a variety of processes (Evans and Sadler, 2008). At the command area level, altered irrigation water distribution to reduce the number of water users is a common measure for adapting to insufficient water availability (Bouman et al., 2007; Perry and Narayanamurthy, 1998). At the farm level, fallowing can be performed to spatially optimize irrigation distribution (i.e. temporarily or permanently retiring land from production to allocate the remaining water to a smaller area), or to preserve soil moisture for upcoming cultivation cycles (Evans and Sadler, 2008; Debaeke and Aboudrare, 2004; Kahil et al., 2015). Additionally, long-term irrigation mismanagement and lack of drainage systems can deteriorate soil productivity, ultimately leading to temporary or permanent land abandonment (Evans and Sadler, 2008; Qadir et al., 2014; Wood et al., 2000).

In the light of increasing demands for food, feed, fuel, and fiber, the further exploitation of reservoir-based irrigation is part of the option space for increasing the productivity of cropping systems (Manikowski and Strapasson, 2016; van Ittersum et al., 2016; You et al., 2011). Assessing the scope of these productivity increases requires investigating the cropping frequency in reservoir-based irrigation schemes and its spatial determinants on a global scale. Specifically, identifying technological limitations for agricultural production will help to better target infrastructure investment. Delays and failures to meet cropping intensity targets are prevalent for large dams and thus potentially relate to infrastructure size (WCD, 2000). Since the causes of such variations remain weakly understood, a comparative analysis of

cropping frequency determinants in command areas of large versus small reservoirs is needed to disentangle the underlying processes. Here, we first approximated the command areas of a global sample of irrigation dams and assessed cropping frequencies therein. We then investigated the effects of the technological, biophysical, and socio-economic properties of irrigation dam command areas on cropping frequency using Boosted Regression Trees. Specifically, we addressed the following research questions:

- What are the spatial patterns of irrigation dam command areas at the global scale and cropping frequencies therein?
- How do the technological, socio-economic and biophysical properties of command areas determine cropping frequency in command areas?
- Which command area properties are related to low cropping frequencies and how do these differ for smaller and larger reservoirs, respectively?

3.2 Material and methods

3.2.1 Command area allocation

We collected data on geolocations of single-purpose and multi-purpose irrigation dams from the GRanD and AQUASTAT databases (Lehner et al., 2011; FAO, 2015), while restricting our analyses to dams commissioned since 1985 (n = 1,626). We fused the two databases, since GRanD comprised highly detailed data on geolocation and dam attributes, while AQUASTAT included dams not represented in GRanD. As a large fraction of the AQUASTAT entries missed information on geolocation, we used available data on dam and river name, closest city, and administrative unit to locate these missing entries in Google Maps (n = 596). Existing coordinates were checked and corrected, if necessary (n = 412). After fusion with the GRanD database and duplicate removal, the database comprised a total of 1,370 irrigation dams in 71 countries worldwide (Figure 3.1).

A globally concise definition of command area size and location is challenging, since regional biophysical, technological, and socio-economic factors co-determine conveyance and irrigation efficiencies (Daccache et al., 2014; Jägermeyr et al., 2015; Rohwer et al., 2007), and thus the extent of land that can be irrigated given a quantity of water. To account for these differences, we calculated country-level ratios between total area of cropland irrigated with surface water [ha] and total reservoir storage capacity (Mm^3). We used the global map of irrigated areas (Siebert et al., 2013) to derive national surface-water irrigated land extent, and AQUASTAT statistics (FAO, 2015) to extract the national reservoir storage capacity in the year 2005

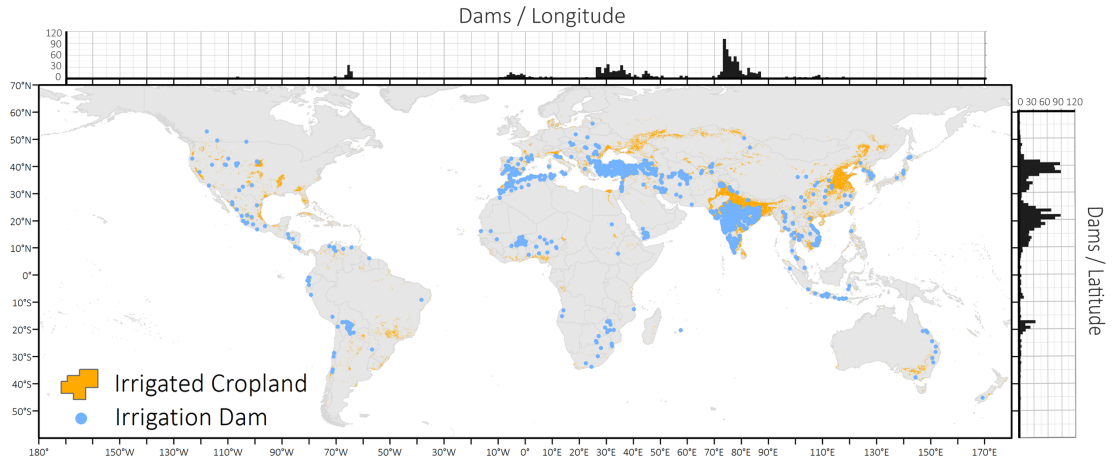

Figure 3.1: Spatial distribution of irrigation dams (blue, n=1,370) and irrigated croplands (orange; Salmon et al., 2015). Histograms represent the number of dams by latitude and longitude.

or the most proximate year for which data was available. The resulting ratio represented the potential area that can be irrigated given a unit of water (ha/Mm^3) in a given country. Assuming that reservoir storage capacity is a primary determinant of command area size (Strobl and Strobl, 2011), we multiplied the storage capacity of each dam (Mm^3) with the country-specific ratio to estimate the command area size (ha) for each dam. Finally, we compared the resulting estimates with reported command area sizes (n = 266) gathered from independent national databases, reports, and the World Register of Dams (Table S3.1; see Figure 3.4 and Table S3.2 for results).

We spatially allocated the estimated command area extent for each dam, accounting for parameters representing: irrigated cropland abundance (P1), topography (P2), watershed structures (P3), reservoir size (P4), national borders (P5), and distance to the dam (P6) (Figure 3.2 a-f). To understand the sensitivity of the allocation, we tested 24 different allocation schemes with varying parameter settings (Table 3.1, Figure 3.2 g).

For our allocation routine, we only considered irrigated or paddy irrigated areas in the year 2005 (P1, Salmon et al., 2015). Assuming that gravity-based water allocation dominates across the globe (Biemans et al., 2011; Duflo and Pande, 2007; Haddeland et al., 2006; You et al., 2011), we restricted the allocation of water to areas topographically below the impoundment point (P2). We accounted for three different elevation thresholds, namely exclusively areas below the impoundment (0 m), areas of up to 10 m above the impoundment point (10 m) to account for uncertain-

ties in the elevation dataset (Jarvis et al., 2008), as well as areas of up to 50 m above the impoundment point (50 m) to test for the effect of pump-based water allocation schemes.

We used USGS HydroBASINS watershed boundaries (Lehner and Grill, 2013) to limit the allocation to areas in the watershed of the dam location and the downstream watershed (P3), as effects of irrigation reservoirs dominantly occur in these regions (Blanc and Strobl, 2014; Duflo and Pande, 2007; Strobl and Strobl, 2011). We altered the hydrographic watershed delineation according to the Pfafstetter System (Pfafstetter, 1989) which delineates drainage areas according to hierarchical levels. Level 1 represents a continental-scale watershed delineation, which is then divided into higher-level sub-watersheds. Increasing the Pfafstetter level thus reduces the maximum possible distance of command area allocation. We tested four different approaches to account for watershed boundaries during the allocation, namely allocation without any watershed restrictions (NONE), allocation within Pfafstetter level 5 (L5) and the finer level 6 (L6) watershed boundaries, as well as a dynamic scheme (DYN). The dynamic allocation scheme assumes that large irrigation dam projects can entail complex and costly water allocation schemes, which partly bridge local topographical barriers (e.g., through tunneled canals). Such allocation schemes are unlikely to be economically viable for smaller dam-related irrigation schemes. Accordingly, we varied the scale of watershed delineation of the command area allocation based on the respective reservoir's storage capacity (P4). This resulted in potentially greater allocation distances for large reservoirs. We assigned decreasing Pfafstetter levels for increasing reservoir capacities: $<$100 Mm^3 = level 7; 100 Mm^3-1,000 Mm^3 = level 6; $>$1,000 Mm^3 = level 5. We further tested the inclusion (YES) and exclusion (NO) of trans-boundary water allocation (P5), since earlier studies assumed domestic irrigation schemes to be prioritized in water allocation (Biemans et al., 2011; You et al., 2011).

The pixels for which all criteria (P1-P5) in a given configuration were met, were qualified as suitable land for command areas. Namely, these are irrigated areas (P1) of lower elevation relative to the dam (P2), which are located within the respective watershed boundaries (P3, P4) and national borders (P5). Since increasing distance of water allocation is commonly associated with high evaporative losses and seepage, it decreases the economic viability of irrigation water allocation (Singh, 2016; You et al., 2011). Assuming that stakeholders and planning authorities aim for minimized conveyance losses, we allocated the command area size estimate over the suitable pixels with the least Euclidean distance to the dam location (P6). In several cases, the estimated command area extent (derived by multiplying reservoir storage volume with the country-level efficiency factor) exceeded the suitable land identified by the allocation model. Consequently, we prioritized our spatial allocation model

and reduced the estimated extent of a given command area to fit the extent of suitable land identified by the allocation model (see "Command Area Reduction" in Table 3.1).

We identified non-irrigated control areas of similar size and site characteristics for the comparison of cropping frequency within and outside of dam command areas (Table 3.1). We therefore repeated the allocation procedure for areas under rainfed cultivation (Salmon et al., 2015), using the extent estimates and allocation criteria described above (P2-P6). An overview of the datasets used for the definition of command and control areas as well as the reference data is presented in Table S3.1.

While the highest share of estimated command area extent was generally allocated when no watershed restrictions were included (NONE, 95.9% - 97.9%), the resulting command areas were partly located in neighboring watersheds without connection to the respective dam and its canal scheme (Figure 3.2 g, blue areas). The dynamic watershed restriction (DYN) further prevented the command area allocation over implausibly long distances for small reservoirs, while enabling sufficiently distant allocations for large reservoirs. We therefore selected the conservative allocation scheme with dynamic watershed restriction (DYN), a 10 m elevation difference threshold (10 m) and without cross-country water allocation (NO) for further analyses (Figure 3.2 a-f). The selected allocation scheme successfully allocated command areas for 1,288 irrigation reservoirs, while 81 command areas associated mostly with small reservoirs could not be allocated (accounting for 0.03 Mha or 0.1% of the total command area). The total extent of the 1,288 command areas was reduced by 8.69 Mha (36.9% of the total command area) to match the available suitable command area. This reduction included high shares of mega-projects such as Sardar Sarovar (India) and Hoa Binh (Vietnam). The command area datasets used for further analyses as well as the overlay of all 24 allocation schemes are publicly available (Rufin et al., 2017).

3.2.2 Mapping cropping frequency

We used *cropping frequency* as a metric describing the cropping intensity in irrigation dam command areas. Here, we defined cropping frequency as the number of years in which arable land has been cultivated (Estel et al., 2016) between 2001 and 2012. Consequently, we focus on cropping frequencies smaller than or equal to 1 per year, whereas the difference between observed cropping frequencies and the maximum observable cropping frequency (12) translates into the number of fallow years. This definition allows for identifying areas where cropping intensity can be increased (independent of multi-cropping practices), which represent up to a third of global croplands on an annual basis (Siebert et al., 2010b).

We derived a global map of cropping frequency at 500 m spatial resolution from

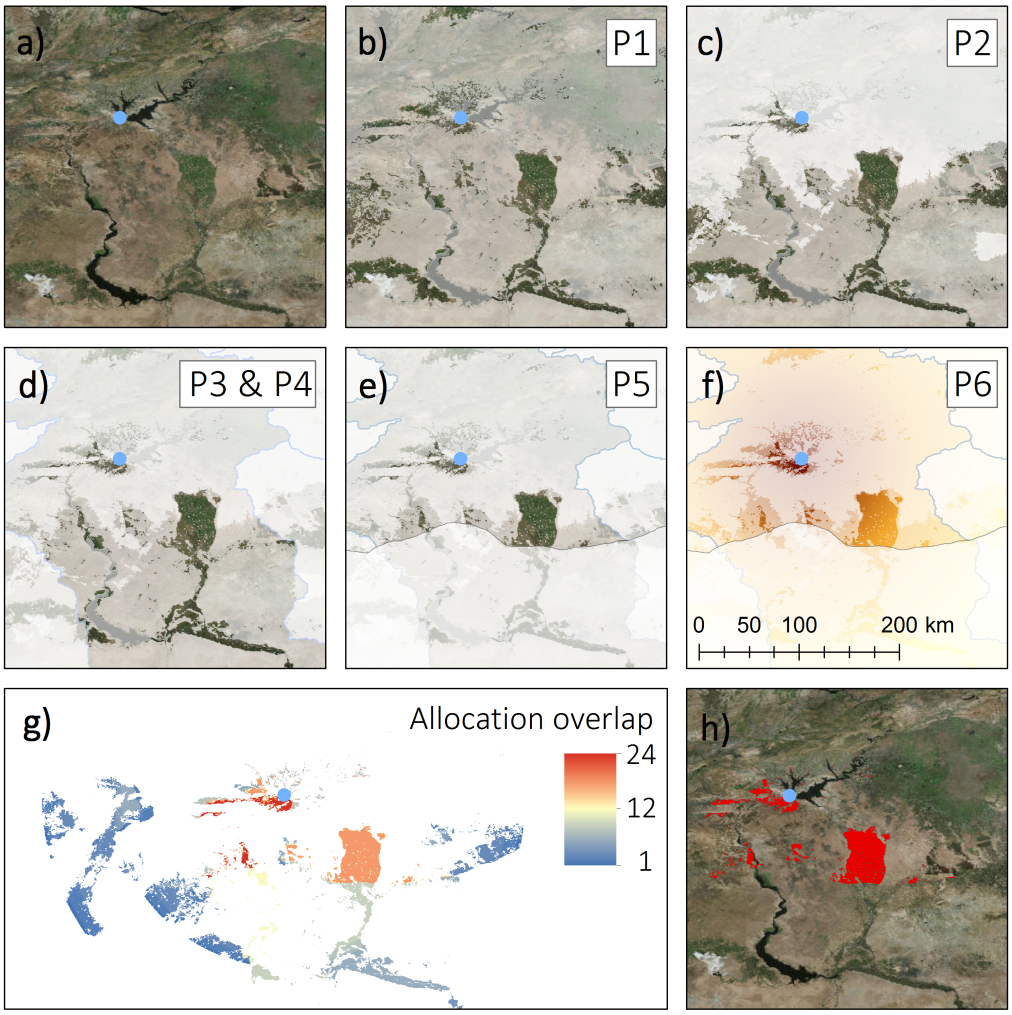

Figure 3.2: Example of the spatial allocation of command areas for the Atatürk dam in Turkey (a, blue dot). Transparent white areas are masked out. Allocation parameters include irrigated cropland (b, P1), elevation relative to the dam (c, P2), watershed boundaries (d, P3 & P4), national borders (e, P5), and distance to the dam (f, P6). Overlapping command areas resulting from 24 allocation schemes reveal the robustness of the allocation (g). The allocated command area is presented in red (h).

an annual time-series of MODIS land-cover maps for 2001 to 2012 (Friedl et al., 2010). This dataset has high accuracies in the cropland domain (Friedl et al., 2010) and provides uncertainty layers, which render it highly suitable for the purpose of our study. We preprocessed and converted the data into annual binary cropland and non-cropland layers. We summarized these binary maps into a cropping frequency layer with values between 0 (no cropland in any year) to 12 (cropland in all years; Figure 3.3). We focused on pixels with the class label "cropland", which refers to pixels that are dominated by cropland, as the sub-pixel cropland extent in the class "agricultural mosaic" (composed of natural vegetation and cropland) remains uncertain and is lower than 60% (Vintrou et al., 2012).

Table 3.1: Sensitivity of command and control area allocation to parameter configurations of the allocation algorithm. We report successfully allocated command and control areas (Mha), area reductions due to lack of suitable areas (Mha), as well as reservoirs for which no allocation was possible (n).

Trans-boundary allocation	Watershed restric-tions	Allocation above dam (m)	Allocated command areas (Mha)	Command area re-duction (Mha)	Dropped command areas (n)	Allocated control areas (Mha)	Control area re-duction (Mha)	Dropped control areas (n)
NO	NONE	0	22.52	0.97	3	18.72	4.77	7
NO	NONE	10	22.59	0.90	2	19.00	4.49	6
NO	NONE	50	22.64	0.85	2	19.46	4.03	6
YES	NONE	0	22.87	0.62	0	20.45	3.04	2
YES	NONE	10	22.95	0.54	0	20.66	2.83	2
YES	NONE	50	22.99	0.50	0	21.12	2.37	2
NO	L5	0	15.19	8.30	19	10.27	13.23	66
NO	L5	10	15.37	8.12	17	10.53	12.96	63
NO	L5	50	15.79	7.70	14	11.27	12.22	58
YES	L5	0	15.71	7.78	7	10.39	13.10	60
YES	L5	10	15.89	7.60	7	10.66	12.83	58
YES	L5	50	16.25	7.24	6	11.41	12.09	53
NO	L6	0	11.37	12.12	43	6.73	16.76	128
NO	L6	10	11.57	11.92	42	7.06	16.43	124
NO	L6	50	12.05	11.44	41	8.15	15.34	117
YES	L6	0	11.58	11.91	37	6.78	16.71	122
YES	L6	10	11.79	11.70	36	7.12	16.37	119
YES	L6	50	12.26	11.23	34	8.22	15.27	111
NO	DYN	0	14.52	8.97	82	9.46	14.03	184
NO	DYN	10	14.72	8.77	81	9.76	13.73	178
NO	DYN	50	15.15	8.34	75	10.65	12.84	169
YES	DYN	0	15.04	8.45	77	9.55	13.95	176
YES	DYN	10	15.23	8.26	76	9.86	13.63	171
YES	DYN	50	15.60	7.89	70	10.76	12.73	163

We performed an independent validation of the binary cropland maps based on 527 random samples from all areas that were under cropland use at least once. We visualized each sample pixel extent in Google Earth and verified the classification labels (cropland or non-cropland) year by year using the very-high-resolution satellite images available in Google Earth. We identified croplands through clear indications of management or cultivation, such as tillage or crop rows. In total, 73.1% of the points were classified correctly as cropland, with annual accuracies ranging between 66.7% in 2001 and 79.5% in 2006 (Figure S3.2).

We extracted and averaged cropping frequencies across the command areas and the corresponding control areas identified in each of the 24 allocation procedures (see Command Area Allocation). We performed analyses of variance (ANOVA) and linear regressions to test for differences in cropping frequencies between irrigated command areas and rainfed control areas on a global scale as well as stratified by UN world regions (Hijmans, 2015).

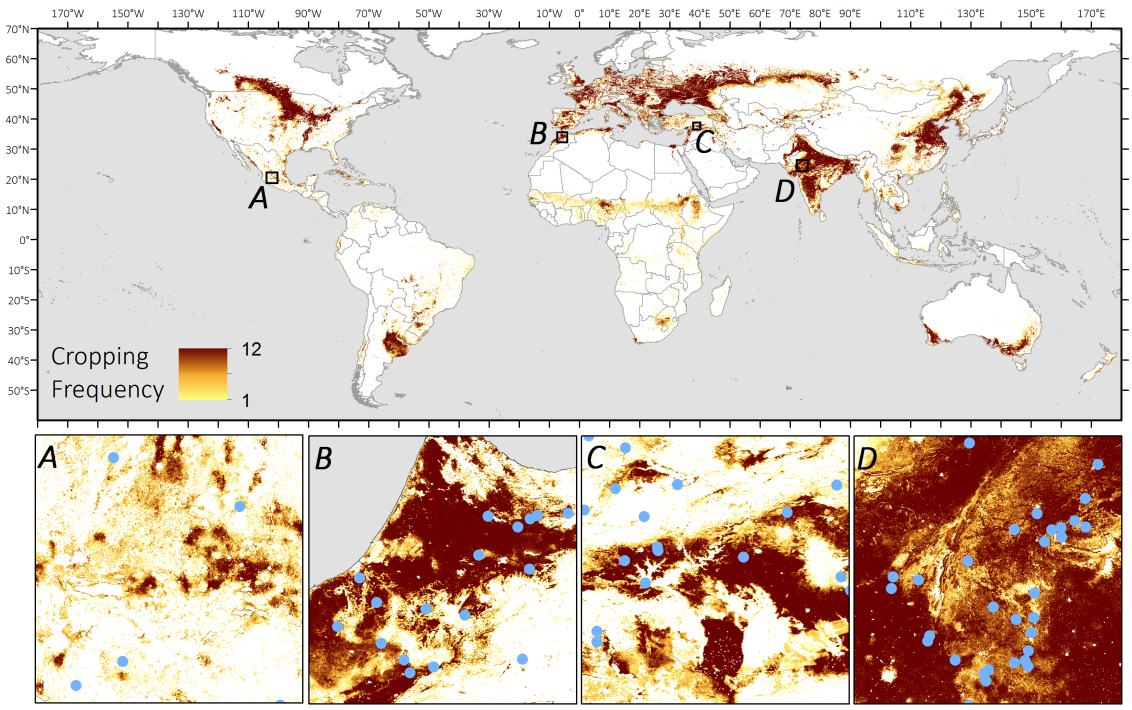

Figure 3.3: Global distribution of cropping frequencies for the time period 2001 - 2012. Image chips (A-D, locations marked in global map) include locations of irrigation dams (blue dots).

3.2.3 Spatial determinants of cropping frequency

The selection of spatial determinants of cropping frequency in command areas was motivated by existing literature and data availability (Table 3.2). We gathered datasets describing relevant properties of dams and irrigation systems, as well as biophysical, and socio-economic properties of the command areas (for data sources and variable units see Table S3.3). The non-spatial data (dam attributes, country-level, and world region variables) were associated with each individual command area. We averaged the spatially explicit variables across command areas, except the terrain variable for which we calculated the standard deviation of elevation across each command area. We computed variance inflation factors (VIF; Table S3.3) and pairwise Pearson correlation coefficients (Figure S3.3) to detect collinearity between our set of predictor variables (Dormann, 2013). The VIF quantifies collinearity between predictor variables in regression models by trying to explain each predictor variable with the remaining predictors in a linear regression model. VIF values were below the common critical threshold of 10.0 (Alin, 2010; Dormann, 2013), except for three UN world region factors, namely South Asia, South-Eastern Asia and Western Asia.

3.2.4 Explaining variation in cropping frequency

We aimed at explaining the observed variation in cropping frequency across irrigation dam command areas using a set of predictor variables describing the characteristics of dam and irrigation systems, as well as the biophysical and socio-economic attributes of the command area location (Table 3.2). We used Boosted Regression Trees (BRTs) to model and explore the relationships between the predictor variables and cropping frequency. BRTs are a machine learning technique capable of handling non-linearity without imposing a priori relationships between target and predictor variables (Elith et al., 2008). BRTs combine decision trees with boosting and are a particularly useful tool for assessing drivers of land change (Müller et al., 2013). Calibrating BRTs requires determining a set of parameters known as: bag fraction, learning rate (lr), tree complexity (tc), and number of trees to be built (n_tree). The bag fraction determines the share of observations from the input data that is randomly withheld while fitting each new decision tree to avoid overfitting. We set the bag fraction to 0.5 following (Friedman, 2001), i.e. randomly drawing 50% of the training data without replacement. The learning rate reduces the contribution of each additional tree when added to the model, with a lower learning rate relating to a smaller contribution. Tree complexity defines the number of nodes within a single tree and determines the levels of interaction between spatial determinants.

Both tree complexity and learning rate strongly influence model performance and finding the parameter combination with minimum predictive error is therefore important. To do so, we tested multiple combinations of learning rate (0.001, 0.0025, 0.005, 0.0075, 0.01, 0.025, 0.05, 0.075, 0.1) and tree complexity (1-15) similar to (Levers et al., 2014) and optimized model parameters with respect to the cross-validated (CV) correlation coefficient. The number of trees is a measure of model complexity and defines how many single decision trees are included in the model. We determined the optimal number of trees by minimizing the holdout deviance using the gbm.step function implemented in the dismo package in R (Hijmans et al., 2011).

Optionally, BRTs allow a weighting of observations according to auxiliary variables representing, for example, the importance or certainty of single observations. The MODIS land-cover product provides pixel-based uncertainty information (hereafter termed "class probability"). We found higher class probabilities in the correctly classified validation samples (median of correctly classified samples: 74%, median of misclassified samples: 63%) and therefore considered them as a useful measure of uncertainty in our response variable. We calculated the mean class probability across all years as a per-pixel measure of classification confidence (Gross et al., 2013) and used these as observation weights in the BRT models. We assessed differences between large and small reservoirs by building two additional BRT models on the

data from the largest and smallest 50% of the reservoirs, respectively, split by the median storage capacity of 7.9 Mm^3.

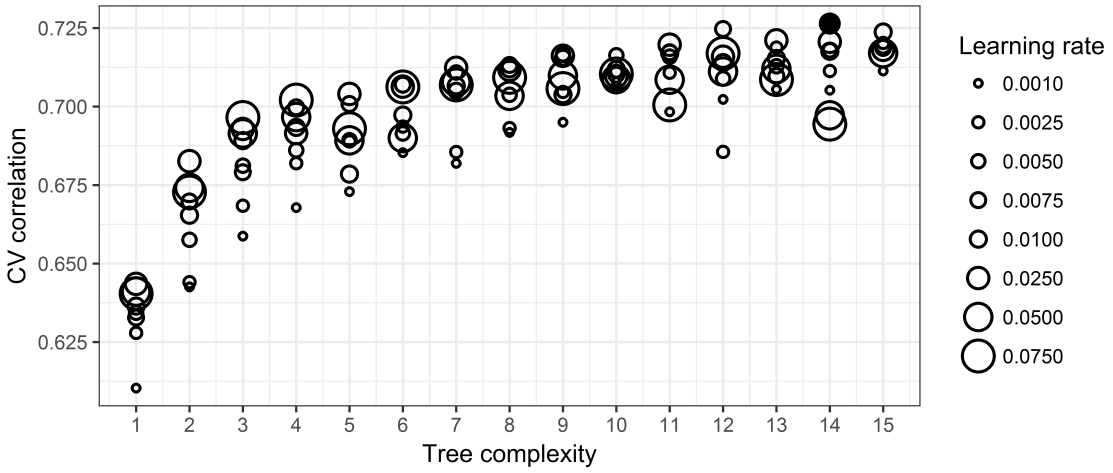

Figure 3.4: Cross-validated (CV) correlation coefficients across all combinations of tree complexity (x-axis) and learning rate (size of circles). Final model is shown as filled circle.

Table 3.2: List of predictor variables considered for explaining variation of cropping frequency in command areas with the underlying hypothesis and supporting literature.

Category	Variable name	Explanation	Hypothesis	Supporting Literature
Dam	comm_year	Commissioning year	Sediment accumulation successively reduces storage capacity and long-term irrigation can degrade soil fertility, leading to increased fallow frequencies.	WCD (2000); Hu et al. (2009); Singh (2016)
	hydropower	Hydropower	Water releases for hydropower generation can interfere with irrigation water supply.	Lacombe et al. (2014); Zeng et al. (2017)
	water_supp	Water supply	Abstraction for urban or industrial water supply can interfere with irrigation water supply.	Rosenzweig et al. (2004); Scott et al. (2007)
	area	Command area extent	Large and small reservoirs can have systematically differing cropping intensity in their command areas.	Blanc and Strobl (2014); WCD (2000)
Irrigation System	surface_perc	Share of surface irrigation	Surface irrigation can be inefficient and increase water logging under insufficient drainage, which can affect cropping negatively.	Jägermeyr et al. (2015); Rohwer et al. (2007)
	sprnk_drp_perc	Share of sprinkler and drip irrigation	More efficient irrigation technology can reduce water consumption and thus the risk of reduced cropping intensity associated with water scarcity.	Jägermeyr et al. (2015); Fader et al. (2016)
	conv_loss	Conveyance loss (% of water withdrawn)	High conveyance losses due to seepage and evaporation can constrain irrigation water availability.	Singh (2016); Fader et al. (2016)
	dist_dam	Distance to dam	Long water allocation distances increase conveyance losses and can hence affect irrigation water availability.	Thakkar (2000); Burney et al. (2013)
Biophysical	gdd	Growing degree days	Agro-climatological characteristics co-determine cropping intensities.	Iizumi and Ramankutty (2015); Levers et al. (2016)
	terrain	Terrain	Water allocation in rugged landscapes is challenging and cultivation prone to soil erosion.	Neumann et al. (2011)
	humidity	Humidity Index	Cropping intensities vary across gradients of aridity to humidity.	Neumann et al. (2011); Siebert et al. (2010b)
	prcp_dry	Precipitation in driest quarter of the year	Seasonal precipitation extremes and droughts can affect agricultural production.	Neumann et al. (2011); Iizumi and Ramankutty (2015)
Socio-economic	access	Travel time to major cities	Access to supplementary agricultural inputs such as labor or technology, is beneficial for irrigation and can increase cropping intensity.	Neumann et al. (2011)
	pop_dens	Population density	Intensive irrigated agriculture occurs under high population densities.	Neumann et al. (2011)
	UN	UN world region	Country- and region-specific characteristics determine water use efficiency and cropping intensity.	Rohwer et al. (2007); WCD (2000)
	gov_effectiv	Government effectiveness	National governance influences water security and strengthens irrigation infrastructure decision making.	Neumann et al. (2011); Klümper et al. (2017)

3.3 Results

3.3.1 Command areas and cropping frequencies

We found a good agreement between estimated command area extent and the reference data (Table S3.1) (Spearman's $\rho = 0.69$, mean absolute error = 33,290 ha, mean command area size in reference data = 53,007 ha). The model showed a tendency to underestimate reference command area extent, especially in the lower value range (Figure 3.5). The total extent of all estimated command areas of irrigation dams constructed since 1985 (n=1,370) was 23.49 Mha.

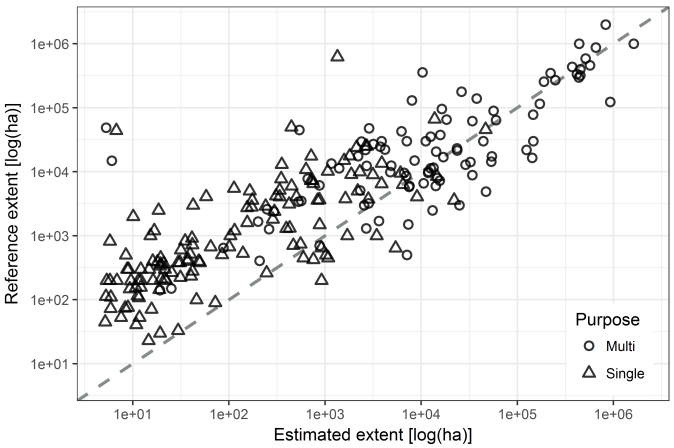

Figure 3.5: Log-scale scatterplot of reference (y-axis) and estimated command area extent (x-axis). Dots denote single-purpose dams, triangles multi-purpose dams. Dotted line indicates 1:1 agreement. Reported command area sizes (n = 266) gathered from independent national databases, reports, and the World Register of Dams (Table S3.1).

The total extent of the 1,288 allocated command areas comprised 14.77 Mha, distributed across 67 countries. Large fractions were located in India (5.90 Mha), Indonesia (1.47 Mha), China (1.42 Mha), Vietnam (0.87 Mha), Turkey (0.71 Mha), Iran (0.68 Mha), and Thailand (0.60 Mha). Despite the reduction in command area extent due to our allocation criteria, their country-wise distribution was well captured (Figure S3.1).

The ANOVA revealed significantly higher cropping frequencies within command areas compared to the rainfed control regions ($p < 0.001$), independent of the underlying spatial allocation criteria. On a global scale, the average effect of $\beta_{irrigation}$ equals 1.90 (standard deviation $\beta_{irrigation} = 0.03$), hence irrigation dam command areas showed nearly two fallow years (or 15.8% fallow periods) less than the rainfed control areas. A stratification by UN world region further revealed that these differences are consistent across most regions of the globe (Figure 3.6). Northern Africa was an exception, where irrigation was negatively related to cropping frequency,

likely because cropping frequencies in rainfed control areas were also high. Strong positive effects of reservoir-based irrigation on cropping frequency were observed in Western Europe (mean $\beta_{irrigation} = 4.3$) and Eastern Asia (mean $\beta_{irrigation} = 3.6$) (Table S3.4).

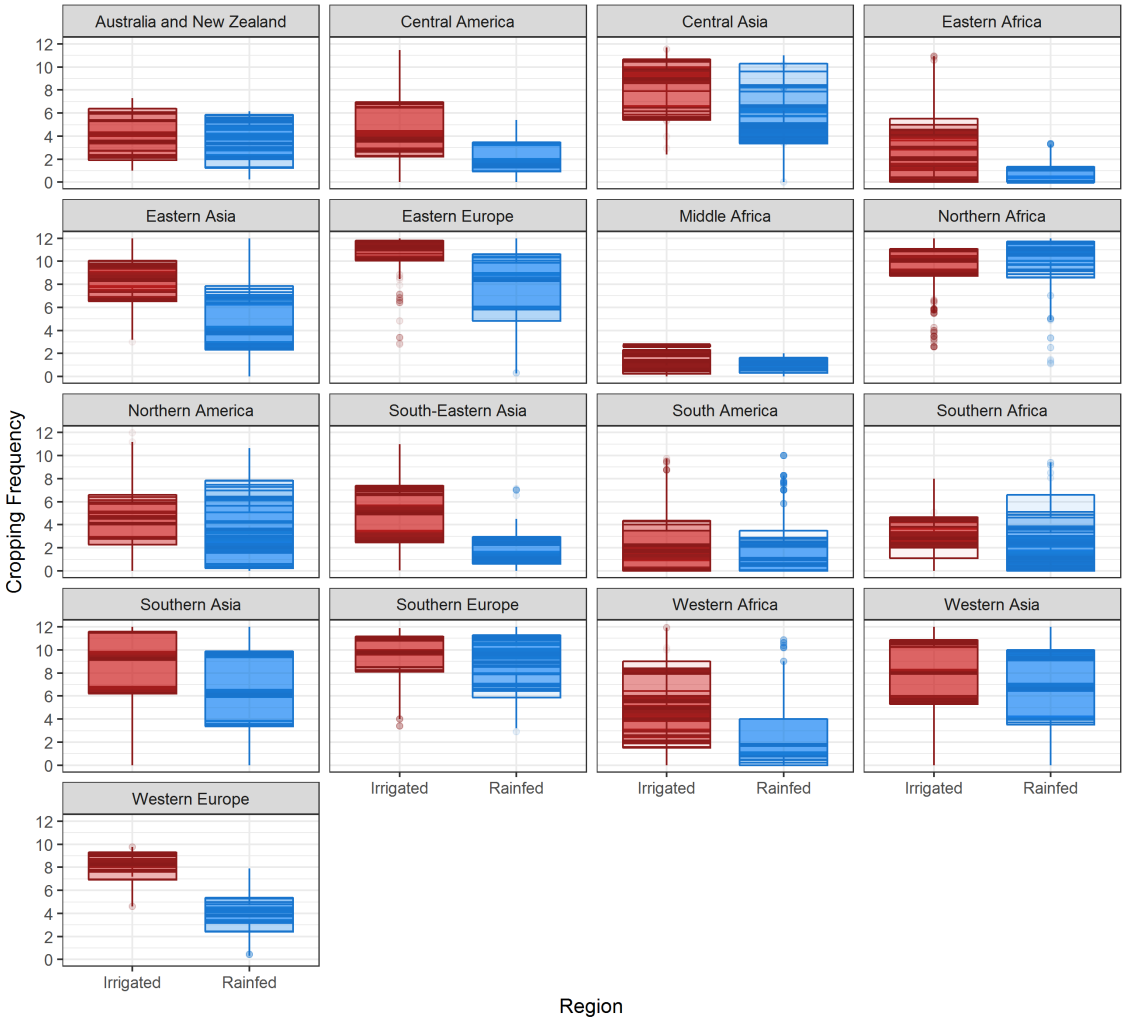

Figure 3.6: Boxplots representing the distribution of mean cropping frequency in command areas (red) and control areas under rainfed agriculture (blue). Overlaid boxplots represent the variability across the 24 allocation schemes presented in Table 3.1.

3.3.2 Model performance and relative importance of spatial determinants

Generally, the model performance increased with increasing tree complexity and decreasing learning rate, with an optimum at lr = 0.0075 and tc = 14 (cross-validation correlation r = 0.726, Figure 3.4). The optimal number of trees was fixed at 1,090 in the full model (small dams = 740, large dams = 760). The full model explained

51.3% (small reservoirs: 49.9%; large reservoirs: 50.9%) of the variation in cropping frequency with an RMSE of 1.5 cultivation years in the 12-year period (small reservoirs: 1.5; large reservoirs: 1.3). Using the uncertainty measure as observation weights improved the model performance throughout (full model: +0.6%, small reservoirs: +1.3%, large reservoirs +1.6%). In the full model, the biophysical and socio-economic properties of the command areas were the most important, accounting for 33.9% and 33.4% of the total variable importance (Table 3.3). The variable categories dam and irrigation system summed up to 11.7% and 20.9% of the variable importance. The most important single variable describing the variations in cropping frequency in our command areas was UN world region (20.8%). The importance of the remaining variables was relatively balanced, with command area extent (9.9%), humidity (9.8%), and terrain (9.0%) substantially contributing to explaining cropping frequency patterns (Figure 3.7).

Table 3.3: Summed variable importance (%) of the four categories describing the operational realities of irrigation dams. See Table 3.2 for an overview of variables in each category.

Category	All reservoirs	Small reservoirs	Large reservoirs
Dam	11.7	10.0	9.6
Irrigation System	20.9	31.9	17.2
Biophysical	33.9	32.7	34.1
Socio-Economic	33.4	25.5	39.1

We observed marked changes in the proportions of variable categories and single variable contributions when stratifying command areas according to larger and smaller reservoirs (Table 3.3; Figure 3.7). In the small reservoir model, the relative importance of dam and irrigation system properties (41.9%) increased, and exceeded those of the socio-economic (25.5%) and biophysical (32.7%) variables. For large reservoirs, the socio-economic variables (39.1%) gained importance, while biophysical variables were less important compared to the full model. Specifically, we observed a large gain in variable importance for the UN world region variable (+6.9%). For small reservoirs, we noted a strong increase in relative importance of distance to dam (+8.3%), but also government effectiveness (+2.2%), while the UN world regions lost importance (-13.0%).

3.3.3 Relationships between spatial determinants and cropping frequency

The PDPs revealed that the relationships between the spatial determinants and cropping frequencies were mostly non-linear (Figure 3.8). Command area extent was positively related to cropping frequency, yet this trend saturated toward higher val-

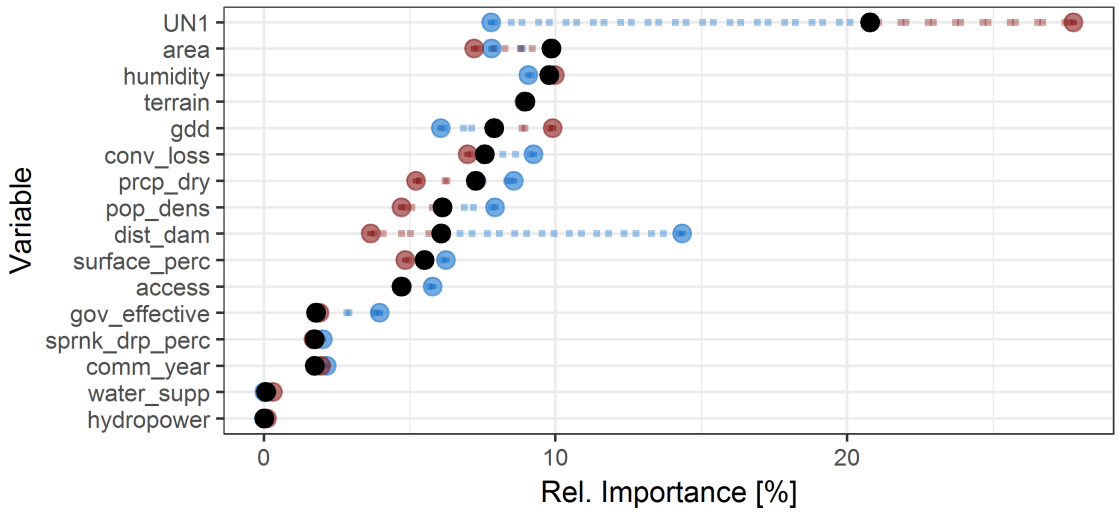

Figure 3.7: Relative variable importance of the three models. Values of the full model in black circles, small reservoirs in blue circles and large reservoirs in red circles.

ues (area $\geq$ 10,000 ha). Earlier commissioning years showed slightly lower cropping frequencies, and additional reservoir functions (hydropower, water_supp) decreased cropping frequencies marginally. Command areas distant from the dam (dist_dam $>$ 20km) were characterized by below-average cropping frequencies. Cropping frequency declined with increasing conveyance losses (conv_loss $\geq$ 16%). Increasing fractions of surface irrigation had a positive effect on cropping frequency (up to surface_perc = 20%), and a similar trend was found for sprinkler and drip irrigation fractions (sprnk_drp_perc $>$ 10%). Command areas with below-average cropping frequencies were located in regions with high terrain variability (terrain $>$ 100 m). Low amounts of precipitation in the driest quarter of the year (prcp_dry $<$ 150 mm) and extreme humidity (humidity $>$ 1.0, i.e. regions where mean annual precipitation exceeds mean annual potential evapotranspiration) were negatively related to cropping frequency. A very high number of growing degree days (gdd $>$ 7000) was associated with declines in cropping frequency. We further observed below-average cropping frequencies in remote areas (access $>$ 300 minutes), under low population density (pop_dens $<$ 100 people / km^2), and in countries with low government effectiveness (gov_effective $<$ -0.7). World regions with low cropping frequencies under reservoir-based irrigation include Australia and New Zealand, Central America, Eastern Africa, South-Eastern Asia, South America and Southern Africa.

The PDPs showed significant variations in the functional relationships between determinant and response when comparing size stratified models (Figure 3.8). Compared to the full model, the large reservoir model showed higher responsiveness (i.e. variation in fitted values) toward command area extent, commissioning year, and accessibility. Small reservoirs were more sensitive to variations in distance to dam

and government effectiveness but less responsive toward dry-season precipitation, growing degree days, and world region.

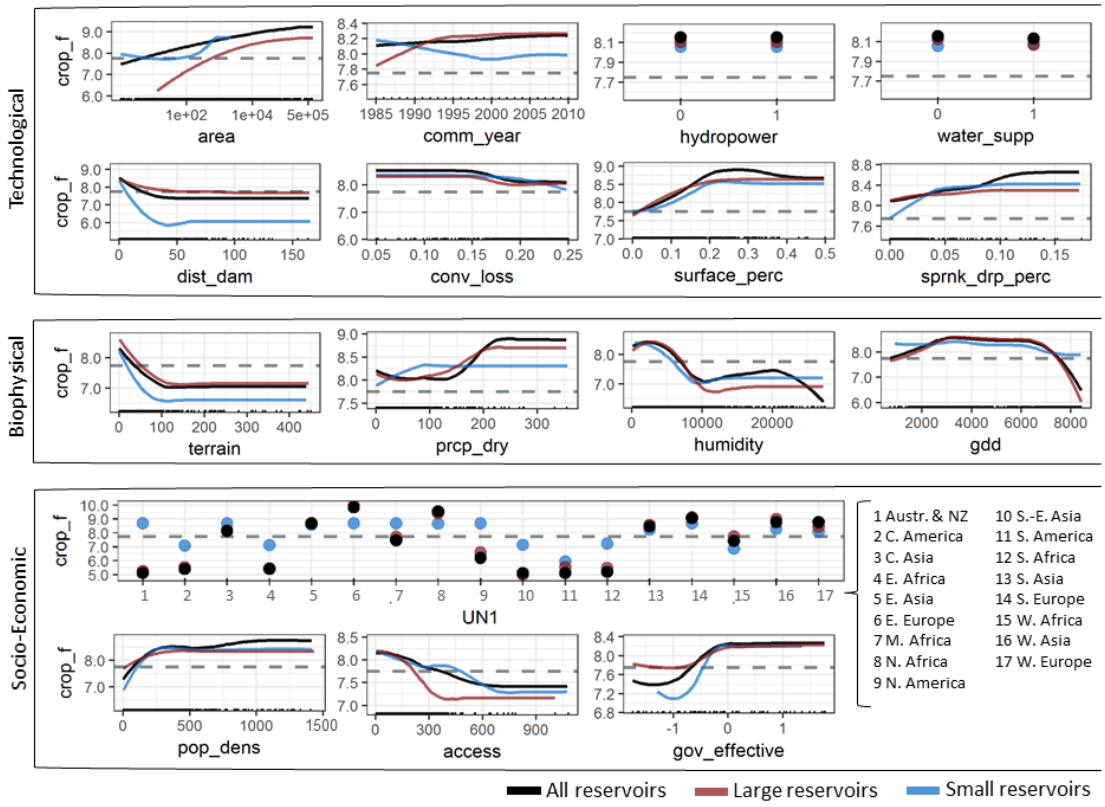

Figure 3.8: LOESS-smoothed (span = 0.5) partial dependence plots of predictor variables. Plots represent value range of predictor (x-axis) and fitted response (y-axis) for all dams (black); small reservoirs (blue) and large reservoirs (red). Rug plots on the x-axis depict the data distribution. Horizontal dashed line represents the mean cropping frequency across all command areas (x = 7.75).

3.4 Discussion

We studied the patterns and determinants of cropping frequency in irrigation dam command areas at a global scale. A number of key insights emerged from our analysis. First, while the irrigation dam command areas we studied here were dispersed across 67 countries, hotspots of reservoir-based irrigation were found in India, Indonesia, China, Vietnam, Turkey, Iran and Thailand. Globally, cropping frequencies of command areas were 16% higher compared to nearby and topographically similar areas under rainfed cultivation. Second, our models suggested that dam and irrigation system properties rival socio-economic and biophysical determinants in explaining cropping frequency. Third, we observed lower cropping frequency in

small command areas, and those which were characterized by inefficient water transfer. These two properties thus potentially constrain intensive cropping in command areas, highlighting their relevance for irrigation infrastructure planning. High remoteness, as well as extremely warm and humid climates were further associated with low cropping frequency, which indicates that agro-ecologically suitable locations are critical for irrigation dam benefits. Finally, by comparing the functional relationships of cropping frequency and operational realities among large and small reservoirs, we found an improved versatility of small reservoirs for supporting high cropping frequencies across wide ranges of biophysical conditions.

3.4.1 Irrigation dam command areas

We reported estimates of the extent and spatial distribution of irrigation dam command areas for the period after 1985 and found satisfactory agreement between command area extent estimates and independent data (Spearman's $\rho = 0.69$, mean absolute error = 33,290 ha). However, due to frequent underestimation of command area extent, especially at lower values, the estimates presented here are conservative. This underestimation is potentially related to a systemic bias in the reference data which overstate project benefits (Ansar et al., 2014). In these cases, large command areas ($> 10^3$ ha) are allegedly irrigated by very small reservoirs (capacity $<$ 0.1 Mm^3), such as in several cases in Turkey. Our model for estimating command area extent proportionally performs best for command areas between 10,000 ha and 1,000,000 ha (Table S3.2). Due to the remaining discrepancies between estimates and reference data, we encourage further research on this topic.

Our data provide deeper insights into the spatial distribution of irrigation dam beneficiaries (Strobl and Strobl, 2011). Nevertheless, the global-scale assumptions underlying the presented command area allocation potentially mask local to regional scale realities of irrigation water allocation. For example, the shares of reservoir storage capacity actually used for irrigation can vary with fractions of active storage (the water quantity available for outtake), as well as the number and types of reservoir purposes. As there is no data available to account for these in-situ variations, we rely on a country-scale ratio of reservoir storage capacity and irrigated area. While this ratio is created by averaging on a country-scale and thus suppressing sub-national heterogeneity in live storage fractions, it captures variations in live storage fractions in higher detail than commonly used global scale coefficients. Further, the effects of multiple and potentially conflicting reservoir purposes on irrigation are as yet weakly understood. The effects of such conflicts on irrigation water availability were found to underlie significant spatial variation, which can partly be explained by climate (Zeng et al., 2017). In the context of our study, the lack of knowledge and data on the effects of conflicting reservoir purposes did not allow us to account for these

effects. Nevertheless, our reference data did not reveal a systematic bias between single-purpose and multi-purpose reservoirs during the command area extent estimation. Further, variables describing hydropower and water supply functions were of low importance for explaining global-scale variations in cropping frequency.

An additional source of uncertainty for global-scale command area identification is a lack of information on the type of water allocation. Whereas previous studies generally assumed gravity-based water allocation (Biemans et al., 2011), pump-based water allocation can allow for water transfer to elevated croplands. To account for this effect, we tested a global elevation tolerance of 50 m, but found no significant changes in terms of allocated command area extent and global-scale patterns of cropping frequency.

While the lack of spatially explicit reference data on command areas hampered a systematic assessment of the presented spatial allocation procedure, we would like to highlight three major improvements compared to existing approaches which relied on aggregated areal units, such as administrative districts (Duflo and Pande, 2007), or watershed boundaries (Strobl and Strobl, 2011). First, we accounted for six different allocation criteria, reducing the error of commission regarding false attribution of command areas to lands that are not within the actual command area. Second, we performed a sensitivity analysis to report variations in allocated command area extent under changing baseline assumptions. Third, our command area allocation operates on a global scale, producing spatially explicit maps of command areas in high spatial detail (spatial resolution of 500 m). We made the data publicly available for further use and investigation.

3.4.2 Cropping frequency in command areas

We mapped cropping frequency at a global scale and our independent validation attests to the reliability of the resulting map. Uncertainties inherent in global cropland maps demand careful evaluation (Bontemps et al., 2012; Fritz et al., 2011), especially for some regions where cropland is hard to map using MODIS satellite data (e.g., in the Sahel belt). The product used here outperformed other global land-cover products, even in heterogeneous and low intensity cropping systems (Vintrou et al., 2012). Regional investigations of these data further indicated high potential for capturing cropland dynamics (Bai et al., 2015; Kuenzer et al., 2014). Our cropping frequency map provides a conservative estimate, as we excluded agricultural mosaic landscapes, which are composed of varying fractions of annual croplands ($\leq$ 60%) and natural vegetation. We did not consider agricultural mosaic landscapes in our analyses since the sub-pixel cropland fraction within such areas is variable, and class-specific uncertainties are comparably high compared to the cropland class (Friedl et al., 2010; Vintrou et al., 2012). The implications of excluding this class

can lead to lower values in our cropping frequency measure, as well as the exclusion of agricultural mosaic landscapes from the command area allocation.

Comparing our data with national-level cropping frequencies (Ray and Foley, 2013) confirmed the general spatial patterns in our response variable, while we observed regional disagreements, for instance, in European Russia. Aggregated to the global scale, the estimated average cropping frequency (8.9 years, or cultivation in 74.2% of all years), or fallow land (25.8% of all years) respectively, is very well in line with previous global-scale estimates of fallow land extent (Siebert et al., 2010b). Further, the spatial patterns and hotspots of high (western Europe, eastern China, northeastern Argentina and the northeastern United States) and low cropping frequency (western United States, Central Asia, South-Eastern Asia, parts of tropical Africa) compare well between datasets. Comparing cropping frequency estimates including with those excluding agricultural mosaics reveal spatial clusters of differences, most notably in the Sahel belt, the eastern United States, South-Eastern Asia and parts of European Russia. As most of these regions do not contain extensive command areas commissioned since 1985 (Figure S3.4), the potential bias resulting from this disagreement is likely negligible for our study.

Despite the higher cropping frequencies within command areas, as compared to rainfed control areas, we registered frequent fallow periods in these locations. The global-scale average of 7.75 cultivation years in the 12-year study period reveals that fallow years account for 35.4% of all cultivation years and are thus substantially above global-scale estimates for all cropland areas (Siebert et al., 2010b). These values indicate a vast potential for increasing agricultural intensity in irrigation dam command areas on a global scale.

3.4.3 Spatial determinants of cropping frequency in command areas

We studied the technological, biophysical and socio-economic determinants of cropping frequency in command areas on a global scale to identify the conditions under which below-average cropping frequencies were prevalent. Two of the technological properties with a limiting effect on cropping frequency are water allocation distance and conveyance losses. In light of the need for improved water management (Jägermeyr et al., 2016; Mueller et al., 2012; Rosenzweig et al., 2004), de-centralized water storage facilities appear as a suitable solution to overcome these inefficiencies (Burney et al., 2013; van der Zaag and Gupta, 2008). Such distributed irrigation schemes also facilitate access to irrigation resources and could thus counteract the unequal spatial distribution of irrigation dam benefits (Duflo and Pande, 2007; Palmer et al., 2015). Our models revealed positive effects of increasing the share of surface irrigation on cropping frequency, indicating that water-intensive irrigation techniques

increase cropping frequency. Surface irrigation is the dominant technique worldwide (FAO, 2015), but the resulting productivity gains are unlikely to be sustainable. Excessive water application increases soil salinity, which consequently degrades the productivity of an estimated 1.5 Mha of agricultural land annually (Wood et al., 2000), often with limited options for restoration (Qadir et al., 2014). We found indications for declining land productivity, as we observed a negative relationship between the time since dam commissioning and cropping frequency in the full and large reservoir model.

Increasing humidity and a high number of growing degree days had a negative effect on cropping frequency, as observed in the command areas of the humid tropics of the Americas, Africa and Asia. These trends are in line with country-wise data on cropping frequency (Ray and Foley, 2013) and a global scale study that identified humidity as a constraining factor for irrigation suitability (Neumann et al., 2011). The unfavorable biophysical conditions in the humid tropics, such as excessive rainfall during sensitive phenological stages and poor soil quality likely constrain intensive cropping. As water scarcity is not necessarily limiting agricultural production in regions with ample precipitation, the benefits of irrigation reservoirs can be low in the tropics (McCully, 2001; Weaving, 1991).

Reservoirs are built to de-couple agricultural production from periodic water scarcity. Contrastingly, our findings imply that humidity and dry-season precipitation determine cropping frequency regardless of the buffering effect of water storage infrastructure; the intended de-coupling of cropping systems from precipitation-related water scarcity was not apparent from our data. Investigating this finding further by comparing the functional relationships between cropping frequency and seasonal precipitation inside and outside of command areas is subject of future analysis.

The UN world regions captured a significant proportion of the variation in cropping frequency, especially in the large dam model. This variable incorporates a variety of political, economic and institutional attributes, which were not otherwise captured by the included spatial determinants. A growing amount of scientific evidence suggests that governance and management of irrigation systems are vital for the functioning of water distribution and irrigation. For example, full irrigation potential was hampered by a lack of on-farm water management and infrastructure maintenance in Pakistan (Ashraf et al., 2007). In Ethiopia, lacking governance capacity limited the effectiveness of local small-scale irrigation projects (Yami, 2015). Farm-level irrigation water security in Tajikistan was determined by local governance, expressed as transparency, accountability and participation (Klümper et al., 2017). Additional country-level governance indicators besides government effectiveness were available (Kraay et al., 2010), yet we did not include these in the model

due to their internal collinearity (Neumann et al., 2011).

Command areas of small reservoirs (here defined as reservoirs with a capacity < 7.9 Mm^3) showed cropping frequencies similar to large reservoirs, yet under reduced responsiveness to variations in technological, biophysical, and socio-economic factors. Especially the tolerance to dry-season precipitation scarcity and growing degree days was greater for small reservoirs than for large ones. Hence small reservoirs are vital components for improving resilience against climatic variability and thereby improving productivity in low-yielding regions (Ashraf et al., 2007; Wisser et al., 2010; Dile et al., 2013). Earlier research found positive effects of small reservoirs on cropland productivity, while their economic viability exceeds that of large dams, especially when considering the lower environmental and socio-economic externalities (Blanc and Strobl, 2014).

3.5 Conclusion

This study presents the first global-scale, spatially explicit analysis of the technological, biophysical and socio-economic realities of irrigation dam command areas and their effects on cropping frequency. Our results show that the technicalities of dams and irrigation systems co-determine cropping frequency, and highlight the potential for increasing cropping frequency in dam-and-canal irrigation schemes through minimizing water allocation distances and related conveyance losses. Further, our findings indicate that small reservoirs are versatile measures for increasing cropping frequency, although suitable topography and short water allocation distances are critical factors for success. Our findings thus speak in favor of considering decentralized water storage facilities in proximity to command areas as an appropriate infrastructure for improving agricultural production by means of irrigation.

Our analysis provides new insights into the determinants of cropping frequency on reservoir-irrigated croplands at the global scale. Nevertheless, local-level deviations from the identified general trends might be masked in such global-scale analyses. We therefore highlight the need to complement the presented inductive approach with regional- or national-level analyses, for which data with finer spatial resolution are available and associated uncertainties may thus be lower. This will help to contextualize our insights into operational realities of irrigation reservoirs and their benefits for agricultural production.

Recent research provided growing evidence that institutional settings on local to regional levels are key elements for managing irrigated cropland to its full potential. While organizations such as the United Nation's Food and Agriculture Organization recognized the importance of irrigation governance, restrictions in data availability hamper the investigation of the effects of in-situ irrigation infrastructure mainte-

nance and governance beyond the local level. For future studies, we thus suggest a focus on the effects of irrigation governance on cropping intensities across scales, and highly encourage complementing the collection of agricultural production statistics with data on irrigation system governance at sub-national scales.

Acknowledgments

Philippe Rufin gratefully acknowledges funding from the Elsa Neumann Scholarship of the Federal State of Berlin, Germany. IRI THESys is funded through the German Excellence Initiative. This research contributes to the Global Land Programme (https://glp.earth/).

Chapter 3

Supplementary materials

Table S3.1: Sources and characteristics of datasets used for the command area allocation.

Analysis	Dataset Name	Reference
Dam geolocations and command area attributes	AQUASTAT Georeferenced Dam Database	FAO (2015)
	Global Reservoir and Dam Database V1.01	Lehner et al. (2011)
	India Water Resource Information System	CWC and ISRO (2015)
	World Register of Dams	ICOLD (2015)
	Register of Large Dams in Australia V1.0	ANCOLD (2010)
	Irrigation Dam Command Areas in Turkey	DSI (2015)
Command area extent estimation	GMIA V5.0	Siebert et al. (2013)
	AQUASTAT	FAO (2015)
Spatial allocation of command areas	GRIPC	Salmon et al. (2015)
	SRTM V4.1 500 m	Jarvis et al. (2008)
	Hydrobasins V1.2	Lehner and Grill (2013)
	GADM V2.8	Hijmans (2015)

Table S3.2: Mean absolute error of the estimated command area extent, stratified by command area extent classes in the reference data. Command area sizes stratified by reference size groups.

Reference command area extent [ha]	Reference data points [n]	Mean Absolute Error [ha]
1 – 10	0	-
10 – 100	19	54.8
100 – 1,000	76	519.7
1,000 – 10,000	87	4,622.6
10,000 – 100,000	62	27,481.7
100,000 – 1,000,000	20	223,580.2
> 1,000,000	2	1,176,975.0
overall	266	33,990.5

Table S3.3: Sources and characteristics of spatial determinant datasets as well as variance inflation factors (VIF).

Variable name	Data source	Spatial Unit	Unit	VIF
comm_year	FAO (2015); Grill et al. (2015)	Dam	Year	1.21
hydropower	FAO (2015); Grill et al. (2015)	Dam	Binary	1.37
water_supp	FAO (2015); Grill et al. (2015)	Dam	Binary	1.35
area	FAO (2015); Grill et al. (2015)	Dam	Mm^3	1.34
surface_perc	Jägermeyr et al. (2015)	0.5°	%	1.33
sprnk_drp_perc	Jägermeyr et al. (2015)	0.5°	%	1.13
conv_loss	Jägermeyr et al. (2015)	0.5°	%	1.23
dist_dam	this study	500 m	km	1.79
terrain	Jarvis et al. (2008)	500 m	m	1.34
gdd	New et al. (2000)	0.5°	index	4.31
humidity	Trabucco and Zomer (2009)	1 km	aridity index ($x10^3$)	1.55
prcp_dry	Hijmans et al. (2005)	1 km	mm during dry quarter	1.80
access	Nelson (2008)	1 km	min	1.10
pop_dens	CIESIN et al. (2011)	1 km	people / km^2	1.22
gov_effectiv	Kraay et al. (2010)	Country	index	3.30
UN1	Hijmans (2015)	UN world region	factor	C. America: 3.45
				C. Asia: 3.13
				E. Africa: 1.74
				E. Asia: 6.25
				E. Europe: 1.75
				N. Africa: 8.63
				N. America: 2.33
				S.E. Asia: 11.71
				S. America: 7.78
				S. Africa: 1.43
				S. Asia: 46.88
				S. Europe: 6.49
				W. Africa: 3.07
				W. Asia: 27.59
				W. Europe: 1.56

Table S3.4: Mean and standard deviation of regression coefficients and p-values of irrigation factor across allocation schemes for each UN world region.

UN world region	mean $\beta_{irrigation}$	sd $\beta_{irrigation}$	mean p	sd p
Austr. & NZ	0.419	0.346	0.682	0.237
C. America	2.476	0.087	0.004	0.002
C. Asia	2.443	0.773	0.185	0.172
E. Africa	2.240	0.352	0.017	0.017
E. Asia	3.647	0.258	0.000	0.000
E. Europe	2.657	0.217	0.009	0.007
M. Africa	0.611	0.720	0.685	0.250
N. Africa	-0.650	0.217	0.155	0.167
N. America	0.933	0.289	0.447	0.156
S. America	0.765	0.375	0.157	0.195
S.E. Asia	3.542	0.091	0.000	0.000
S. Africa	0.260	0.710	0.742	0.197
S. Asia	2.315	0.103	0.000	0.000
S. Europe	0.679	0.230	0.216	0.189
W. Africa	2.184	0.714	0.017	0.021
W. Asia	1.061	0.152	0.001	0.002
W. Europe	4.251	0.391	0.038	0.018

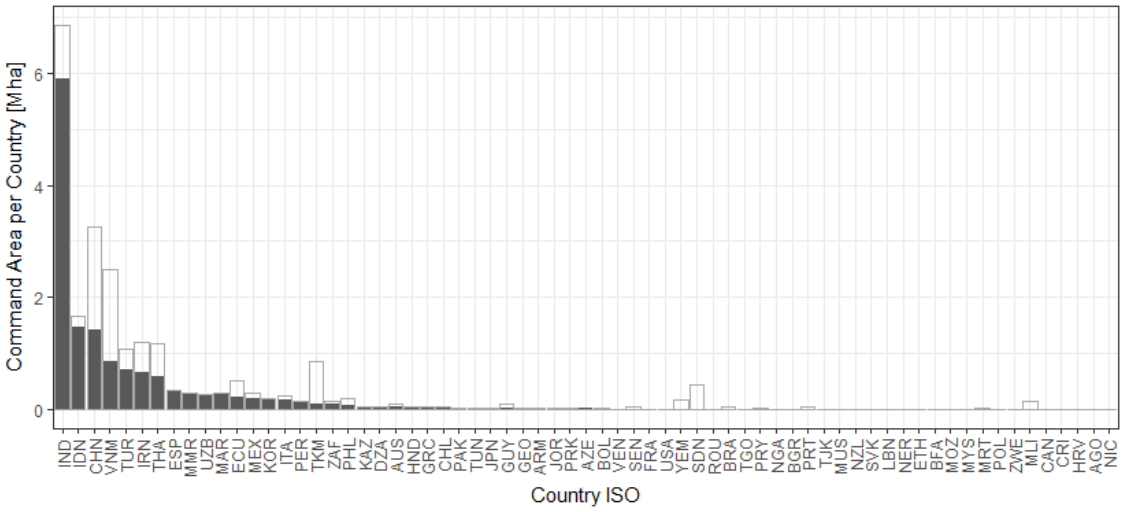

Figure S3.1: Distribution of allocated command area in countries with more than 5,000 ha allocated (filled bars). Hollow bars show total estimated command area extent by country, the difference between both indicates the area not allocated in a country.

Figure S3.2: Annual distribution of validation samples with error of omission (EO), correctly classified (Correct) and error of commission (EC). Color of the bars represents the number of samples in each bar.

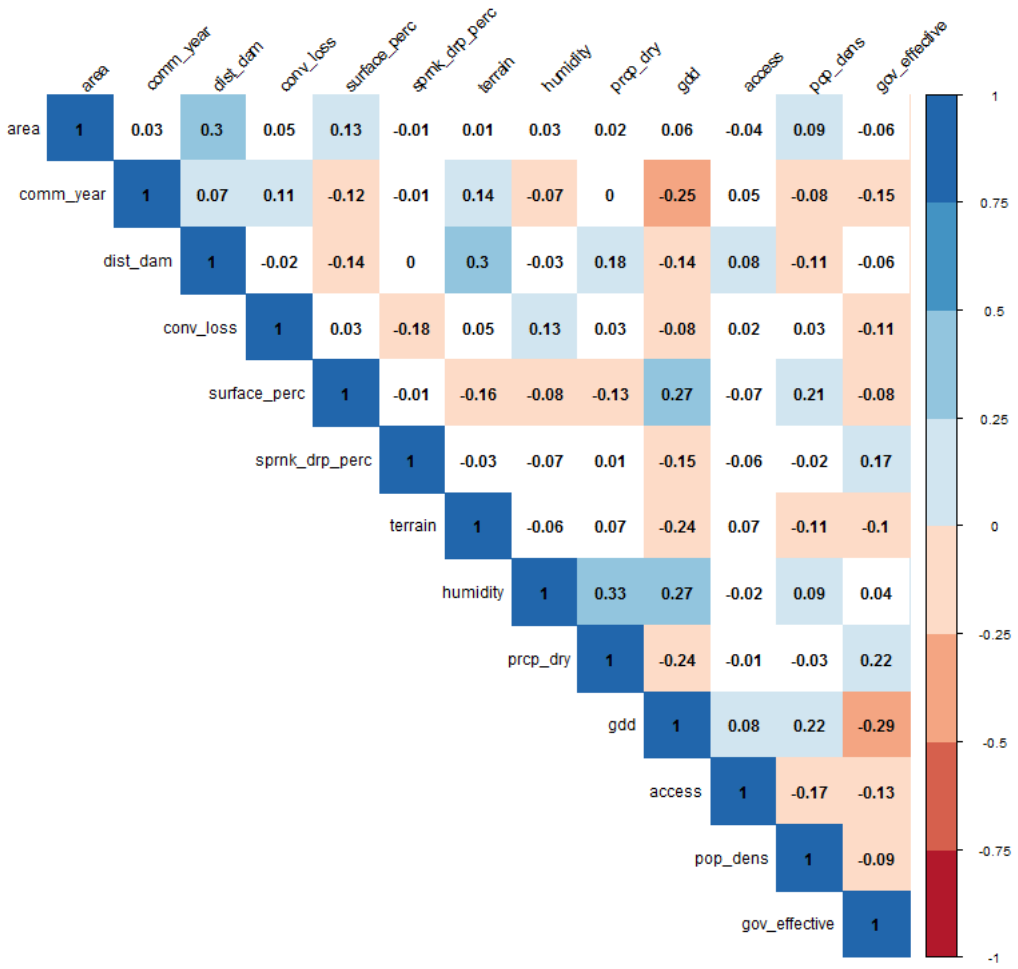

Figure S3.3: Pairwise Pearson correlation coefficients between predictor variables. Correlations in white boxes are insignificant, blue boxes represent positive, red boxes negative correlations. Saturation increases with correlation coefficient.

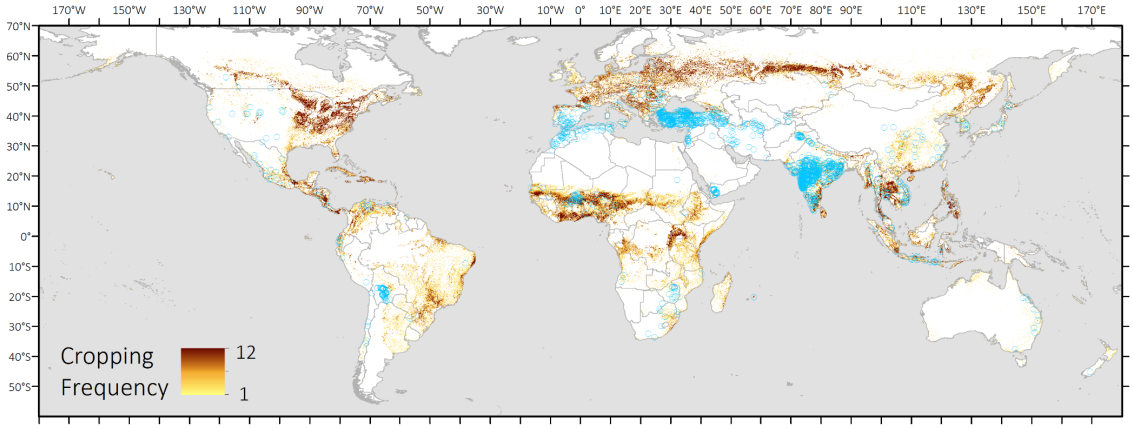

Figure S3.4: Changes in cropping frequency values under inclusion of the agricultural mosaic class. For reasons of simplification, we neglected the defined cropland share ($\leq 60\%$) in each pixel and counted the occurrence of the class as if it was cropland (100%). Blue circles represent dam locations.

Chapter 4

Mapping cropping practices on a national scale using intra-annual Landsat time series binning

Philippe Rufin, David Frantz, Stefan Ernst, Andreas Rabe, Patrick Griffiths, Mutlu Özdoğan, and Patrick Hostert
Remote Sensing, 2019

DOI: 10.3390/rs11030232
Submitted 21 December 2018; Revised 15 January 2018; Accepted: 17 January 2019

Abstract

Spatially explicit information on cropland use intensity is vital for monitoring land and water resource demands in agricultural systems. Cropping practices underlie substantial spatial and temporal variability, which can be captured through the analysis of image time series. Temporal binning helps to overcome limitations concerning operability and repeatability for mapping large areas and can improve the thematic detail and consistency of maps in agricultural systems. We here assessed the use of annual, quarterly, and eight-day temporal features for mapping five cropping practices on annual croplands across Turkey. We used 2,403 atmospherically corrected and topographically normalized Landsat Collection 1 L1TP images of 2015 to compute quarterly best-pixel composites, quarterly and annual spectral-temporal metrics, as well as gap-filled eight-day time series of Tasseled Cap components. We tested 22 feature sets for binary cropland mapping, and subsequent discrimination of five cropping practices: spring and winter cropping, summer cropping, semi-aquatic cropping, double cropping, greenhouse cultivation. We evaluated area-adjusted accuracies and compared cropland area estimates at province-level with official statistics. We achieved overall accuracies above 90%, when using either all quarterly features, or the eight-day Tasseled Cap time series, indicating that temporal binning of intra-annual image time-series into multiple temporal features improves representations of cropping practices. Class accuracies of winter and spring, summer, and double cropping were robust, while omission errors for semi-aquatic cropping and greenhouse cultivation were high. Our mapped cropland extent was in good agreement with province-level statistics (r^2 = 0.85, RMSE = 7.2%). Our results indicate that 71.3% (± 2.3%) of Turkey's annual croplands were cultivated during winter and spring, 15.8% (± 2.2%) during summer, while 8.5% (± 1.6%) were double-cropped, 4% (± 1.9%) were cultivated under semi-aquatic conditions and 0.32% (± 0.2%) was greenhouse cultivation. Our study presents an open and readily available framework for detailed cropland mapping over large areas, which bears potential to inform assessments of land use intensity, as well as land and water resource demands.

4.1 Introduction

Growing pressure on agricultural systems under rising requirements for sustainable production results in a growing need for land use intensity and land management datasets (Pongratz et al., 2017). Spatially explicit information on land use intensity is crucial for tracking resource demands in the nexus of land, water and food over space and time (Kümmerle et al., 2013). It is, therefore, crucial to develop mapping approaches that move beyond broad representations of cropland extent towards enabling the distinction of management-driven cropland use intensity (Erb et al., 2013; Bégué et al., 2018). Better information on the areal extent and spatial distribution of cropping practices across large areas improves estimation of current and future land and water resource demands (Portmann et al., 2010; Estel et al., 2016; Jägermeyr et al., 2015).

The strong spatio-temporal variability of croplands and irregular clear-sky image acquisitions for optical data pose challenges for robust mapping of annual cropping practices (Whitcraft et al., 2015). Mapping efforts thus frequently relied on coarse-resolution imagery such as MODIS or AVHRR (500 m – 8 km), for instance in the context of cropping intensity (Estel et al., 2016; Jain et al., 2013; Biradar and Xiao, 2011), or irrigation (Salmon et al., 2015; Thenkabail et al., 2009). Landsat(-like) medium spatial resolution data (10 m - 30 m) represent cropland management more accurately (Bégué et al., 2018; Velpuri et al., 2009), specifically in small-holder cropping systems (Jain et al., 2013). Consequently, a variety of studies recently improved the remote-sensing based characterization of cropland management practices, such as irrigation (Deines et al., 2017; Ferrant et al., 2017; Chen et al., 2018), field sizes (Graesser and Ramankutty, 2017), or selected crop types (Song et al., 2017). However, many studies target regional characterization of single management indicators, while large area mapping efforts trying to characterize various management practices remain scarce (Bégué et al., 2018).

Major challenges for mapping cropping practices with medium resolution sensors stem from low revisit frequencies, and resulting sparse and irregular observation densities. The Landsat sensor family has a nominal repeat frequency of 16 days at nadir. During times with two operational satellites, repeat coverage can be up to 8 days, which can, however, be spatially and temporally fragmented, e.g., due to the failure of Landsat 7's scan line corrector (Wulder et al., 2008), or changes in long-term acquisition plans (Arvidson et al., 2001). Higher repeat frequency can occur in lateral overlaps of two orbits (Kovalskyy and Roy, 2013). However, cloud contamination largely reduces data availability on a pixel-level (Kovalskyy and Roy, 2015), limiting the large-scale applicability of traditional classification approaches, which relied on a manual selection of cloud-free single or multi-date imagery. Deriving temporally aggregated, (e.g., seasonal or annual) features from

Landsat image time series can help to overcome such issues, and aid in improving the thematic detail, consistency, and quality of maps in agricultural systems (Gómez et al., 2016; Waldner et al., 2015; Phalke and Özdoğan, 2018). Common techniques to generate standardized gap-free spectral features include pixel-based compositing (Griffiths et al., 2013b; Frantz et al., 2017), the computation of spectral-temporal metrics (Pasquarella et al., 2018; Müller et al., 2015; Schmidt et al., 2016), as well as data fusion (Gao et al., 2006, 2017) or gap-filling techniques (Schwieder et al., 2016). Such temporal features can be produced consistently for multiple periods and large areas (Waldner et al., 2017). Furthermore, they contain information on land surface phenology, which renders them suitable for mapping cropping practices across gradients of climate, topography, or land use intensity (Waldner et al., 2016a).

Land-surface phenology on annual croplands is particularly heterogeneous and dynamic, due to a variety of management-regimes. In water-scarce regions, for instance, growing cycles of cultivated lands are largely precipitation-driven. However, irrigation locally decouples cropland cultivation from precipitation-based restrictions in water availability. Consequently, the timing and amplitude of growing cycles of irrigated lands strongly deviate from the phenological cycles of rainfed crops (Ambika et al., 2016; Son et al., 2014). Identifying the timing of phenological events relevant for characterizing different cropland management practices is a challenging task (Özdoğan et al., 2010) and requires either regional expert knowledge or data-driven approaches to identify key phenological events in a spatially explicit manner (Jönsson and Eklundh, 2004). This problem is further aggravated in case of large area mapping, where diverse management regimes control for additional heterogeneity in the timing and number of growing cycles, as opposed to natural ecosystems, where climate or topography are primary drivers of shifts in phenology (Frantz, 2017). Additionally, the inter-annual variability of cropland management decisions, such as crop rotations, prohibits data pooling across multiple years, as can be used in more persistent environments such as forested ecosystems (Griffiths et al., 2014; Melaas et al., 2013).

Turkey has been and is undergoing policy-driven agricultural intensification. In this context, land consolidation efforts increased productivity by reducing parcel fragmentation across the country (Yaslioglu et al., 2009), and the expansion of irrigation infrastructure fostered regional development through increased agricultural production (Kibaroğlu et al., 2012). On the one hand, these policies boosted crop production over decades, ranking Turkey amongst the world's leading producers of cereals and other industrial crops (Kibaroğlu et al., 2011). On the other hand, they also resulted in a diverse agricultural landscape, dispersed along gradients in climate and topography, with a strong inter-annual variability in management practices (FAO, 2009b). Furthermore, low irrigation water use efficiencies (Kibaroğlu

et al., 2011; FAO, 2009b), as well as the limited availability of land and water resources require optimization of cropland management towards higher resource use efficiency. In this context, spatially explicit data on cropping practices is of high value to understand past and current patterns and drivers of land use intensity and associated resource consumption.

Growing information needs demand for accessible and operational methodologies, and analysis-ready data (ARD), defined as cloud-screened surface reflectance products delivered in regular tiles (Dwyer et al., 2018), or higher level time-series products (Frantz, 2017). Such data can enable large area cropland management mapping, independent of costly calibration efforts, which rely on ancillary ground data or large area characterization of vegetation phenology (Bégué et al., 2018). The Landsat archive is the longest uninterrupted global satellite dataset and thus provides an accessible and consistent data basis for deriving such information. In this study, we compare different approaches for Landsat time-series aggregation. We used consistently produced Landsat Collection 1 data, and openly available processing frameworks for generating ARD to promote readily applicable data and methods for large area mapping at medium spatial resolution. The key aim of this paper is to present a set of scientifically sound and openly accessible good practice recommendations for operational national scale mapping of cropland use intensity, demonstrated using the case of mapping cropping practices across Turkey. Specifically, our objectives are to:

- Test the performance of Landsat time-series binning methods for mapping cropping practices on annual croplands in Turkey.
- Investigate the spatial patterns of cropping practices across Turkey.
- Compile a set of good practice recommendations for Landsat-based mapping of cropping practices over large areas.

4.2 Data and methods

4.2.1 Study area

Located at the intersection of the European and Asian continent, Turkey's geopolitical role in agricultural production and trade has persisted through centuries. Turkey covers an area of 783,000 km^2. To date, roughly one-third of the country's land is cultivated (FAO, 2009b). Due to strong biophysical and cultural gradients, Turkey's agricultural lands comprise nine distinct agro-ecosystems that differ in biophysical characteristics, crop types, and cropping practices (FAO, 2009b). In 2015, Turkey's cultivated lands included 15.7 Mha of annual cropland, plus an additional

4.1 Mha of temporary fallow land (TSI, 2015). Cereals represent nearly two-thirds of the harvested land in Turkey, most notably wheat (35%), barley (12%) and maize (10%) (TSI, 2015). Additionally, sugar beets (25%), potatoes (7%), sunflower (3%), cotton (3%), and pulses (2%) are grown. As extensive parts of the country have semi-arid to arid climate, irrigation is key for economically viable agricultural production (Kibaroğlu et al., 2011). Rainfed cultivation during spring and the first summer months is possible in most parts of the country. Contrarily, cultivation during the dry summer months requires irrigation for successful crop development in the water-limited regions of Turkey, like Central and South-Eastern Anatolia. Summer cropping in these regions is indicative of irrigation (Özdoğan et al., 2006). Irrigation is widespread and currently present on 4.9 Mha, being subject to further expansion and projected to reach 8.5 Mha by 2030 (FAO, 2009b). 78% of the irrigated land is irrigated with surface water, which is mostly applied through surface irrigation (92%), followed by sprinkler (6%) and drip (2%) irrigation. However, national water use efficiency was below 50%, causing substantial water losses (FAO, 2009b). Furthermore, up to 55% of the area equipped for irrigation was not irrigated on an annual basis due to mismanagement, water shortages and institutional barriers at the local level, reflecting underused investments into irrigation infrastructure (Kibaroğlu et al., 2011), which can cause strong spatio-temporal dynamics of rainfed and irrigated cropping and thus to a high variability in land use intensity.

4.2.2 Data pre-processing and class catalog

We downloaded 1,143 Landsat 7 ETM+ and 1,269 Landsat 8 OLI images for the year 2015 that cover our study area of 63 WRS-2 scenes. As we aimed for achieving high radiometric and geometric consistency, we used exclusively Landsat Collection 1 Level 1 Tier 1 precision terrain corrected (C1 L1TP T1) images with a cloud cover of less than 80%. For conversion into topographically normalized surface reflectance, we performed atmospheric correction and topographic normalization using a modified C-correction for topographic normalization to avoid topography-driven misclassification (Radeloff et al., 2018; Tan et al., 2013). Generation of ARD, i.e. cloud and cloud shadow masking, radiometric correction (atmospheric, topographic, BRDF and adjacency effect correction), and data cubing (reprojection to ETRS89-LAEA projection and tiling into a 30 km x 30 km grid) were performed with the Framework for Operational Radiometric Correction for Environmental Monitoring (FORCE v. 1.1, freely available at http://force.feut.de), based on the algorithm described in (Frantz et al., 2016).

For classification, we included several auxiliary features. We used the 1 Arc-Second (30 m) digital elevation model acquired by the Shuttle Radar Topography Mission (USGS, 2015) to derive elevation and hillslope. Additionally, we generated

per-pixel latitude and longitude in geographic coordinates to account for large-scale variability in land cover characteristics.

We used a hierarchical class definition, first distinguishing annual cropland from other land cover and land use classes. In a next step, we classified annual croplands into five distinct classes of cropping practices, which characterize the annual cropland system of Turkey and relate to its use intensity (Table 4.1). The hierarchical approach enables the evaluation of the cropping practice maps independently of the respective cropland mask used. The areal extent of the cropping practice classes was expected to vary strongly. While wheat production in Turkey covers extensive areas, greenhouse cultivation only accounts for a marginal share of the cropland area (FAO, 2009b; TSI, 2015). Accurately capturing small classes in large area mapping poses additional challenges related to training data collection and validation (Olofsson et al., 2014). However, due to our objective to characterize the annual crop production system in a holistic manner, as well as the relevance of classes like semi-aquatic cropping and greenhouse cultivation regarding land and water resource consumption, we decided to integrate these classes in our class catalog. Examples of the spectral-temporal dynamics of our target classes are available in Figure S4.1 - S4.5.

Table 4.1: Description of the class catalog.

Category	Cropland classes	Description
Annual cropland	Winter and spring cropping	Start of the green-up possible in 2014, peak of the season in April to May 2015, followed by harvest.
	Summer cropping	Summer crops, start of the season in 2015, peak of the season between June and August, harvest in 2015.
	Semi-aquatic cropping	Phenology similar to summer crops, with visible flooding of parcels before green-up.
	Double cropping	Two growing cycles and harvests within 2015, comprising winter and spring as well as summer cropping.
	Greenhouse cultivation	Spectrally bright due to foil cover with transmitted vegetation signal, which shows clear seasonality. Single or multiple seasons are possible.
Other	-	Includes deciduous and evergreen forests and shrublands with a closed canopy, open woodland and shrubland canopy with exposed soil background, plantations and perennial crops, natural, semi-natural and managed grasslands, marginal lands, such as bare soils without distinct phenology as well as built-up areas, wetlands and surface water.

4.2.3 Generation of temporal features

We used all available clear-sky observations (CSO) for temporal binning of all images into gap-filled eight-day, quarterly and annual temporal features. While previous studies relied on annual temporal binning, we here introduced the quarterly binning as an intermediate trade-off between a high temporal resolution and an observation availability, which is sufficient for producing near gap-free coverage. The gap-filled eight-day temporal window represents an ideal case, where clear observations are available on a near-weekly basis. We derived temporally aggregated features using time-series gap filling, best-observation compositing, as well as the computation of spectral-temporal metrics. All higher-level products were generated using FORCE v.1.1.

Best-observation composites

We used 2,403 atmospherically corrected and topographically normalized, cloud-screened Landsat Collection 1 L1TP T1 images to compute four best-observation composites (Griffiths et al., 2013b) across Turkey. To identify the best observation, we conducted a parametric scoring which considered the temporal distance to the target day of the year, as well as the distance to clouds and cloud shadows and a haze score as parameters (Frantz, 2017). We used all available imagery from each quarter of 2015 to produce composites for the target days 15 February, 17 May, 16 August, and 16 November for the blue, green, red, near infrared, and both shortwave infrared bands, summing up to 24 features. For quality checking and interpretation, we derived compositing flags containing information on the quality, number of CSOs per pixel, the acquisition date of the best observation, the difference between the acquisition date and target day of the year (DOY), as well as the sensor. Additionally, we computed the CSO count for the entire year, considering all areas free of clouds, cloud shadows, snow and ice, which were not compromised by radiometric saturation.

Spectral-temporal metrics

We generated eleven band-wise spectral-temporal metrics for each quarter and the entire year using the CSOs available in the respective period. We computed minimum, 25^{th} percentile, median, 75^{th} percentile, maximum, mean spectral reflectance as well as the inter-quartile-range, range, and standard deviation of all reflectance values during each period. Additionally, we calculated the skewness and kurtosis of the distribution of reflectance values in the respective period. In total, the eleven spectral-temporal metrics for each quarter and spectral band sum up to 264 quarterly features, plus 66 spectral-temporal metrics from all observations of 2015.

Equidistant time series of Tasseled Cap components

The Tasseled Cap transformation represents a linear transformation of the Landsat spectral bands into components which express selected physical scene characteristics (Crist and Cicone, 1984). We applied the Tasseled Cap transformation based on the coefficients for Landsat surface reflectance (Crist, 1985) on the CSOs to generate an equidistant eight-day interval time series of the Tasseled Cap Brightness, Greenness, and Wetness components. We used a data-density weighted ensemble of three Radial Basis Function (RBF) convolution filters for smoothing and gap-filling of the time series (Schwieder et al., 2016). We chose to produce a time series of three Tasseled Cap components over a time series of standard vegetation indices since the Tasseled Cap transformation integrates the entire spectral information content of the six Landsat bands. While the vegetation signal is emphasized by the Tasseled Cap greenness component, the Tasseled Cap wetness, and brightness components potentially aid in the classification of our target classes such as semi-aquatic croplands and greenhouses.

The RBF approach is an ensemble technique, which combines multiple kernels to reduce noise and outliers in a time series, while enabling to capture the variability of the signal in managed systems. We defined an ensemble of Gaussian kernels with σ_1=8, σ_2=16, and σ_3=32 days, respectively and applied a kernel-cutoff parameter that restricted the absolute width of the Gaussian kernels to ± 21, 41, and 82 days relative to the target date. These kernels are relatively narrow compared to previous studies with a focus on natural ecosystems (Schwieder et al., 2016, 2018) and provide a trade-off between data gap reduction and the description of dynamic events, such as harvests. We finally aggregated the three kernels by calculating a data-density weighted mean, which gives preference to kernels with a higher data density for the final estimation.

The procedure resulted in a near gap-free eight-day time-series of three Tasseled Cap components for the year 2015, which consisted of 135 features. We further calculated mean, standard deviation, minimum, and maximum of the Brightness, Greenness, and Wetness time series for the entire year, resulting in 12 additional features.

4.2.4 Training data and classification

We collected training polygons with a minimum extent of nine pixels (0.8ha), using the composites, an Enhanced Vegetation Index (EVI) time series for the years 2014-2016 (produced following the methods for the Tasseled Cap time series), and high-resolution imagery available in Google Earth. We collected 1,925 training polygons in the different agricultural regions, comprising the Middle North, Aegean, Thrace,

Mediterranean, Northeast, Southeast, Black Sea, Middle East and Middle South regions (FAO, 2009b), to capture the heterogeneous management regimes across Turkey. We reduced the number of training samples to 15% of the pixels in each polygon, with a minimum of two and a maximum of 30 pixels, resulting in 10,340 training points (of which 50.2% represented annual croplands).

We compiled 22 different subsets of the 505 input features (Table 4.2). We categorized the feature subsets based on the employed temporal binning. The annual scheme refers to annual spectral-temporal metrics, combinations of composites and spectral-temporal metrics from all quarters of the year, all quarterly composites, all quarterly spectral-temporal metrics, or annual statistics derived from the Tasseled Cap time series. The bi-quarterly scheme refers to six combinations of two quarterly composites and spectral-temporal metrics; whereas the quarterly feature sets include composites and spectral-temporal metrics from one quarter only. For the quarterly and annual scheme, we further combined all quarterly feature subsets with annual spectral-temporal metrics. For the weekly scheme, we used the eight-day time series of Brightness, Greenness and Wetness, as well as the time series together with the annual Tasseled Cap statistics. We used Random Forest classification models (Breiman, 2001) for classification of each feature subset using n = 500 trees and included the square root of the number of features at each split. This procedure was used to separately produce binary cropland maps, as well as cropping practice maps for the study region.

4.2.5 Validation data and accuracy assessment

Assuming user's accuracies of 0.85 for all classes and targeting a standard error of the overall accuracy of 1% regarding binary cropland mapping and 2% for the cropping practice mapping, we determined a required sample size of 1,275 for the binary and 391 for the cropping practices map, respectively (Cochran, 1977). We performed a stratified allocation of the reference samples due to high imbalances in the extent of specific land uses. We produced a preliminary classification based on all quarterly spectral-temporal metrics and composites, which represented the five cropping practice classes plus nine sub-classes not related to annual croplands. This map provided the strata for implementing a stratified random sampling, allowing us to allocate samples in diverse types of non-cropland areas, such as grasslands, shrublands, or urban environments. We calculated the confidence intervals of accuracies and area estimates for four different sample allocation schemes and determined an allocation scheme with a class-wise minimum of 50 samples, and the remainder distributed according to class weights derived from the preliminary map as a suitable allocation (Olofsson et al., 2014). The final sample comprised 1,447 validation points, 465 of which were annual cropland samples (166 samples for winter cropping: 106 for

Table 4.2: Feature subsets and abbreviations, as well as total number of features, and number of features including the four auxiliary variables (latitude, longitude, elevation, and hillslope).

Scheme	Feature set	Model abbreviation	Number of features
Annual	All features	ALL	505
	Annual spectral-temporal metrics	ANNUAL_STM	70
	Quarterly composites & quarterly spectral-temporal metrics	QRT_STM_CMP	292
	Quarterly spectral-temporal metrics	QRT_STM	268
	Quarterly composites	QRT_CMP	28
	TC statistics	TC_STATS	16
Bi-quarterly	Q1 + Q2 composites & spectral-temporal metrics	Q1Q2_STM_CMP	148
	Q1 + Q3 composites & spectral-temporal metrics	Q1Q3_STM_CMP	148
	Q1 + Q4 composites & spectral-temporal metrics	Q1Q4_STM_CMP	148
	Q2 + Q3 composites & spectral-temporal metrics	Q2Q3_STM_CMP	148
	Q2 + Q4 composites & spectral-temporal metrics	Q2Q4_STM_CMP	148
	Q3 + Q4 composites & spectral-temporal metrics	Q3Q4_STM_CMP	148
Quarterly	Q1 composites & spectral-temporal metrics	Q1_STM_CMP	76
	Q2 composites & spectral-temporal metrics	Q2_STM_CMP	76
	Q3 composites & spectral-temporal metrics	Q3_STM_CMP	76
	Q4 composites & spectral-temporal metrics	Q4_STM_CMP	76
Quarterly & annual	Q1 composites & spectral-temporal metrics & annual spectral-temporal metrics	Q1_STM_CMP_ANN_STM	142
	Q2 composites & spectral-temporal metrics & annual spectral-temporal metrics	Q2_STM_CMP_ANN_STM	142
	Q3 composites & spectral-temporal metrics & annual spectral-temporal metrics	Q3_STM_CMP_ANN_STM	142
	Q4 composites & spectral-temporal metrics & annual spectral-temporal metrics	Q4_STM_CMP_ANN_STM	142
Weekly	8-day TC time series & annual TC statistics	WKL_TC_STATS	154
	8-day TC time series	WKL_TC	139

summer cropping, 63 for semi-aquatic cropping, 67 for double cropping, and 63 for greenhouse cultivation).

We pre-compiled relevant information for each validation point, containing image chips of pixel-based composites displayed in false-color RGB at three different zoom levels, pixel spectra of the point locations, and an EVI time series spanning 2014-2016 (see Figure S4.1 - S4.5 for examples). Based on this phenological information, we determined the class label for each validation sample. We further considered the pixel extent of each sample in Google Earth to verify the label against high-resolution imagery from 2015, or the closest acquisition year available. This was particularly useful to increase the certainty for separating cropland from grassland and for identifying greenhouses. Two trained interpreters crosschecked 25% of the samples, finding interpreter agreement in more than 95% of all cases. Reference points where class labels could not be determined with high confidence were removed. We predicted the reference data points for each classification model and computed area-adjusted overall accuracies as well as area-adjusted class accuracies (Olofsson et al., 2014).

4.3 Results

4.3.1 Clear sky observation density

We registered an average of 20.42 CSOs per pixel (minimum 0; maximum 62) during the study period. A spatially explicit visualization of CSOs (Figure 4.1) revealed data-scarce areas in the Eastern parts of the Black Sea region, while observation density in the across-track overlap areas in South Eastern Anatolia (southeast Turkey, alongside the Syrian border) was highest. Time windows covering single quarters of the year showed few gaps, except for the first quarter, where 9% of the study area remained unobserved (Table 4.3).

Table 4.3: Landsat clear sky observation statistics for Turkey, 2015.

Quarter	Mean CSOs	Maximum CSOs	No data	$\geq$ three CSOs	$\geq$ five CSOs	$\geq$ ten CSOs
1 (Jan – Mar)	3.14	16	9.17%	57.92%	23.78%	0.67%
2 (Apr – Jun)	6.37	22	1.09%	91.66%	70.13%	15.58%
3 (Jul – Sep)	10.70	24	0.07%	99.48%	96.74%	55.74%
4 (Oct - Nov)	6.61	22	1.12%	91.59%	73.91%	18.51%

4.3.2 Classification accuracies

We calculated the area-adjusted overall accuracies as well as their 95% confidence intervals for each binary cropland and cropping practice classification for all 22 input feature sets. The binary classification was robust (Figure 4.2, black signature) with

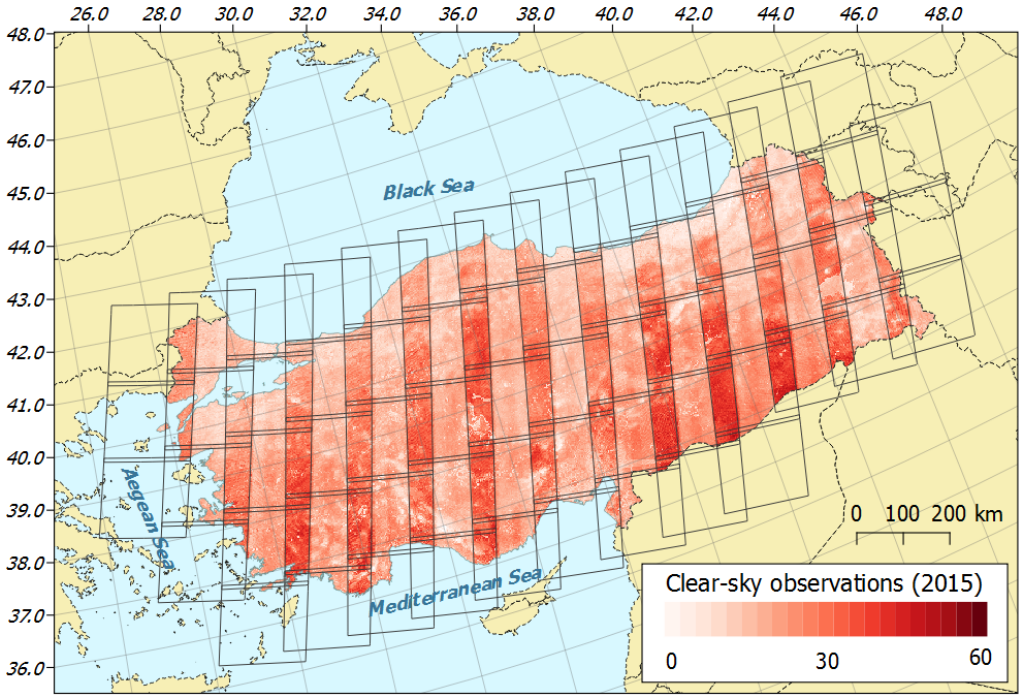

Figure 4.1: Study area and clear-sky observation count for 2015. Overlay represents the 63 Landsat WRS-2 scenes covering Turkey.

overall accuracies exceeding 92% throughout, whereas variations in accuracies were apparent for the cropping practice classification (Figure 4.2, grey signature).

Generally, features generated from annual data outperformed the seasonally restricted approaches, while the low accuracies of TC_STATS and ANNUAL_STM suggest that retaining seasonal information in temporal aggregates through seasonal binning is essential. We found no differences in overall accuracy when using only composites or only spectral-temporal metrics. Combining both however improved overall accuracy. In the category of bi-quarterly inputs, involving data from the spring and summer months performed well. Similarly, the single-quarter classifications showed that spectral-temporal metrics and composites from the summer quarter were sufficient for achieving overall accuracies above 85%. Using spectral-temporal metrics and composites from the data-scarce first and fourth quarters, however, yielded the lowest accuracies. Adding feature sets from other seasons generally increased accuracy. Including geographic location (latitude, longitude) and topography (elevation, slope) as auxiliary variables increased overall accuracies by 1 - 3% throughout, indicating their benefit for large area mapping.

Four models exceeded 90% overall accuracy in both binary cropland and cropping practice mapping (Table A1 - A4). These were ALL (all features), QRT_STM_CMP (quarterly composites and spectral-temporal metrics), WKL_TC (eight-day time series of three Tasseled Cap components) and WKL_TC_STATS (eight-day time series of three Tasseled Cap components complemented with four annual statistics).

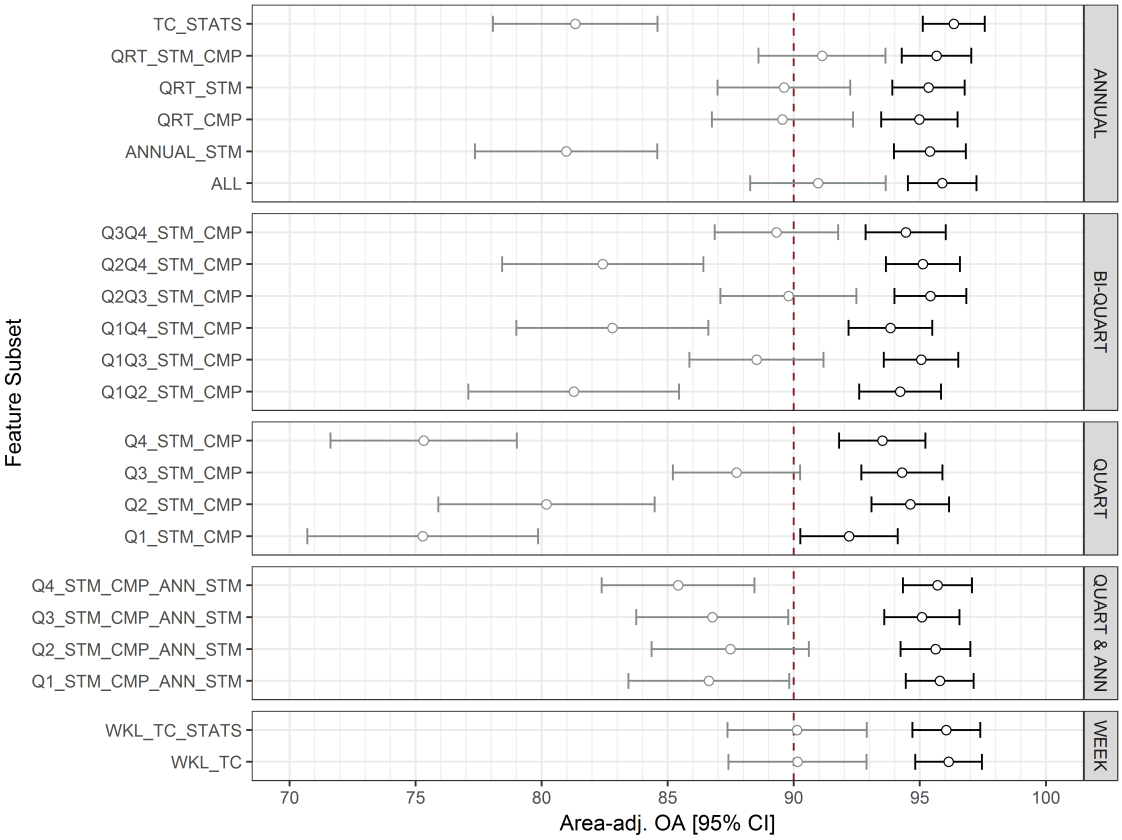

Figure 4.2: Area adjusted overall accuracies for binary annual cropland classification (black) and cropping practice classification (grey), for 22 feature subsets. Error bars indicate 95% confidence intervals, vertical dashed line marks 90% accuracy.

All these feature sets retain temporal information throughout the different seasons. Class wise user's and producer's accuracies of these four best models showed robust mapping of spring and winter cropping, summer cropping, and double cropping, whereas semi-aquatic cropping and greenhouse cultivation showed low producer's accuracies (Figure 4.3).

We based the following analyses on model WKL_TC_STATS, because the cropland extent was closest to official statistics (see Section on Cropland Area Estimates), and the spatial consistency was found to be highest.

4.3.3 Evaluating cropland maps

Cropland area estimates of the maps with the highest accuracies ranged between 10.73 Mha and 11.72 Mha (± 0.8 Mha; Table 4.4), thereby being substantially lower than reported statistics of cropland area extent, with a country total of 15.7 Mha (TSI, 2015).

We compared province-level (NUTS3) cropland proportions (%) from the binary cropland map WKL_TC_STATS, CORINE Land Cover 2012 (European Commis-

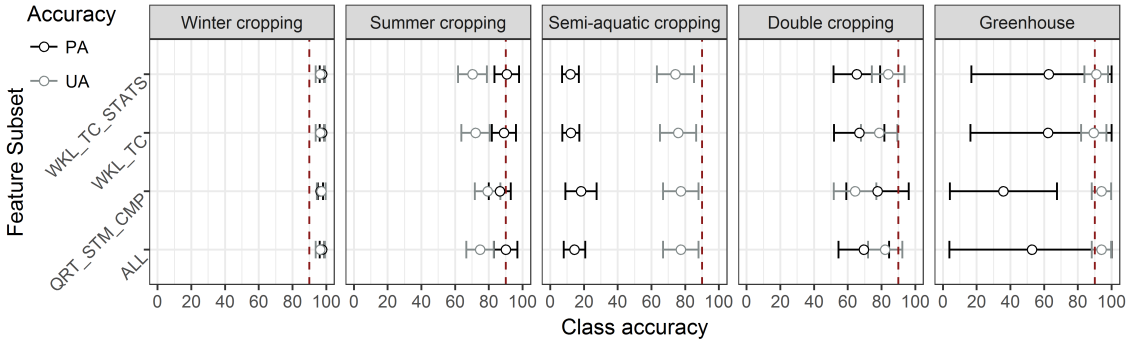

Figure 4.3: Area-adjusted producer's (black) and user's accuracies (grey) for the selected models. Error bars indicate 95% confidence intervals. Vertical dashed lines mark 90% accuracy.

Table 4.4: Error-adjusted cropland area estimates for Turkey in 2015. See Table 4.2 for abbreviations of model names.

Feature subset	Estimated cropland (Mha)	95% Confidence interval (Mha)
ALL	11.41	0.81
QRT_CMP_STM	10.73	0.83
WKL_TC	11.36	0.77
WKL_TC_STATS	11.72	0.79

sion, 2017) as well as the GFSAD30 cropland extent product with the baseline year 2015 (Phalke et al., 2017) with reported statistics of the sown area for the year 2015 (TSI, 2015) (Figure 4.4). Linear regression revealed high correlation of the cropland extent estimates from WKL_TC_STATS ($r^2 = 0.85$) and CORINE 2012 ($r^2 = 0.84$), whereas the correlation with estimates from GFSAD30 was comparatively low ($r^2 = 0.64$). Regression coefficients revealed the systematic underestimation of cropland area for our cropland mask (slope of regression: $\beta = 1.1$), although it was much lower than the overestimation in CORINE 2012 ($\beta = 0.7$) and GFSAD30 ($\beta = 0.5$). For a more detailed comparison of the province-level estimates, we investigated the accuracy (bias), precision (repeatability) and uncertainty (root mean squared error) of mapped versus reported cropland for all three products. We found lower accuracy compared to CORINE 2012 (i.e. a higher bias) but higher precision (i.e. higher consistency of the prediction) and similar uncertainty (Table 4.5). Our cropland area estimates had the highest precision of all products investigated here and their uncertainty was similar to estimates obtained from CORINE 2012. However, the overestimation of cropland in GFSAD30 as well as CORINE 2012 as compared to the national statistics might partly be related to the product class definitions, which include temporary fallow croplands.

We overlaid the binary cropland masks resulting from the four best classifications, finding agreement in 93.2% of the area, corresponding to 11.3% of cropland and 81.9% of the other class. Disagreement across cropland masks (Figure 4.5, first

Table 4.5: Model performance and summary statistics of linear regressions with NUTS3-level (n=81), using cropland extent statistics as a dependent, and mapped cropland extent from WKL_TC_STATS, CORINE 2012, and GFSAD30 products as the independent variable. Accuracy, precision and uncertainty in thousand hectares.

Model	Accuracy	Precision	Uncertainty	r^2
WKL_TC_STATS	5.45	4.70	7.20	0.85
CORINE 2012	-2.60	6.54	7.04	0.84
GFSAD30	-21.84	12.38	25.11	0.64

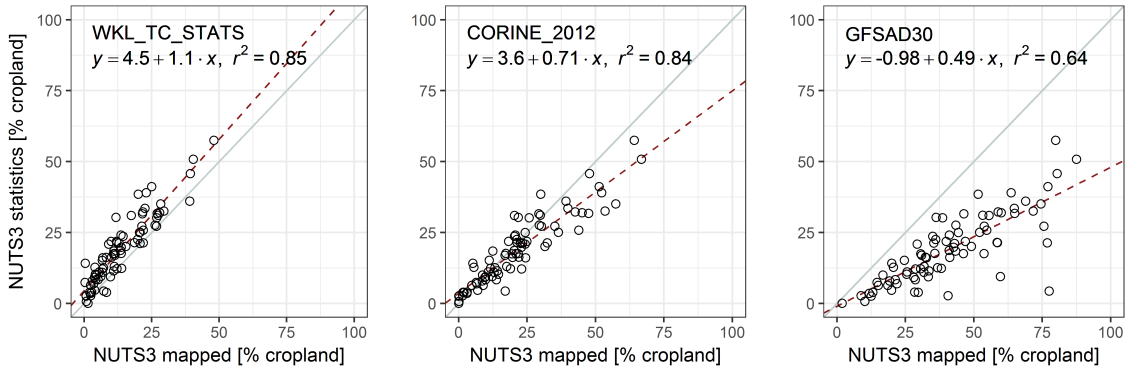

Figure 4.4: Comparison of province level fraction of cropland derived from maps and statistics from Turkish Statistical Institute at NUTS3-level (provinces; n=81). Cropland extent mapped from WKL_TC_STATS (left), CORINE 2012 (center), and GFSAD30 (right). Grey line shows 1:1 line, red dashed line represents linear regression line of mapped area against statistics.

column) occurred on parcel boundaries, within seasonally inundated wetlands and lakes, and in small-scale, fragmented or low-intensity cropping systems.

A comparison of the map products further demonstrated how these differences unfolded spatially and revealed some advantages of the presented cropping practice map (Figure 4.5). For instance, we captured parcels of temporary fallow croplands (e.g., Figure 4.5 A, B, C). Furthermore, our mapping methods are pixel-based and thus not restricted to a minimum mapping unit, which allowed for capturing small parcels in fragmented landscapes (e.g., Figure 4.5 C). Additionally, we found very high agreement between our semi-aquatic cropping class and CORINE's rice field class (Figure 4.5 D, E). The thematic detail of our maps allowed for identifying greenhouse cultivation (Figure 4.5 C) or the distinction between winter, summer, and double cropping in intensively irrigated systems (Figure 4.5 F).

4.3.4 Spatial patterns of cropping practices

Error-adjusted class area estimates across the four models were consistent (Figure 4.5). According to the selected model (WKL_TC_STATS), spring and winter

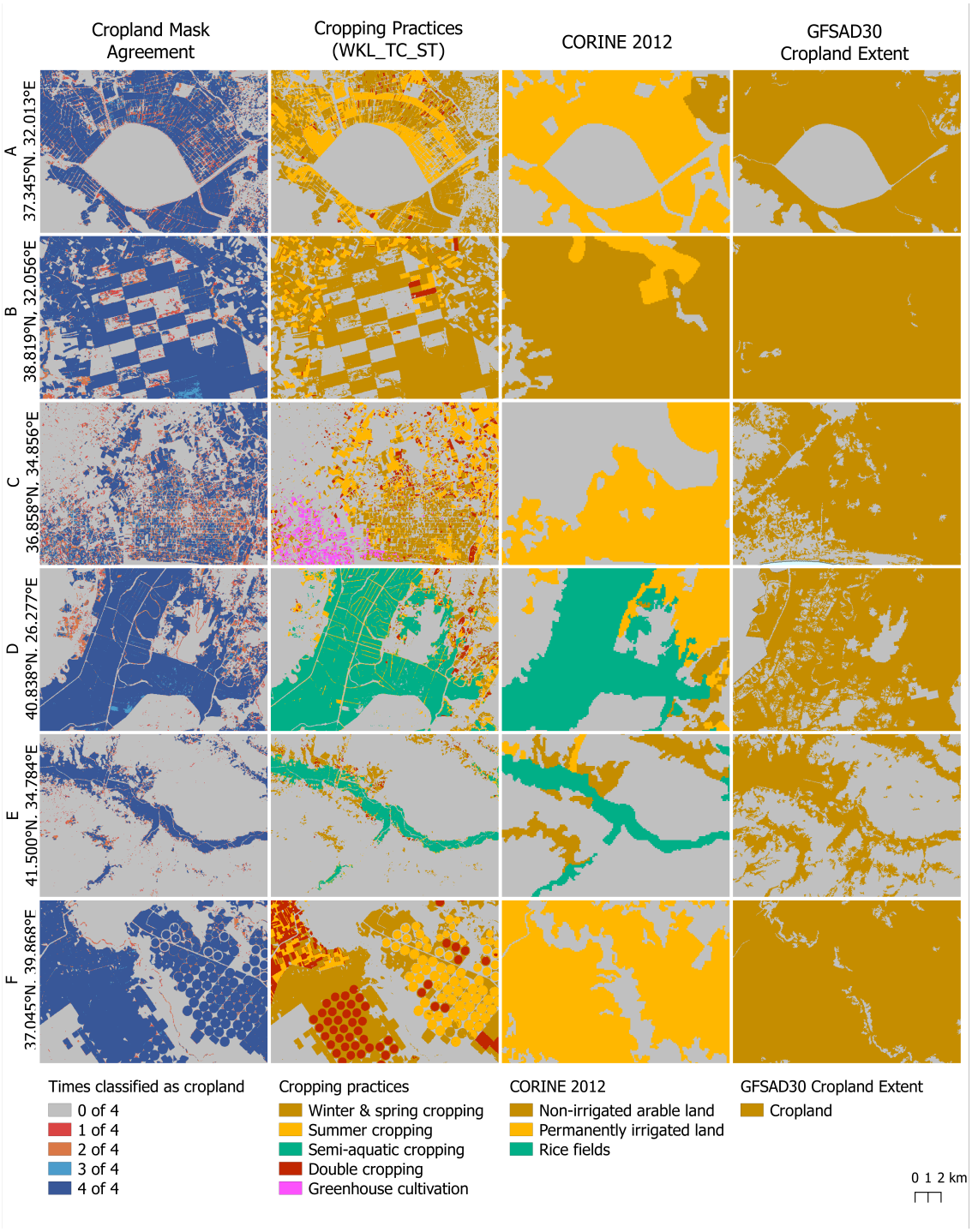

Figure 4.5: Image subsets (rows A to F) of cropland mask overlay (first column), cropping practice product (second column), CORINE 2012 (third column) and GFSAD30 product (fourth column). Center coordinates of each subset indicated to the left.

crops cover 71.3% (± 2.3%), and summer crops 15.8% (± 2.2%) of the total cropland area. Double cropping occurred on 8.5% (± 1.6%) and semi-aquatic crops were cultivated on 4.0% (± 1.9%) of the cropland area. Greenhouses accounted for only

0.32% (± 0.2%) of the cropland area, corresponding to an estimated 36,752 ha, which is well in line with the 38,605 ha reported in official statistics (TSI, 2015).

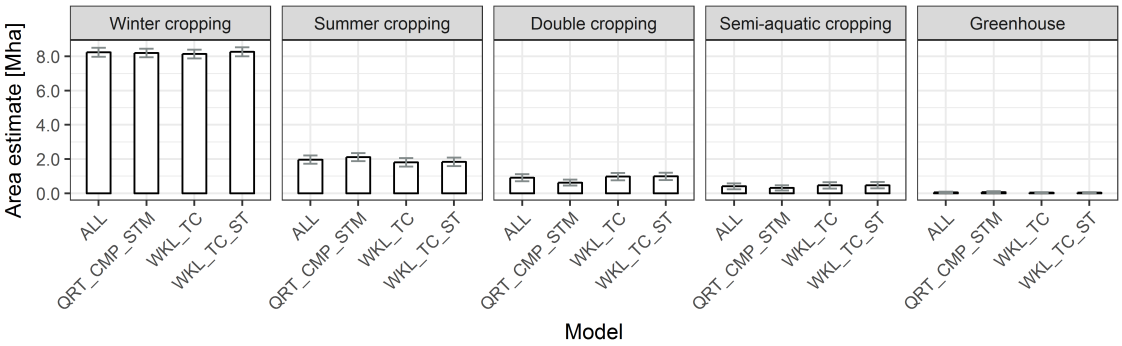

Figure 4.6: Error-adjusted area estimates of cropping practice classes (from left to right: winter/spring cropping, summer cropping, double cropping, semi-aquatic cropping, greenhouse cultivation) across the four best classification models (see Table 4.2 for abbreviations). Error bars indicate 95% confidence intervals.

We visually identified regional differences in cropping practices across Turkey (Figure 4.7). Semi-aquatic cropping, i.e. paddy rice cultivation, was prevalent in Sinop province in the Black Sea region (Figure 4.7 A) and the Evros river valley alongside the Turkish-Greek border. Here, misclassifications of summer crops on the unflooded parcel-boundaries were apparent (Figure 4.7 B). Distinct patterns of summer and double cropping occurred in the river valleys flowing into the Aegean Sea, most notably in the provinces of Aydın, Maniza, and İzmir (Figure 4.7 C). Central parts of Anatolia contained large-scale cropping systems (Figure 4.7 E). Agglomerations of greenhouses characterized the agricultural landscape along the Mediterranean coastline, e.g., east of Antalya (Figure 4.7 D, F). We found intensive cultivation patterns in the Şanlıurfa and Mardin provinces of the South-East Anatolia Project irrigation scheme (Figure 4.7 G). The cropping system in Eastern Anatolia showed heterogeneous parcel sizes and management systems, consisting of winter, summer, and double cropping (Figure 4.7 H, I).

Province-level (NUTS-3) shares of annual cropland by province showed spatial hotspots of cropland in the northwest, Central Anatolia, and South-Eastern Anatolia (Figure 4.8). Fractions of cropping practices in 2015 revealed the dominance of spring and winter cropping across Turkey. Fifty-three provinces were dominated (>60%) by winter and spring cropping. Summer cropping was the second most common cultivation strategy and distributed across almost all provinces, with spatial clusters along the Aegean Sea and the Eastern Mediterranean Sea. Double cropping occurred on less than 9% of croplands and clustered spatially in South-East Anatolia, e.g., Mardin (40%) and Şanlıurfa (21%), in the river valleys of the Aegean Sea region, e.g., İzmir (37%), and parts of the Black Sea region where cropland was limited. Semi-aquatic cropping was relevant in Edirne (21%) along the Greek border and

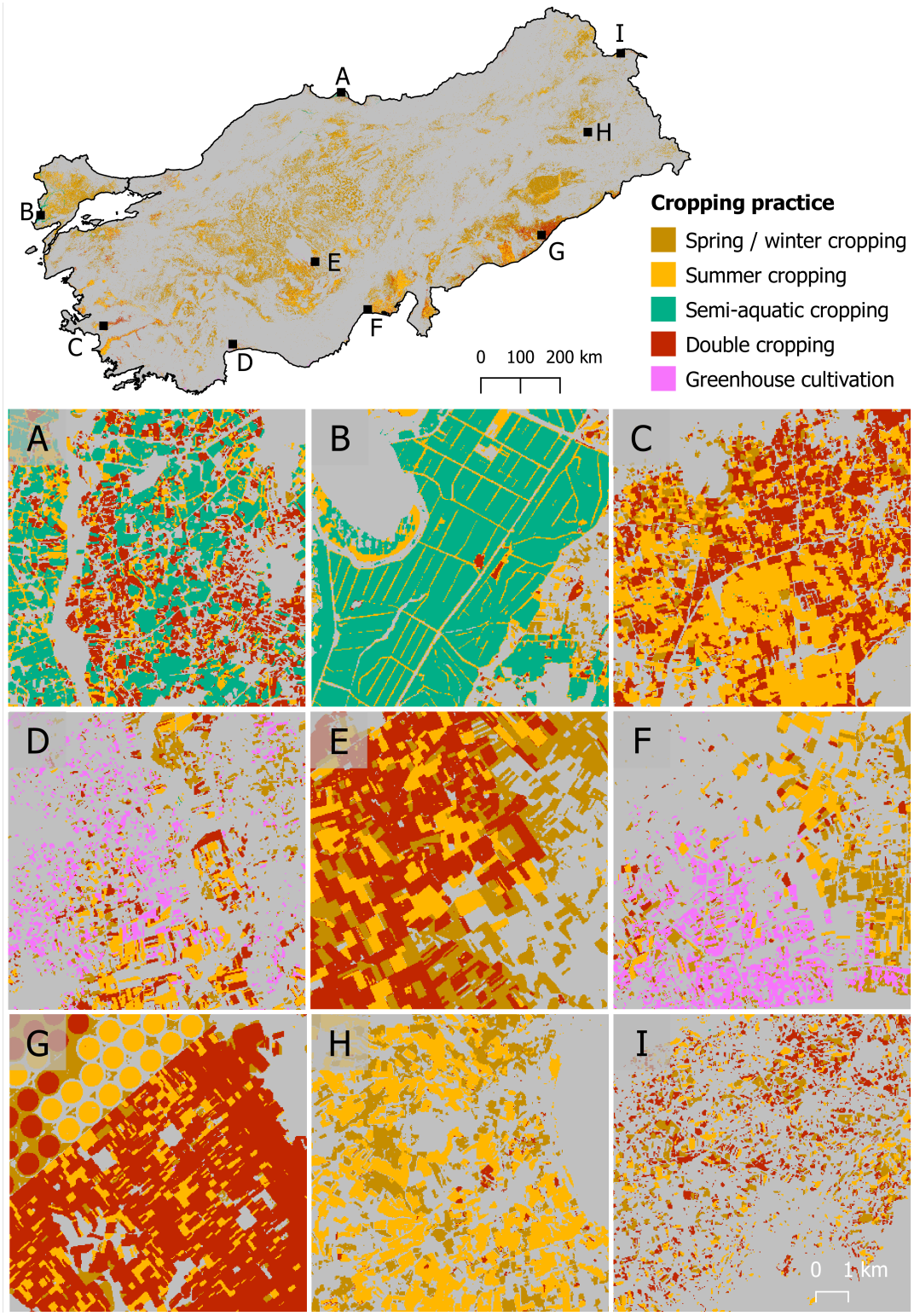

Figure 4.7: National-scale cropping practice map for the year 2015 (upper section), based on eight-day time-series of Tasseled Cap Brightness, Greenness, and Wetness including four annual statistics (WKL_TC_STATS). Black rectangles indicate location of subsets A to I (lower section).

Sinop (21%) in the Central Black Sea region. Greenhouse cultivation clustered along the Mediterranean coastline, especially Antalya (17%) and İçel (10%).

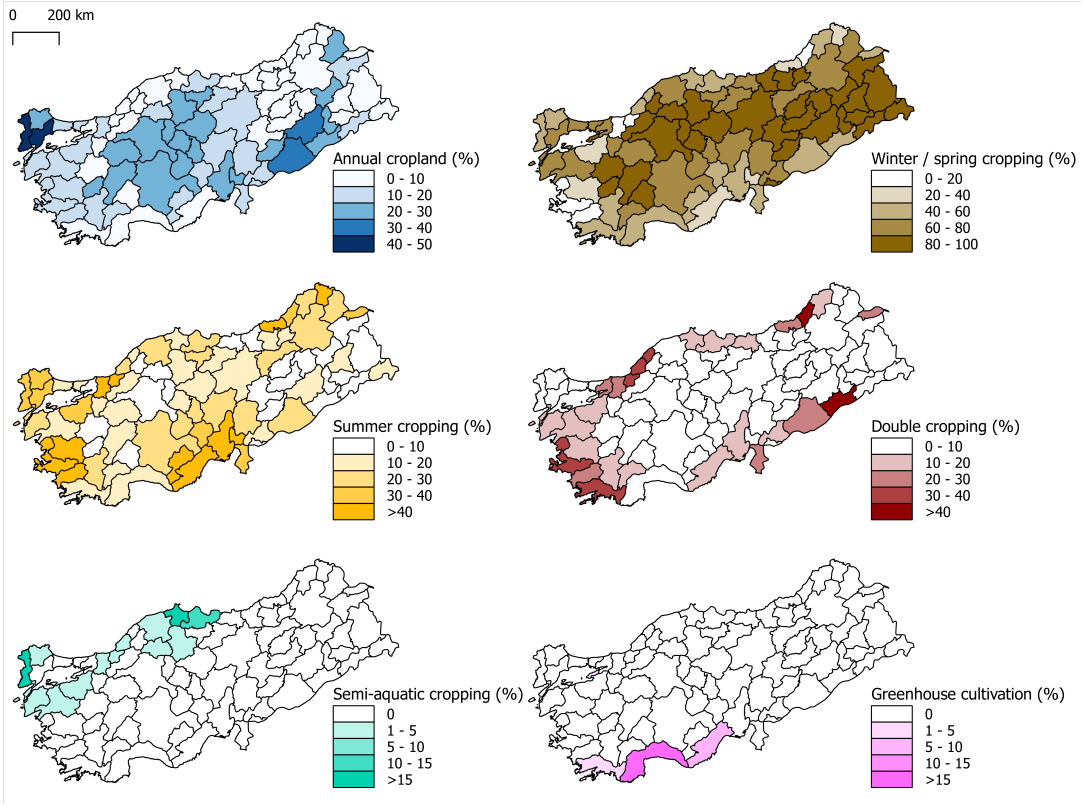

Figure 4.8: Province-level (NUTS-03) share of annual cropland on total province area (top left) and shares of cropping practices in percent of all cropland.

4.4 Discussion

The openly accessible Landsat archive provides unseen opportunities for informing land use intensity assessments over large areas. The presented study generated a set of good practice recommendations for mapping cropping practices over large areas, considerations for transferring the presented approaches into eras with different sensor constellations, uncertainties related to our approach, as well as insights concerning Turkey's cropland management regimes.

4.4.1 Good practice recommendations

We highlight that the binning of dense image time series within pre-defined temporal windows is an efficient technique to produce widely consistent image features over space and time. Overall, the robustness, high classification accuracies and spatial consistency of our maps demonstrate the applicability of currently operational

sensor constellations for mapping cropping practices across environmental and management gradients. We were able to identify some patterns when testing several temporal binning schemes and methods, which translate into a set of good practice recommendations.

First, retaining the seasonal information contained in the intra-annual time series is of utmost importance for mapping cropping practices. Our tests revealed that annual binning into spectral-temporal metrics or time series statistics performed poorly, as the phenological information is lost (Figure 4.2). In line with a recently presented approach on crop type mapping (Griffiths et al., 2019), increasing the temporal resolution of the included features had a positive impact on classification accuracies. We thus suggest narrow, e.g., near-weekly binning wherever data availability allows for satisfactory spatial coverage during cloud-prone seasons. Alternatively, quarterly binning provided a good trade-off between temporal detail and observation availability that allowed for producing robust results on national, up to continental scales (Phalke and Özdoğan, 2018).

Second, summer composites and spectral-temporal metrics produced satisfactory overall accuracies for Turkey. Thus, images from June to September essentially describe the spectral-temporal characteristics of our target classes. However, other seasonal windows might be more important when applying the approach in regions with different climate or management regimes. Similar to a study focusing on continental scale cropland mapping (Phalke and Özdoğan, 2018), classification accuracies increased when features from all quarters were included. Doing so presents an alternative to data-driven identification of the phenologically relevant season for accurate class discrimination or expert knowledge acquisition, as the first is challenging to implement and the latter is commonly not available in a spatially explicit manner across large areas.

Third, including auxiliary features describing geographic location and topography improved mapping accuracy. In line with other studies (Pflugmacher et al., 2019), we thus recommend the integration of such features in large area mapping as a common practice.

Our mapping efforts were relatively inexpensive. Two trained interpreters conducted the collection of training data and labeling of validation points in 320 work hours. Overall computation times were below two weeks for pre-processing, computation of all temporal features, and classification. However, we performed all computations using multi-core processing, which reduced processing times substantially. Storage space requirements were highest for pre-processed Landsat data (2.6 TB), composites and spectral-temporal metrics (0.8 TB) as well as Tasseled Cap time series and statistics (0.4 TB), but can be further reduced via image compression. In cases where processing and storage infrastructure is not available, processing can al-

ternatively be performed using readily available ARD on cloud processing platforms (Gorelick et al., 2017). The map product presented in this paper is available online (https://doi.pangaea.de/10.1594/PANGAEA.897547).

4.4.2 Temporal transferability

The applicability of individual methods is dependent on the operational sensor constellation during the period of interest. For past decades, highly irregular inter-annual acquisition densities in the Landsat archive pose challenges for long-term mapping approaches (Griffiths et al., 2018). Seasonally restricted spectral-temporal metrics are promising tools for mapping land use across large areas in past decades (Schmidt et al., 2016). Average clear-sky observation density across Turkey between 1984 and 2017 is rarely below three observations during summer, suggesting that efforts targeting the mapping of cropping practices in Turkey over past decades are potentially worthwhile. However, these demand analyses of the quality of spectral-temporal features under scenarios of scarce and temporally disperse observations.

On the contrary, mapping cropping practices in the years past 2015 will benefit from novel sensor constellations with higher revisit frequency, which increases the probability of cloud-free acquisitions. Improvements of sensor integration (Zhang et al., 2018; Claverie et al., 2018) and automated image processing (Frantz et al., 2018) now enable the combined use of intra-annual Landsat 8 and Sentinel 2A+B acquisitions for agricultural mapping applications (Griffiths et al., 2019). Increased observation density will likely improve the mapping of cropland management interventions, such as harvests, or flooding of semi-aquatic crops. Recent advances suggest also the applicability of radar data to further supplement mapping efforts at high thematic detail (Mansaray et al., 2017), which can also be temporally aggregated for large area applications (Baumann et al., 2018).

4.4.3 Uncertainties and limitations

The products generated here meet common quality criteria regarding classification accuracy, and the high spatial consistency and thematic detail of these maps have the potential to satisfy the growing need for land use intensity datasets covering large areas (Pongratz et al., 2017; Kümmerle et al., 2013). However, remaining uncertainties relate to underestimated cropland extent and the omission of semi-aquatic cropping. We underestimated cropland extent by 25%, mostly due to confusion between spring crops and grasslands, as both classes represent herbaceous vegetation layers underlying precipitation-driven phenology and management interventions. Differences in cropland area estimates can be reduced by employing adaptive thresholds for classification probability, in order to match higher quality area estimates, such as

province-level statistics (Song et al., 2017). The omission of semi-aquatic cropping occurred due to the confusion with summer cropping, owing to strong phenological similarities. This insight supports the hypothesis that image availability during the flooding stage is crucial for accurate representation of semi-aquatic crops, such as paddy rice (Kontgis et al., 2015). While our study aims at the characterization of annual croplands, spatially explicit information on grasslands and perennial croplands is essential for a better characterization of agricultural land use intensity (Pongratz et al., 2017). In 2015, permanent pastures accounted for 14.6 Mha and perennial croplands for 3.3 Mha in Turkey (TSI, 2015), highlighting the need for detailed characterization of perennial crop systems to improve the understanding of the entire production system. However, the mapping of perennial croplands and grasslands poses various challenges from a remote sensing perspective (Vieira et al., 2012; Senf et al., 2013; Ali et al., 2016). These arise from heterogeneous class characteristics (crop type, grass species, phenology, planting density, irrigation, mowing frequency) and the lack of datasets that allow for discriminating natural from managed grasslands, as well as cropped plantations from timber plantations.

4.4.4 Cropland intensity and water resources in Turkey

Cropland management strongly determines agricultural water requirements (Döll and Siebert, 2002; Rockström et al., 2010). We show that vast areas of annual croplands exist in semi-arid parts of Turkey, where total annual precipitation ranges between 200 mm and 600 mm, with near-zero precipitation during summer and particularly high evaporation rates (FAO, 2009a). While we show that spring and winter cropping, covering extensive areas of winter cereals with relatively low water requirements, dominate in Turkey (FAO, 2009a; Lopes et al., 2018), our results reveal that 28% of the national cropland area was cultivated during summer in 2015 (including summer, double, and semi-aquatic cropping). The recent expansion of irrigated agriculture, coupled with high irrigation water requirements led to a 48% increase in agricultural water requirements between 1992 and 2008 (FAO, 2015). In the case of the South-East Anatolia Project, the expansion of irrigated cotton cultivation successfully boosted the regional economy (Altinbilek and Tortajada, 2012), yet this occurred at the cost of drastic water consumption increases (Özdoğan and Woodcock, 2006a; Yesilnacar and Uyanik, 2005).

Current irrigation water use in Turkey is excessive and inefficient (Kibaroğlu et al., 2011). Generally low water prices due to a lack of volumetric pricing schemes foster excessive water use (Cakmak, 2010). Irrigation efficiencies in Turkey commonly do not exceed 50%, mostly due to the prevalence of surface irrigation, and high conveyance losses (Koç, 2017). While the Turkish government envisions a 73% expansion of irrigated agriculture until 2030 (Büyükcangaz et al., 2007), doing so

without drastic institutional, agronomic and engineering changes poses a threat to the national water resource base. Climate change further aggravates crop water deficits across Turkey (EEA, 2016), causing yield declines on rainfed and irrigated croplands (Saadi et al., 2015; Yano et al., 2007). The adoption of more efficient irrigation techniques offers water savings potential in the region (Ertek and Yilmaz, 2014), whereas saved water can be re-allocated and enable irrigation in other production systems (Büyükcangaz et al., 2007; Jägermeyr et al., 2016). Improving water use efficiency through reduced conveyance and evaporative losses is thus imperative to foster more sustainable production and should be of utmost priority of planning authorities to prevent water scarcity and maintain environmental flow requirements in future intensification pathways (Jägermeyr et al., 2017).

4.5 Conclusion

We based our approach exclusively on openly available datasets (Landsat Collection 1 imagery) and algorithms (FORCE v1.1) that allow for streamlining pre-processing chains and producing analysis-ready datasets. We thereby demonstrated the benefits of openly accessible satellite image datasets and pre-processing frameworks for improving our understanding of agricultural land use intensity across large areas. This study provides a robust mapping framework to disentangle annual cropland management, using Turkey as a case study.

The fine spatial and temporal detail of the resulting maps allow for tracking cropping practices at 30 m spatial resolution and at annual intervals. Our maps can reveal areas of low cropland use intensity, such as rainfed cultivation on small parcels or fallow croplands, as opposed to intensity hotspots, such as double-cropped areas, flood-irrigated croplands, or areas with greenhouse cultivation. This is a substantial improvement compared to statistics at aggregated units, or other map products of reduced thematic detail, or coarser spatial or temporal resolution. The detail of our maps has the potential to inform stakeholder-related processes and assessments of land and water resource consumption over large areas.

We formulated good practice recommendations for binning Landsat time-series into temporal features for wall-to-wall characterization of cropping practices. We recommend binning into quarterly or finer temporal windows, wherever data availability is sufficient. We achieved the best classification results by using quarterly composites and spectral-temporal metrics, or gap-filled time series of Tasseled Cap components as input features. Auxiliary features on topography and geographic location improved classification accuracies throughout. Knowledge of regional phenological characteristics of the target classes is essential. However, we generally recommend the integration of features from multiple seasons, when difficulties in

identifying key phenological windows prevail.

The generic temporal binning of all available clear sky observations into eight-day or quarterly time windows was a successful strategy in a Mediterranean setting, but is likely applicable in climatic zones with a good data availability in the growing season. In this light, transferring our approach to other regions and eras requires investigating the effect of observation density on the consistency of temporal features, to determine minimum data requirements and subsequent trade-offs in mapping accuracies. The presented methods are potentially applicable across yearly time series to get insights into the inter-annual cropland management dynamics and to derive efficiency indicators such as irrigation ratios. Complementing the presented methods with techniques for detecting parcel sizes (e.g., Graesser and Ramankutty, 2017; Yan and Roy, 2016) could enable the long-term evaluation of governmental land consolidation policies. Such information could ultimately improve our understanding of long-term developments of cropland management and thus land and water resource demand at the regional to continental scale.

Acknowledgments

This research contributes to the Landsat Science Team and the Global Land Programme. All authors acknowledge and appreciate the United States Geological Survey's efforts in providing Landsat data. We thank the Turkish Statistical Institute for providing province-level statistics and the Global Food Security-Support Analysis Data at 30 m project for their efforts in global scale cropland mapping.

Supplementary materials

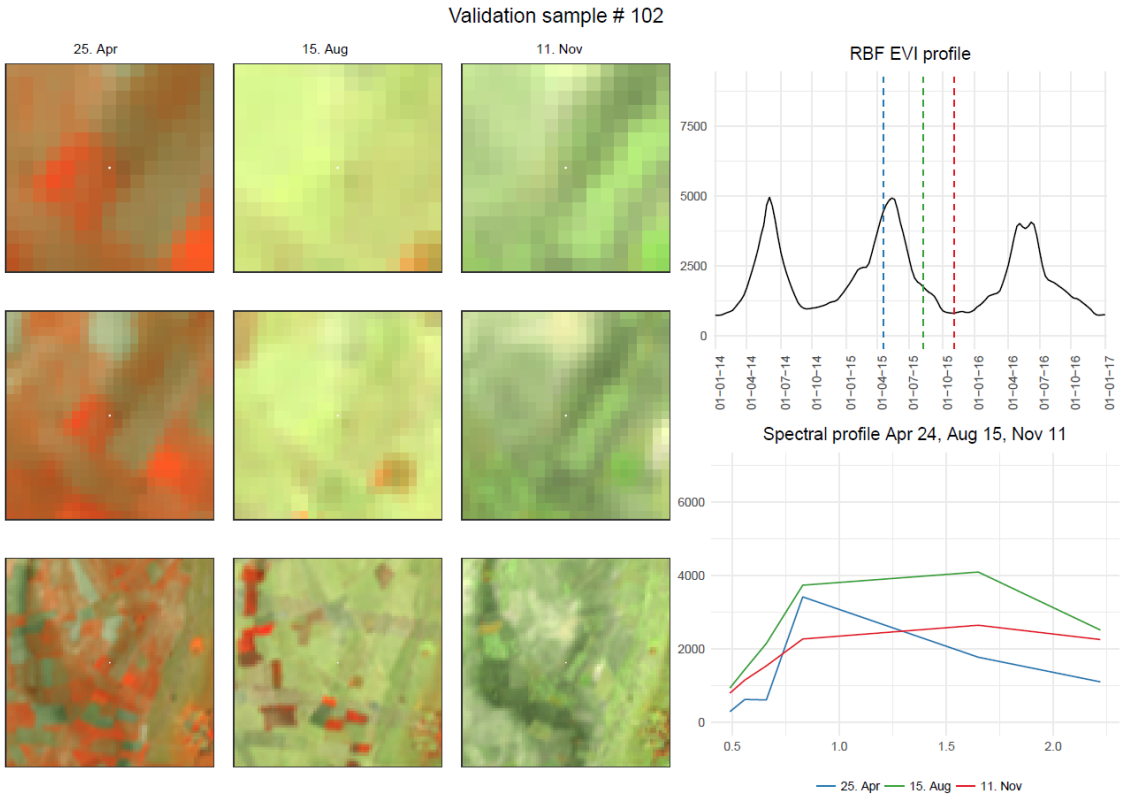

Figure S4.1: Validation pixel protocol for class spring / winter cropping.

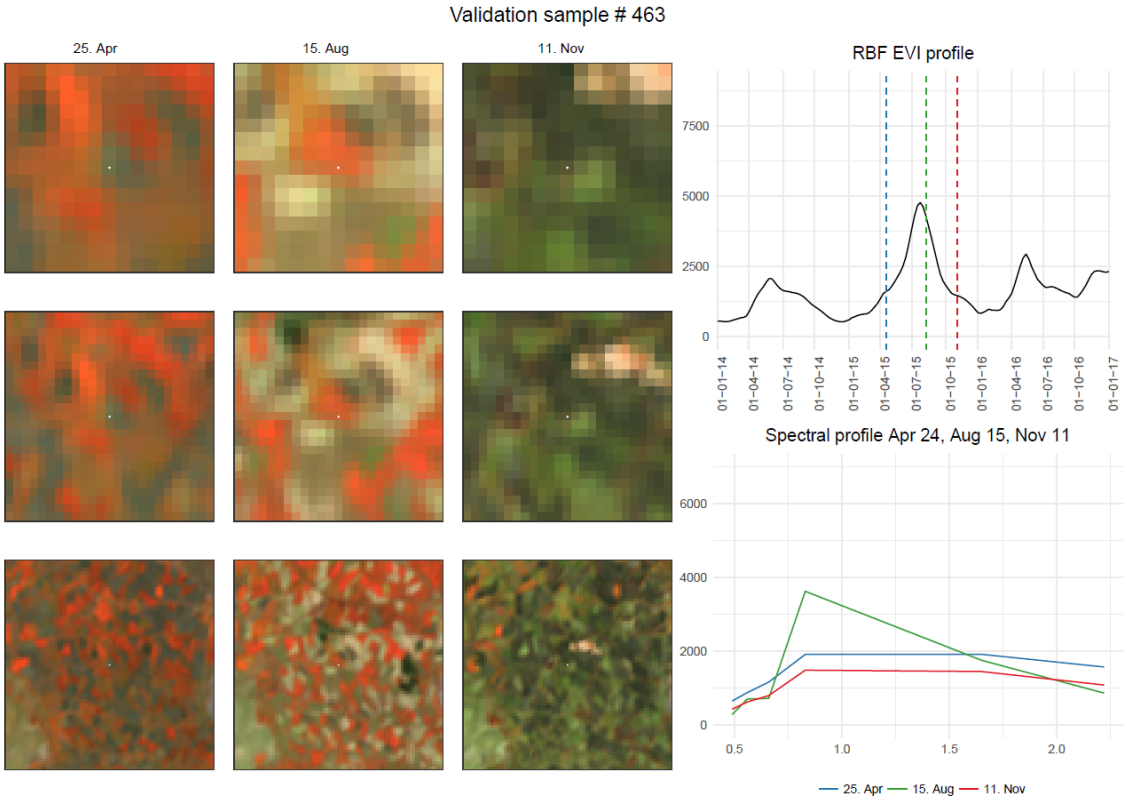

Figure S4.2: Validation pixel protocol for class summer cropping.

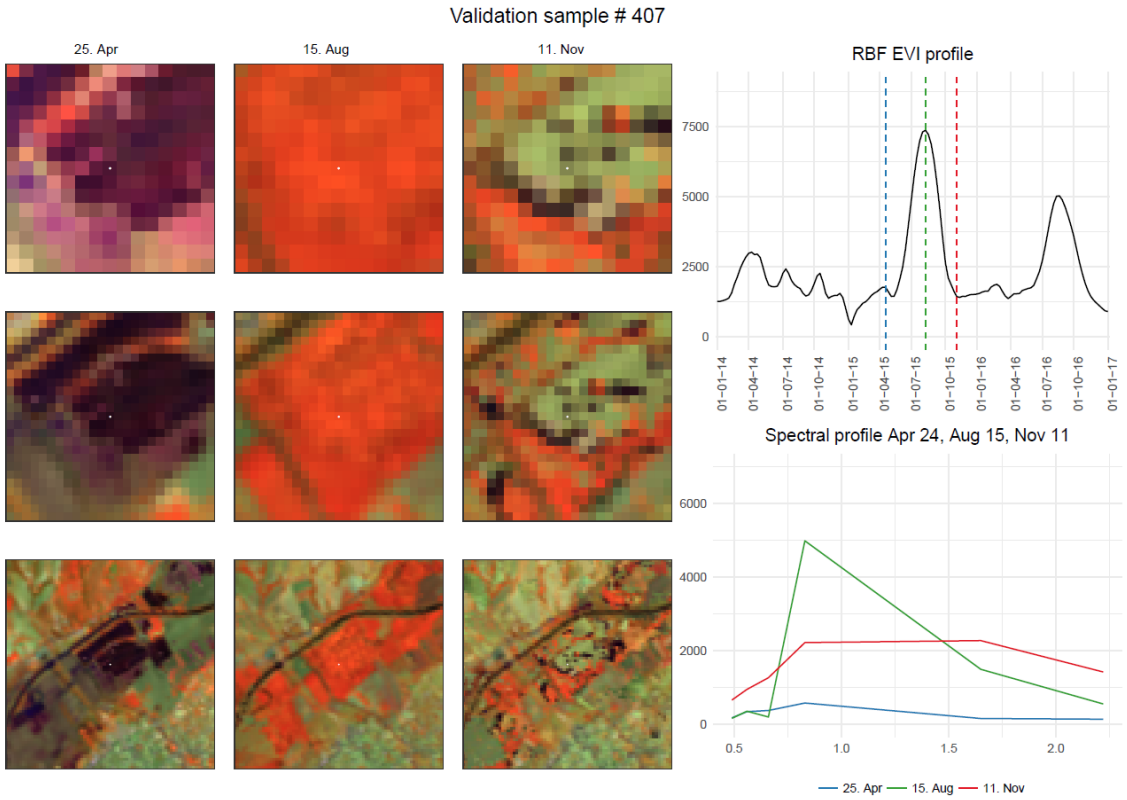

Figure S4.3: Validation pixel protocol for class semi-aquatic cropping.

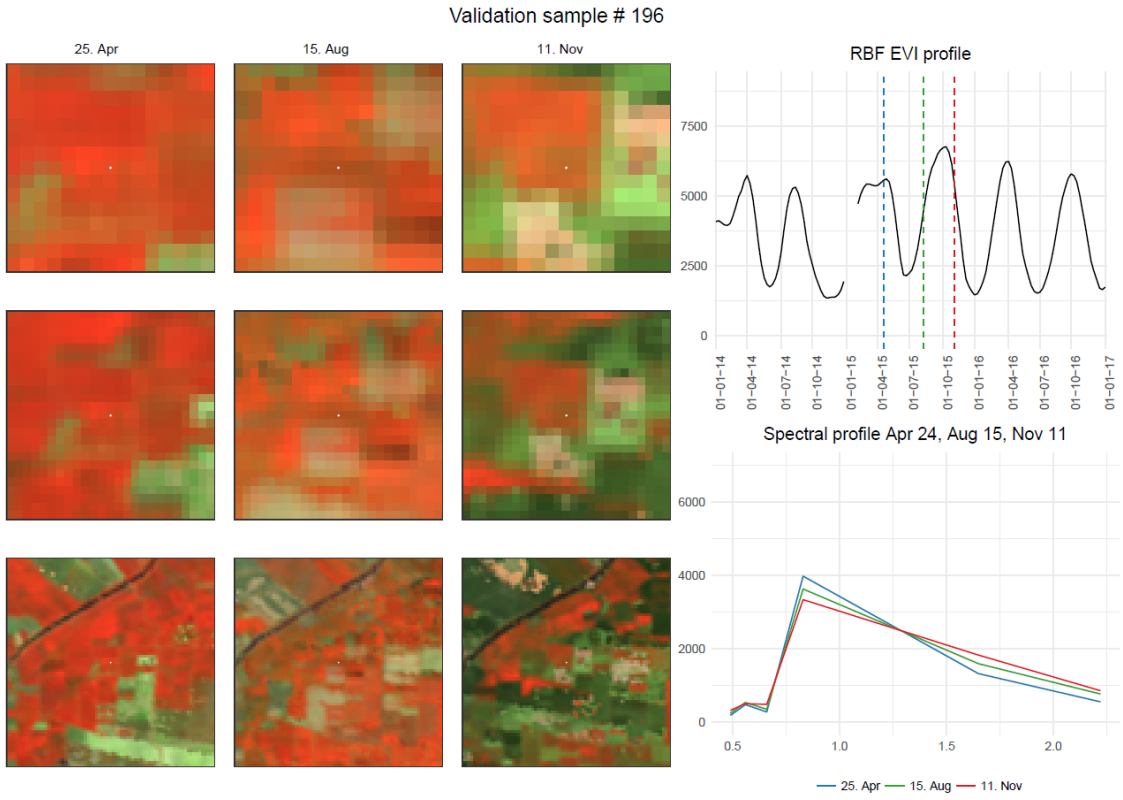

Figure S4.4: Validation pixel protocol for class double cropping.

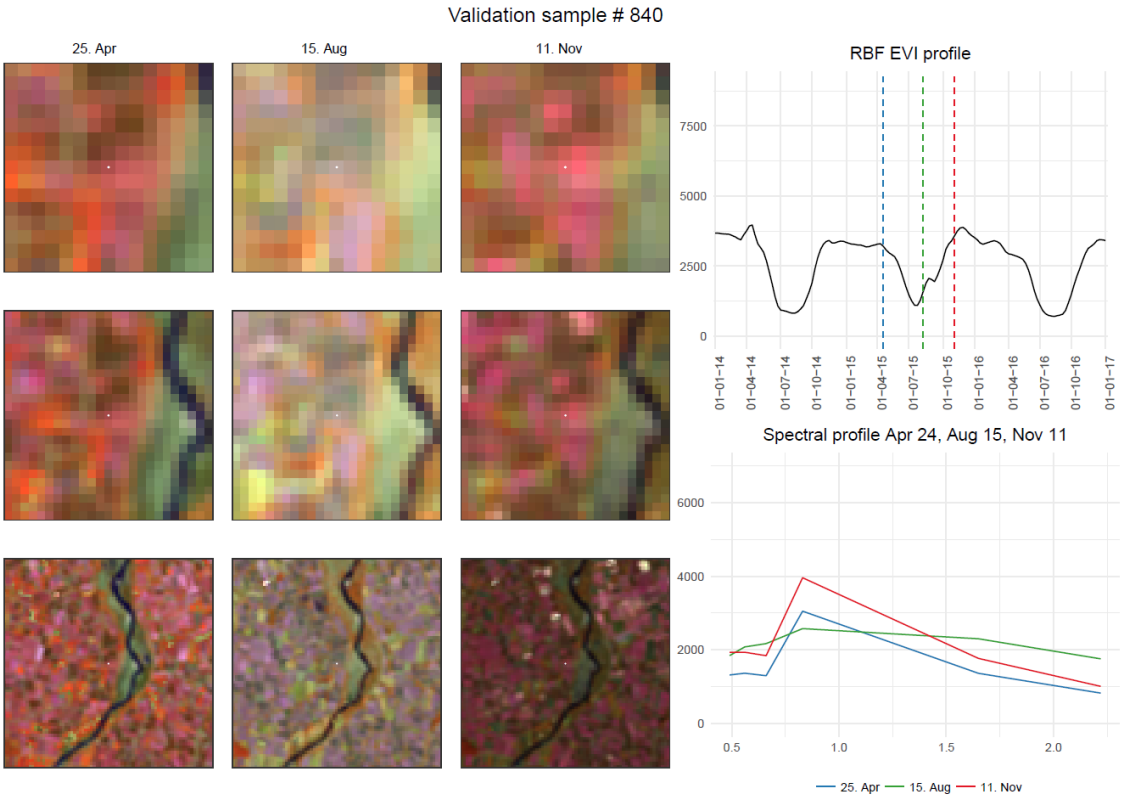

Figure S4.5: Validation pixel protocol for class greenhouse cultivation.

Table S4.1: Confusion matrix for variable subset "ALL". Rows contain map information, columns contain reference dataset. Cells populated with probabilities according to Olofsson et al. (2014). WC: winter cropping, SC: summer cropping, AC: semi-aquatic cropping, DC: double-cropping, GH: greenhouse cultivation.

	WC	SC	AC	DC	GH
WC	0.6953	0.0085	0.0042	0.0127	0.0000
SC	0.0129	0.1528	0.0258	0.0110	0.0018
AC	0.0000	0.0014	0.0050	0.0001	0.0000
DC	0.0047	0.0071	0.0000	0.0544	0.0000
GH	0.0000	0.0001	0.0000	0.0000	0.0021

Table S4.2: Confusion matrix for variable subset "QRT_CMP_STM". Rows contain map information, columns contain reference dataset. Cells populated with probabilities according to Olofsson et al. (2014). WC: winter cropping, SC: summer cropping, AC: semi-aquatic cropping, DC: double-cropping, GH: greenhouse cultivation.

	WC	SC	AC	DC	GH
WC	0.6996	0.0085	0.0042	0.0085	0.0000
SC	0.0166	0.1620	0.0184	0.0037	0.0037
AC	0.0000	0.0014	0.0050	0.0001	0.0000
DC	0.0083	0.0154	0.0000	0.0426	0.0000
GH	0.0000	0.0001	0.0000	0.0000	0.0021

Table S4.3: Confusion matrix for variable subset "WKL_TC". Rows contain map information, columns contain reference dataset. Cells populated with probabilities according to Olofsson et al. (2014). WC: winter cropping, SC: summer cropping, AC: semi-aquatic cropping, DC: double-cropping, GH: greenhouse cultivation.

	WC	SC	AC	DC	GH
WC	0.6953	0.0085	0.0042	0.0127	0.0000
SC	0.0129	0.1473	0.0313	0.0129	0.0000
AC	0.0000	0.0015	0.0049	0.0001	0.0000
DC	0.0047	0.0083	0.0000	0.0520	0.0012
GH	0.0000	0.0000	0.0000	0.0002	0.0020

Table S4.4: Confusion matrix for variable subset "WKL_TC_STATS". Rows contain map information, columns contain reference dataset. Cells populated with probabilities according to Olofsson et al. (2014). WC: winter cropping, SC: summer cropping, AC: semi-aquatic cropping, DC: double-cropping, GH: greenhouse cultivation.

	WC	SC	AC	DC	GH
WC	0.6953	0.0085	0.0042	0.0127	0.0000
SC	0.0129	0.1436	0.0313	0.0166	0.0000
AC	0.0000	0.0016	0.0048	0.0001	0.0000
DC	0.0047	0.0047	0.0000	0.0556	0.0012
GH	0.0000	0.0000	0.0000	0.0001	0.0020

Chapter 5

Mapping the extent and frequency of irrigated summer cropping in Southeastern Anatolia since 1990 using Landsat data

Philippe Rufin, Daniel Müller, Marcel Schwieder, Dirk Pflugmacher, and Patrick Hostert

In preparation for submission.

Abstract

Irrigation enables more intensive use of land and is thus essential for meeting the world's rapidly growing demands for food, feed, fuel, and fiber. Mapping irrigated croplands at high spatial detail over long periods allows assessing the state and performance of irrigated agricultural systems, for instance, regarding the area equipped with irrigation infrastructure, the frequency of annual cropping, or water consumption. We used intra-annual Landsat time series to map the expansion and frequency of irrigated summer cropping for the largest irrigation scheme of Turkey. We combined spectral-temporal features with a generalized classification model for producing annual maps of summer cropping from 1990 to 2018 at 30 m spatial resolution. Overall accuracies of the resulting annual maps ranged between 98.1% and 99.8%. We found a tendency for the omission of summer crops in the early years of our study period, which was sensitive to the number of available clear sky observations per year ($R^2 = 0.3$). We used post-classification analyses to reveal the spatial patterns and trends of summer-cropped area as well as cropping frequency. In 2018, the region comprised a summer-cropped area of 577,887 ha (± 47,932 ha), corresponding to a 617% expansion compared to 1990. The croplands in the study region were cropped during summer only every second year, indicating that half of the irrigation infrastructure remained idle on an annual basis. High summer cropping frequency (cropped in more than 80% of the years) were found in only 16% of the study area. Summer cropping frequency remained temporally stable in almost half of the study area. Contrastingly, 19% of the observed area showed a significant trend for decreasing, and 43% for increasing levels of cropping frequency over time. Our approach highlights novel opportunities for detailed mapping of the spatio-temporal evolution of irrigation schemes and their performance using openly accessible satellite imagery.

5.1 Introduction

Land use intensification boosted crop production globally, specifically since the onset of the Green Revolution in the middle of the 20^{th} century (Ramankutty et al., 2018). Irrigation has been a core component for the global increase in crop production, as it enabled to overcome essential limitations for production in water-scarce regions and periods with insufficient precipitation (Johansson et al., 2016; Elliott et al., 2014). However, inefficient use of land and water resources often hampers irrigated agriculture (Gerten et al., 2011; Jägermeyr et al., 2015), and equipped areas are thus underused at the global scale (Siebert et al., 2013). Excessive irrigation increases the risk of water scarcity, leads to soil salinization, and thus poses a threat to future crop production (Mekonnen and Hoekstra, 2016; Porkka et al., 2016; Singh, 2016). Region-specific constraints including, e.g., unfavorable climate and topography, or the necessity to transfer irrigation water over long distances were suggested to hamper the successful implementation of irrigation infrastructure and to compromise irrigation-induced productivity increases (Neumann et al., 2011; Rufin et al., 2018).

Irrigated agriculture offers the potential to overcome production deficits in water-limited regions through more intensive use of land (Rosa et al., 2018; Malek et al., 2018). The water inputs and capital investments required for irrigation enable for boosting yields (Lobell et al., 2009) and for increasing the input of land into the production system (Erb et al., 2013). The latter comprises cropland expansion on previously unused land, a reduction of fallow years, or the introduction of additional cropping cycles (Foley et al., 2011; Rufin et al., 2018). However, the current knowledge of the spatial patterns and magnitudes of these individual processes is scarce (Ray and Foley, 2013). Statistics and reports on the extent and use intensity of irrigated lands are costly to produce and underlie potential bias due to over- or under-reporting of water use. In this light, cost-efficient monitoring of land and water resource use in irrigated production systems is necessary.

Remote sensing offers great potential for monitoring the extent and land use intensity of irrigated agriculture across administrative borders, institutional settings, as well as management regimes (Deines et al., 2017; Löw et al., 2018; Özdoğan et al., 2010). Annual information on irrigated area extent at appropriate spatial resolution provides useful means for understanding the spatio-temporal patterns and trends of land-use intensity across spatial scales, which can support land-use planning and policy towards attaining more efficient land and water resource use in water-limited production systems (Ambika et al., 2016; Chen et al., 2018). In recent years, openly available remote sensing data archives fueled data-driven applications, encompassing decadal historical analyses and near-real-time monitoring applications over large areas (Wulder et al., 2012; Wulder and Coops, 2014). Specifically, the Landsat data record provides a suitable basis for such applications, as it spans more than

three decades at 30 m spatial resolution with global coverage (Wulder et al., 2008). Utilizing standardized spectral-temporal features from intra-annual time series was highlighted as a means to improved classification of land cover or land use at high thematic details and across large areas (Rufin et al., 2019b; Wulder et al., 2018). Spectral-temporal features in combination with state-of-the-art machine learning algorithms enable cost-efficient production of multi-decadal thematic maps in agricultural systems (Schmidt et al., 2016; Waldner and Defourny, 2017), which in turn allow for capturing land-use intensity indicators (Deines et al., 2017).

The Güneydoğu Anadolu Projesi (GAP) represents one of Turkey's largest infrastructure investments, located in the semi-arid southeast of Anatolia. The GAP aimed at diverting and storing water from the Euphrates and Tigris rivers to irrigate 1.8 million hectares (Mha) of arable land. Construction of the GAP commenced in 1989 and completion was originally envisioned for 2005. However, the currently operational irrigation infrastructure covers only 0.5 Mha (GAP, 2017). Large parts of the GAP are delayed or on hold due to geopolitical and socio-cultural disputes, which hampered the development of the planned irrigation infrastructure (Hommes et al., 2016). The operational areas are widely used for the production of water-intensive export commodities such as cotton (Bilgen, 2018a; USDA, 2018). However, a substantial fraction of the croplands equipped with irrigation infrastructure is not irrigated on an annual basis, causing a strong spatio-temporal variability in cropping frequency, the determinants of which remain elusive (Degirmenci et al., 2006).

Irrigation can contribute to an intensification of the production systems in Southeastern Anatolia, and a better understanding of the performance of irrigation systems is therefore urgently needed (Malek et al., 2018). Tracking the spatio-temporal evolution of irrigated areas in the GAP region can shed light on the spatial patterns of irrigated land, its long-term cropping frequency, and on the conditions under which varying levels of cropping frequency occur. In this study, we analyzed the Landsat archive from 1990 through 2018 to create annual maps of summer-cropped areas at 30 m resolution, which serve as proxies for irrigation in the semi-arid GAP region. We thereby tracked the temporal evolution of irrigated summer cropping and evaluated the cropping frequency on these lands. Furthermore, we identified areas which experienced distinct intensification or dis-intensification trends during their operational lifetime. We specifically investigated the following research questions:

- How did summer-cropped areas in the GAP region expand between 1990 and 2018?
- What are the spatial patterns of summer cropping frequency in the GAP region?
- Which trends in summer cropping frequency were apparent in the GAP region

between 1990 and 2018?

5.2 Data and methods

5.2.1 Study area

The Güneydoğu Anadolu Projesi (GAP) is a large-scale development project covering 75,000 km^2, accounting for nearly 10% of the Turkish land area across nine provinces in South-Eastern Anatolia (Figure 5.1). The region has a semi-arid climate with precipitation between 200 and 600 mm/year, while potential evaporation frequently exceeds 2,000 mm/year. The GAP was developed in the late 1970s by the Turkish State Hydraulic Works, with envisioned completion in 2005 (Bilgen, 2018b), but is currently still under development due to numerous delays (Kankal et al., 2016). The land and water resource program of the GAP comprised infrastructure development, including 22 dams for electricity generation and irrigation water provision, as well as 1,400 km of irrigation canal networks and tunnels for long-distance water allocation. Two major tunnel systems deliver irrigation water from the Atatürk reservoir in Adıyaman province to the Harran and Ceylanpınar plains in Şanlıurfa since April 1995 (UNEP, 2004). The overall target of the GAP was the expansion of irrigation on 1.8 Mha of land. However, by 2017, the total land area under irrigation was reported to cover 545,938 ha; thus only 30% of the target was reached (GAP, 2017).

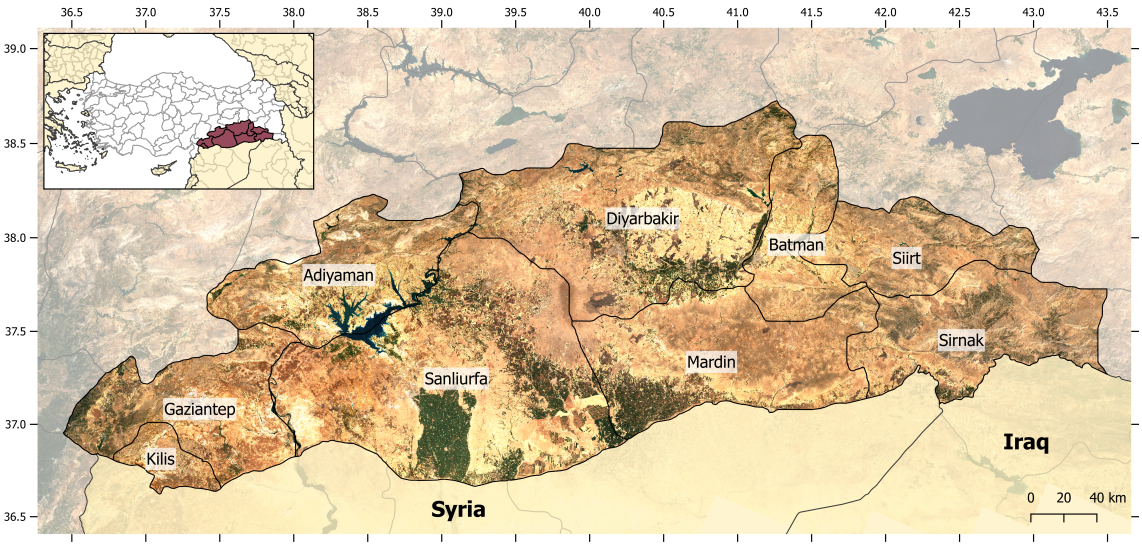

Figure 5.1: Provinces of the GAP region in Turkey. True color satellite image (composited from Landsat ETM+ and OLI data) represents mid-August 2015.

Near-zero precipitation during July, August, and September requires irrigation for summer cultivation (Özdoğan et al., 2006). Consequently, the region was domi-

nated by rainfed cultivation of winter and spring crops before initiation of the GAP irrigation scheme. The main winter and spring crops are wheat, barley, and pulses such as lentils and chickpeas. Winter crops, such as wheat are commonly harvested until the end of June (Metin Sezen and Yazar, 2006), while irrigated summer crops are mostly cotton and corn (Figure 5.2). Since project launch, the share of irrigated cotton cultivation increased drastically in the GAP region, covering 310,000 ha in 2018, which corresponds to 56% of the national cotton production area of Turkey (USDA, 2018). Cotton cultivation in the GAP region has very high irrigation water demands, in comparison with other regions of Turkey (Ertek and Yilmaz, 2014).

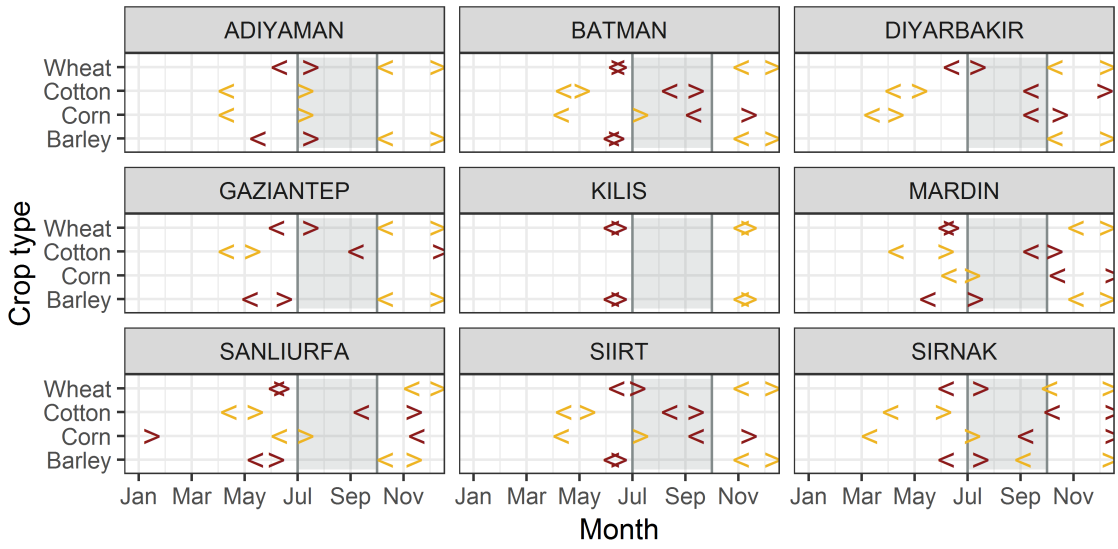

Figure 5.2: Regional crop calendar, indicating the start (<) and end (>) of the planting phase (yellow) as well as the start (<) and end (>) of the harvest period (red) for four major crops in the GAP region. Grey shading indicates the observation time window defined in this study. Data compiled by the Turkish Ministry of Agriculture and Forestry (TARIM, 2015). Planting and harvesting dates were not available for all crops and provinces.

5.2.2 Mapping summer-cropped areas

We produced a total of 29 annual maps of summer-cropped areas for the period 1990-2018 in several steps. First, we collected training data for a single year of good data availability (2015). Second, we computed Landsat-based spectral-temporal variability metrics for each summer growing season between 1990 and 2018. Third, we trained a generalized classification model for the year 2015 and applied it to the spectral-temporal features of the yearly data from 1990 to 2018. Finally, we assessed the mapping accuracy and area estimates.

Training data collection

We targeted a binary class catalog consisting of summer-cropped areas and other types of land cover or land use. The summer-cropped class included areas of summer cultivation and areas with two harvests in the same year. Other land cover categories included water, non-vegetated land, grassland, open to closed canopy shrublands and forests, but also irrigated winter crops (cereals and pulses), irrigated perennials (pistachio and olive trees), as well as summer-fallowed areas. We collected training data as polygons with a minimum mapping unit of nine pixels (0.81 ha) and a maximum size of 30 ha using pixel-based Landsat composites (Frantz, 2017; Griffiths et al., 2013a), a gap-filled time series of the Enhanced Vegetation Index (EVI) covering 2014-2016 (Rufin et al., 2019b), and very high resolution imagery available in Google Earth. We collected 568 training polygons across the GAP provinces, of which 37% represented summer-cropped areas. We used all pixels entirely located within the polygons (n = 10,780) for classification model training.

Spectral-temporal variability metrics

Spectral-temporal metrics are suitable to generate gap-free datasets over large areas, while at the same time providing information on land surface phenology, and have been used in large-area mapping applications in agricultural landscapes (Phalke and Özdoğan, 2018; Rufin et al., 2019b; Waldner et al., 2017). We used Google Earth Engine (Gorelick et al., 2017) for producing a set of spectral-temporal metrics to discriminate summer cultivated areas from the remaining land use and land cover classes in the GAP region. We used all available precision terrain corrected images of the Landsat Collection 1 Surface Reflectance product (L1TP Tier 1), covering the growing season of summer crops (July 1st to September 30th, Figure 5.2) in the GAP area for the years 1990 to 2018. This time window coincides with the maturity stage of summer crops and has been shown to provide valuable information for Landsat-based mapping of summer cropping amongst other cropping practices across Turkey (Rufin et al., 2019b). We performed cloud, cloud-shadow, and snow masking based on the cloud information contained in the Landsat Collection 1 quality bands (Zhu et al., 2015). We compiled six spectral-temporal metrics for each of the six spectral bands of Landsat 5, Landsat 7, and Landsat 8 at the pixel level, resulting in a total of 36 spectral-temporal features. We calculated band-wise spectral-temporal features that capture the distribution of reflectance values (25^{th} percentile, median, 75^{th} percentile, interquartile mean), as well as the variability of reflectance in the summer period (standard deviation and interquartile range). We further derived the average number of clear sky observations available each year.

Classification

We trained a Random Forest classification model (Breiman, 2001) based on the training samples and the spectral-temporal features of 2015. We used 250 trees and the square root of the number of input features at each split to identify the best feature. We subsequently used this generalized classification model to classify the spectral-temporal features from all years, resulting in a time series of 29 binary maps covering the years 1990 to 2018. We eliminated areas with only one year of summer cultivation over the study period for the subsequent analyses to reduce the effect of one-time commission errors on further analysis steps (Deines et al., 2017).

Post-classification analyses

We derived indicators of changes in land use and land use intensity in the study region. First, we derived a layer with the first year under summer cropping to characterize the expansion of irrigated area over time. Second, we calculated the total number of years under summer cropping in the study period. Third, we derived summer cropping frequency (SCF) as the percentage of all summer cultivated years after (i.e., excluding) the first year of summer cropping (Figure 5.3 A). Fourth, we derived five-year summer-cropping frequency (5-year SCF) at an annual basis. 5-year SCF was calculated within a five-year moving window, yielding the share of years under summer cultivation. Due to the five-year window, this indicator was derived only two years after the initial cultivation, and until 2016. Fifth, we performed a pixel-wise linear regression analysis between 5-year SCF and time to identify trends in the 5-year SCF. We performed this analysis for time series with a minimum length of five years, thus excluding areas commissioned after 2012. The analysis yielded a spatially explicit representation of the linear regression coefficients and their standard error. The regression slopes revealed positive and negative changes in cropping frequency during the operational lifetime of the summer-cropped areas, which were interpreted as indicators of intensification, or dis-intensification, respectively (Figure 5.3 B). We assessed the overall trend magnitude over the individual time series for each pixel and categorized the resulting positive or negative trend magnitudes into weak (trend magnitude of 25% - 50%), moderate (50% - 75%), and strong (75% - 100%), besides unsubstantial trend magnitudes (0% - 25%).

Accuracy assessment and area estimation

We used a stratified random sample of 1,260 Landsat pixels to estimate map accuracies and class areas. The validation sample size was estimated by targeting a 1% standard error of overall accuracy and assuming 90% user's accuracy for the summer cropping and other classes (Cochran, 1977). As strata, we used a map of

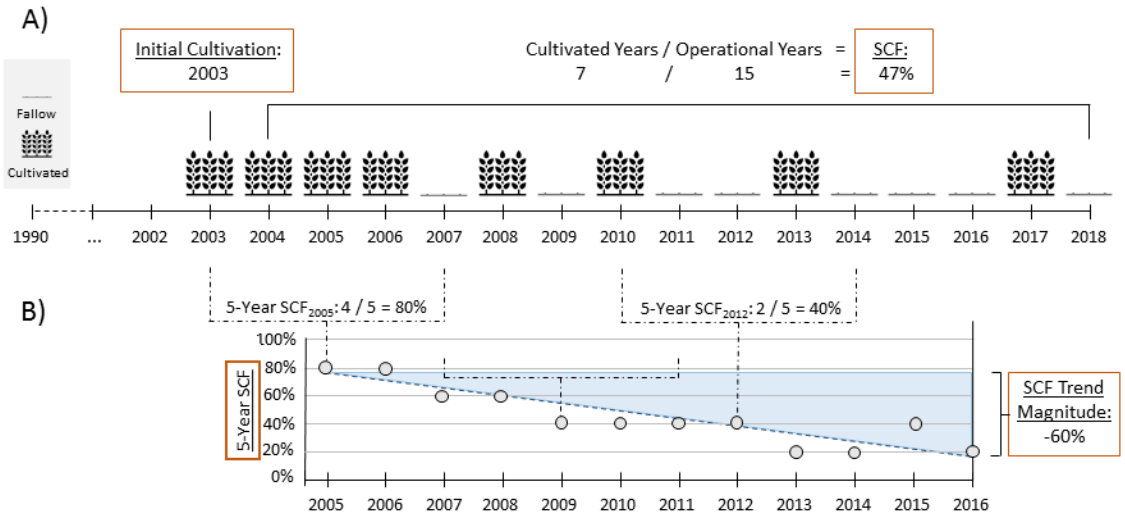

Figure 5.3: Schematic representation of pixel-level post-classification analyses. A time series of binary information on fallow or cultivated land was used to derive the initial cultivation year, SCF, 5-year SCF, and the linear trend.

the initial cultivation year to cover different cropping periods, leading to 40 samples per year and 100 samples in permanent non-cropped areas. Each validation pixel was labeled as either summer-cropped or other land cover using spectral time series plots and annual medoid composites (Flood, 2013), assuming that crop cover prevails throughout most parts of the summer period (Özdoğan and Woodcock, 2006b). We downloaded the composite time series using code produced for the TimeSync Legacy software (Kennedy et al., 2018) and visualized the composite time series in the EO Time Series Viewer (Jakimow et al., in prep). To aid interpretation and to exclude potential areas of permanent vegetation or seasonally inundated areas, we visually inspected each point location in high-resolution imagery available in Google Earth.

Class labels for 179 samples could not be determined due to mixed pixel effects, i.e., where samples were located amidst neighboring parcels and those in highly fragmented landscapes. The resulting 1,081 reference samples were used to estimate area-adjusted accuracies and area proportions of the summer-cropped area (Olofsson et al., 2014; Stehman, 2014). Additionally, we calculated the first year of summer cultivation, the number of years under summer cropping, and the SCF for the reference samples. These values were used to assess the accuracy of the mapped cropping intensity measures by calculating the R^2 and the RMSE. All spatially explicit analyses, as well as estimates of summer-cropped area at the province-level, were derived from the land cover maps.

5.3 Results

5.3.1 Map accuracy assessment

Area adjusted accuracies for the binary cropland maps underline the robustness of our approach (Table S5.1). Overall map accuracies range between 98.1% (± 0.8%) in 2009 and 99.8% (± 0.3%) in 1990. Map uncertainties mainly relate to the omission of summer crops, which resulted in varying producer's accuracies of the summer crop class (Figure 5.4, between 45.9% in 1995 and 97.5% in 2015). Producer's accuracies of the other land cover class were above 99% throughout. User's accuracies for summer crops ranged from 67.3% in 1993 to 97.1% in 1990 and were consistently above 98% for the other class. Generally, the producer's accuracies of the summer cropping class were lower in some of the early years of the study period, which partly corresponded with reduced data availability (Figure 4). In contrast, individual years with low data availability had high accuracies (e.g., 1990), and vice versa (e.g., 2009), and thus no clear relationship between data availability and accuracy was apparent. Linear regression analyses between the annual number of clear observations and overall accuracies, as well as class-wise user's and producer's accuracies revealed that the number of observations did not explain much of the variations in any accuracy measure (Table S5.2), except for the producer's accuracy of the summer cropping class (β_{nobs} = 2.42, standard error = 0.71, p-value = 0.002). Here, the number of clear sky observations explained nearly one third of the observed variance (R^2 = 0.30).

We found good agreement between the sum of summer-cropped years derived from our reference sample versus the predicted maps (R^2 = 0.93, RMSE = 1.8 years), whereas the most frequent errors represented one-time commission on permanent non-cropland (n = 77). The mapped year of initial summer cultivation also correlated well with values obtained from reference data (R^2 = 0.85, RMSE = 3.4 years), similarly to the cropping frequency measure (R^2 = 0.85 and an RMSE of 11.8%; Figure S5.1).

5.3.2 Expansion of summer-cropped areas

The start of the water transfer to Şanlıurfa and Mardin in 1995 marked the onset of summer cropping expansion in the GAP region. Error-adjusted area estimates revealed a 617% increase of summer-cropped area since 1990 (Figure 5.5), i.e., summer-cropped area increased from 93,553 ha (± 19,200 ha) in 1990 to 577,887 ha (± 47,932 ha) in 2018. While the expansion of summer-cropped areas follows a linear trend over time with an annual increase of 17,086 ha (standard error = 922 ha, R^2 = 0.93), individual years deviated from the trend (1995, 1998, 2007, and 2008).

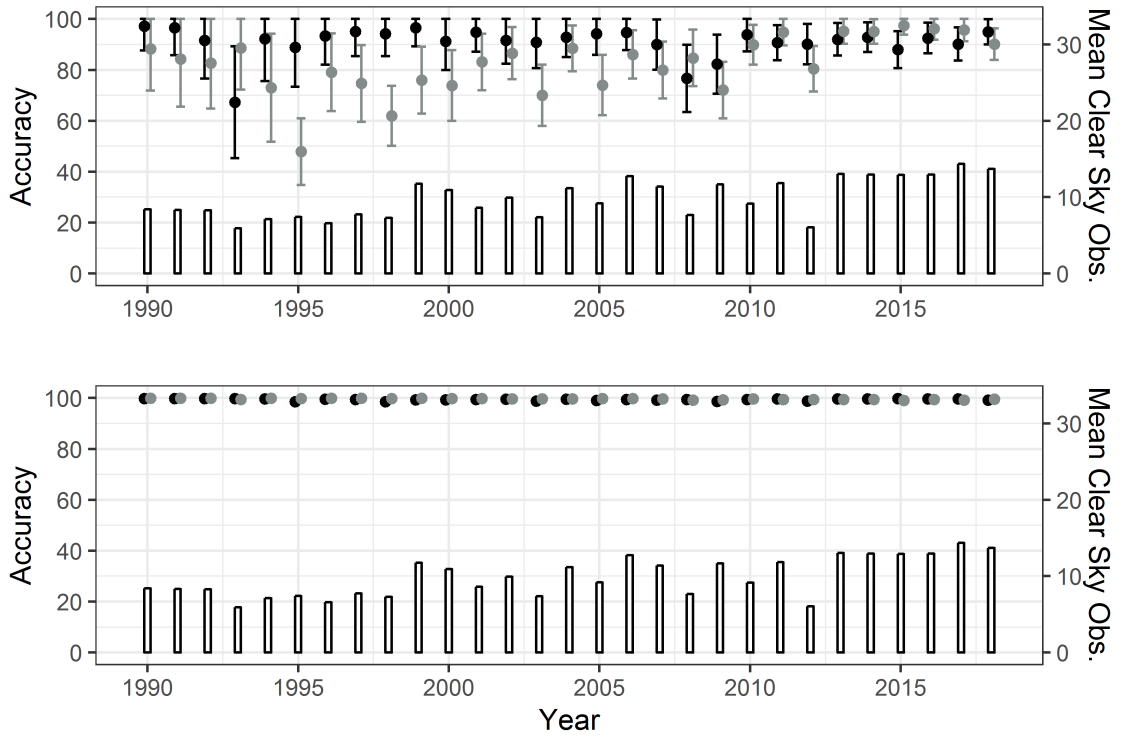

Figure 5.4: Estimates of user's (black) and producer's (grey) accuracy of the summer cropping (top) and others class (bottom). Error bars indicate 95% confidence intervals. Bars indicate the average number of clear sky observations in the respective year.

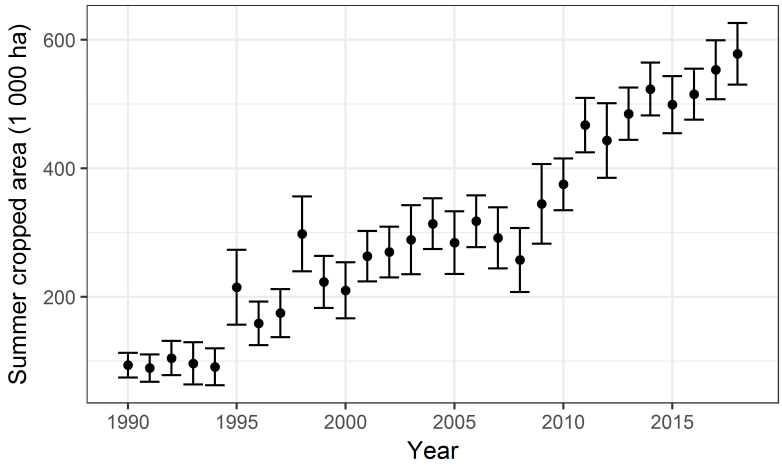

Figure 5.5: Annual error-adjusted area estimates of the summer-cropped area with 95% confidence intervals.

The year of initial summer cropping reveals past and present patterns of summer cropping expansion (Figure 5.6). Summer cropping expansion in the 1990-2000 period dominated in parts of Adıyaman (Figure 6 A), Şırnak (Figure 5.6 I) and the Şanlıurfa Harran plain (Figure 5.6 G), while more recent expansion was evident in parts of Diyarbakır (Figure 5.6 B), Gaziantep (Figure 5.6 C), western and

eastern Şanlıurfa (Figure 5.6 D, H), and Mardin (Figure 5.6 F). Large agglomerations of pivot-irrigated croplands replaced older rectangular parcels in the border region of Şanlıurfa and Mardin after 2010 (Figure 5.6 E). Regarding absolute area, the expansion of summer cropping concentrated widely in the central and southern provinces (Şanlıurfa, Mardin, and Diyarbakır; Table S5.3 and Figure S5.2). Expansion of summer-cropped area occurred continuously in the Şanlıurfa and Diyarbakır provinces, whereas the expansion in Mardin accelerated since the early 2000s. Relative increases of the summer-cropped area in comparison with the summer-cropped area in 1990 were highest in Mardin (1,026%), Kilis (607%), Şanlıurfa (503%), Adıyaman (205%), and Diyarbakır (201%).

5.3.3 Patterns of summer cropping frequency (SCF)

We calculated summer cropping frequency (SCF) as fractions of years with summer cropping relative to all years after initial summer cropping for each pixel. The average SCF in the study region was 49.1% (or 50.8% excluding the years before 1995) , with distinct variability between provinces. Mean SCF was highest in Şanlıurfa (56.7% / 57.4%), Mardin (53.6% / 55.7%), and Diyarbakır (43.4% / 42.7%), whereas all other provinces had a mean SCF below 35%. The lowest mean SCF was found in Siirk (20.7% / 21.0%), Kilis (24.3% / 26.0%), and Şırnak (27.0% / 26.3%). We considered an SCF of 80% as a benchmark threshold for permanent cultivation (Deines et al., 2017). Following this definition, 15.6% of the summer croplands established since 1995 were permanently cultivated. The least and most intensively used 10% of the study area each covered an area of 73,112 ha and had a cropping frequency of 13.6%, and 92.8%, respectively. Spatially explicit patterns reveal differences in cropping frequency across and within regions (Figure 5.7). SCF was generally high in Şanlıurfa and Mardin. For instance, SCF >80% were common in the Harran plain (Figure 5.7 G), where some croplands exist since the mid-to-late 1990s. Likewise, croplands in western Mardin (Figure 5.7 F) were frequently used. Intermediate SCF of 40-80% occurred in Adıyaman and Şırnak (Figure 5.7 A, I), while lower SCF occurred in recently activated regions in eastern Şanlıurfa (Figure 5.7 E, H), or Diyarbakır (Figure 5.7 B).

5.3.4 Trends of five-year summer cropping frequency (5-year SCF)

We calculated pixel-wise linear regressions of 5-year SCF to identify areas, in which substantial changes in cropping frequency occurred between the initial cultivation and the year 2016 (Table 5.1). The analysis revealed that 62.7% of the summer-cropped lands underwent substantial changes in cropping frequency over time. Neg-

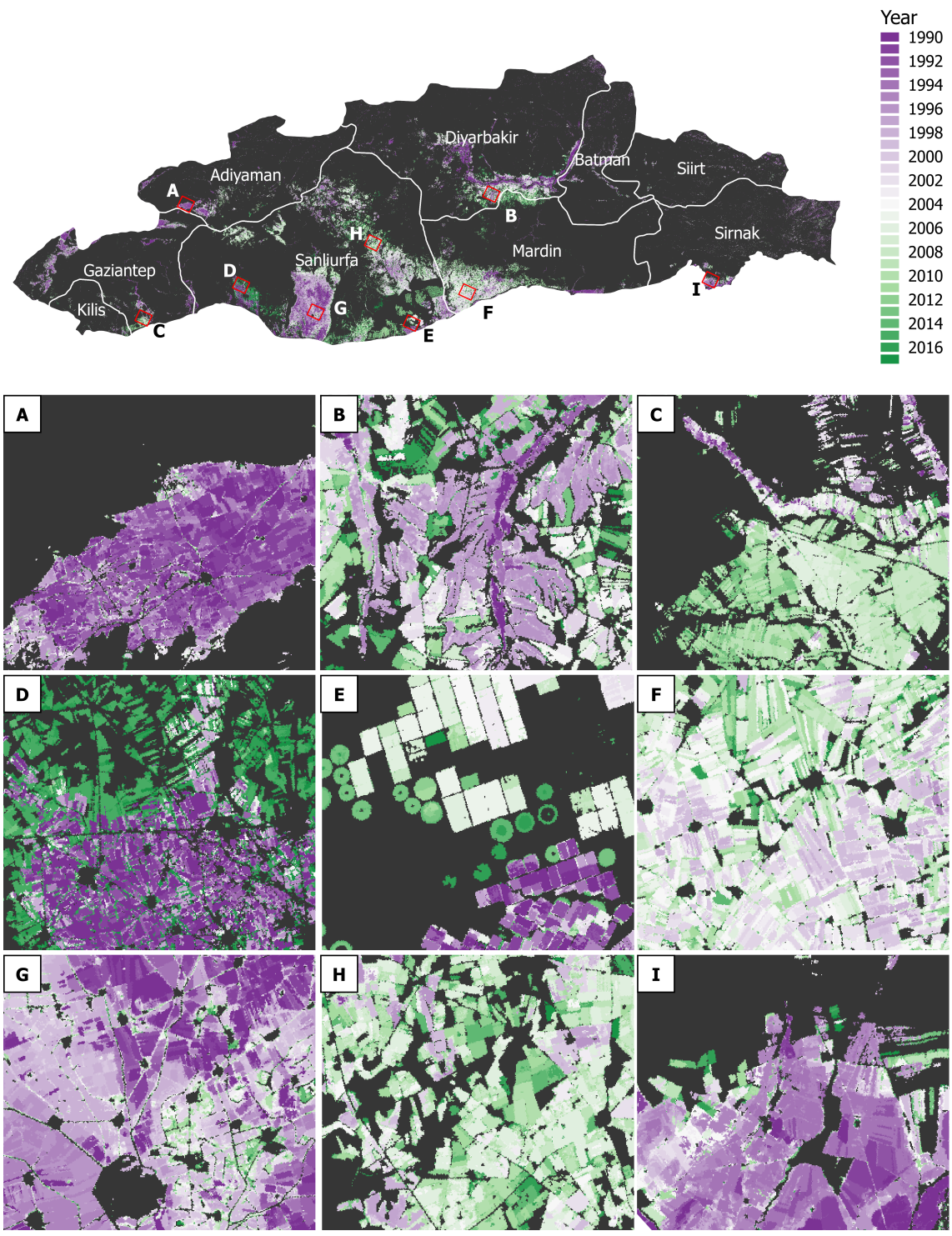

Figure 5.6: Post-classification analysis showing the first year of summer cropping for selected areas.

ative trends were detected on 19.0% and positive trends in 43.3% of the study area, indicating that intensification processes dominate in the study period. On the contrary, 37.7% of the croplands in the study region did not show substantial trend magnitudes. This suggests that no substantial changes in terms of SCF occurred

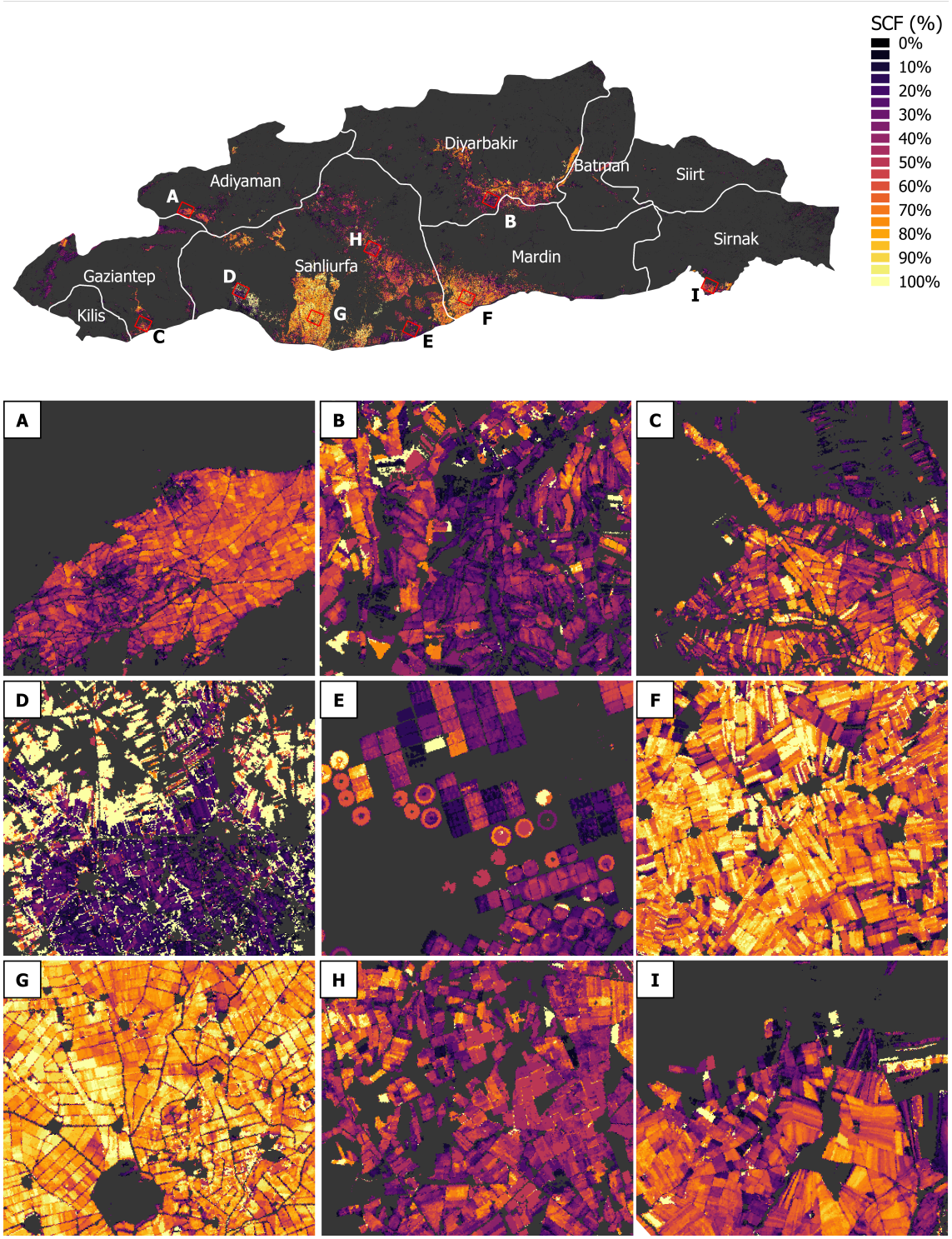

Figure 5.7: Fraction of years with summer cropping after the initial summer cropping year (SCF; in %).

over the study period, or that no clear trend was apparent within the period of investigation.

Contrasting spatial patterns of frequency trends were visible at the regional and at the local level, (Figure 5.8). Intensification patterns dominated in most parts

Table 5.1: Categorization of trend magnitudes into classes of unsubstantial, weak, moderate, and strong trends.

Trend Direction	Trend Magnitude	Change class	Share of croplands
Negative	< -75%	Strong negative	2.2%
	-50% - -75%	Moderate negative	4.8%
	-25% - -50%	Weak negative	12.0%
None	0%	Unsubstantial	37.7%
Positive	+25% - +50%	Weak positive	19.1%
	+50% - +75%	Moderate positive	13.7%
	> +75%	Strong positive	10.5%

of Şanlıurfa and Mardin (Figure 5.8 D, F, G), with the exception of abandoned fields in the Southeast of Şanlıurfa (Figure 5.8 E). Dis-intensification on the other hand was apparent on the croplands of the western provinces Gaziantep and Kilis, Adıyaman, and the southern parts of Diyarbakır (Figure 5.8 A, B, C). Generally, a strong local-level variability regarding trend strength and direction was abundant between neighboring parcels throughout most parts of the GAP (e.g., Figure 5.8 A, B, F, H, I).

5.4 Discussion

5.4.1 Methods and mapping accuracies

We presented a satellite-based long-term characterization of the spatio-temporal evolution of Turkey's largest irrigation scheme. We derived annual extent and frequency of summer cropping at 30 m spatial resolution over 29 years. The approach offered unique opportunities for identifying hotspots of cropland expansion as well as cropping frequency in irrigated production systems of semi-arid areas of Turkey. Our method for producing annual maps of summer cropping over nearly three decades relied on standardized spectral-temporal features. Similar to previous studies, we assumed that Landsat-based spectral-temporal metrics provide temporally consistent means for cropland mapping (Deines et al., 2017; Schmidt et al., 2016). Based on this assumption, we trained a generalized non-parametric classifier to predict spectral-temporal metrics across the study period, similar to a recent study targeting long-term mapping of deforestation (Griffiths et al., 2018). We could thereby restrict training data collection to a year, for which very-high resolution imagery was available in Google Earth.

The accuracies of the summer cropping class were less stable in the early years of the time series, and a relationship between the number of clear sky observations and producer's accuracy could be determined (Figure 5.4). However, the number of observations explained less than a third of the variance in accuracy. We thus

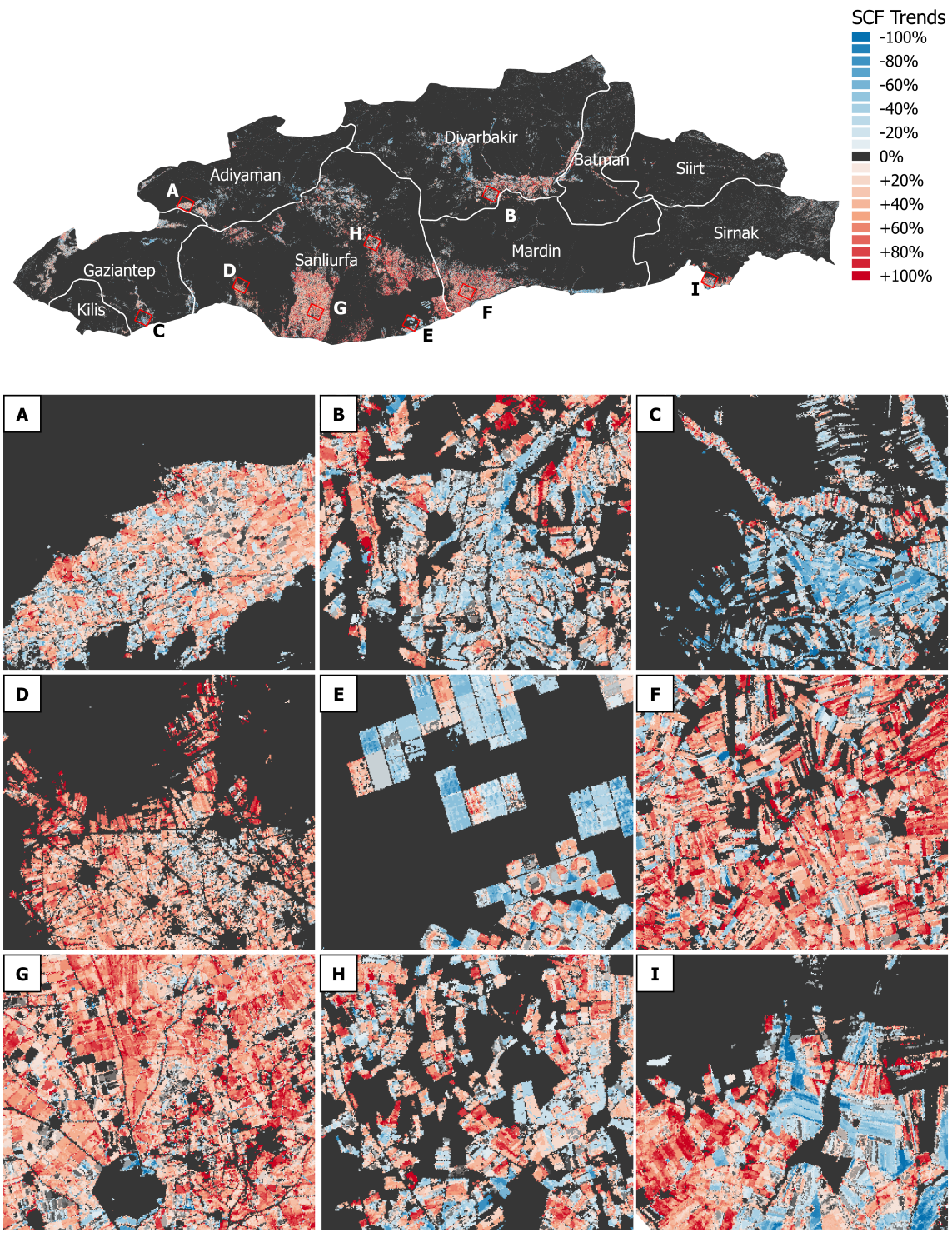

Figure 5.8: SCF trend magnitudes, showing varying magnitudes of increasing (red) and decreasing 5-year SCF (blue).

reason that variation in accuracy is additionally driven by the temporal distribution of the observations relative to the phenological cycle in the given year, which varies with annual precipitation and temperature patterns. The robustness of spectral-temporal metrics under varying observation densities and distributions, therefore,

needs to be investigated in experimental setups on a case by case basis (e.g., Muller et al., 2015; Rufin et al., 2015). Further research is needed to quantify the effects of the number and timing of available observations on the consistency and quality of spectral-temporal features to assess the spatial transferability of the presented methods. However, the annual summer-crop maps presented here were highly accurate (overall accuracies: 98.09% ± 0.80% and 99.83% ± 0.25%) and the post-classification derivates underlie low uncertainties (total number of years cropped RMSE = 1.79 years; first year summer cropping RMSE = 3.43 years; cropping frequency RMSE = 11%), which speak in favor of the consistency of spectral-temporal metrics under varying observation availability.

5.4.2 Changes in summer cropping extent and frequency

Since 1990, the summer-cropped area in the GAP provinces has increased by a staggering 617%. Our error-adjusted area estimates of the summer-cropped area of 553,088 ha in 2017 are well in line with the reported operationally irrigable area of 545,938 ha in 2017 (GAP, 2017). We likely underestimate the total irrigable area in the GAP region, as our maps did not include irrigated winter crops, perennials, as well as summer-fallowed areas. If we consider the cumulative summer-cropped area since 1995 and assume that installed irrigation infrastructure is not removed, our maps suggest that the region comprises an operationally irrigable area of 731,118 ha. This estimate exceeds the official estimates of the irrigable area by 33.92%, which could be indicative of irrigation water use outside the GAP irrigation schemes and supports previous hypotheses that irrigation extent and water usage are underreported in the region (Özdoğan and Woodcock, 2006b). However, our estimates of the total irrigable area include low-intensity smallholder agriculture outside of the GAP core areas. For instance, we mapped the expansion of summer cultivation on 32,468 ha in the mountainous north-eastern parts of the study region (Sirnak, Siirt), which are unlikely to receive water from the water storage infrastructures of the GAP.

One-sixth of the croplands activated after 1995 (15.6%, or 114,182 ha) was cultivated with a cropping frequency exceeding 80%. Relative to these levels, the observed average SCF (50%) implied that on average half of the irrigation infrastructure remains idle at an annual basis and that investments are not used to their potential. Besides fallowing as a strategy to avoid depletion of soil nutrients, causes of low SCFs entail preferences for rainfed cropping due to economic, engineering and managerial constraints, which vary in dependence of the institutions for irrigation and maintenance (Harris, 2009; Kibaroğlu et al., 2011). In the GAP region, irrigation schemes were developed by governmental authorities (State Hydraulic Works), but their operation, management, and maintenance were transferred to irrigation

unions (Bilgen, 2018a). Differences in SCF might thus be related to the management of individual irrigation unions, its members' land ownership structure, and prevailing management practices (Degirmenci et al., 2006). Investigating cropping frequencies across the different irrigation unions in the GAP region could, therefore, reveal effects of water licensing schemes and management strategies on long-term cropping frequency and changes therein.

The trend analysis of 5-year SCF revealed changes in land use intensity over the study period. The presented trend maps can serve as an indicator of areas which experienced dis-intensification (negative trend), or intensification towards their later operational phases (positive trend). The reasons for the observed changes should be assessed on a case-by-case basis, but potentially include shifts in crop rotations, which alter the frequency of summer cultivation. In the GAP region, few major crops dominate the production system. Cotton cultivation expanded drastically and is currently the major crop in the GAP region, covering 310,000 ha or 53.6% of the summer-cropped area in 2018 (USDA, 2018). Cotton does not allow for double-cropping due to conflicting growth schedule with winter crops in the region (Figure 2), and as a consequence, cotton fields are commonly fallowed in winter and spring (Özdoğan and Woodcock, 2006b). A recent study suggested relatively high shares of double-cropping in some GAP provinces in 2015 (Rufin et al., 2019b), which is likely related to the cultivation of winter cereals in rotation with corn (Figure 5.2).

Negative trends could be induced by long-term degradation of irrigation infrastructure under improper management, which can hamper sufficient and timely water delivery. Water prices in Turkey relate to the irrigated area by crop type and thus do not impose volumetric restrictions on the water use, thereby promoting excessive irrigation (Cakmak, 2010). Excessive irrigation and insufficient drainage drastically raised the extent of saline lands in the GAP region (Altinbilek and Tortajada, 2012; Kendirli et al., 2005), and can ultimately lead to the abandonment of irrigation infrastructure, as was documented in other regions (Deines et al., 2017; Löw et al., 2018).

5.4.3 Implications for water use

Our results suggest that the impact of irrigated summer cropping on the regional water resource base should be investigated in more detail. The production of summer crops in the GAP region is spatially dispersed and water intensive, which likely causes additional evaporative conveyance losses in the open secondary canal network. Trade-offs between the expansion of irrigated fields and intensification on existing irrigated fields should thus be assessed before engaging in further expansion of irrigation infrastructure. In this regard, the combination of spatially explicit variables on cropland expansion or cropping frequency presented here, with data on the

local land management (e.g., irrigation technique, crop rotations, irrigation union governance) and production output (e.g., yield, or market value) is key for disentangling the implications of varying cropping frequency in regards to the overall system performance and efficiency.

5.5 Conclusions

Assessing the performance of irrigation schemes is essential to inform land and water resource management. We used a 29-year time series of Landsat imagery to quantify the expansion and frequency of irrigated summer cropping in Turkey's largest irrigation scheme. Our annual maps showed a six-fold expansion in summer cropping since 1990, and most irrigated fields were cropped in less than half of the years, but intensification trends were apparent in 43% of the study area.

The combination of Landsat-derived spectral-temporal metrics and a generalized non-parametric classification algorithm proved efficient for producing a robust long-term characterization of the regional cropping system at 30 m spatial resolution. The approach significantly reduced the costs of training data collection and associated uncertainties that arise when training data is required for years where no high-resolution data are available. However, our approach relied on the assumption that spectral-temporal metrics are temporally consistent, which is potentially compromised by historically varying sensor constellations and in areas with different cloud patterns. Our findings indicate that the number of clear observations can in parts be associated with varying classification accuracies, but that the temporal distribution of observations in relation to the local land surface phenology is likely to be a dominant contributing factor.

Further irrigation expansion in the region is foreseen. Better knowledge about land use intensity and its spatial and temporal distribution can help to assess the impacts of the future expansion of irrigated agriculture on the regional water resource base, environmental flow requirements, and downstream water users. The methods and outcomes of our study can potentially be of value to inform such spatial planning and decision-making processes and help to improve land and water use efficiencies in irrigated agricultural production systems.

Acknowledgments

This research contributes to the Landsat Science Team 2018-2023 and the Global Land Programme. We gratefully acknowledge the open cloud processing platform provided by Google.

Supplementary materials

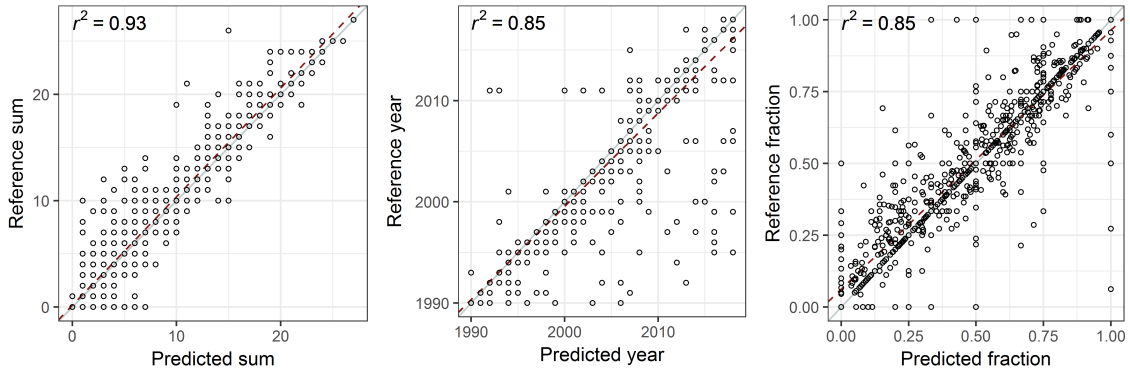

Figure S5.1: Mapped against reference data values (n = 1,081) for three variables derived in post-classification analysis: the sum of years under summer cultivation (left), the earliest year where summer cultivation occurred (middle), and the derived summer cropping frequency (SCF), defined as the fraction of years cultivated after (i.e., excluding) the initial year (right).

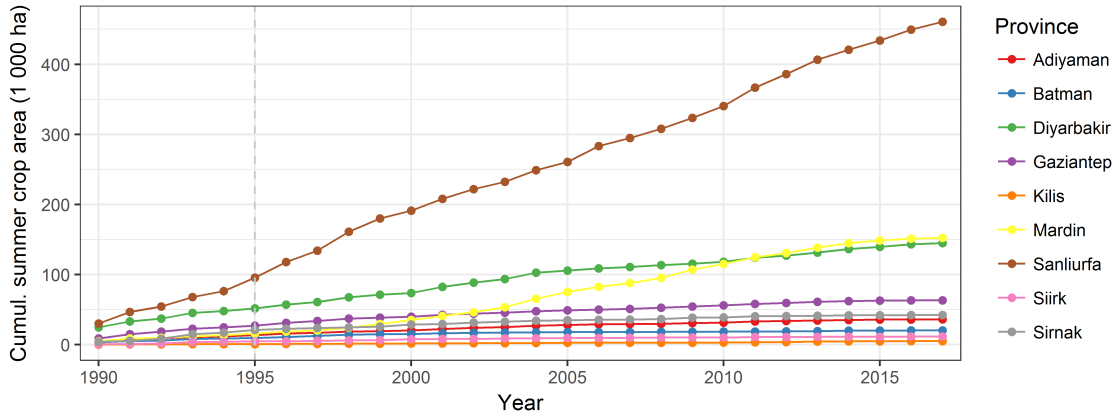

Figure S5.2: Map-based cumulative summer-cropped area in thousand hectares between 1990 and 2015. These estimates consider all areas, which were under summer cultivation at least twice between 1990 and 2018.

Table S5.1: Annual area-adjusted overall and class-wise user's and producer's accuracies (%) with corresponding 95% confidence intervals.

				Summer Crop				Others			
Year	N Obs	OA	95% CI	PA	95% CI	UA	95% CI	PA	95% CI	UA	95% CI
1990	8.4	99.83%	0.25%	88.32%	16.47%	97.14%	9.52%	99.97%	0.10%	99.86%	0.23%
1991	8.3	99.79%	0.28%	84.24%	18.74%	96.60%	10.85%	99.97%	0.11%	99.82%	0.25%
1992	8.3	99.67%	0.34%	82.64%	17.88%	91.64%	15.02%	99.90%	0.18%	99.76%	0.29%
1993	5.9	99.33%	0.43%	88.63%	16.38%	67.31%	21.96%	99.46%	0.36%	99.86%	0.23%
1994	7.1	99.61%	0.37%	73.03%	21.23%	92.26%	16.60%	99.93%	0.15%	99.68%	0.34%
1995	7.4	98.40%	0.75%	47.89%	13.08%	88.85%	15.42%	99.83%	0.23%	98.55%	0.72%
1996	6.6	99.46%	0.44%	79.07%	15.24%	93.40%	11.29%	99.88%	0.20%	99.57%	0.39%
1997	7.7	99.35%	0.48%	74.71%	15.07%	95.13%	9.69%	99.91%	0.17%	99.43%	0.45%
1998	7.3	98.41%	0.75%	62.00%	11.80%	94.20%	8.80%	99.85%	0.23%	98.52%	0.73%
1999	11.8	99.24%	0.52%	75.94%	13.18%	96.55%	7.26%	99.92%	0.17%	99.30%	0.50%
2000	10.9	99.11%	0.56%	73.87%	13.90%	91.29%	11.40%	99.81%	0.25%	99.28%	0.51%
2001	8.6	99.28%	0.50%	83.12%	11.12%	94.82%	7.69%	99.84%	0.23%	99.41%	0.46%
2002	9.9	99.26%	0.51%	86.57%	10.23%	91.57%	9.18%	99.72%	0.31%	99.52%	0.42%
2003	7.4	98.63%	0.69%	70.05%	12.05%	90.90%	10.16%	99.73%	0.30%	98.86%	0.64%
2004	11.2	99.27%	0.51%	88.46%	8.96%	92.89%	7.84%	99.72%	0.31%	99.52%	0.42%
2005	9.2	98.89%	0.62%	74.03%	11.86%	94.20%	8.25%	99.83%	0.24%	99.03%	0.59%
2006	12.8	99.24%	0.52%	86.09%	9.51%	94.70%	6.95%	99.80%	0.27%	99.41%	0.46%
2007	11.4	98.92%	0.61%	79.97%	11.14%	89.95%	9.84%	99.65%	0.34%	99.23%	0.53%
2008	7.7	98.65%	0.64%	84.72%	11.09%	76.71%	13.22%	99.13%	0.49%	99.48%	0.44%
2009	11.7	98.09%	0.80%	72.11%	11.11%	82.25%	11.59%	99.28%	0.46%	98.72%	0.68%
2010	9.2	99.24%	0.52%	89.90%	7.78%	93.89%	6.66%	99.71%	0.32%	99.49%	0.43%
2011	11.8	99.11%	0.55%	94.87%	5.24%	90.70%	6.93%	99.38%	0.46%	99.67%	0.35%
2012	6.1	98.39%	0.74%	80.43%	8.96%	90.10%	7.91%	99.47%	0.42%	98.83%	0.66%
2013	13.1	99.19%	0.52%	95.22%	4.99%	92.04%	6.37%	99.46%	0.43%	99.68%	0.35%
2014	12.9	99.19%	0.53%	95.14%	4.83%	92.90%	5.85%	99.48%	0.43%	99.65%	0.36%
2015	12.9	98.99%	0.57%	97.48%	3.66%	87.97%	7.29%	99.09%	0.55%	99.83%	0.26%
2016	13.0	99.24%	0.51%	96.19%	4.36%	92.52%	5.99%	99.45%	0.44%	99.73%	0.32%
2017	14.4	98.96%	0.59%	95.71%	4.44%	90.17%	6.48%	99.21%	0.52%	99.67%	0.35%
2018	13.7	98.92%	0.61%	90.15%	6.20%	94.97%	4.92%	99.62%	0.37%	99.22%	0.54%

Table S5.2: Linear regression analyses between accuracy measures (response) and mean number of observations (predictor) in each year. Intercept, β_{nobs}, standard error of β_{nobs} given in %.

Accuracy	Class	Intercept	β_{nobs}	SE(β_{nobs})	R^2	p-value
Overall	-	99.130	0.000	0.004	0.001	0.906
Producer's	Summer cropping	58.526	2.420	0.709	0.302	0.002
	Others	100.083	-0.043	0.018	0.180	0.022
User's	Summer cropping	88.580	0.544	0.452	0.051	0.239
	Others	99.065	0.034	0.029	0.049	0.247

Table S5.3: Map-based summer-cropped area by provinces. Total cumulative area, total cumulative area activated after 1995, the largest annual expansion, and the according year.

Province	Cumulative SC area (ha)	Cumulative SC area after 1995 (ha)	Post 1995 (%)	Max. annual expansion after 1995 (ha)	Year of max. expansion
Adıyaman	36,351	24,438	67.23%	2,143	1996
Batman	20,515	11,685	56.96%	1,919	1998
Diyarbakır	144,809	96,744	66.81%	9,242	2004
Gaziantep	63,267	38,339	60.60%	4,010	1996
Kilis	5,135	4,409	85.85%	678	2013
Mardin	152,521	138,977	91.12%	1,226	2004
Şanlıurfa	460,483	384,058	83.40%	26,824	1998
Siirt	11,582	7,398	63.88%	1,219	2000
Şırnak	42,379	25,070	59.16%	3,706	1995
Total	937,044	731,118	78.02%	48,383	2011

Chapter 6

Synthesis

6.1 Summary

This thesis aimed at expanding the current knowledge about the effects of dam construction and operation on land systems on a global and regional scale by means of remote sensing. The first research question of this thesis targeted an improved understanding of dam-induced agricultural land change. The second research questions aimed at exploring the potential of remote sensing data products and methods for capturing land change processes on a global and a regional scale. A synthesis of the current literature (chapter II) revealed the types and directions of dam-induced land system change across the globe, strengthening the hypothesis of the positive effects of dams on land use intensity. This link was further explored using remote sensing products for investigating cropping frequencies in irrigation dam command areas as well as the spatial determinants thereof (chapter III). On a regional scale, Landsat time series analyses were tested in order to compile good practice recommendations for mapping cropping practices on a national scale, exemplified for Turkey (chapter IV). The resulting methodological insights were considered for a detailed investigation of the long-term patterns and trends of irrigated summer cropping in Turkey's major dam-and-canal irrigation scheme (chapter V).

Overall, the work of this thesis contributed to the understanding of the effects of dam construction and operation on land systems, both on a global and regional scale. Analyses on different scales revealed that dams commonly increased land use intensity and that these processes underlie a pronounced spatial and temporal variability. The presented approaches greatly benefited from the use of remote sensing datasets and methods. State-of-the-art datasets and methods were used to produce novel representations of irrigation dam command areas and land use intensity therein. According to the overarching research questions, the work of the individual chapters can be briefly summarized as follows:

Research Question I: *How did irrigation dams affect agricultural land systems on a global and regional scale?*

A link between irrigation dams and land use intensity could be observed on a global scale. The scientific literature frequently reported positive effects of irrigation dams on land use intensity in many world regions (chapter II). Due to a lack of data on the direction and magnitude of these effects, this relationship was subject to further investigation using MODIS-based data products. Global measurements of cropping frequency in irrigation dam command areas revealed that fallow years occurred less frequent in irrigated command areas, as compared to rainfed croplands under similar conditions (chapter III). The magnitude of this effect accounted for a 16% reduction in fallow years, but inter-regional variability was high, and some world regions showed no, or only weak responses. Cropping frequencies in the in-

vestigated command areas were sensitive to the technological properties of the dam and irrigation system (e.g., conveyance losses, water allocation distance), as well as the biophysical (e.g., humidity, terrain) and socio-economic (e.g., accessibility, population density) characteristics of the command area locations.

A Landsat-based investigation of irrigated summer cropland extent and cropping frequency in Turkey's largest dam-and-canal irrigation scheme revealed a six-fold (617%) increase of summer cropped land in the region between 1990 and 2018 (chapter V). However, this drastic expansion accounted for only a third of the anticipated irrigated area extent of 1.8 million ha. The mapped patterns and trends within the irrigated lands revealed a substantial spatial and temporal variability of cropping frequency on a regional level. On average, summer cropping occurred bi-annually, and only a few areas were used continuously. However, an intensification trend was apparent in most parts of the study region (43%). On the contrary, nearly one-fifth of the summer croplands (19%) have undergone declines in cropping frequency throughout their operational phase.

Research Question II: *How can remote sensing contribute to our understanding of dam-induced agricultural change?*

MODIS-based products essentially enabled novel insights on dam-induced agricultural change at the global scale (chapter III). First, a time series of MODIS land cover datasets (Friedl et al., 2010) was used to derive cropping frequency at 500 m spatial resolution on the global scale. The spatially explicit uncertainty layer contained in the product was an asset for the analysis presented here. Independent validation of the MODIS cropland layers confirmed that the classification uncertainty measure relates to mapping accuracy, and thus allowed for integrating map uncertainties in subsequent analyses. Second, a spatially explicit representation of irrigated and rainfed croplands (Salmon et al., 2015), paired - among other datasets - with a remotely sensed surface elevation model (Jarvis et al., 2008), enabled a spatially explicit approximation of the location of 15 million ha of irrigation dam command areas established since 1985. In combination, these two MODIS-based products offered unique and novel insights on the effect of irrigation dams on cropping frequency on a global scale.

On a regional scale, intra-annual Landsat time series analysis enabled a detailed and accurate characterization of cropping practices across Turkey (chapter IV). The procedure relied on temporal binning of integrated Landsat ETM+ and OLI time series, which allowed for integrating the spectral signal of the target classes, as well as its temporal variation in predefined time windows. The best results (area-adjusted overall accuracies $> 90\%$) were achieved using spectral-temporal metrics and pixel-based composites in quarterly intervals, or an ensemble gap-filling approach to achieve eight-day temporal coverage. Interestingly, high accuracies (88%)

were also achieved using only spectral-temporal metrics and composites from the third quarter of the year (July through September), suggesting that the land surface phenological trajectories of this period contain relevant information for the defined class catalog.

Using this insight, a 29-year intra-annual Landsat time series enabled a long-term characterization of irrigated summer cropping in Turkey's largest irrigation scheme (chapter V). All available Landsat observations in each year's third quarter were aggregated into a standardized set of spectral-temporal metrics and classified using a generalized classification model. The resulting time series of irrigated summer cropping maps was spatially consistent and had high accuracies through most parts of the study period. These Landsat-based maps thereby enabled a spatially and temporally detailed characterization of summer cropland expansion and cropping frequencies, yielding novel insights into the patterns and trends of land use intensity in Turkey's major dam-and-canal irrigation scheme.

6.2 Main conclusions

The following conclusions can be drawn regarding research question I:

Dams modify the configuration of land systems, as they induced changes in land cover, land use, and land use intensity through a multitude of direct and indirect processes across spatial, and temporal scales. The findings of this thesis support the hypothesis that irrigation dams cause increases in land use intensity, i.e., cropping frequency. This effect was apparent from the literature synthesis and was subsequently investigated on a global, and a regional scale. The higher levels of cropping frequency in irrigation dam command areas attested to the results obtained from previous national to continental-scale studies which examined the impacts of irrigation dams on agricultural production (Duflo and Pande, 2007; Strobl and Strobl, 2011).

The results highlighted the immense spatio-temporal variability of irrigated agriculture. A global-scale analysis revealed a strong variability of cropping frequency between individual command areas, as well as the inter-regional variability in the difference between rainfed and irrigated croplands (Figure 3.6). The regional insights further emphasized the high spatial variability of cropping frequency at the field-scale (Figure 5.7). Moreover, temporal variability was observed. The literature synthesis suggested that the direction of dam-induced land use intensity changes inverted with increasing time since dam commissioning. Land use intensity increases were mostly observed shortly after dam commissioning, whereas dis-intensification trends were visible in the long term (Figure S2.5). The regionally observed intensification and dis-intensification processes further attested to the high temporal

variability of irrigation activities (Figure 5.8). On average, only 50% of the irrigated summer croplands in Turkey were cultivated each year. This widely exceeded previous global estimates that suggested 12% - 17% of the area equipped with irrigation infrastructure are commonly not irrigated (Rohwer et al., 2007; Siebert et al., 2013). In combination, these findings highlight that the high spatial and temporal variability should be considered for future assessments of land use intensity in command areas.

The global-scale analysis suggested sensitivity towards biophysical, socio-economic, and technological determinants of cropping frequency. However, the selected predictors explained only half of the variation in cropping frequency. The high variability on the regional scale indicated that irrigation system governance and management decisions on a local level dominate over biophysical constraints in these highly engineered irrigation schemes. Appropriate data on irrigation system management and governance are thus needed to disentangle the mechanisms underlying the observed patterns. To that end, in-depth case studies are of outstanding value to improve the knowledge on the specific processes and causal mechanisms of land change (Meyfroidt, 2016), as could for instance be impressively demonstrated in the pioneering work of Thomas and Adams (1999), or the comprehensive case study of de Fraiture et al. (2014).

Concerning research question II, the following can be concluded:

The global scale insights produced here heavily profited from map products derived from remotely sensed time series. This thesis, therefore, attested to the scientific value of such globally consistent datasets on land cover and land use, as they enabled the production of global-scale insights on the link between dam-based irrigation and cropping frequency in agricultural land systems. As the level of uncertainty of global map products is comparably high (Fritz et al., 2011; Waldner et al., 2016b), accounting for regional and class-specific inaccuracies is essential. The spatially explicit representations of classification confidence provided in the MODIS land cover product were an asset in this regard.

The openly accessible Landsat archive enabled the production of robust, consistent, and accurate estimates of the extent and spatial distribution of cropping practices over large areas, and cropping frequency over long time frames. Current demands for spatially explicit information about land management and land use intensity can thus in parts be met with existing datasets and methods. Temporal binning of intra-annual time series (e.g., through spectral-temporal metrics) was key for mapping cropping practices and cropping frequency from Landsat data. Specifically, eight-day or quarterly temporal bins enabled to produce near gap-free data coverage over large areas while capturing information on land surface phenology in sufficient detail for the discrimination of cropping practices. Additionally, current

sensor constellations allow for producing spatially and thematically detailed representations in narrow, e.g., annual, temporal intervals. Thereby, requirements for the monitoring of highly dynamic areas, such as irrigation schemes, can potentially be met in many world regions.

Overall, the findings of this thesis stress that the recent developments regarding open data availability and accessibility, as well as processing capabilities concerning hardware and software currently allow for the generation of accurate, large area map products at fine temporal, spatial and thematic detail. Remote sensing and Landsat-level analyses in specific represent an effective tool which allows for producing quantitative and spatially explicit estimations of the state and dynamics of land systems. As an example, the findings from chapter V could complement the investigation of irrigated areas over time presented by the WCD (2000, cf. Figure 1.4), revealing a low performance of the GAP in meeting irrigated area targets. Ultimately, similar Landsat-based land use maps can assist in spatial planning and decision-making processes, or inform assessments of land and water resource consumption. Thereby, these presented methods can facilitate improvements in land and water use efficiencies in irrigated agricultural production systems.

6.3 Implications

This thesis revealed novel insights about the impacts of dams on the land system, with a focus on irrigation-induced changes in agricultural production systems. The results provided answers to the two overarching research questions, thereby filling previous knowledge gaps in dam-induced agricultural land change and suitable methods in this context. Additionally, the insights, methods, and datasets generated in the context of this thesis have the following scientific implications.

The novel framework for identifying command areas can support future analyses. Detailed knowledge about the locations of irrigation dam command areas is essential for studying the spatial distribution and variability of social, economic, and environmental outcomes of irrigation dam construction (Strobl and Strobl, 2011). This thesis presented the first global-scale framework for approximating the size and location of irrigation dam command areas (Rufin et al., 2017). Previous studies focusing on the effect of dams on agricultural production relied on aggregated areal units (Blanc and Strobl, 2014; Duflo and Pande, 2007). As a consequence, the presented spatial allocation framework can substantially increase the spatial detail of such analyses in the future. The flexibility of the presented framework allows for modifications to match various scales, contextual settings, or data situations. For instance, nationally available data on command area extents could be integrated (DSI, 2015), or the predefined topographic relationships between dams and command ar-

eas could be adjusted to account for regional configurations of water transfer. Global Landsat-based maps of irrigated areas likely emerge in the coming years (Thenkabail, 2013), which - combined with other land use maps - facilitate a more detailed characterization of cropping activities and land management in command areas.

The data produced in this thesis can facilitate a better understanding of the relationship between land inputs and production outputs. The ratio of harvested land relative to total available cropland increased in recent decades, which served as a means to increase global crop production (Ray and Foley, 2013). While it can be assumed that additional cultivation cycles, e.g., through reduced fallow periods, or multi-cropping will have a significant effect on production output, it remains unclear how land input changes explicitly relate to output metrics (Erb et al., 2013). Current yield increases are potentially insufficient to meet growing demands in the future (Ray et al., 2013). Maximizing cropping frequency represents a valuable complementary strategy, as it could increase total agricultural production by 44% (Ray and Foley, 2013). Investigating the relationships between land inputs and changes in production outputs for different crop types and rotations, varying levels of agrochemical inputs, or irrigation type and intensity, is challenging. Central to this issue is the lack of appropriate datasets on the respective input indicators (e.g., land management, fertilizer use, water input, cropping frequency), and production outputs (Erb et al., 2013; Kümmerle et al., 2013). This thesis delivered datasets to serve this endeavor, including a global cropping frequency layer, a national scale map of cropping practices, as well as the data on long-term cropping frequency in Turkey's major irrigation scheme. It should be noted that the ongoing enhancements of global land cover products result in higher temporal resolution (e.g., ESA CCI Land Cover v2; (Li et al., 2018)), or improved temporal consistency (e.g., MODIS Collection 6 Land Cover Type product; (Sulla-Menashe et al., 2019)), and thus allow for a re-investigation of the presented approach for deriving global cropping frequency maps.

First insights on the role of dam-based irrigation for increased resilience of production systems were generated. Agricultural production is sensitive to climatic variability, both regarding yields (Iizumi and Ramankutty, 2016; Ray et al., 2015), and cropping frequency (Cohn et al., 2016; Ray and Foley, 2013; Wu et al., 2018). Irrigation dams buffer against water shortages and thus reduces the sensitivity to climatic variability (Lindström et al., 2012; Muller et al., 2015). However, it remains unclear to which degree climate-induced variation in water availability can be overcome through irrigation dams and how that translates into reduced fallow years, e.g., by avoiding crop failures. Anecdotic evidence from this thesis raised questions about the capability of water storage infrastructures to de-couple production from precipitation-based water restrictions.

At the global scale, cropping frequency was variable and sensitive towards aridity and precipitation. Moreover, the temporal variability of the extent of summer cropped area in Southeastern Anatolia was high, and strong declines were observed in years of major droughts in this water-dependent region. To this end, it could be assumed that irrigation water demand periodically exceeded the supply. In light of the hypothesis that increasing reservoir storage amplifies water demand and thus inverses the buffering effect of existing storage (Di Baldassarre et al., 2018), an investigation of the covariance of climatic variables and cropping frequency in irrigated systems is suggested. Comparing regions with and without water storage infrastructures could help to determine the presence of the buffering effect and its magnitude.

Landsat time series gap-filling techniques and spectral-temporal metrics offer great potential for large-area mapping of cropping systems. The gap-filling method applied in chapter IV was based on a novel data-density-weighted ensemble of Radial Basis Convolution Filters (RBF). The approach was originally developed and applied for the mapping of vegetation properties in natural savanna ecosystems (Schwieder et al., 2016, 2018). For the first time, this approach has been successfully applied for thematically detailed, large area mapping in agricultural systems. The results presented here proved the potential of the method for a spatially consistent mapping of dynamic cropping practices over large areas. The RBF technique is suitable to generate equidistant time series at narrow temporal intervals, which can be digested by algorithms for the derivation of phenological metrics (Jönsson and Eklundh, 2004; Jönsson et al., 2018). The first step in this direction indicated the great potential of RBF-based phenological metrics derived from Landsat time series for discriminating diverse crop rotations in agricultural landscapes of Brazil (Bendini et al., in review).

Moreover, the work in chapter IV and V yielded novel insights concerning the use of spectral-temporal metrics. First, a definition of appropriate temporal bins for mapping cropping systems was approached. The results suggested that annual binning of spectral-temporal metrics is not advisable for this purpose, as the seasonal land-surface phenological information becomes essentially blurred. Quarterly features provided a suitable compromise to capture sufficient temporal detail for discriminating the cultivation of winter, summer, semi-aquatic crops, as well as double cropping and greenhouse cultivation. Simultaneously, near gap-free coverage over Turkey could be achieved in quarterly intervals. The temporal transferability of quarterly spectral-temporal metrics was investigated in chapter V. Here, a time series of summer spectral-temporal metrics was paired with a generalized classification model predict land cover over 29 years. Class-specific accuracies were partly lower in years with reduced data availability, but this was only partly related to the number of observations. The temporal distribution of observations in relation to the

phenological cycle was consequently suggested as a critical factor for mapping with spectral-temporal metrics across time. The impacts of changing quantity and distribution of clear observations likely vary with the classes of interest (Müller et al., 2015). The effects of varying observation density and distribution on classification performance or spatial consistency could thus be assessed for binary discrimination of individual classes, as defined in common land cover or land use class catalogs (e.g., the CORINE Land Cover Classification System; (EEA, 2017)). Such analyses could be conducted computationally inexpensive across large regions, by using a sample-based approach which relies on ground-based land cover information, such as the European Land Use/Land Cover Areal Survey (Martino and Fritz, 2008).

6.4 Outlook

The challenges and insights presented in this thesis translate into several research strands which should be pursued in order to disentangle dam-induced land system change in more detail.

A comprehensive spatial database on dam locations is missing to date. The global-scale analyses conducted in this thesis investigated more than one thousand dams. However, as compared to the 59,000 existing water storage infrastructures, this represents only a small fraction of currently operational dams (ICOLD, 2017). Surprisingly, a spatially explicit global inventory of dams and reservoirs lacks to date. Existing spatial datasets (Lehner et al., 2011; FAO, 2015) should, therefore, be amended to enable comprehensive analyses at the global scale. This endeavor can largely profit from Landsat-based datasets that characterize global surface water extent and changes since 1984 (Donchyts et al., 2016; Pekel et al., 2016). An integration of Landsat MSS data to extend the temporal coverage of such products into the early 1970s should be targeted to cover the periods of highest dam construction rates. Developing methods to distinguish artificial reservoirs from natural surface waters based on Landsat- and MODIS-based products (Klein et al., 2017), could be a vital step towards characterizing and quantifying the effects of dams on a variety of land system components. Such a comprehensive dataset on global surface water reservoirs could, for instance, be used for estimating the total area submerged by artificial reservoirs since 1973, or for improving global scale estimations of reservoir greenhouse gas emissions (St. Louis et al., 2000).

An improved characterization of cropping frequency is needed. Analyses of land input remain challenging, as spatially explicit datasets on cropping frequency are limited in their extent (Estel et al., 2016), temporal coverage (Siebert et al., 2010a) or are only available at aggregate areal units (Ray and Foley, 2013). However, datasets on land input are essential for an improved understanding of land use

intensity and its change over the globe (Kümmerle et al., 2013; Pongratz et al., 2017). An initial step in this regard could be a large-area characterization of cropping frequency, including double-cropped lands. Double-cropped lands have been mapped across the globe, only with low (8 km) spatial detail (Wu et al., 2018). In light of the recent advances in data availability and cloud computing capabilities, such an indicator could potentially be derived at 30 m or finer spatial resolution, and for several years. Time series of Landsat, Sentinel 2, or a combination of the two, could be combined with algorithms for gap-filling and the characterization of land surface phenological metrics over multiple growing seasons (Jönsson and Eklundh, 2004; Jönsson et al., 2018). The dynamic inter- and intra-annual spectral-temporal behavior of multi-cropped land poses extremely high requirements towards clear sky observation availability, due to which a region with good data availability is preferable for examining the operationality of such approaches.

The relevance of dams for food production and food security remain unknown. Irrigation improves the access and availability to nutrition (Domènech, 2015). Surprisingly, the contribution of dams for improving food security was not part of the investigation by the WCD and remains widely unknown to date (Perry, 2001). On the contrary, adverse effects on food security were observed regarding hydropower dam construction, e.g., concerning fisheries (Sabo et al., 2017; Baran and Myschowoda, 2009; Orr et al., 2012). The degree to which dam-based irrigation can support the production of food for local or domestic consumption should be investigated and related to the degree to which command areas are used for the cultivation of bioenergy crops for global markets or non-food crops, such as cotton. Moving beyond the question of input-output relationships is required in this context, as the production purposes and market dynamics must be accounted for. First insights could be generated by combining datasets on irrigation dam or command area location with coarse-scale datasets on crop types (Monfreda et al., 2008), or calorie allocation to food, biofuels, and animal feed in the respective regions (Cassidy et al., 2013).

Identifying pathways for sustainable intensification are a core task for society at large (Rockström et al., 2016). Generally, the impacts of dams on land systems are not well understood. This involves the direction and magnitude of effects, their interactions with related land system components, their spatial variability, as well as changes over time. Better understanding the past role of dam-based irrigation for production systems can support the process of designing future intensification pathways, in which the growing demands for agricultural production need to be coupled with minimized ecological trade-offs (Pretty, 2018). To this end, the expansion of agricultural land into pristine ecosystems needs to be fully avoided, and a 50% increase in water productivity should be achieved until 2030 (Rockström et al., 2016). Positive effects of dam-based irrigation on cropping frequency were observed

in this thesis. However, the effects were variable across space and time, and sensitive to climate, topography, as well as engineering constraints. The causal mechanisms underlying this variability remain weakly understood. To this end, it will be increasingly important to consider the spatio-temporal variability of land use intensity within irrigation systems and couple it with detailed information which can help to disentangle the processes underlying this variability. Irrigation technologies (e.g., surface, sprinkler, drip irrigation), conveyance and application efficiencies, management (e.g., water licensing schemes, withdrawal quantities), and maintenance (e.g., investments) could be essential determinants and should be investigated. In light of the currently limited knowledge, case study research has an outstanding value to improve the insights on the underlying processes of dam-induced agricultural change.

Remote sensing is an ideal complement to this endeavor due to its capability to provide measures of land system responses, as was demonstrated in this thesis. Specifically, the potential for applying Landsat time series for capturing long-term processes related to agricultural expansion and intensification was highlighted, and good practice recommendations for mapping annual croplands in Mediterranean landscapes could be provided. The open access to data and processing algorithms provide options for operational monitoring schemes in irrigation districts in future years, opening novel opportunities to track the regional variability in intensity indicators and to combine those insights with local-level management information. To facilitate such developments, all tools and map products presented in this thesis were or will be made, publicly available. These include a global scale approximation of irrigation dam command areas commissioned since 1985 (Rufin et al., 2017), a national-scale map of cropping practices in the year 2015 for Turkey (Rufin et al., 2019a), as well as the map products on the expansion and land use intensity of irrigated summer cropping in a major dam-and-canal irrigation scheme in Southeastern Anatolia. Combining these data with integrative research perspectives is encouraged and might facilitate novel insights which can improve our understanding of past patterns of dam-induced agricultural land change. Bridging disciplinary boundaries and combining scientific perspectives and skillsets from diverse fields, such as hydrology, agronomy, ecology, anthropology, or geography, appears imperative to understand the social-ecological costs and benefits of dam-based irrigation in more detail.

Bibliography

Alahiane, N., Elmouden, A., Aitlhaj, A., Boutaleb, S., 2016. Small dam reservoir siltation in the Atlas Mountains of Central Morocco: Analysis of factors impacting sediment yield. Environmental Earth Sciences 75 (12).

Alexandratos, N., Bruinsma, J., 2012. World Agriculture towards 2030/2050: the 2012 revision. FAO, Rome, Italy.

Ali, I., Cawkwell, F., Dwyer, E., Barrett, B., Green, S., 2016. Satellite remote sensing of grasslands: from observation to management. Journal of Plant Ecology 9 (6), 649–671.

Alin, A., 2010. Multicollinearity. Wiley Interdisciplinary Reviews: Computational Statistics 2 (3), 370–374.

Altinbilek, D., Tortajada, C., 2012. The Atatürk Dam in the Context of the Southeastern Anatolia (GAP) Project. In: Tortajada, C., Altinbilek, D., Biswas, A. K. (Eds.), Impacts of Large Dams: A Global Assessment. Water Resources Development and Management. Springer, Berlin/Heidelberg, Germany, pp. 171–199.

Ambika, A. K., Wardlow, B., Mishra, V., 2016. Remotely sensed high resolution irrigated area mapping in India for 2000 to 2015. Scientific data 3, 160118.

ANCOLD, 2010. Register of Large Dams in Australia. Australian National Committee on Large Dams, Hobart, Tasmania, Australia.

Andersen, D. C., Cooper, D. J., Northcott, K., 2007. Dams, floodplain land use, and riparian forest conservation in the semiarid upper Colorado river basin, USA. Environmental Management 40 (3), 453–475.

Ansar, A., Flyvbjerg, B., Budzier, A., Lunn, D., 2014. Should we build more large dams? The actual costs of hydropower megaproject development. Energy Policy 69, 43–56.

Arvidson, T., Gasch, J., Goward, S. N., 2001. Landsat 7's long-term acquisition plan — an innovative approach to building a global imagery archive. Remote Sensing of Environment 78 (1-2), 13–26.

Ashraf, M., Kahlown, M. A., Ashfaq, A., 2007. Impact of small dams on agriculture and groundwater development: A case study from Pakistan. Agricultural Water Management 92 (1-2), 90–98.

Assahira, C., Piedade, M. T. F., Trumbore, S. E., Wittmann, F., Cintra, B. B. L., Batista, E. S., Resende, A. F. d., Schöngart, J., 2017. Tree mortality of a flood-adapted species in response of hydrographic changes caused by an Amazonian river dam. Forest Ecology and Management 396, 113–123.

Atzberger, C., 2013. Advances in Remote Sensing of Agriculture: Context Description, Existing Operational Monitoring Systems and Major Information Needs. Remote Sensing 5 (2), 949–981.

Awlachew, S. B., M. Loulseged., Yilma, A. D., 2008. Impact of Irrigation on Poverty and Environment in Ethiopia. International Water Management Institute, Colombo, Sri Lanka.

Azami, K., Suzuki, H., Toki, S., 2004. Changes in riparian vegetation communities below a large dam in a monsoonal region: Futase Dam, Japan. River Research and Applications 20 (5), 549–563.

Bai, Y., Feng, M., Jiang, H., Wang, J., Liu, Y., 2015. Validation of Land Cover Maps in China Using a Sampling-Based Labeling Approach. Remote Sensing 7 (8), 10589–10606.

Baran, E., Myschowoda, C., 2009. Dams and fisheries in the Mekong Basin. Aquatic Ecosystem Health & Management 12 (3), 227–234.

Barros, N., Cole, J. J., Tranvik, L. J., Prairie, Y. T., Bastviken, D., Huszar, V. L. M., del Giorgio, P., Roland, F., 2011. Carbon emission from hydroelectric reservoirs linked to reservoir age and latitude. Nature Geoscience 4 (9), 593–596.

Bartholomé, E., Belward, A. S., 2005. GLC2000: a new approach to global land cover mapping from Earth observation data. International Journal of Remote Sensing 26 (9), 1959–1977.

Baumann, M., Levers, C., Macchi, L., Bluhm, H., Waske, B., Gasparri, N. I., Kuemmerle, T., 2018. Mapping continuous fields of tree and shrub cover across the Gran Chaco using Landsat 8 and Sentinel-1 data. Remote Sensing of Environment 216, 201–211.

Bégué, A., Arvor, D., Bellon, B., Betbeder, J., de Abelleyra, D., P. D. Ferraz, R., Lebourgeois, V., Lelong, C., Simões, M., R. Verón, S., 2018. Remote Sensing and Cropping Practices: A Review. Remote Sensing 10 (2), 1–32.

Bendini, H. N., Fonseca, L. M. G., Schwieder, M., Sehn Körting, T., Rufin, P., Del Arco Sanches, I., Leitão, P. J., Hostert, P., in review. Detailed Agricultural Land Classification in the Brazilian Cerrado based on Phenological Information from Dense Satellite Image Time Series. International Journal of Applied Earth Observation and Geoinformation.

Benhin, J. K., 2008. South African crop farming and climate change: An economic assessment of impacts. Global Environmental Change 18 (4), 666–678.

Biemans, H., Haddeland, I., Kabat, P., Ludwig, F., Hutjes, R. W. A., Heinke, J., von Bloh, W., Gerten, D., 2011. Impact of reservoirs on river discharge and irrigation water supply during the 20th century. Water Resources Research 47 (3), 1–15.

Bilgen, A., 2018a. The Southeastern Anatolia Project (GAP) in Turkey: An Alternative Perspective on the Major Rationales of GAP. Journal of Balkan and Near Eastern Studies, 1–21.

Bilgen, A., 2018b. The Southeastern Anatolia Project (GAP) revisited: The evolution of GAP over forty years. New Perspectives on Turkey 58, 125–154.

Biradar, C. M., Xiao, X., 2011. Quantifying the area and spatial distribution of double- and triple-cropping croplands in India with multi-temporal MODIS imagery in 2005. International Journal of Remote Sensing 32 (2), 367–386.

Biswas, A. K., 2012. Impacts of Large Dams: Issues, Opportunities and Constraints. In: Tortajada, C., Altinbilek, D., Biswas, A. K. (Eds.), Impacts of Large Dams: A Global Assessment. Springer, Berlin/Heidelberg, Germany, pp. 1–18.

Biswas, A. K., Tortajada, C., 2001. Development and Large Dams: A Global Perspective. International Journal of Water Resources Development 17 (1), 9–21.

Blanc, E., Strobl, E., 2014. Is Small Better? A Comparison of the Effect of Large and Small Dams on Cropland Productivity in South Africa. The World Bank Economic Review 28 (3), 545–576.

Bonsch, M., Popp, A., Biewald, A., Rolinski, S., Schmitz, C., Weindl, I., Stevanovic, M., Högner, K., Heinke, J., Ostberg, S., Dietrich, J. P., Bodirsky, B., Lotze-Campen, H., Humpenöder, F., 2015. Environmental flow provision: Implications for agricultural water and land-use at the global scale. Global Environmental Change 30, 113–132.

Bontemps, S., Defourny, P., Bogaert, E. V., Arino, O., Kalogirou, V., Perez, J. R., 2011. GLOBCOVER 2009 - Products description and validation report. European Space Agency, Frascati, Roma, Italy.

Bontemps, S., Herold, M., Kooistra, L., van Groenestijn, A., Hartley, A., Arino, O., Moreau, I., Defourny, P., 2012. Revisiting land cover observation to address the needs of the climate modeling community. Biogeosciences 9 (6), 2145–2157.

Boserup, E., 1965. The conditions of agricultural growth: The economics of agrarian change under population pressure. Transaction Publishers.

Bouman, B. A. M., Lampayan, R. M., Tuong, T. P., 2007. Water management in irrigated rice: Coping with water scarcity. International Rice Research Institute, Los Baños, Philippines.

Braatne, J. H., Rood, S. B., Goater, L. A., Blair, C. L., 2008. Analyzing the impacts of dams on riparian ecosystems: A review of research strategies and their relevance to the Snake River through Hells Canyon. Environmental Management 41 (2), 267–281.

Breiman, L., 2001. Random Forests. Machine Learning 45 (1), 5–32.

Brouwer, C., 1989. Irrigation Water Management: Irrigation Scheduling: Training manual no. 4. Rome, Italy.

Burney, J. A., Naylor, R. L., Postel, S. L., 2013. The case for distributed irrigation as a development priority in sub-Saharan Africa. Proceedings of the National Academy of Sciences 110 (31), 12513–12517.

Butsic, V., Lewis, D. J., Radeloff, V. C., Baumann, M., Kuemmerle, T., 2017. Quasi-experimental methods enable stronger inferences from observational data in ecology. Basic and Applied Ecology 19, 1–10.

Büyükcangaz, H., Demirtas, C., Yazgan, S., Korukcu, A., 2007. Efficient water use in agriculture in Turkey: The need for pressurized irrigation systems. Water International 32, 776–785.

Cakmak, E. H., 2010. Agricultural Water Pricing in Turkey: Economic Co-Operation and Development. Sustainable Management of Water Resources in Agriculture. OECD, Paris, France.

Campbell, B. M., Beare, D. J., Bennett, E. M., Hall-Spencer, J. M., Ingram, J. S. I., Jaramillo, F., Ortiz, R., Ramankutty, N., Sayer, J. A., Shindell, D., 2017. Agriculture production as a major driver of the Earth system exceeding planetary boundaries. Ecology and Society 22 (4).

Cao, M., Prince, S. D., Small, J., Goetz, S. J., 2004. Remotely Sensed Interannual Variations and Trends in Terrestrial Net Primary Productivity 1981–2000. Ecosystems 7 (3), 233–242.

Cao, Y., Zhou, W., Wang, J., Yuan, C., 2011. Spatial-temporal pattern and differences of land use changes in the Three Gorges Reservoir Area of China during 1975–2005. Journal of Mountain Science 8 (4), 551–563.

Casado, A., Peiry, J.-L., Campo, A. M., 2016. Geomorphic and vegetation changes in a meandering dryland river regulated by a large dam, Sauce Grande River, Argentina. GEOMORPHOLOGY 268, 21–34.

Cassidy, E. S., West, P. C., Gerber, J. S., Foley, J. A., 2013. Redefining agricultural yields: From tonnes to people nourished per hectare. Environmental Research Letters 8 (3), 034015.

Chen, Y., Lu, D., Luo, L., Pokhrel, Y., Deb, K., Huang, J., Ran, Y., 2018. Detecting irrigation extent, frequency, and timing in a heterogeneous arid agricultural region using MODIS time series, Landsat imagery, and ancillary data. Remote Sensing of Environment (204), 197–211.

CIESIN, IFPRI, CIAT, 2011. Global Rural-Urban Mapping Project, Version 1 (GRUMPv1): Population Density Grid. NASA Socioeconomic Data and Applications Center (SEDAC), New York, USA.

Claverie, M., Ju, J., Masek, J. G., Dungan, J. L., Vermote, E. F., Roger, J. C., Skakun, S. V., Justice, C. O., 2018. The Harmonized Landsat and Sentinel-2 surface reflectance data set. Remote Sens. Environ.

Cochran, W. G., 1977. Sampling Techniques: 3d Ed. Wiley, Hoboken, NJ, USA.

Cohn, A. S., VanWey, L. K., Spera, S. A., Mustard, J. F., 2016. Cropping frequency and area response to climate variability can exceed yield response. Nature Climate Change 6 (6), 601–604.

Congalton, R. G., Yadav, K., McDonnell, K., Poehnelt, J., Stevens, B., Gumma, M. K., Teluguntla, P., Thenkabail, P. S., 2017. Global Food Security-support Analysis Data (GFSAD) Cropland Extent 2015 Validation 30 m V001. NASA EOSDIS Land Processes DAAC, SD, USA.

Conijn, J. G., Bindraban, P. S., Schröder, J. J., Jongschaap, R., 2018. Can our global food system meet food demand within planetary boundaries? Agriculture, Ecosystems & Environment 251, 244–256.

Crist, E., 1985. A TM tasseled cap equivalent transformation for reflectance factor data. Remote Sensing of Environment (17), 301–306.

Crist, E., Cicone, R., 1984. A Physically Based Transformation of Thematic Mapper Data - The TM Tasseled Cap. IEEE Transactions on Geoscience and Remote Sensing.

CWC, ISRO, 2015. Indian Water Resource Information System. Central Water Commission, New Delhi, Delhi, India.

Daccache, A., Ciurana, J. S., Rodriguez Diaz, J. A., Knox, J. W., 2014. Water and energy footprint of irrigated agriculture in the Mediterranean region. Environmental Research Letters 9 (12), 124014.

Dara, A., Baumann, M., Kuemmerle, T., Pflugmacher, D., Rabe, A., Griffiths, P., Hölzel, N., Kamp, J., Freitag, M., Hostert, P., 2018. Mapping the timing of cropland abandonment and recultivation in northern Kazakhstan using annual Landsat time series. Remote Sensing of Environment 213, 49–60.

de Faria, F., Jaramillo, P., Sawakuchi, H. O., Richey, J. E., Barros, N., 2015. Estimating greenhouse gas emissions from future Amazonian hydroelectric reservoirs. Environmental Research Letters 10 (12), 124019.

de Fraiture, C., Kouali, G. N., Sally, H., Kabre, P., 2014. Pirates or pioneers? Unplanned irrigation around small reservoirs in Burkina Faso. Agricultural Water Management 131, 212–220.

Debaeke, P., Aboudrare, A., 2004. Adaptation of crop management to water-limited environments. European Journal of Agronomy 21 (4), 433–446.

Defourny, P., Kirches, G., Brockmann, C., Boettcher, M., Peters, M., Bontemps, S., Lamarche, C., Schlerf, M., Santoro, M., 2012. Land Cover CCI: Product User Guide Version 2. European Space Agency, Frascati, Roma, Italy.

Defourny, P., Vancutsem, C., Bicheron, P., Brockmann, C., Nino, F., Schouten, L., Leroy, M., 2006. GLOBCOVER: a 300 m global land cover product for 2005 using Envisat MERIS time series. In: Proceedings of the ISPRS commission.

DeFries, R. S., Foley, J. A., Asner, G. P., 2004. Land-use choices: balancing human needs and ecosystem function. Frontiers in Ecology and the Environment 2 (5), 249–257.

Degirmenci, H., Büyükcangaz, H., Merdun, H., 2006. Assessment of irrigation schemes in Turkey with irrigation Ratio and relative water supply. Water International 31 (2), 259–265.

Deines, J. M., Kendall, A. D., Hyndman, D. W., 2017. Annual Irrigation Dynamics in the U.S. Northern High Plains Derived from Landsat Satellite Data. Geophysical Research Letters 44 (18), 9350–9360.

Delang, C. O., Toro, M., Charlet-Phommachanh, M., 2013. Coffee, mines and dams: conflicts over land in the Bolaven Plateau, southern Lao PDR. Geographical Journal 179 (2), 150–164.

Destouni, G., Jaramillo, F., Prieto, C., 2013. Hydroclimatic shifts driven by human water use for food and energy production. Nature Climate Change 3 (3), 213–217.

Di Baldassarre, G., Wanders, N., AghaKouchak, A., Kuil, L., Rangecroft, S., Veldkamp, T. I. E., Garcia, M., van Oel, P. R., Breinl, K., van Loon, A. F., 2018. Water shortages worsened by reservoir effects. Nature Sustainability 1 (11), 617.

Diamond, J., 2001. Ecology - Dammed experiments! Science 294 (5548), 1847–1848.

Dile, Y. T., Karlberg, L., Temesgen, M., Rockström, J., 2013. The role of water harvesting to achieve sustainable agricultural intensification and resilience against water related shocks in sub-Saharan Africa. Agriculture, Ecosystems & Environment 181, 69–79.

Döll, P., Siebert, S., 2002. Global modeling of irrigation water requirements. Water Resources Research 38 (4), 1–10.

Domènech, L., 2015. Improving irrigation access to combat food insecurity and undernutrition: A review. Global Food Security 6, 24–33.

Donchyts, G., Baart, F., Winsemius, H., Gorelick, N., Kwadijk, J., van de Giesen, N., 2016. Earth's surface water change over the past 30 years. Nature Climate Change 6 (9), 810–813.

Dormann, C. F., 2013. Parametrische Statistik: Verteilungen, maximum likelihood und GLM in R. Springer Spektrum, Berlin Heidelberg.

DSI, 2015. DSI Barajlar Uygulaması v1.4: Register of Dams in Turkey. General Directorate of the State Hydraulic Works, Ankara, Turkey.

Duflo, E., Pande, R., 2007. Dams. The Quarterly Journal of Economics 122 (2), 601–646.

Dwyer, J., Roy, D., Sauer, B., Jenkerson, C., Zhang, H., Lymburner, L., 2018. Analysis Ready Data: Enabling Analysis of the Landsat Archive. Remote Sensing 10 (1363), 1–19.

EEA, 2016. Crop water demand: How is climate change affecting the water requirement of agricultural crops across Europe? European Environment Agency, Copenhagen, Denmark.

EEA, 2017. Updated CLC illustrated nomenclature guidelines. European Environment Agency, Wien, Austria.

Elith, J., Leathwick, J. R., Hastie, T., 2008. A working guide to boosted regression trees. The Journal of animal ecology 77 (4), 802–813.

Elliott, J., Deryng, D., Müller, C., Frieler, K., Konzmann, M., Gerten, D., Glotter, M., Flörke, M., Wada, Y., Best, N., Eisner, S., Fekete, B. M., Folberth, C., Foster, I., Gosling, S. N., Haddeland, I., Khabarov, N., Ludwig, F., Masaki, Y., Olin, S., Rosenzweig, C., Ruane, A. C., Satoh, Y., Schmid, E., Stacke, T., Tang, Q., Wisser, D., 2014. Constraints and potentials of future irrigation water availability on agricultural production under climate change. Proceedings of the National Academy of Sciences of the United States of America 111 (9), 3239–3244.

Ellis, E. C., 2011. Anthropogenic transformation of the terrestrial biosphere. Philosophical transactions. Series A, Mathematical, physical, and engineering sciences 369 (1938), 1010–1035.

Ellis, E. C., Kaplan, J. O., Fuller, D. Q., Vavrus, S., Klein Goldewijk, K., Verburg, P. H., 2013. Used planet: a global history. Proceedings of the National Academy of Sciences of the United States of America 110 (20), 7978–7985.

Erb, K.-H., Haberl, H., Jepsen, M. R., Kuemmerle, T., Lindner, M., Muller, D., Verburg, P. H., Reenberg, A., 2013. A conceptual framework for analysing and measuring land-use intensity. Current Opinion in Environmental Sustainability 5 (5), 464–470.

Ersado, L., 2005. Small-Scale Irrigation Dams, Agricultural Production, and Health: Theory and Evidence from Ethiopia. Policy Research Working Paper; No. 3494. World Bank, Washington DC., USA.

Ertek, A., Yilmaz, H., 2014. The agricultural perspective on water conservation in Turkey. Agricultural Water Management 143, 151–158.

Estel, S., Kuemmerle, T., Levers, C., Baumann, M., Hostert, P., 2016. Mapping cropland-use intensity across Europe using MODIS NDVI time series. Environmental Research Letters 11 (2), 24015.

European Commission, 2017. Corine Land Cover (CLC) 2012. European Environment Agency, Copenhagen, Denmark.

Evans, R. G., Sadler, E. J., 2008. Methods and technologies to improve efficiency of water use. Water Resources Research 44 (7), 263.

Evenson, R. E., Gollin, D., 2003. Assessing the impact of the green revolution, 1960 to 2000. Science (New York, N.Y.) 300 (5620), 758–762.

Fader, M., Shi, S., von Bloh, W., Bondeau, A., Cramer, W., 2016. Mediterranean irrigation under climate change: More efficient irrigation needed to compensate for increases in irrigation water requirements. Hydrology and Earth System Sciences 20 (2), 953–973.

FAO, 1985. Irrigation Water Management: Training Manual No. 1: Introduction to Irrigation. FAO, Rome, Italy.

FAO, 2009a. Euphrates-Tigris Basin. Water Report No 34. FAO, Rome, Italy.

FAO, 2009b. Irrigation in the Middle East region. Country Profile: Turkey: AQUASTAT Survey. FAO, Rome, Italy.

FAO, 2015. AQUASTAT Database. FAO, Rome, Italy.

Fearnside, P. M., 2005. Deforestation in Brazilian Amazonia: History, Rates and Consequences. Conservation Biology 19 (3), 680–688.

Feng, L., Han, X., Hu, C., Chen, X., 2016. Four decades of wetland changes of the largest freshwater lake in China: Possible linkage to the Three Gorges Dam? Remote Sensing of Environment 176, 43–55.

Ferrant, S., Selles, A., Le Page, M., Herrault, P.-A., Pelletier, C., Al-Bitar, A., Mermoz, S., Gascoin, S., Bouvet, A., Saqalli, M., Dewandel, B., Caballero, Y., Ahmed, S., Maréchal, J.-C., Kerr, Y., 2017. Detection of Irrigated Crops from Sentinel-1 and Sentinel-2 Data to Estimate Seasonal Groundwater Use in South India. Remote Sensing 9 (11), 1119.

Flood, N., 2013. Seasonal Composite Landsat TM/ETM+ Images Using the Medoid (a Multi-Dimensional Median). Remote Sensing 5 (12), 6481–6500.

Foley, J. A., DeFries, R. S., Asner, G. P., Barford, C., Bonan, G., Carpenter, S. R., Chapin, F. S., Coe, M. T., Daily, G. C., Gibbs, H., Helkowski, J. H., Holloway, T., Howard, E. A., Kucharik, C. J., Monfreda, C., Patz, J. A., Prentice, I. C., Ramankutty, N., Snyder, P. K., 2005. Global consequences of land use. Science (New York, N.Y.) 309 (5734), 570–574.

Foley, J. A., Ramankutty, N., Brauman, K. A., Cassidy, E. S., Gerber, J. S., Johnston, M., Mueller, N. D., O'Connell, C., Ray, D. K., West, P. C., Balzer, C.,

Bennett, E. M., Carpenter, S. R., Hill, J., Monfreda, C., Polasky, S., Rockström, J., Sheehan, J., Siebert, S., Tilman, D., Zaks, David P. M., 2011. Solutions for a cultivated planet. Nature 478 (7369), 337–342.

Foody, G. M., 2005. Local characterization of thematic classification accuracy through spatially constrained confusion matrices. International Journal of Remote Sensing 26 (6), 1217–1228.

Frantz, D., 2017. Generation of Higher Level Earth Observation Satellite Products for Regional Environmental Monitoring. Doctoral thesis, Universität Trier, Trier, Germany.

Frantz, D., Haß, E., Uhl, A., Stoffels, J., Hill, J., 2018. Improvement of the Fmask algorithm for Sentinel-2 images: Separating clouds from bright surfaces based on parallax effects. Remote Sensing of Environment (215), 471–481.

Frantz, D., Roder, A., Stellmes, M., Hill, J., 2016. An Operational Radiometric Landsat Preprocessing Framework for Large-Area Time Series Applications. IEEE Transactions on Geoscience and Remote Sensing 54 (7), 3928–3943.

Frantz, D., Röder, A., Stellmes, M., Hill, J., 2017. Phenology-adaptive pixel-based compositing using optical earth observation imagery. Remote Sensing of Environment 190, 331–347.

Friedl, M. A., Sulla-Menashe, D., Tan, B., Schneider, A., Ramankutty, N., Sibley, A., Huang, X., 2010. MODIS Collection 5 global land cover: Algorithm refinements and characterization of new datasets. Remote Sensing of Environment 114 (1), 168–182.

Friedman, J. H., 2001. Greedy Function Approximation: A Gradient Boosting Machine. The Annals of Statistics 29 (5), 1189–1232.

Fritz, S., See, L., McCallum, I., Schill, C., Obersteiner, M., van der Velde, Marijn, Boettcher, H., Havlík, P., Achard, F., 2011. Highlighting continued uncertainty in global land cover maps for the user community. Environmental Research Letters 6 (4), 44005.

Fritz, S., See, L., McCallum, I., You, L., Bun, A., Moltchanova, E., Duerauer, M., Albrecht, F., Schill, C., Perger, C., Havlik, P., Mosnier, A., Thornton, P., Wood-Sichra, U., Herrero, M., Becker-Reshef, I., Justice, C., Hansen, M., Gong, P., Abdel Aziz, S., Cipriani, A., Cumani, R., Cecchi, G., Conchedda, G., Ferreira, S., Gomez, A., Haffani, M., Kayitakire, F., Malanding, J., Mueller, R., Newby, T., Nonguierma, A., Olusegun, A., Ortner, S., Rajak, D. R., Rocha, J., Schepaschenko, D., Schepaschenko, M., Terekhov, A., Tiangwa, A., Vancutsem, C.,

Vintrou, E., Wenbin, W., van der Velde, Marijn, Dunwoody, A., Kraxner, F., Obersteiner, M., 2015. Mapping global cropland and field size. Global Change Biology 21 (5), 1980–1992.

Fung, Z., Pomun, T., Charles, K. J., Kirchherr, J., 2018. Mapping the social impacts of small dams: The case of Thailand's Ing River basin. Ambio 15, 2134.

Gao, F., Anderson, M. C., Zhang, X., Yang, Z., Alfieri, J. G., Kustas, W. P., Mueller, R., Johnson, D. M., Prueger, J. H., 2017. Toward mapping crop progress at field scales through fusion of Landsat and MODIS imagery. Remote Sensing of Environment 188, 9–25.

Gao, F., Masek, J., Schwaller, M., Hall, F., 2006. On the blending of the Landsat and MODIS surface reflectance: predicting daily Landsat surface reflectance. IEEE Transactions on Geoscience and Remote Sensing 44 (8), 2207–2218.

GAP, 2017. Latest state in GAP. GAP Regional Development Administration, Sanliurfa, Turkey.

Gaur, A., Biggs, T. W., Gumma, M. K., Parthasaradhi, G., Turral, H., 2008. Water Scarcity Effects on Equitable Water Distribution and Land Use in a Major Irrigation Project—Case Study in India. Journal of Irrigation and Drainage Engineering 134 (1), 26–35.

Geist, H. J., Lambin, E. F., 2001. What Drives Tropical Deforestation? A meta-analysis of proximate and underlying causes of deforestation based on subnational case study evidence. LUCC Report Series 4. UCL, Louvain, Belgium.

Gerland, P., Raftery, A. E., Sevčíková, H., Li, N., Gu, D., Spoorenberg, T., Alkema, L., Fosdick, B. K., Chunn, J., Lalic, N., Bay, G., Buettner, T., Heilig, G. K., Wilmoth, J., 2014. World population stabilization unlikely this century. Science (New York, N.Y.) 346 (6206), 234–237.

Gerten, D., Heinke, J., Hoff, H., Biemans, H., Fader, M., Waha, K., 2011. Global Water Availability and Requirements for Future Food Production. Journal of Hydrometeorology 12 (5), 885–899.

Gibbs, H. K., Ruesch, A. S., Achard, F., Clayton, M. K., Holmgren, P., Ramankutty, N., Foley, J. A., 2010. Tropical forests were the primary sources of new agricultural land in the 1980s and 1990s. Proceedings of the National Academy of Sciences 107 (38), 16732–16737.

Gibson, L., Lee, T. M., Koh, L. P., Brook, B. W., Gardner, T. A., Barlow, J., Peres, C. A., Bradshaw, C. J. A., Laurance, W. F., Lovejoy, T. E., Sodhi, N. S., 2011.

Primary forests are irreplaceable for sustaining tropical biodiversity. Nature 478, 378.

Godfray, H. C. J., Beddington, J. R., Crute, I. R., Haddad, L., Lawrence, D., Muir, J. F., Pretty, J., Robinson, S., Thomas, S. M., Toulmin, C., 2010. Food security: the challenge of feeding 9 billion people. Science (New York, N.Y.) 327 (5967), 812–818.

Gómez, C., White, J. C., Wulder, M. A., 2016. Optical remotely sensed time series data for land cover classification: A review. ISPRS Journal of Photogrammetry and Remote Sensing 116, 55–72.

Gómez-Limón, J. A., Picazo-Tadeo, A. J., 2012. Irrigated Agriculture in Spain: Diagnosis and Prescriptions for Improved Governance. International Journal of Water Resources Development 28 (1), 57–72.

Gordon, E., Meentemeyer, R. K., 2006. Effects of dam operation and land use on stream channel morphology and riparian vegetation. Geomorphology 82 (3-4), 412–429.

Gorelick, N., Hancher, M., Dixon, M., Ilyushchenko, S., Thau, D., Moore, R., 2017. Google Earth Engine: Planetary-scale geospatial analysis for everyone. Remote Sensing of Environment 202, 18–27.

Graesser, J., Ramankutty, N., 2017. Detection of cropland field parcels from Landsat imagery. Remote Sensing of Environment 201, 165–180.

Grafton, R. Q., Williams, J., Perry, C. J., Molle, F., Ringler, C., Steduto, P., Udall, B., Wheeler, S. A., Wang, Y., Garrick, D., Allen, R. G., 2018. The paradox of irrigation efficiency. Science (New York, N.Y.) 361 (6404), 748–750.

Griffiths, P., Jakimow, B., Hostert, P., 2018. Reconstructing long term annual deforestation dynamics in Pará and Mato Grosso using the Landsat archive. Remote Sensing of Environment 216, 497–513.

Griffiths, P., Kuemmerle, T., Baumann, M., Radeloff, V. C., Abrudan, I. V., Lieskovsky, J., Munteanu, C., Ostapowicz, K., Hostert, P., 2014. Forest disturbances, forest recovery, and changes in forest types across the Carpathian ecoregion from 1985 to 2010 based on Landsat image composites. Remote Sensing of Environment 151, 72–88.

Griffiths, P., Müller, D., Kuemmerle, T., Hostert, P., 2013a. Agricultural land change in the Carpathian ecoregion after the breakdown of socialism and expansion of the European Union. Environmental Research Letters 8 (4), 45024.

Griffiths, P., Nendel, C., Hostert, P., 2019. Intra-annual reflectance composites from Sentinel-2 and Landsat for national-scale crop and land cover mapping. Remote Sensing of Environment 220, 135–151.

Griffiths, P., van der Linden, S., Kuemmerle, T., Hostert, P., 2013b. A Pixel-Based Landsat Compositing Algorithm for Large Area Land Cover Mapping. IEEE Journal of Selected Topics in Applied Earth Observations and Remote Sensing 6 (5), 2088–2101.

Grill, G., Lehner, B., Lumsdon, A. E., MacDonald, G. K., Zarfl, C., Liermann, C. R., 2015. An index-based framework for assessing patterns and trends in river fragmentation and flow regulation by global dams at multiple scales. Environmental Research Letters 10 (1), 015001.

Gross, D., Dubois, G., Pekel, J.-F., Mayaux, P., Holmgren, M., Prins, H., Rondinini, C., Boitani, L., 2013. Monitoring land cover changes in African protected areas in the 21st century. Ecological Informatics 14, 31–37.

Haddeland, I., Skaugen, T., Lettenmaier, D. P., 2006. Anthropogenic impacts on continental surface water fluxes. Geophysical Research Letters 33 (8).

Hall, J. W., Grey, D., Garrick, D., Fung, F., Brown, C., Dadson, S. J., Sadoff, C. W., 2014. Water Security. Coping with the curse of freshwater variability. Science (New York, N.Y.) 346 (6208), 429–430.

Han, X., Feng, L., Hu, C., Chen, X., 2018. Wetland changes of China's largest freshwater lake and their linkage with the Three Gorges Dam. Remote Sensing of Environment 204, 799–811.

Hansen, M. C., Loveland, T. R., 2012. A review of large area monitoring of land cover change using Landsat data. Remote Sensing of Environment 122, 66–74.

Hansen, M. C., Potapov, P. V., Moore, R., Hancher, M., Turubanova, S. A., Tyukavina, A., Thau, D., Stehman, S. V., Goetz, S. J., Loveland, T. R., Kommareddy, A., Egorov, A., Chini, L., Justice, C. O., Townshend, J. R. G., 2013. High-Resolution Global Maps of 21st-Century Forest Cover Change. Science 342 (6160), 850–853.

Harris, L. M., 2009. Contested sustainabilities: assessing narratives of environmental change in southeastern Turkey. Local Environment 14 (8), 699–720.

Hijmans, R., 2015. Database of Global Administrative Areas: Version 2.8. University of California-Berkeley, California, USA.

Hijmans, R., Phillips, S., Leathwick, J., Elith, J., 2011. Package: dismo. https://CRAN.R-project.org/package=dismo.

Hijmans, R. J., Cameron, S. E., Parra, J. L., Jones, P. G., Jarvis, A., 2005. Very high resolution interpolated climate surfaces for global land areas. International Journal of Climatology 25 (15), 1965–1978.

Hillel, D., Braimoh, A., Vlek, P., 2008. Soil Degradation Under Irrigation. In: Braimoh, A., Vlek, P. (Eds.), Land Use and Soil Resources. Springer Netherlands, pp. 101–119.

Hommes, L., Boelens, R., Maat, H., 2016. Contested hydrosocial territories and disputed water governance: Struggles and competing claims over the Ilisu Dam development in southeastern Turkey. Geoforum 71, 9–20.

Hu, B., Yang, Z., Wang, H., Sun, X., Bi, N., Li, G., 2009. Sedimentation in the Three Gorges Dam and the future trend of Changjiang (Yangtze River) sediment flux to the sea. Hydrology and Earth System Sciences 13 (11), 2253–2264.

ICOLD, 2015. World Register of Dams. International Commission on Large Dams, Paris, France.

ICOLD, 2017. General Synthesis on the Register of Dams. International Commission on Large Dams, Paris, France.

Iizumi, T., Ramankutty, N., 2015. How do weather and climate influence cropping area and intensity? Global Food Security 4, 46–50.

Iizumi, T., Ramankutty, N., 2016. Changes in yield variability of major crops for 1981–2010 explained by climate change. Environmental Research Letters 11 (3), 34003.

Immitzer, M., Vuolo, F., Atzberger, C., 2016. First Experience with Sentinel-2 Data for Crop and Tree Species Classifications in Central Europe. Remote Sensing 8 (3), 166.

IPCC, 2018. Global warming of 1.5 C: An IPCC Special Report on the impacts of global warming of 1.5 C above pre-industrial levels and related global greenhouse gas emission pathways, in the context of strengthening the global response to the threat of climate change, sustainable development, and efforts to eradicate poverty. Special report. World Meteorological Organization,, Geneva, Switzerland.

Jafari, R., Hasheminasab, S., 2017. Assessing the effects of dam building on land degradation in central Iran with Landsat LST and LULC time series. Environmental Monitoring and Assessment 189 (2), 74.

Jägermeyr, J., Gerten, D., Heinke, J., Schaphoff, S., Kummu, M., Lucht, W., 2015. Water savings potentials of irrigation systems: global simulation of processes and linkages. Hydrology and Earth System Sciences 19 (7), 3073–3091.

Jägermeyr, J., Gerten, D., Schaphoff, S., Heinke, J., Lucht, W., Rockström, J., 2016. Integrated crop water management might sustainably halve the global food gap. Environmental Research Letters 11 (2), 25002.

Jägermeyr, J., Pastor, A., Biemans, H., Gerten, D., 2017. Reconciling irrigated food production with environmental flows for Sustainable Development Goals implementation. Nature communications 8, 15900.

Jain, M., Mondal, P., DeFries, R. S., Small, C., Galford, G. L., 2013. Mapping cropping intensity of smallholder farms: A comparison of methods using multiple sensors. Remote Sensing of Environment 134, 210–223.

Jakimow, B., Griffiths, P., van der Linden, S., Hostert, P., 2018. Mapping pasture management in the Brazilian Amazon from dense Landsat time series. Remote Sensing of Environment 205, 453–468.

Jakimow, B., van der Linden, S., Thiel, F., Hostert, P., in prep. Visualizing and labeling multi-sensor Earth observation data in QGIS: The EO Time Series Viewer.

Jaramillo, F., Destouni, G., 2015. Local flow regulation and irrigation raise global human water consumption and footprint. Science (New York, N.Y.) 350 (6265), 1248–1251.

Jarvis, A., Reuter, H. I., Nelson, A., Guevara, E., 2008. Hole-filled SRTM for the globe Version 4: Available from the CGIAR-CSI SRTM 90m Database.

Johansson, E. L., Fader, M., Seaquist, J. W., Nicholas, K. A., 2016. Green and blue water demand from large-scale land acquisitions in Africa. Proceedings of the National Academy of Sciences of the United States of America 113 (41), 11471–11476.

Jönsson, P., Cai, Z., Melaas, E., Friedl, M., Eklundh, L., 2018. A Method for Robust Estimation of Vegetation Seasonality from Landsat and Sentinel-2 Time Series Data. Remote Sensing 10 (4), 635.

Jönsson, P., Eklundh, L., 2004. TIMESAT—a program for analyzing time-series of satellite sensor data. Computers & Geosciences 30 (8), 833–845.

Kahil, M. T., Connor, J. D., Albiac, J., 2015. Efficient water management policies for irrigation adaptation to climate change in Southern Europe. Ecological Economics 120, 226–233.

Kankal, M., Nacar, S., Uzlu, E., 2016. Status of hydropower and water resources in the Southeastern Anatolia Project (GAP) of Turkey. Energy Reports 2, 123–128.

Kawasaki, K., 2018. Two Harvests Are Better than One: Double Cropping as a Strategy for Climate Change Adaptation. American Journal of Agricultural Economics 7 (2), 181.

Keiser, J., Caldas de Castro, Marcia, Maltese, M. F., Bos, R., Tanner, M., Singer, B. H., Utzinger, J., 2005. Effect of Irrigation and Large Dams on the Burden of Malaria on a Global and Regional Scale. Am J Trop Med Hyg 72 (4), 392–406.

Keken, Z., Panagiotidis, D., Skalos, J., 2015. The influence of damming on landscape structure change in the vicinity of flooded areas: Case studies in Greece and the Czech Republic. Ecological Engineering 74, 448–457.

Kellogg, C. H., Zhou, X., 2014. Impact of the construction of a large dam on riparian vegetation cover at different elevation zones as observed from remotely sensed data. International Journal of Applied Earth Observation and Geoinformation 32, 19–34.

Kendirli, B., Cakmak, B., Ucar, Y., 2005. Salinity in the southeastern Anatolia project (GAP), Turkey: issues and options. Irrigation and Drainage 54 (1), 115–122.

Kennedy, R., Yang, Z., Gorelick, N., Braaten, J., Cavalcante, L., Cohen, W., Healey, S., 2018. Implementation of the LandTrendr Algorithm on Google Earth Engine. Remote Sensing 10 (5), 691.

Khlifi, S., Ameur, M., Mtimet, N., Ghazouani, N., Belhadj, N., 2010. Impacts of small hill dams on agricultural development of hilly land in the Jendouba region of northwestern Tunisia. Agricultural Water Management 97 (1), 50–56.

Kibaroğlu, A., Kramer, A., Scheumann, W., 2011. Turkey's water policy: National frameworks and international cooperation. Springer, Heidelberg, Germany and New York, NY, USA.

Kibaroğlu, A., Sümer, V., Scheumann, W., 2012. Fundamental Shifts in Turkey's Water Policy. Méditerranée (119), 27–34.

Kingsford, R. T., Thomas, R. F., 2004. Destruction of wetlands and waterbird populations by dams and irrigation on the Murrumbidgee River in arid Australia. Environmental Management 34 (3), 383–396.

Kirchherr, J., Charles, K. J., 2016. The social impacts of dams: A new framework for scholarly analysis. Environmental Impact Assessment Review 60, 99–114.

Kirchherr, J., Pohlner, H., Charles, K. J., 2016. Cleaning up the big muddy: A meta-synthesis of the research on the social impact of dams. Environmental Impact Assessment Review 60, 115–125.

Klein, I., Gessner, U., Dietz, A. J., Kuenzer, C., 2017. Global WaterPack – A 250 m resolution dataset revealing the daily dynamics of global inland water bodies. Remote Sensing of Environment 198, 345–362.

Klümper, F., Herzfeld, T., Theesfeld, I., 2017. Can Water Abundance Compensate for Weak Water Governance? Determining and Comparing Dimensions of Irrigation Water Security in Tajikistan. Water 9 (4), 286.

Koç, C., 2017. Sustainability of Irrigation Schemes Transferred in Turkey. Irrigation and Drainage 7 (4), 231.

Koluvek, P. K., Tanji, K. K., Trout, T. J., 1993. Overview of Soil Erosion from Irrigation. Journal of Irrigation and Drainage Engineering 119 (6), 929–946.

Kontgis, C., Schneider, A., Özdoğan, M., 2015. Mapping rice paddy extent and intensification in the Vietnamese Mekong River Delta with dense time stacks of Landsat data. Remote Sensing of Environment 169, 255–269.

Kovalskyy, V., Roy, D., 2015. A One Year Landsat 8 Conterminous United States Study of Cirrus and Non-Cirrus Clouds. Remote Sensing 7 (1), 564–578.

Kovalskyy, V., Roy, D. P., 2013. The global availability of Landsat 5 TM and Landsat 7 ETM+ land surface observations and implications for global 30m Landsat data product generation. Remote Sensing of Environment 130, 280–293.

Kraay, A., Kaufmann, D., Mastruzzi, M., 2010. The worldwide governance indicators: Methodology and analytical issues. World Bank, Washington DC., USA.

Kuenzer, C., Leinenkugel, P., Vollmuth, M., Dech, S., 2014. Comparing global land-cover products – implications for geoscience applications: An investigation for the trans-boundary Mekong Basin. International Journal of Remote Sensing 35 (8), 2752–2779.

Kümmerle, T., Erb, K., Meyfroidt, P., Müller, D., Verburg, P. H., Estel, S., Haberl, H., Hostert, P., Jepsen, M. R., Kastner, T., Levers, C., Lindner, M., Plutzar, C., Verkerk, P. J., van der Zanden, Emma H, Reenberg, A., 2013. Challenges and opportunities in mapping land use intensity globally. Current opinion in environmental sustainability 5 (5), 484–493.

Labahn, S., 2018. Landsat Global Archive Consolidation (LGAC) Status. USGS Landsat Science Team Meeting, Colorado, USA.

Lacombe, G., Douangsavanh, S., Baker, J., Hoanh, C. T., Bartlett, R., Jeuland, M., Phongpachith, C., 2014. Are hydropower and irrigation development complements or substitutes? The example of the Nam Ngum River in the Mekong Basin. Water International 39 (5), 649–670.

Lambin, E. F., Meyfroidt, P., 2011. Global land use change, economic globalization, and the looming land scarcity. Proceedings of the National Academy of Sciences of the United States of America 108 (9), 3465–3472.

Lehner, B., Grill, G., 2013. Global river hydrography and network routing: baseline data and new approaches to study the world's large river systems. Hydrological Processes 27 (15), 2171–2186.

Lehner, B., Liermann, C. R., Revenga, C., Vörösmarty, C., Fekete, B., Crouzet, P., Döll, P., Endejan, M., Frenken, K., Magome, J., Nilsson, C., Robertson, J. C., Rödel, R., Sindorf, N., Wisser, D., 2011. High-resolution mapping of the world's reservoirs and dams for sustainable river-flow management. Frontiers in Ecology and the Environment 9 (9), 494–502.

Levers, C., van Butsic, Verburg, P. H., Müller, D., Kuemmerle, T., 2016. Drivers of changes in agricultural intensity in Europe. Land Use Policy 58, 380–393.

Levers, C., Verkerk, P. J., Müller, D., Verburg, P. H., van Butsic, Leitão, P. J., Lindner, M., Kuemmerle, T., 2014. Drivers of forest harvesting intensity patterns in Europe. Forest Ecology and Management 315, 160–172.

Li, W., MacBean, N., Ciais, P., Defourny, P., Lamarche, C., Bontemps, S., Houghton, R. A., Peng, S., 2018. Gross and net land cover changes in the main plant functional types derived from the annual ESA CCI land cover maps (1992–2015).

Lillesand, T., Kiefer, R., Chipman, J., 2011. Remote Sensing and Image Interpretation, sixth edition Edition. Wiley, Hoboken, NJ.

Lindström, A., Granit, J., Weinberg, J., 2012. Large-scale water storage in the water, energy and food nexus: Perspectives on benefits, risks and best practices. Stockholm International Water Institute, Stockholm, Sweden.

Lipton, M., Litchfield, J., Faurès, J.-M., 2003. The effects of irrigation on poverty: a framework for analysis. Water Policy 5 (5-6), 413–427.

Liu, J., et al., 2007. Complexity of Coupled Humand and Natural Systems. Science (317), 1513–1516.

Lobell, D. B., Cassman, K. G., Field, C. B., 2009. Crop Yield Gaps: Their Importance, Magnitudes, and Causes. Annual Review of Environment and Resources 34 (1), 179–204.

Loker, W. M., 2003. Dam impacts in a time of globalization: Using multiple methods to document social and environmental change in rural Honduras. Current Anthropology 44 (S), S112–S121.

Lopes, M. S., Royo, C., Alvaro, F., Sanchez-Garcia, M., Ozer, E., Ozdemir, F., Karaman, M., Roustaii, M., Jalal-Kamali, M. R., Pequeno, D., 2018. Optimizing Winter Wheat Resilience to Climate Change in Rain Fed Crop Systems of Turkey and Iran. Frontiers in plant science 9, 563.

Löw, F., Prishchepov, A., Waldner, F., Dubovyk, O., Akramkhanov, A., Biradar, C., Lamers, J., 2018. Mapping Cropland Abandonment in the Aral Sea Basin with MODIS Time Series. Remote Sensing 10 (2), 159.

Magliocca, N. R., Ellis, E. C., Allington, G. R., de Bremond, A., Dell'Angelo, J., Mertz, O., Messerli, P., Meyfroidt, P., Seppelt, R., Verburg, P. H., 2018. Closing global knowledge gaps: Producing generalized knowledge from case studies of social-ecological systems. Global Environmental Change 50, 1–14.

Magliocca, N. R., van Vliet, J., Brown, C., Evans, T. P., Houet, T., Messerli, P., Messina, J. P., Nicholas, K. A., Ornetsmüller, C., Sagebiel, J., Schweizer, V., Verburg, P. H., Yu, Q., 2015. From meta-studies to modeling: Using synthesis knowledge to build broadly applicable process-based land change models. Environmental Modelling & Software 72, 10–20.

Main, H., 1990. Dam Projects and Urbanization in Kano State, Nigeria. Singapore Journal of Tropical Geography 11 (2), 87–99.

Malek, Ž., Verburg, P. H., R Geijzendorffer, I., Bondeau, A., Cramer, W., 2018. Global change effects on land management in the Mediterranean region. Global Environmental Change 50, 238–254.

Manikowski, S., Strapasson, A., 2016. Sustainability Assessment of Large Irrigation Dams in Senegal: A Cost-Benefit Analysis for the Senegal River Valley. Frontiers in Environmental Science 4, 308.

Mansaray, L., Huang, W., Zhang, D., Huang, J., Li, J., 2017. Mapping Rice Fields in Urban Shanghai, Southeast China, Using Sentinel-1A and Landsat 8 Datasets. Remote Sensing 9 (3), 257.

Margulies, J. D., Magliocca, N. R., Schmill, M. D., Ellis, E. C., 2016. Ambiguous Geographies: Connecting Case Study Knowledge with Global Change Science. Annals of the American Association of Geographers 106 (3), 572–596.

Martino, L., Fritz, M., 2008. New insight into land cover and land use in Europe. Eurostat, Luxembourg.

Masek, J. G., Vermote, E. F., Saleous, N. E., Wolfe, R., Hall, F. G., Huemmrich, K. F., Gao, F., Kutler, J., Lim, T.-K., 2006. A Landsat Surface Reflectance Dataset for North America, 1990-2000. IEEE Geoscience and Remote Sensing Letters 3 (1), 68–72.

Maxwell, A. E., Warner, T. A., Fang, F., 2018. Implementation of machine-learning classification in remote sensing: An applied review. International Journal of Remote Sensing 39 (9), 2784–2817.

McCully, P., 2001. Silenced rivers: The ecology and politics of large dams, enl. & updated ed Edition. Zed Books, London and New York.

Mekonnen, M. M., Hoekstra, A. Y., 2016. Four billion people facing severe water scarcity. Science advances 2 (2), e1500323.

Melaas, E. K., Friedl, M. A., Zhu, Z., 2013. Detecting interannual variation in deciduous broadleaf forest phenology using Landsat TM/ETM+ data. Remote Sensing of Environment 132, 176–185.

Metin Sezen, S., Yazar, A., 2006. Wheat yield response to line-source sprinkler irrigation in the arid Southeast Anatolia region of Turkey. Agricultural Water Management 81 (1-2), 59–76.

Meyfroidt, P., 2016. Approaches and terminology for causal analysis in land systems science. Journal of Land Use Science 11 (5), 501–522.

Micklin, P., 2007. The Aral Sea Disaster. Annual Review of Earth and Planetary Sciences 35 (1), 47–72.

Monfreda, C., Ramankutty, N., Foley, J. A., 2008. Farming the planet: 2. Geographic distribution of crop areas, yields, physiological types, and net primary production in the year 2000. Global Biogeochemical Cycles 22 (1), GB1022.

Mueller, N. D., Gerber, J. S., Johnston, M., Ray, D. K., Ramankutty, N., Foley, J. A., 2012. Closing yield gaps through nutrient and water management. Nature 490 (7419), 254–257.

Müller, D., Leitão, P. J., Sikor, T., 2013. Comparing the determinants of cropland abandonment in Albania and Romania using boosted regression trees. Agricultural Systems 117, 66–77.

Müller, H., Rufin, P., Griffiths, P., Barros Siqueira, Auberto José, Hostert, P., 2015. Mining dense Landsat time series for separating cropland and pasture in a heterogeneous Brazilian savanna landscape. Remote Sensing of Environment 156, 490–499.

Müller, H., Rufin, P., Griffiths, P., de Barros Viana Hissa, Letícia, Hostert, P., 2016. Beyond deforestation: Differences in long-term regrowth dynamics across land use regimes in southern Amazonia. Remote Sensing of Environment 186, 652–662.

Muller, M., Biswas, A., Martin-Hurtado, R., Tortajada, C., 2015. Built infrastructure is essential. Science (New York, N.Y.) 349 (6248), 585–586.

Murray, N. J., Phinn, S. R., DeWitt, M., Ferrari, R., Johnston, R., Lyons, M. B., Clinton, N., Thau, D., Fuller, R. A., 2018. The global distribution and trajectory of tidal flats. Nature.

Nelson, A., 2008. Travel time to major cities: A global map of Accessibility. Joint Research Centre of the European Commission, Ispra, Italy.

Neumann, K., Stehfest, E., Verburg, P. H., Siebert, S., Müller, C., Veldkamp, T., 2011. Exploring global irrigation patterns: A multilevel modelling approach. Agricultural Systems 104 (9), 703–713.

New, M., Hulme, M., Jones, P., 2000. Representing Twentieth-Century Space–Time Climate Variability. Part II: Development of 1901–96 Monthly Grids of Terrestrial Surface Climate. Journal of Climate 13 (13), 2217–2238.

Nilsson, C., Berggren, K., 2000. Alterations of Riparian Ecosystems Caused by River Regulation. BioScience 50 (9), 783–792.

Olofsson, P., Foody, G. M., Herold, M., Stehman, S. V., Woodcock, C. E., Wulder, M. A., 2014. Good practices for estimating area and assessing accuracy of land change. Remote Sensing of Environment 148, 42–57.

Orr, S., Pittock, J., Chapagain, A., Dumaresq, D., 2012. Dams on the Mekong River: Lost fish protein and the implications for land and water resources. Global Environmental Change 22 (4), 925–932.

Ostrom, E., 2009. A general framework for analyzing sustainability of social-ecological systems. Science (New York, N.Y.) 325 (5939), 419–422.

Özdoğan, M., Gutman, G., 2008. A new methodology to map irrigated areas using multi-temporal MODIS and ancillary data: An application example in the continental US. Remote Sensing of Environment 112 (9), 3520–3537.

Özdoğan, M., Woodcock, C. E., 2006a. Resolution dependent errors in remote sensing of cultivated areas. Remote Sensing of Environment 103 (2), 203–217.

Özdoğan, M., Woodcock, C. E., 2006b. Resolution dependent errors in remote sensing of cultivated areas. Remote Sensing of Environment 103 (2), 203–217.

Özdoğan, M., Woodcock, C. E., Salvucci, G. D., Demir, H., 2006. Changes in Summer Irrigated Crop Area and Water Use in Southeastern Turkey from 1993 to 2002: Implications for Current and Future Water Resources. Water Resources Management 20 (3), 467–488.

Özdoğan, M., Yang, Y., Allez, G., Cervantes, C., 2010. Remote Sensing of Irrigated Agriculture: Opportunities and Challenges. Remote Sensing 2 (9), 2274–2304.

Palmer, M. A., Liu, J., Matthews, J. H., Mumba, M., D'Odorico, P., 2015. Manage water in a green way. Science (New York, N.Y.) 349 (6248), 584–585.

Pasquarella, V. J., Holden, C. E., Woodcock, C. E., 2018. Improved mapping of forest type using spectral-temporal Landsat features. Remote Sensing of Environment 210, 193–207.

Pekel, J.-F., Cottam, A., Gorelick, N., Belward, A. S., 2016. High-resolution mapping of global surface water and its long-term changes. Nature 540, 418–437.

Pérez-Hoyos, A., Rembold, F., Kerdiles, H., Gallego, J., 2017. Comparison of Global Land Cover Datasets for Cropland Monitoring. Remote Sensing 9 (11), 1118.

Perry, C., 2001. World Commission on Dams: Implications for food and irrigation1. Irrigation and Drainage 50 (2), 101–107.

Perry, C. J., Narayanamurthy, S. G., 1998. Farmer Response to Rationed and Uncertain Irrigation Supplies: Research Report 24. Colombo, Sri Lanka.

Pfafstetter, O., 1989. Classification of hydrographic basins: coding methodology. Unpublished manuscript. Departamento Nacional de Obras de Saneamento, Brazil.

Pflugmacher, D., Cohen, W. B., E. Kennedy, R., 2012. Using Landsat-derived disturbance history (1972–2010) to predict current forest structure. Remote Sensing of Environment 122, 146–165.

Pflugmacher, D., Krankina, O. N., Cohen, W. B., Friedl, M. A., Sulla-Menashe, D., Kennedy, R. E., Nelson, P., Loboda, T. V., Kuemmerle, T., Dyukarev, E., Elsakov, V., Kharuk, V. I., 2011. Comparison and assessment of coarse resolution land cover maps for Northern Eurasia. Remote Sensing of Environment 115 (12), 3539–3553.

Pflugmacher, D., Rabe, A., Peters, M., Hostert, P., 2019. Mapping pan-European land cover using Landsat spectral-temporal metrics and the European LUCAS survey. Remote Sensing of Environment 221, 583–595.

Phalke, A., Özdoğan, M., Thenkabail, P., Congalton, R., Yadav, K., Massey, R., Teluguntla, P., Poehnelt, J., Smith, C., 2017. Global Food Security-support Analysis Data (GFSAD) Cropland Extent 2015 Europe, Central Asia, Russia, Middle East 30 m V001. Sioux Falls, South Dakota, USA.

Phalke, A. R., Özdoğan, M., 2018. Large area cropland extent mapping with Landsat data and a generalized classifier. Remote Sensing of Environment 219, 180–195.

Poff, N. L., Hart, D. D., 2002. How Dams Vary and Why It Matters for the Emerging Science of Dam Removal. BioScience 52 (8), 659.

Pongratz, J., Dolman, H., Don, A., Erb, K.-H., Fuchs, R., Herold, M., Jones, C., Kuemmerle, T., Luyssaert, S., Meyfroidt, P., Naudts, K., 2017. Models meet data: Challenges and opportunities in implementing land management in Earth system models. Global Change Biology, 1–18.

Pongratz, J., Reick, C., Raddatz, T., Claussen, M., 2008. A reconstruction of global agricultural areas and land cover for the last millennium. Global Biogeochemical Cycles 22 (3), n/a–n/a.

Porkka, M., Gerten, D., Schaphoff, S., Siebert, S., Kummu, M., 2016. Causes and trends of water scarcity in food production. Environmental Research Letters 11 (1), 015001.

Portmann, F. T., Siebert, S., Döll, P., 2010. MIRCA2000-Global monthly irrigated and rainfed crop areas around the year 2000: A new high-resolution data set for agricultural and hydrological modeling. Global Biogeochemical Cycles 24 (1), 1–24.

Power, A. G., 2010. Ecosystem services and agriculture: tradeoffs and synergies. Philosophical transactions of the Royal Society of London. Series B, Biological sciences 365 (1554), 2959–2971.

Pretty, J., 2018. Intensification for redesigned and sustainable agricultural systems. Science (New York, N.Y.) 362 (6417).

Qadir, M., Quillérou, E., Nangia, V., Murtaza, G., Singh, M., Thomas, R. J., Drechsel, P., Noble, A. D., 2014. Economics of salt-induced land degradation and restoration. Natural Resources Forum 38 (4), 282–295.

Radeloff, V., Yin, H., Tan, B., Frantz, D., Buchner, J., 2018. Topographic Correction of Landsat imagery in the Caucasus Mountains. USGS Landsat Science Team Meeting, Colorado, USA.

Rakhmatullaev, S., Huneau, F., Celle-Jeanton, H., Le Coustumer, P., Motelica-Heino, M., Bakiev, M., 2013. Water reservoirs, irrigation and sedimentation in Central Asia: a first-cut assessment for Uzbekistan. Environmental Earth Sciences 68 (4), 985–998.

Ramankutty, N., Foley, J. A., 1998. Characterizing patterns of global land use: An analysis of global croplands data. Global Biogeochemical Cycles 12 (4), 667–685.

Ramankutty, N., Mehrabi, Z., Waha, K., Jarvis, L., Kremen, C., Herrero, M., Rieseberg, L. H., 2018. Trends in Global Agricultural Land Use: Implications for Environmental Health and Food Security. Annual review of plant biology 69, 789–815.

Rasmussen, L. V., Coolsaet, B., Martin, A., Mertz, O., Pascual, U., Corbera, E., Dawson, N., Fisher, J. A., Franks, P., Ryan, C. M., 2018. Social-ecological outcomes of agricultural intensification. Nature Sustainability 1 (6), 275–282.

Ray, D. K., Foley, J. A., 2013. Increasing global crop harvest frequency: Recent trends and future directions. Environmental Research Letters 8 (4), 44041.

Ray, D. K., Gerber, J. S., MacDonald, G. K., West, P. C., 2015. Climate variation explains a third of global crop yield variability. Nature communications 6, 5989.

Ray, D. K., Mueller, N. D., West, P. C., Foley, J. A., 2013. Yield Trends Are Insufficient to Double Global Crop Production by 2050. PLoS ONE 8 (6), e66428.

Robinson, D. T., Di Vittorio, A., Alexander, P., Arneth, A., Barton, C. M., Brown, D. G., Kettner, A., Lemmen, C., O&apos, Neill, B. C., Janssen, M., Pugh, T. A. M., Rabin, S. S., Rounsevell, M., Syvitski, J. P., Ullah, I., Verburg, P. H., 2018. Modelling feedbacks between human and natural processes in the land system. Earth System Dynamics 9 (2), 895–914.

Rockström, J., Karlberg, L., Wani, S. P., Barron, J., Hatibu, N., Oweis, T., Bruggeman, A., Farahani, J., Qiang, Z., 2010. Managing water in rainfed agriculture—The need for a paradigm shift. Agricultural Water Management 97 (4), 543–550.

Rockström, J., Williams, J., Daily, G., Noble, A., Matthews, N., Gordon, L., Wetterstrand, H., DeClerck, F., Shah, M., Steduto, P., de Fraiture, C., Hatibu, N., Unver, O., Bird, J., Sibanda, L., Smith, J., 2016. Sustainable intensification of agriculture for human prosperity and global sustainability. AMBIO 46, 4–17.

Rohwer, J., Gerten, D., Lucht, W., 2007. Development of Functional Irrigation Types for Improved Global Crop Monitoring: Report No. 104. Potsdam Institute for Climate Impact Research, Potsdam, Germany.

Rosa, L., Rulli, M. C., Davis, K. F., Chiarelli, D. D., Passera, C., D'Odorico, P., 2018. Closing the yield gap while ensuring water sustainability. Environmental Research Letters 13 (10), 104002.

Rosegrant, M. W., Ringler, C., Zhu, T., 2009. Water for Agriculture: Maintaining Food Security under Growing Scarcity. Annual Review of Environment and Resources 34 (1), 205–222.

Rosenberg, D. M., McCully, P., Pringle, C. M., 2000. Global-Scale Environmental Effects of Hydrological Alterations: Introduction. BioScience 50 (9), 746.

Rosenzweig, C., Strzepek, K. M., Major, D. C., Iglesias, A., Yates, D. N., McCluskey, A., Hillel, D., 2004. Water resources for agriculture in a changing climate: International case studies. Global Environmental Change 14 (4), 345–360.

Roy, D. P., Yan, L., 2018. Robust Landsat-based crop time series modelling. Remote Sensing of Environment (in press).

Rufin, P., Frantz, D., Ernst, S., Rabe, A., Griffiths, P., Özdoğan, M., Hostert, P., 2019a. A Landsat-based national-scale map of cropping practices for Turkey (2015). PANGAEA, Hamburg, Germany.

Rufin, P., Frantz, D., Ernst, S., Rabe, A., Griffiths, P., Özdoğan, M., Hostert, P., 2019b. Mapping Cropping Practices on a National Scale Using Intra-Annual Landsat Time Series Binning. Remote Sensing 11 (3), 232.

Rufin, P., Levers, C., Baumann, M., Jägermeyr, J., Krueger, T., Kuemmerle, T., Hostert, P., 2017. CA1985: A global approximation of irrigation dam command areas commissioned since 1985. GFZ Data Services, Potsdam, Germany.

Rufin, P., Levers, C., Baumann, M., Jägermeyr, J., Krueger, T., Kuemmerle, T., Hostert, P., 2018. Global-scale patterns and determinants of cropping frequency in irrigation dam command areas. Global Environmental Change 50, 110–122.

Rufin, P., Müller, H., Pflugmacher, D., Hostert, P., 2015. Land use intensity trajectories on Amazonian pastures derived from Landsat time series. International Journal of Applied Earth Observation and Geoinformation 41, 1–10.

Saadi, S., Todorovic, M., Tanasijevic, L., Pereira, L. S., Pizzigalli, C., Lionello, P., 2015. Climate change and Mediterranean agriculture: Impacts on winter wheat and tomato crop evapotranspiration, irrigation requirements and yield. Agricultural Water Management 147, 103–115.

Sabo, J. L., Ruhi, A., Holtgrieve, G. W., Elliott, V., Arias, M. E., Ngor, P. B., Räsänen, T. A., Nam, S., 2017. Designing river flows to improve food security futures in the Lower Mekong Basin. Science (New York, N.Y.) 358 (6368).

Salmon, J., Friedl, M. A., Frolking, S., Wisser, D., Douglas, E. M., 2015. Global rain-fed, irrigated, and paddy croplands: A new high resolution map derived from remote sensing, crop inventories and climate data. International Journal of Applied Earth Observation and Geoinformation 38, 321–334.

Scanlon, B. R., Faunt, C. C., Longuevergne, L., Reedy, R. C., Alley, W. M., McGuire, V. L., McMahon, P. B., 2012. Groundwater depletion and sustainability of irrigation in the US High Plains and Central Valley. Proceedings of the National Academy of Sciences of the United States of America 109 (24), 9320–9325.

Schmidt, M., Pringle, M., Devadas, R., Denham, R., Tindall, D., 2016. A Framework for Large-Area Mapping of Past and Present Cropping Activity Using Seasonal Landsat Images and Time Series Metrics. Remote Sensing 8 (4), 312.

Schug, F., Okujeni, A., Hauer, J., Hostert, P., Nielsen, J. Ø., van der Linden, S., 2018. Mapping patterns of urban development in Ouagadougou, Burkina Faso, using machine learning regression modeling with bi-seasonal Landsat time series. Remote Sensing of Environment 210, 217–228.

Schwieder, M., Leitão, P. J., da Cunha Bustamante, Mercedes Maria, Ferreira, L. G., Rabe, A., Hostert, P., 2016. Mapping Brazilian savanna vegetation gradients with Landsat time series. International Journal of Applied Earth Observation and Geoinformation 52, 361–370.

Schwieder, M., Leitão, P. J., Pinto, J. R. R., Teixeira, A. M. C., Pedroni, F., Sanchez, M., Bustamante, M. M., Hostert, P., 2018. Landsat phenological metrics and their relation to aboveground carbon in the Brazilian Savanna. Carbon balance and management 13 (1), 7.

Scott, C. A., Flores-López, F., Gastélum, J. R., 2007. Appropriation of Río San Juan water by Monterrey City, Mexico: Implications for agriculture and basin water sharing. Paddy and Water Environment 5 (4), 253–262.

Scudder, T., 2012. Resettlement Outcomes of Large Dams. In: Tortajada, C., Altinbilek, D., Biswas, A. K. (Eds.), Impacts of Large Dams: A Global Assessment. Water Resources Development and Management. Springer, Berlin/Heidelberg, Germany, pp. 37–67.

Scudder, T., 2019. Large Dams: Long Term Impacts on Riverine Communities and Free Flowing Rivers. Water Resources Development and Management. Springer Singapore, Singapore.

Seifert, C. A., Lobell, D. B., 2015. Response of double cropping suitability to climate change in the United States. Environmental Research Letters 10 (2), 024002.

Senf, C., Leitão, P. J., Pflugmacher, D., van der Linden, S., Hostert, P., 2015. Mapping land cover in complex Mediterranean landscapes using Landsat: Improved classification accuracies from integrating multi-seasonal and synthetic imagery. Remote Sensing of Environment 156, 527–536.

Senf, C., Pflugmacher, D., van der Linden, S., Hostert, P., 2013. Mapping Rubber Plantations and Natural Forests in Xishuangbanna (Southwest China) Using Multi-Spectral Phenological Metrics from MODIS Time Series. Remote Sensing 5 (6), 2795–2812.

Shao, J.-A., Huang, X.-Q., Qu, M., Wei, C.-F., Xie, D.-T., 2005. Land Use Change and its Socio-Economic Driving Forces - A Case Study of Linshui Reservoir Area of Dahonghe Reservoir in Sichuan Province. CHINESE GEOGRAPHICAL SCIENCE 15 (4), 315–324.

Shumilova, O., Tockner, K., Thieme, M., Koska, A., Zarfl, C., 2018. Global Water Transfer Megaprojects: A Potential Solution for the Water-Food-Energy Nexus? Frontiers in Environmental Science 6, 150.

Siebert, S., Burke, J., Faures, J. M., Frenken, K., Hoogeveen, J., Döll, P., Portmann, F. T., 2010a. Groundwater use for irrigation – a global inventory. Hydrology and Earth System Sciences 14 (10), 1863–1880.

Siebert, S., Döll, P., 2010. Quantifying blue and green virtual water contents in global crop production as well as potential production losses without irrigation. Journal of Hydrology 384 (3-4), 198–217.

Siebert, S., Henrich, V., Frenken, K., Burke, J., 2013. Update of the digital global map of irrigation areas to version 5: Project report. Institute of Crop Science and Resource Conservation, Bonn, Germany.

Siebert, S., Kummu, M., Porkka, M., Döll, P., Ramankutty, N., Scanlon, B. R., 2015. A global data set of the extent of irrigated land from 1900 to 2005. Hydrology and Earth System Sciences 19 (3), 1521–1545.

Siebert, S., Portmann, F. T., Döll, P., 2010b. Global Patterns of Cropland Use Intensity. Remote Sensing 2 (7), 1625–1643.

Singh, A., 2016. Evaluating the effect of different management policies on the long-term sustainability of irrigated agriculture. Land Use Policy 54, 499–507.

Son, N.-T., Chen, C.-F., Chen, C.-R., Duc, H.-N., Chang, L.-Y., 2014. A Phenology-Based Classification of Time-Series MODIS Data for Rice Crop Monitoring in Mekong Delta, Vietnam. Remote Sensing 6 (1), 135–156.

Song, X.-P., Hansen, M. C., Stehman, S. V., Potapov, P. V., Tyukavina, A., Vermote, E. F., Townshend, J. R., 2018. Global land change from 1982 to 2016. Nature 560 (7720), 639–643.

Song, X.-P., Potapov, P. V., Krylov, A., King, L., Di Bella, C. M., Hudson, A., Khan, A., Adusei, B., Stehman, S. V., Hansen, M. C., 2017. National-scale soybean mapping and area estimation in the United States using medium resolution satellite imagery and field survey. Remote Sensing of Environment 190, 383–395.

St. Louis, V. L., Kelly, C. A., Duchemin, É., Rudd, J., Rosenberg, D. M., 2000. Reservoir Surfaces as Sources of Greenhouse Gases to the Atmosphere: A Global Estimate. BioScience 50 (9), 766–775.

Stanhill, G., 1986. Water Use Efficiency. Vol. 39. pp. 53–85.

Steffen, W., Broadgate, W., Deutsch, L., Gaffney, O., Ludwig, C., 2015. The trajectory of the Anthropocene: The Great Acceleration. The Anthropocene Review 2 (1), 81–98.

Steffen, W., Rockström, J., Richardson, K., Lenton, T. M., Folke, C., Liverman, D., Summerhayes, C. P., Barnosky, A. D., Cornell, S. E., Crucifix, M., Donges, J. F., Fetzer, I., Lade, S. J., Scheffer, M., Winkelmann, R., Schellnhuber, H. J., 2018. Trajectories of the Earth System in the Anthropocene. Proceedings of the National Academy of Sciences of the United States of America 115 (33), 8252–8259.

Stehman, S. V., 2014. Estimating area and map accuracy for stratified random sampling when the strata are different from the map classes. International Journal of Remote Sensing 35 (13), 4923–4939.

Stevenson, J. R., Villoria, N., Byerlee, D., Kelley, T., Maredia, M., 2013. Green Revolution research saved an estimated 18 to 27 million hectares from being brought into agricultural production. Proceedings of the National Academy of Sciences of the United States of America 110 (21), 8363–8368.

Strobl, E., Strobl, R. O., 2011. The distributional impact of large dams: Evidence from cropland productivity in Africa. Journal of Development Economics 96 (2), 432–450.

Sueltenfuss, J. P., Cooper, D. J., Knight, R. L., Waskom, R. M., 2013. The Creation and Maintenance of Wetland Ecosystems from Irrigation Canal and Reservoir Seepage in a Semi-Arid Landscape. Wetlands 33 (5), 799–810.

Sulla-Menashe, D., Gray, J. M., Abercrombie, S. P., Friedl, M. A., 2019. Hierarchical mapping of annual global land cover 2001 to present: The MODIS Collection 6 Land Cover product. Remote Sensing of Environment 222, 183–194.

Tan, B., Masek, J. G., Wolfe, R., Gao, F., Huang, C., Vermote, E. F., Sexton, J. O., Ederer, G., 2013. Improved forest change detection with terrain illumination corrected Landsat images. Remote Sensing of Environment 136, 469–483.

TARIM, 2015. Crop calendar for Turkey: A compilation of planting and harvesting dates for selected Turkish provinces. Data not published. Turkish Ministry of Agriculture and Forestry, Ankara, Turkey.

Thakkar, H., 2000. Assessment of Irrigation Options in India: Contributing Papers World Commission on Dams. South Asia Network on Dams, Rivers and People.

Thenkabail, P. S., 2013. Global Food Security-support data at 30 m (GFSAD30). In: AGU Fall Meeting Abstracts. American Geophysical Union, Washington D.C., USA.

Thenkabail, P. S., Dheeravath, V., Biradar, C. M., Gangalakunta, O. R. P., Noojipady, P., Gurappa, C., Velpuri, M., Gumma, M., Li, Y., 2009. Irrigated Area Maps and Statistics of India Using Remote Sensing and National Statistics. Remote Sensing 1 (2), 50–67.

Thomas, D. H., Adams, W. M., 1999. Adapting to dams: Agrarian change downstream of the Tiga Dam, Northern Nigeria. World Development 27 (6), 919–935.

Tilman, D., Balzer, C., Hill, J., Befort, B. L., 2011. Global food demand and the sustainable intensification of agriculture. Proceedings of the National Academy of Sciences 108 (50), 20260–20264.

Torres, R., Snoeij, P., Geudtner, D., Bibby, D., Davidson, M., Attema, E., Potin, P., Rommen, B., Floury, N., Brown, M., Traver, I. N., Deghaye, P., Duesmann, B., Rosich, B., Miranda, N., Bruno, C., L'Abbate, M., Croci, R., Pietropaolo, A., Huchler, M., Rostan, F., 2012. GMES Sentinel-1 mission. Remote Sensing of Environment 120, 9–24.

Tortajada, C., 2014. Dams: An Essential Component of Development. Journal of Hydrologic Engineering 20 (1).

Tortajada, C., Altinbilek, D., Biswas, A. K., 2012. Impacts of Large Dams: A Global Assessment. Springer, Berlin/Heidelberg, Germany.

Trabucco, A., Zomer, R. J., 2009. Global Potential Evapo-Transpiration (Global-PET) and Global Aridity Index (Global-Aridity) Geo-Database. CGIAR CSI, https://cgiarcsi.community/data/global-aridity-and-pet-database/.

TSI, 2015. Crop Production Statistics: Agricultural Land. Turkish Statistical Institute. Ankara, Turkey.

Turner, B. L., Doolittle, W. E., 2010. The concept and measure of agricultural intensity. The Professional Geographer 30 (3), 297–301.

UNEP, 2004. Analyzing environmental trends using satellite data: Selected cases. Environment change analysis series. United Nations Environment Programme, Division of Early Warning and Assessment, Nairobi, Kenya and Sioux Falls, S.D., USA.

USDA, 2018. Turkey Cotton and Products Annual. USDA Foreign Agricultural Service, Washington D.C., USA.

USGS, 2015. SRTM 1 Arc-Second Global. USGS, Denver, CO, USA.

van der Zaag, P., Gupta, J., 2008. Scale issues in the governance of water storage projects. Water Resources Research 44 (10), 1–14.

van Ittersum, M. K., van Bussel, Lenny G. J., Wolf, J., Grassini, P., van Wart, J., Guilpart, N., Claessens, L., de Groot, H., Wiebe, K., Mason-D'Croz, D., Yang, H., Boogaard, H., van Oort, Pepijn A. J., van Loon, M. P., Saito, K., Adimo, O., Adjei-Nsiah, S., Agali, A., Bala, A., Chikowo, R., Kaizzi, K., Kouressy, M., Makoi, Joachim H. J. R., Ouattara, K., Tesfaye, K., Cassman, K. G., 2016. Can

sub-Saharan Africa feed itself? Proceedings of the National Academy of Sciences 113 (52), 14964–14969.

van Vliet, J., de Groot, H. L., Rietveld, P., Verburg, P. H., 2015a. Manifestations and underlying drivers of agricultural land use change in Europe. Landscape and Urban Planning 133, 24–36.

van Vliet, J., Magliocca, N. R., Büchner, B., Cook, E., Rey Benayas, José M, Ellis, E. C., Heinimann, A., Keys, E., Lee, T. M., Liu, J., Mertz, O., Meyfroidt, P., Moritz, M., Poeplau, C., Robinson, B. E., Seppelt, R., Seto, K. C., Verburg, P. H., 2015b. Meta-studies in land use science: Current coverage and prospects. AMBIO 45 (1), 15–28.

Velpuri, N. M., Thenkabail, P. S., Gumma, M. K., Biradar, C., Dheeravath, V., Noojipady, P., Yuanjie, L., 2009. Influence of Resolution in Irrigated Area Mapping and Area Estimation. Photogrammetric Engineering & Remote Sensing 75 (12), 1383–1395.

Verburg, P. H., Crossman, N., Ellis, E. C., Heinimann, A., Hostert, P., Mertz, O., Nagendra, H., Sikor, T., Erb, K.-H., Golubiewski, N., Grau, R., Grove, M., Konaté, S., Meyfroidt, P., Parker, D. C., Chowdhury, R. R., Shibata, H., Thomson, A., Zhen, L., 2015. Land system science and sustainable development of the earth system: A global land project perspective. Anthropocene 12, 29–41.

Verburg, P. H., Erb, K.-H., Mertz, O., Espindola, G., 2013. Land System Science: between global challenges and local realities. Current Opinion in Environmental Sustainability 5 (5), 433–437.

Verburg, P. H., Neumann, K., NOL, L., 2011. Challenges in using land use and land cover data for global change studies. Global Change Biology 17 (2), 974–989.

Vieira, M. A., Formaggio, A. R., Rennó, C. D., Atzberger, C., Aguiar, D. A., Mello, M. P., 2012. Object Based Image Analysis and Data Mining applied to a remotely sensed Landsat time-series to map sugarcane over large areas. Remote Sensing of Environment 123, 553–562.

Vintrou, E., Desbrosse, A., Bégué, A., Traoré, S., Baron, C., Lo Seen, D., 2012. Crop area mapping in West Africa using landscape stratification of MODIS time series and comparison with existing global land products. International Journal of Applied Earth Observation and Geoinformation 14 (1), 83–93.

Vörösmarty, C. J., McIntyre, P. B., Gessner, M. O., Dudgeon, D., Prusevich, A., Green, P., Glidden, S., Bunn, S. E., Sullivan, C. A., Liermann, C. R., Davies,

P. M., 2010. Global threats to human water security and river biodiversity. Nature 467, 555.

Vuolo, F., Ng, W.-T., Atzberger, C., 2017. Smoothing and gap-filling of high resolution multi-spectral time series: Example of Landsat data. International Journal of Applied Earth Observation and Geoinformation 57, 202–213.

Waldner, F., Canto, G. S., Defourny, P., 2015. Automated annual cropland mapping using knowledge-based temporal features. ISPRS Journal of Photogrammetry and Remote Sensing 110, 1–13.

Waldner, F., de Abelleyra, D., Verón, S. R., Zhang, M., Wu, B., Plotnikov, D., Bartalev, S., Lavreniuk, M., Skakun, S., Kussul, N., Le Maire, G., Dupuy, S., Jarvis, I., Defourny, P., 2016a. Towards a set of agrosystem-specific cropland mapping methods to address the global cropland diversity. International Journal of Remote Sensing 37 (14), 3196–3231.

Waldner, F., Defourny, P., 2017. Where can pixel counting area estimates meet user-defined accuracy requirements? International Journal of Applied Earth Observation and Geoinformation 60, 1–10.

Waldner, F., Fritz, S., Di Gregorio, A., Plotnikov, D., Bartalev, S., Kussul, N., Gong, P., Thenkabail, P., Hazeu, G., Klein, I., Löw, F., Miettinen, J., Dadhwal, V. K., Lamarche, C., Bontemps, S., Defourny, P., 2016b. A Unified Cropland Layer at 250 m for Global Agriculture Monitoring. Data 1 (1), 3.

Waldner, F., Hansen, M. C., Potapov, P. V., Löw, F., Newby, T., Ferreira, S., Defourny, P., 2017. National-scale cropland mapping based on spectral-temporal features and outdated land cover information. PLoS ONE 12 (8), e0181911.

WCD, 2000. Dams and development: A new framework for decision-making: the report of the World Commission on Dams: an overview. Earthscan, London and Sterling, VA.

Weaving, R., 1991. Irrigation in the humid tropics: Project design issues in Indonesia and Thailand. World Bank, Washington D.C., USA.

Whitcraft, A. K., Vermote, E. F., Becker-Reshef, I., Justice, C. O., 2015. Cloud cover throughout the agricultural growing season: Impacts on passive optical earth observations. Remote Sensing of Environment (156), 438–447.

Wiejaczka, L., Oledzki, J. R., Bucala-Hrabia, A., Kijowska-Strugala, M., 2017. A Spatial and Temporal Analysis of Land Use Changes in Two Mountain Valleys: With and without Dam Reservoir (Polish Carpathians). Quaestiones Geographicae 36 (1), 887.

Wilmsen, B., 2018. Damming China's rivers to expand its cities: the urban livelihoods of rural people displaced by the Three Gorges Dam. Urban Geography 39 (3), 345–366.

Winemiller, K. O., McIntyre, P. B., Castello, L., Fluet-Chouinard, E., Giarrizzo, T., Nam, S., Baird, I. G., Darwall, W., Lujan, N. K., Harrison, I., Stiassny, M. L. J., Silvano, R. A. M., Fitzgerald, D. B., Pelicice, F. M., Agostinho, A. A., Gomes, L. C., Albert, J. S., Baran, E., Petrere, JR, M., Zarfl, C., Mulligan, M., Sullivan, J. P., Arantes, C. C., Sousa, L. M., Koning, A. A., Hoeinghaus, D. J., Sabaj, M., Lundberg, J. G., Armbruster, J., Thieme, M. L., Petry, P., Zuanon, J., Torrente Vilara, G., Snoeks, J., Ou, C., Rainboth, W., Pavanelli, C. S., Akama, A., van Soesbergen, A., Saenz, L., 2016. Balancing hydropower and biodiversity in the Amazon, Congo, and Mekong. Science (New York, N.Y.) 351 (6269), 128–129.

Wisser, D., Frolking, S., Douglas, E. M., Fekete, B. M., Schumann, A. H., Vörösmarty, C. J., 2010. The significance of local water resources captured in small reservoirs for crop production – A global-scale analysis. Journal of Hydrology 384 (3-4), 264–275.

Wood, S., Sebastian, K. L., Scherr, S. J., Batjes, N. H., 2000. Pilot analysis of global ecosystems: Agroecosystems. Pilot analysis of global ecosystems. World Resources Institute, Washington, D.C.

World Bank, 2007. Project Performance Assessment Report No. 41122: Xiaolangdi Multipurpose Project I & II and Tarim Basin II Project. World Bank, Washington D.C., USA.

Wu, W., Yu, Q., You, L., Chen, K., Tang, H., Liu, J., 2018. Global cropping intensity gaps: Increasing food production without cropland expansion. Land Use Policy 76, 515–525.

Wulder, M. A., Coops, N. C., 2014. Satellites: Make Earth observations open access. Nature 513 (7516), 30–31.

Wulder, M. A., Coops, N. C., Roy, D. P., White, J. C., Hermosilla, T., 2018. Land cover 2.0. International Journal of Remote Sensing 39 (12), 4254–4284.

Wulder, M. A., Masek, J. G., Cohen, W. B., Loveland, T. R., Woodcock, C. E., 2012. Opening the archive: How free data has enabled the science and monitoring promise of Landsat. Remote Sensing of Environment 122, 2–10.

Wulder, M. A., White, J. C., Goward, S. N., Masek, J. G., Irons, J. R., Herold, M., Cohen, W. B., Loveland, T. R., Woodcock, C. E., 2008. Landsat continuity: Issues

and opportunities for land cover monitoring. Remote Sensing of Environment 112 (3), 955–969.

Wulder, M. A., White, J. C., Loveland, T. R., Woodcock, C. E., Belward, A. S., Cohen, W. B., Fosnight, E. A., Shaw, J., Masek, J. G., Roy, D. P., 2016. The global Landsat archive: Status, consolidation, and direction. Remote Sensing of Environment 185, 271–283.

Xiao, X., Boles, S., Frolking, S., Li, C., Babu, J. Y., Salas, W., Moore, B., 2006. Mapping paddy rice agriculture in South and Southeast Asia using multi-temporal MODIS images. Remote Sensing of Environment 100 (1), 95–113.

Yami, M., 2015. Irrigation projects in Ethiopia: What can be done to enhance effectiveness under 'challenging contexts'? International Journal of Sustainable Development & World Ecology 23 (2), 132–142.

Yan, L., Roy, D. P., 2016. Conterminous United States crop field size quantification from multi-temporal Landsat data. Remote Sensing of Environment 172, 67–86.

Yang, J.-j., Liu, S.-l., Wang, C., Deng, L., Dong, S.-k., 2014. Forest pattern dynamics and landscape connectivity changes in the Manwan Basin after dam construction in the Lancang River, China. Landscape and Ecological Engineering 10 (1), 77–83.

Yano, T., Aydin, M., Haraguchi, T., 2007. Impact of Climate Change on Irrigation Demand and Crop Growth in a Mediterranean Environment of Turkey. Sensors 7 (10), 2297–2315.

Yaslioglu, E., Akkaya Aslan, S. T., Kirmikil, M., Gundogdu, K. S., Arici, I., 2009. Changes in Farm Management and Agricultural Activities and Their Effect on Farmers' Satisfaction from Land Consolidation: The Case of Bursa–Karacabey, Turkey. European Planning Studies 17 (2), 327–340.

Yesilnacar, M. I., Uyanik, S., 2005. Investigation of water quality of the world's largest irrigation tunnel system, the Sanliurfa Tunnels in Turkey. Fresenius Environmental Bulletin. 14 (4), 300–306.

You, L., Ringler, C., Wood-Sichra, U., Robertson, R., Wood, S., Zhu, T., Nelson, G., Guo, Z., Sun, Y., 2011. What is the irrigation potential for Africa? A combined biophysical and socioeconomic approach. Food Policy 36 (6), 770–782.

Zarfl, C., Lumsdon, A. E., Berlekamp, J., Tydecks, L., Tockner, K., 2015. A global boom in hydropower dam construction. Aquatic Sciences 77 (1), 161–170.

Zeitoun, M., Lankford, B., Krueger, T., Forsyth, T., Carter, R., Hoekstra, A. Y., Taylor, R., Varis, O., Cleaver, F., Boelens, R., Swatuk, L., Tickner, D., Scott, C. A., Mirumachi, N., Matthews, N., 2016. Reductionist and integrative research approaches to complex water security policy challenges. Global Environmental Change 39, 143–154.

Zeng, R., Cai, X., Ringler, C., Zhu, T., 2017. Hydropower versus irrigation—an analysis of global patterns. Environmental Research Letters 12 (3), 034006.

Zhang, H. K., Roy, D. P., Yan, L., Li, Z., Huang, H., Vermote, E., Skakun, S., Roger, J.-C., 2018. Characterization of Sentinel-2A and Landsat-8 top of atmosphere, surface, and nadir BRDF adjusted reflectance and NDVI differences. Remote Sensing of Environment 215, 482–494.

Zhao, Q., Liu, S., Deng, L., Dong, S., Yang, Z., Liu, Q., 2013. Determining the influencing distance of dam construction and reservoir impoundment on land use: A case study of Manwan Dam, Lancang River. Ecological Engineering 53, 235–242.

Zhu, Z., Wang, S., Woodcock, C. E., 2015. Improvement and expansion of the Fmask algorithm: cloud, cloud shadow, and snow detection for Landsats 4–7, 8, and Sentinel 2 images. Remote Sensing of Environment 159, 269–277.

Eidesstattliche Erklärung

Ich erkläre, dass ich die Dissertation selbständig und nur unter Verwendung der von mir angegebenen Hilfsmittel (gemäß §7 Abs. 3 der Promotionsordnung der Mathematisch-Naturwissenschaftlichen Fakultät, veröffentlicht im Amtlichen Mitteilungsblatt der Humboldt-Universität zu Berlin Nr. 126/2014 am 18.11.2014) angefertigt habe. Ich habe mich nicht anderweitig um einem Doktorgrad im Promotionsfach Geographie beworben und besitze keinen Doktorgrad im Promotionsfach Geographie. Die Promotionsordnung der Mathematisch-Naturwissenschaftlichen Fakultät, veröffentlicht im Amtlichen Mitteilungsblatt der Humboldt-Universität zu Berlin Nr. 126/2014 am 18.11.2014 habe ich zur Kenntnis genommen.

Philippe Rufin

Berlin, den 28.01.2019